DOCTORAL THESIS

Postglacial Climate Change in Eastern Europe: Focus on Chironomid-based Reconstruction of Summer Temperatures and Continentality

Varvara Bakumenko

TALLINNA TEHNIKAÜLIKOOL
TALLINN UNIVERSITY OF TECHNOLOGY
TALLINN 2025

TALLINN UNIVERSITY OF TECHNOLOGY
DOCTORAL THESIS
53/2025

Postglacial Climate Change in Eastern Europe: Focus on Chironomid-based Reconstruction of Summer Temperatures and Continentality

VARVARA BAKUMENKO

TAL TECH PRESS

TALLINN UNIVERSITY OF TECHNOLOGY
School of Science
Department of Geology
This dissertation was accepted for the defence of the degree 14/07/2025

Supervisor: Prof. Siim Veski
School of Science
Tallinn University of Technology
Tallinn, Estonia

Co-supervisors: Dr. Anneli Poska
School of Science
Tallinn University of Technology
Tallinn, Estonia

Dr. Simon Belle
Department of Aquatic Sciences and Assessment
Swedish University of Agricultural Sciences
Uppsala, Sweden

Opponents: Prof Ladislav Hamerlík
Department of Biology and Environmental Studies
Faculty of Natural Sciences
Matej Bel University
Banská Bystrica, Slovakia

PhD Kadri Sohar
Department of GeologyFaculty of Science and Technology
Tartu University
Tartu, Estonia

Defence of the thesis: 19/08/2025, Tallinn

Declaration:
Hereby I declare that this doctoral thesis, my original investigation and achievement, submitted for the doctoral degree at Tallinn University of Technology has not been submitted for doctoral or equivalent academic degree.

Varvara Bakumenko

---
signature

ISSN 2585-6898 (publication)
ISBN 978-9916-80-350-9 (publication)
ISSN 2585-6901 (PDF)
ISBN 978-9916-80-351-6 (PDF)
DOI https://doi.org/10.23658/taltech.53/2025
Printed by Koopia Niini & Rauam

Bakumenko, V. (2025). *Postglacial Climate Change in Eastern Europe: Focus on Chironomid-based Reconstruction of Summer Temperatures and Continentality* [TalTech Press]. https://doi.org/10.23658/taltech.53/2025

TALLINNA TEHNIKAÜLIKOOL
DOKTORITÖÖ
53/2025

Pärastjääaja kliimamuutus Ida-Euroopas: fookus Hironomiidide-põhisele suvetemperatuuride ja kontinentaalsuse rekonstruktsioonile

VARVARA BAKUMENKO

TAL TECH KIRJASTUS

Contents

List of publications

The list of author's publications, on the basis of which the thesis has been prepared:

I Bakumenko, V., Poska, A., Płóciennik, M., Gasteviciene, N., Kotrys, B., Luoto, T.P., Belle, S. and Veski, S. (2024). Chironomid-based inference model for mean July air temperature reconstructions in the eastern Baltic area. Boreas, 53(3), pp. 401–414. doi: 10.1111/bor.12655

II Bakumenko, V., Poska, A., Birks, H. J. B., Huser, B., Veski, S. (2025). Chironomid-climate continentality conundrum. PLOS One, 20(8), e0327780. https://doi.org/10.1371/journal.pone.0327780

III Nosova, M.B., Zakharov, A.L., Lavrenov, N.G., Zaretskaya, N.E., Mazei, N.G., Kupriyanov, D.A., Pastukhova, Y.A., Bakumenko, V.O., Severova, E.E. and Konstantinov, E.A. (2025). A multi-proxy centennial-resolution paleoecological record of Holocene lake sediments in the marginal zone of Last Scandinavian Glaciation (Tver Region, Russia). Quaternary International, 729, p. 109778. doi: 10.1016/j.quaint.2025.109778

IV Bakumenko, V., Lanka, A., Poska, A., Vassiljev, J., Alliksaar, T., Heiri, O., Belle, S., Veski, S. (Manuscript). A 14 500 - year multi-proxy reconstruction of climate and environment change in eastern Baltics: case study from Southern Estonia. Maniscript is under review in: Quaternary Science Reviewes.

Author's contribution to the publications

Contributions to the papers in this thesis are:

I. The author is the principal conceiver of the publication. The author contributed to fieldwork on lake bottom sediments collection and carried out chironomid analysis, data compilation and statistical analysis. The author is partly responsible for result visualisation and interpretation.

II. The author is the principal conceiver of the publication. The author contributed to fieldwork on lake bottom sediments collection and carried out chironomid analysis, data compilation and statistical analysis. The author is partly responsible for result visualisation and interpretation.

III. The author was responsible for chironomid analysis and chironomid-inferred July air temperature and continentality reconstructions. The author is partly responsible for result visualisation and interpretation.

IV. The author is the leading author of the manuscript, and was responsible for chironomid analysis and chironomid-inferred July air temperature and continentality reconstructions. The author is partly responsible for result visualisation and interpretation.

Introduction

Global climate change has a complex impact on the eastern Baltic region, evident in warming air and water temperatures, reduced ice-cover duration, increased precipitation, and alterations in growing season start and duration (Meier et al., 2022). Significant changes in continentality have been recorded both in the eastern Baltic area and globally over the last 50 years (Stonevicius et al., 2018; Alexandrov et al., 2019). Furthermore, these changes are expected to continue in the near future in the context of ongoing climate change (Williams et al., 2007).

The eastern Baltic region, and Estonia in particular, lies at the transition between boreal and temperate vegetation zones and features a pronounced west-east continentality gradient (Edvardsson et al., 2016). Ecosystems of transitional areas like this are highly sensitive to climate variations (Fu, 1992). Thus, the vegetation of the eastern Baltic area has been found to be sensitive to past changes in northern Europe's air circulation patterns (Giesecke et al., 2008; Seppä et al., 2009). This makes Estonian palaeolimnological sites perfect for tracking past and observing present climate changes.

Pollen-based climate reconstructions are most common in the region, with only a few studies utilizing other biotic or abiotic proxies (Heiri et al., 2014; Väliranta et al., 2015; Veski et al., 2015; Stansell et al., 2017; Druzhinina et al., 2020; Šeirienė et al., 2021; Eensalu et al., 2024). While pollen is an excellent indicator of regional and local land cover changes and human impact, and one of the most widely used proxies for past climate reconstructions (Ilyashuk et al., 2009; Salonen et al., 2012; Kaufman et al., 2020), its use in formerly glaciated areas has limitations. For example, studies show terrestrial plant migration after deglaciation lagged behind climate change in Northern and Eastern Europe (Rao et al., 2022; Väliranta et al., 2015; Zani et al., 2023). The cold, highly continental, and dry climate during the glacial and late glacial periods, driven by proximal continental ice sheets, resulted in vegetation assemblages not found today (Magny et al., 2001; Gonzales & Grimm, 2009). Furthermore, boreal forest biomes, widespread in eastern Baltic history, can be insensitive to minor climate fluctuations (Seppä et al., 2007; Stralberg et al., 2020).

Therefore, there is a need for alternative and independent approaches for palaeoclimate reconstruction. The analysis of subfossil chironomid remains, non-biting midges from the family Chironomidae, order Diptera, has been considered one of the most promising methods for quantitative palaeotemperature reconstruction (Battarbee, 2000). The chitinous remains of chironomid larvae are preserved well in Quaternary lake sediments and can be identified at the species, morphotype (species-group), or genus level (Brooks et al., 2007). This enables observations of past chironomid assemblage shifts based on lake sediment records, providing insights into past climatic and environmental changes.

In general, insects are able to follow and respond to rapid climate changes due to their high diversity, sensitivity, narrow ecological niches, and fast reproduction cycle. Mendoza et al. (2024) show that chironomids can provide close modern analogues to the Younger Dryas subfossil communities. To produce a chironomid-inferred climate reconstruction using modern statistical modelling approaches, a training set (TS) of modern chironomid analogues is needed. Such TSs are commonly recommended to be applied within their biogeographic regions of origin (Juggins et al., 2013; Medeiros et al., 2022). The eastern Baltic area is understudied in terms of chironomid analysis. Only a few chironomid-related studies have been conducted here (Seire & Pall, 2000; Agasild et al.,

2018; Stivrins et al., 2021) and even fewer chironomid-inferred climate ones (Heiri et al., 2014; Veski et al., 2015; Šeirienė et al., 2021).

Chironomids demonstrate particular sensitivity to warm season temperatures and duration, factors that directly regulate development, growth, and survival rates in these ectothermic organisms (Foucault et al., 2018). Therefore, not surprisingly, a strong relationship between the taxonomic composition of chironomid assemblages and summer air temperature has been found globally (Eggermont & Heiri, 2012a). Chironomid assemblages are widely used for July air temperature (July air T) reconstructions (Tóth et al., 2015; Hájková et al., 2016; Jiménez-Moreno et al., 2023; Rigterink et al., 2024). However, the mechanisms linking air and surface water temperatures with chironomid assemblages remain debated. Eggermont and Heiri (2012) demonstrate that temperature's indirect effects on lakes' physical and chemical characteristics could play a significant role in determining the distribution of lake-dwelling chironomid larvae. This suggests a more complex climate-chironomid relationship than generally assumed.

Recent studies show that chironomid assemblage composition is also affected by site continentality (Self et al., 2011). The significance of this finding cannot be overstated: continentality represents a fundamental climate characteristic influenced by factors such as distance from the ocean, latitude, and atmospheric circulation patterns (Stonevicius et al., 2018) while integrating not only annual temperature variations but also precipitation patterns, and their seasonal variability. Thus, it was hypothesised that continentality could influence chironomids indirectly through cold season temperature dependent presence and duration of ice-cover and vegetation season properties (Self et al., 2011). However, the field of chironomid-inferred continentality reconstructions is new, the mechanisms of continentality influence on chironomid assemblages have not been studied, and the method has not been fully developed.

While chironomid-based reconstructions of July air T and continentality dynamics during the postglacial time could provide valuable insights into the past, present, and future climate and aquatic environment development of the eastern Baltic area, such reconstructions are largely missing. There is no specialized TS applicable for continentality reconstructions in Europe. Furthermore, although a number of chironomid TSs are available from different parts of Europe (T. P. Luoto, 2009; Heiri et al., 2011; Kotrys et al., 2020), the eastern Baltic region still lacks a chironomid-based TS specifically designed to account for unique characteristics of the region.

The main goal of this thesis is to develop and validate chironomid-based statistical inference models tailored to the eastern Baltic region, and to apply these models to reconstruct past climate conditions using sediment records from the area. The thesis focuses on developing of a new regional chironomid-inferred statistical model for July air T reconstructions, provides justification for using chironomids as a proxy of continentality, and constructs a novel chironomid-based model suitable for continentality reconstructions. Furthermore, the thesis includes the examples of these new models being applied to two sites in the eastern Baltic region presenting chironomid-based July air T and continentality reconstructions of late glacial and Holocene climate changes.

The main chapters of the thesis include a literature review on chironomid ecology and inference model development; a description of the materials and methods used, a presentation of the key results of the published papers, a comprehensive discussion of the findings, and the conclusions.

Aims of study

While most chironomid-based studies have been conducted in central and northern Europe, eastern Europe remains relatively understudied. Specifically, the eastern Baltic region lacks a dataset reflecting local modern chironomid assemblage distributions and reliable chironomid-inferred climate reconstructions. Given its transitional position between boreal and nemoral biomes and oceanic and continental climates, July air T and continentality reconstructions could offer valuable insights into the region's ecosystem functioning. Although the dependence of chironomids on July air T has already been well established, the mechanism by which continentality influences chironomid assemblages has only been hypothesized. Therefore, this mechanism must be clarified before chironomids can be reliably used as a proxy for continentality.

The main aims of this thesis are:

1. To investigate the composition of chironomid assemblages located in the eastern Baltic area and regionally across longitudinal and latitudinal gradients.
2. To develop a chironomid-based inference model suitable for reconstructing July air T in the eastern Baltic area.
3. To explore the application of chironomids as continentality-proxy by developing and testing a chironomid-based inference model.
4. To fill knowledge gaps about the eastern Baltic region’s postglacial climate dynamics.

Abbreviations

air T	mean air temperature
TS	Training set
FBP	Finno-Baltic-Polish
LOI	Loss-on-ignition
KOI	Kerner Oceanity Index
ATR	Annual Temperature Range
WA	Weighted-Average regression
WA-PLS	Weighted Averaging-Partial Least Square regression
INDVAL	Indicator Species Analysis
ANOSIM	Analysis of similarity
GAM	Generalized Additive Model
DCA	Detrended Correspondence Analysis
CCA	Canonical Correlation Analysis
RDA	Redundancy Analysis
PCA	Principal Component Analysis
BP	Before Present
ka	kiloanni
cal	calibrated

1 Background

This chapter provides a literature review on chironomid ecology and inference models development and use.

1.1 Chironomid life cycle

Chironomidae is a family of non-biting midges belonging to the order Diptera, class Insecta. It is one of the most abundant and widely distributed freshwater insects, accounting for up to 15000 species globally, with around 1000 species described in Europe (Armitage et al., 1995; Sæther, 2000).

Chironomids have a four-stage life cycle: imago (adult), egg, larvae, pupae (Figure 1). Eggs are laid in a gelatinous mass or individually, typically on aquatic vegetation (Karima, 2021), and hatch after a specific number of days at a certain temperature (Schütz & Füreder, 2019). The larval stage consists of four instars and is characterized by a well-developed, chitinous head capsule and an elongated, segmented, soft body without thoracic legs. The larval chitinous head capsules are well preserved in Quaternary lake sediments and thus can be used for the lake sediments, allowing their identification at the morphotype level (Brooks et al., 2007). The pupal stage is characterised by a comma-shaped body, and its duration is the shortest in the chironomids' life cycle – from several hours to several days. A key feature of the imago stage is the reduction of the mouthparts and, hence, the absence of feeding (Karima, 2021). This characteristic gives chironomids their common name, "non-biting midges". Depending on the geographic area, chironomids can produce one to four generations per year.

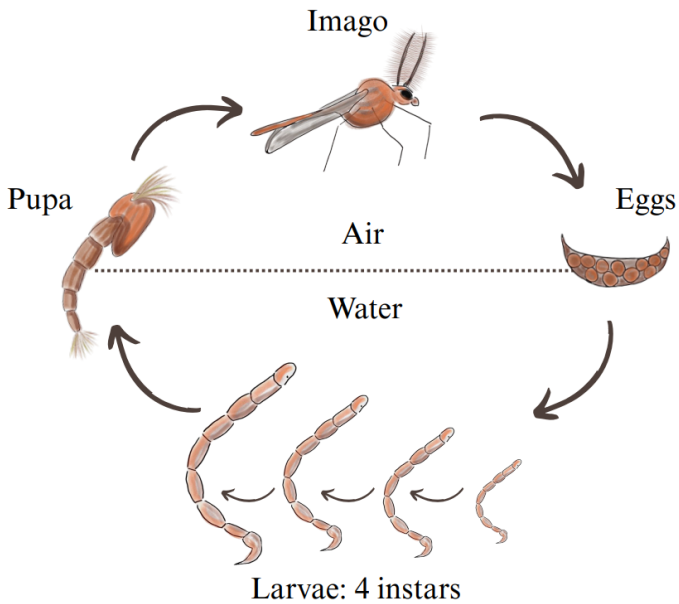

Figure 1 *Chironomid life cycle.*

1.2 Chironomidae ecology

1.2.1 Water depth, pH and heavy metals

Water depth influences bottom-dwelling chironomid assemblages by affecting a variety of environmental parameters (water temperature, oxygen content, food availability, density of aquatic macrophytes, habitat structure etc.) to which chironomids are sensitive (Heiri, 2004; Kurek & Cwynar, 2009; Engels & Cwynar, 2011; Cao et al., 2012; Zhang et al., 2013; Chen et al., 2014). Engels et al. (2012) noted that changes in the ratio between available littoral and profundal habitats are one of the major reasons for chironomid assemblages' sensitivity to water level changes. This could be explained by the fact that chironomid larval feeding behavior and dietary preferences are often linked to the characteristics of their specific habitat (Antczak-Orlewska et al., 2021). Thus, chironomid assemblages have been successfully used to reconstruct depth changes (Ni et al., 2023).

Chironomids are also influenced by pH, a well-established driver affecting aquatic ecosystems and the distribution of chironomid species (Mousavi, 2002; Brooks et al., 2007). The pH values below 4 and above 9 are recognized as unfavourable for limnetic macroinvertebrate communities (Berezina, 2001). Low pH is known to reduce the diversity and ecological stability of chironomids in waterbodies (Brodin & Gransberg, 1993; Orendt, 1999; Woodcock et al., 2005). Also, pH influences the absorption of heavy metals by chironomids (Krantzberg & Stokes, 1988), which they are highly sensitive to (Ruse et al., 2000; Pegler et al., 2020). The chironomid responses to pollution are reflected through mentum deformities (Cortelezzi et al., 2011; Veroli et al., 2014), metal bioaccumulation (Roosa et al., 2016), and shifts in community composition (Ilyashuk et al., 2003; De Bisthoven et al., 2005).

1.2.2 Water trophic state

Trophic state is another key factor influencing chironomid diversity, species composition, and biomass (Brooks et al., 2007). Chironomid diversity has been observed to increase from oligotrophic and mesotrophic conditions towards eutrophic ones, followed by a decline under hypereutrophic conditions (Salonen et al., 1993; Luoto, 2011). Eutrophic lakes typically exhibit elevated total phosphorus levels, stimulating the growth of microorganisms and macrophytes, thereby enhancing food availability and habitat complexity for chironomid larvae (Brooks et al., 2001). These conditions promote the biomass growth and diversity in chironomid communities (Takahashi et al., 2008). The decline in diversity observed in hypereutrophic lakes is most likely a result of oxygen depletion events caused by algal blooms and high microbial activity, typically occurring in late summer before autumn turnover (Brooks et al., 2001; Luoto, 2011).

There is also an inverse relationship between chironomids and the trophic status of a water body. Chironomids play an essential role in the phosphorus flux in the lake ecosystem as agents of phosphorus turnover and as live food for fish, and thus affect the long-term phosphorus budget of lakes (Biswas et al., 2009; Hupfer et al., 2019). Hupfer et al. (2019) notes that, as potential 'ecosystem engineers', chironomid larvae help to control water quality.

Fossil chironomid assemblages can be effectively used to quantitatively reconstruct the trophic history of lakes (Brodersen & Lindegaard, 1999; Brooks et al., 2001; Luoto, 2011). A high degree of precision in such reconstructions can be achieved by applying this method to chironomids in shallow, eutrophic lakes (Langdon et al., 2006).

1.2.3 Dissolved water oxygen concentrations

Oxygen is a critical factor for aquatic organisms relying on aerobic respiration. Seasonal and spatial variations in dissolved oxygen availability can significantly affect chironomid life history strategies, distribution, behaviour, and interactions with other species (J. C. Davis, 1975). Langton et al. (2006) emphasize that in deep, stratified lakes, dissolved oxygen concentrations are the primary driver of chironomid communities.

Chironomid metabolism is directly influenced by oxygen levels, with egg development slowing considerably under low-oxygen conditions (Pinder, 1992). Chironomids do not occur in environments with permanently anoxic conditions, while low oxygen concentrations can trigger entering summer diapause or aestivation (Bryce & Hobart, 1972; Kansanen, 1985; Armitage et al., 1995). Oxygen content was observed to explain the diversity of chironomid profundal communities (Verbruggen et al., 2011; Jyväsjärvi et al., 2013).

Brodersen et al. (2004) proposed a classification of chironomid species based on their oxy-regulatory capacity using experimental approaches, showing that species typical of cold, oligotrophic lakes generally prefer well-oxygenated conditions. In Ontario, Canada, chironomid-based inference models have been successfully developed for reconstructing past hypolimnetic anoxia (Quinlan et al., 1998) and late-summer hypolimnetic oxygen conditions (Little & Smol, 2001) providing valuable information on historical lake oxygen dynamics. The effectiveness of such models is enhanced when supported by other proxies that estimate the duration of the open-water season and nutrient status, key factors regulating hypolimnetic oxygen availability (Luoto & Salonen, 2010).

1.2.4 Climate

Temperature directly influences lake organisms by regulating physiological processes like growth, development, and respiration. In addition it indirectly affects chironomids by shaping limnological factors such as nutrient levels and oxygen concentrations, impacting survival and reproduction. Thus, the taxonomic composition of subfossil chironomid assemblages is known to be responsive to warm season temperature fluctuations (Walker & Mathewes, 1987; Heiri et al., 2011; Fortin et al., 2015; Nazarova et al., 2023) and heat accumulation expressed as growing degree days (GDD; Lotter et al., 1997; Velle et al., 2010). Composition of chironomid larvae communities in lakes across polar and temperate regions of the northern hemisphere is strongly associated with July air T (Barley et al., 2006; Walker, 1987). While the southern hemisphere is understudied in terms of chironomid analysis, the relationships between chironomid assemblages and warm season temperature have also been revealed there (Verschuren & Eggermont, 2006; Rees et al., 2008; Martel-Cea et al., 2021). Chironomid assemblages in lakes can be used to reconstruct past changes in temperature at the local scale (Eggermont & Heiri, 2012b).

Besides summer temperature, chironomids have shown dependency on winter temperature (Larocque et al., 2001; Eggermont & Heiri, 2012b). Chironomid assemblages were hypothesized to be affected by ice-cover length, which is directly related to winter temperatures and is inversely correlated with dissolved oxygen levels, warm season duration, and changes in continentality (Self et al., 2011; Engels et al., 2014).

The relationship between continentality and chironomids, as well as the broader impact of continentality changes on the lake ecosystems, remains largely understudied. However, continentality can indirectly affect aquatic zoobenthos through variations in the start and duration of the growing season (Nishimura & Laroque, 2011), water

turnover timing (Butcher et al., 2015), and ice-cover presence and duration, which influences pH (Preston et al., 2016) and dissolved oxygen levels (Zdorovennova et al., 2021). The annual temperature range (ATR), defined as the difference between the coldest and warmest months, is the most commonly used metric for estimating continentality. However, several other indices accounting for different combinations of its major drivers provide effective measures of continentality gradients. For instance, Kerner oceanity index (KOI; Zambakas, 1992) takes into account October and April air T and Gorzynski continentality index (Gorczyński, 1920) also accounts for latitude.

In 2011, Self et al. presented a TS collected from the European part of Northern Russia and Central Siberia. They demonstrated that chironomid assemblages in Northern Russia are influenced by continentality (Gorzynski continentality index). Since then, no further studies have examined modern chironomid assemblage distribution in relation to continentality.

1.3 Chironomid-based numerical inference models

A calibration dataset of modern analogues that represent a range of climate conditions is necessary to develop a numerical model for quantitative palaeotemperature reconstruction. These datasets are created by analyzing chironomid taxa from the topmost 1–2 cm of lake bottom sediments in a large number of lakes spanning diverse lacustrine environments. Based on the calibration dataset, (Birks & Birks, 1998; Birks, 2010) developed a numerical inference model (transfer/calibration function) to determine chironomid-temperature relationships and quantitatively reconstruct past air T values from fossil Chironomid assemblages. Weighted Averaging-Partial Least Square regression (WA-PLS; ter Braak & Juggins, 1993) is the most widely used approach for chironomid-based inference model building. It allows achieving a prediction error ranging from less than 1° C to 2 °C (Kaufman et al., 2020).

Currently, chironomid-based calibration datasets (training sets; TSs) and July air T inference models have been developed for Switzerland (Lotter et al., 1997), Norway (Brooks & Birks, 2000), northern Sweden (Larocque et al., 2001), Finland (Luoto, 2009), Poland (Kotrys et al., 2020), Tatra Mountains (Chamutiová et al., 2020), the western part of Russia and Northern Siberia (Self et al., 2011; Nazarova et al., 2023), New England and Canada (Suranyi et al., 2025), and Greenland (Brodersen & Anderson, 2002). Calibration functions are recommended to be applied within the biogeographic regions from which they were developed (Heiri et al., 2011; Self et al., 2011). Partially, because the same morphotype can have various ecological requirements in different regions, which can potentially bias temperature reconstructions (Langdon et al., 2008; Kotrys et al., 2020).

The Swiss-Norwegian and Finnish TSs have been used for the reconstruction of July air T change during late glacial and early Holocene climate events in the eastern Baltic area (Heiri et al., 2014; Šeirienė et al., 2021). The estimated air T generally align with other European fossil chironomid-based records and climate model simulated data (Heiri et al., 2014). However, neither Finnish, Swiss-Norwegian, nor the recently published Swiss-Norwegian-Polish (Kotrys et al., 2020) TSs adequately capture the climatic and environmental specifics of the eastern Baltic area.

Modern July air T range in the eastern Baltic area is 17.2–18.4 °C, outside the range of the Finnish TS (12.1–17.5 °C). Thus, the Finnish TS lacks warm-site modern analogues suitable for application in the eastern Baltic area. In addition, the bedrock composition in Fennoscandia is more acidic than in the eastern Baltic, possibly leading to varying water chemistry that influences chironomid assemblages (Eggermont & Heiri, 2012b).

Swiss-Norwegian TS mainly includes high-altitude lakes, and their ecology likely differs from the geographically distant lowland lakes of the eastern Baltic area. The Swiss-Norwegian-Polish TS (Kotrys et al., 2020) expanded the mean July air T range of northeastern European models up to 20 °C. This addition helps to fill the gap in modern "warm" analogues and incorporates sites from carbonate-rich regions, improving reconstructions based on the eastern Baltic region sediments. However, the Swiss-Norwegian-Polish TS, as a combination of spatially separated sampling areas, is not continuous, and lacks modern analogues for the eastern Baltic. This limitation complicates regression-based methods for temperature reconstruction, as they require evenly distributed samples along environmental gradients.

2 Study area, materials and methods

This paragraph provides a general overview of the research area and methods used to study modern chironomid assemblages distribution, and to develop and use chironomid-based TSs for palaeoclimate reconstructions. Please refer to the individual papers for more comprehensive details regarding the study areas, materials, methods, and statistical analyses.

2.1 Study area and sites

The current thesis study area lies within the eastern European Plain and Fennoscandia with a special emphasis on Southern Estonia and the nearby areas, where the palaeoclimate reconstructions were conducted (Paper III, Manuscript) (Figure 2).

The Finno-Baltic-Polish (FBP) TS, developed in Paper I, consists of 121 lakes, evenly distributed across the longitudinal gradient from northernmost Finland until the northern-eastern part of Poland (Figure 2). The eastern Baltic part of the TS was developed as a part of this thesis, while Finnish and Polish have been published before (Table 1). The lakes chosen for the study represent the local water chemistry patterns and have experienced low anthropogenic impact. The FBP TS sampling design reflects the continuous increase in July air T from the north to south (12.1–19.2 °C; Figure 2) with the Baltic Sea as a physical obstacle.

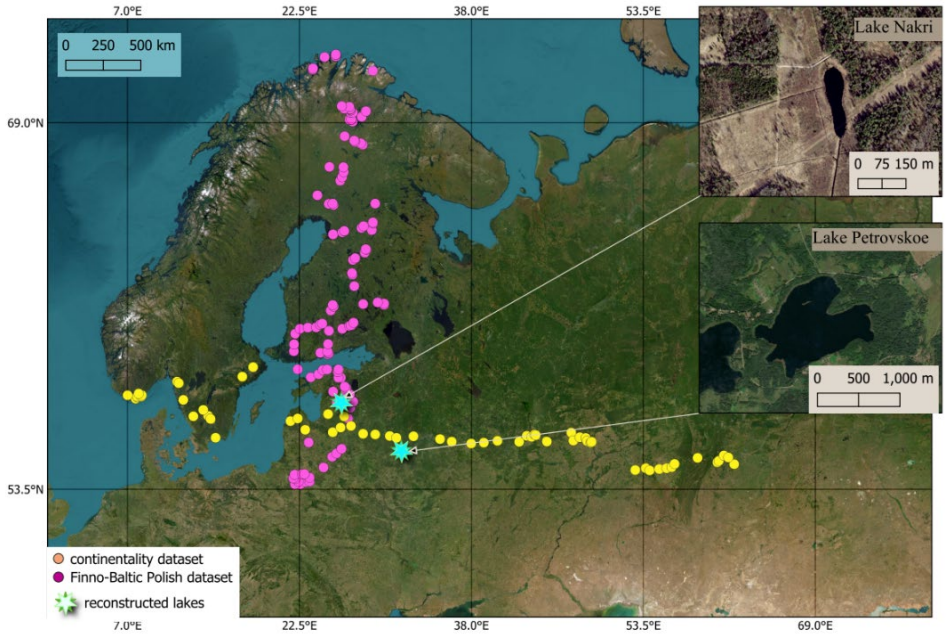

Figure 2 *Location of the sites included in the FBP TS (Paper I) and Continentality Dataset (Paper II); climate reconstruction sites: Lake Nakri (Manuscript), Lake Petrovskoe (Paper III). The Satellite ESRI map was used as a basemap.*

The Continentality Dataset, developed in Paper II, comprises 51 lakes sampled along a longitudinal gradient from the Ural Mountains to the Norwegian Atlantic coast. The Russian and Latvian parts of the dataset were developed within the scope of the

current thesis, while Swedish and Norwegian were obtained from existing datasets (Table 1). The July air T gradient of the dataset remains narrow (14.6–20.2 °C) with a drastic increase from 14.4 up to 33.3 °C in the ATR.

The Swiss-Norwegian TS was downloaded from the National Oceanic and Atmospheric Administration online storage to be used as an inference model (Heiri et al., 2011) along with FBP TS.

Two lakes – Nakri (Manuscript) and Petrovskoe (Paper III) – were chosen to produce a chironomid-based palaeoclimate reconstructions. Lake Nakri is situated in the south of Estonia, while Lake Petrovskoe lies about 400 km southeast, in Russia (Figure 2).

Table 1 *Environmental data for subsets of the FBP TS and Continentality Dataset. The table includes data about July air T (°C), ATR (°C), KOI, number of ice-cover days, and growing degree days with a base temperature 5 °C (GDD5).*

Dataset origin	Number of samples	Publication	July air T(°C)	ATR (°C)	KOI	Ice-cover days	GDD5
Finland	82	Luoto, 2009	12.1–17.5	21.4–27.8	2.8–11.4	105–223	163–583
Poland	9	Kotrys et al., 2020	18.4–19.2	20.9–21.2	–0.3–1.3	82–89	1810–1937
Norway	6	Heiri et al., 2011	16.0–17.3	14.4–16.7	15.8–27.5	35–83	1200–1511
Sweden	7	Huser, unpublished	14.6–16.8	17–19.4	6–11.3	43–65	939–1088
Eastern Baltic	35	Paper I	17.2–18.4	18.6–22.6	–2–11	87–128	1473–1828
Russia	31	Paper II	17.8–20.2	23.0–33.3	–4.5––1.6	126–196	1497–1880

2.1.1 East European Plain and Fennoscandia

The East European Plain is bordered by the Baltic Sea to the west, which acts as a thermal buffer by absorbing excess heat during the summer and releasing it in the winter. This ameliorating effect results in a mild maritime climate in the western part of the East European Plain. In contrast, the eastern part of the Plain experiences a more continental climate due to the influence of the Siberian High (Cohen et al., 2001) and can be characterized by severe winters and hot summers. Summer temperatures gradually rise from north to south, while continentality increases from west to east across the East European Plain.

The North Atlantic borders Fennoscandia to the west, the Arctic Ocean to the north, and the Baltic Sea to the south. Although the distribution of July air T generally follows the same north-to-south gradient observed in the East European Plain, the continentality gradient behaves differently. It increases inland and decreases along the coastal regions.

The bedrock of the East European Plain mainly consists of sandstone and limestone, while Fennoscandia lies predominantly on gneisses and granite/granitoids. The biomes of the area depend on the local environmental and climatic factors. Fennoscandia's landscape is dominated by the boreal forest (taiga) with tundra associations in the

northern and western coastal areas. The East European Plain is characterized by the dry forest-steppes in the areas adjacent to the Ural Mountains, deciduous and mixed deciduous-coniferous forest in the central part, boreal forests in the north-west and tundra biomes in the northernmost parts.

2.1.2 Eastern Baltic area

The last deglaciation of the eastern Baltic took place around 14.7−12.7 ka cal BP (Kalm et al., 2011; Lasberg & Kalm, 2013; Amon et al., 2016; Hughes et al., 2016). Postglacial rebound remains noticeable, particularly in Estonia, with land uplift rates ranging from –0.5 to +2 mm per year, according to rebound models (Kall et al., 2014).

The history of the eastern Baltic area vegetation development after deglaciation has been reconstructed based on pollen data. Late glacial climate and environment in the eastern Baltic revealed several distinct events: Bölling/Alleröd warming followed by the Younger Dryas cooling (Seppä & Poska, 2004; Laumets et al., 2014). Immigration of plant and animal taxa followed shortly after the ice retreat. The late glacial open tundra biome dominated by herbs and cold-tolerant shrub species was replaced by boreal forest during the Early Holocene (Amon et al., 2016; Poska et al., 2022). Later on, from ca 8.5 ka onwards, temperate broad-leaved forests gradually replaced the boreal forests with a distinct reduction in the proportion of temperate trees during 8.2 ka cold event (Saarse & Veski, 2001; Niinemets & Saarse, 2009; Seppä et al., 2009; Seppä & Poska, 2004; Veski et al., 2015). During the Holocene climate optimum, 8 ka cal BP the pollen-based summer air T reconstructions suggest warmer temperatures compared with the present day. Since 6 ka cal BP annual air T gradually decreased to the present level and development of mixed boreal forests. After 4 ka cal BP the eastern Baltic area has experienced considerable anthropogenic deforestation, and change in woodland composition with late successional temperate taxa replaced by early successional ones (Niinemets & Saarse, 2009; Poska et al., 2022).

2.2 Sediment coring and sampling

The modern chironomid assemblages in Latvia, Lithuania, Estonia, and Russia were obtained by sampling lake-bottom sediments with the gravity corer from the deepest part of the lake (Papers I–II). Upper 1–2 centimetres of the sediments were collected and prepared for the analysis.

Lake Nakri palaeosediment coring was conducted from the deepest part of the lake using a Russian corer, and in total 1346 cm long sediment section was recovered (Manuscript). Sediment sequence consists of parallel, overlapping sets of 100 cm long segments. These segments were correlated using loss-on-ignition curves. The coring of Lake Petrovskoe followed the same strategy (Paper III).

2.3 Laboratory analysis and chironomid identification

For chironomid analysis of the eastern Baltic and Russian modern sediments, Lakes Nakri and Petrovskoe palaeo-sediments, 5 cm^3 samples were water-sieved using a 100-µm mesh to remove fine particles. Afterward, each sample was transferred to a Petri dish, where chironomid head capsules were extracted using fine forceps under a stereomicroscope at 25× magnification. The extracted head capsules were air-dried and mounted in Aquatex® or another mounting medium. Taxonomic identification was performed under a light microscope at 100–400× magnification. The identification of

subfossil chironomid head capsules was conducted following the taxonomic framework of Brooks et al. (2007) and supplemented by identification keys from (Klink & Pillot, 2003; T. Andersen et al., 2013; Larocque-Tobler, 2014).

The laboratory procedures for the Finnish, Swiss–Norwegian, and Polish TSs samples are detailed in the original studies (Luoto, 2009; Heiri et al., 2011, p. 20; Kotrys et al., 2020). However, generally they followed the same protocol as described above.

2.4 Other proxies

Pollen, loss-on-ignition (LOI), and Cladoceran analysis of Lake Nakri were done by Siim Veski, Jüri Vassiljev, and Anna Lanka, respectively (Manuscript). Pollen, Cladocera, and charcoal analysis of Lake Petrovskoe were done by Maria Nosova, Yulia Pastukhova, Dmitrii Kupriyanov, respectively (Paper III). In all cases, the standard procedures were used, following methods described in Berglund & Ralska-Jasiewiczowa (1991) and Moore et al. (1991) for pollen analysis; (Frey (1986) and Korhola et al. (2000) for Cladocera analysis; Heiri et al.) 2001) for LOI; Mooney & Tinner (2011) for charcoal analysis. The specifics of laboratory procedures are detailed in respective manuscripts.

2.5 Climate and environmental data

Air T of each month (°C) and ice-cover thickness (mm) for each lake for FBP TS and Continentality Dataset were extracted from the ERA5 dataset with hourly temporal and 0.25° x 0.25° spatial resolution (Hersbach et al., 2020). Using the downloaded climate data, the following variables were calculated based on a 30-year means (1991–2021 for eastern Baltic and Russian sites; 1975–2005 for Finnish sites; 1984–2014 for Polish sites; 1984–2014 for Swedish sites; 1965–1995 for Norwegian sites):

1. Mean January, July, October, and April air T (°C).
2. Continentality indices: ATR (annual temperature range; the difference between the warmest month's mean temperature and the coldest month's mean temperature); KOI (Kerner oceanity index; Zambakas, 1992) reflecting not only annual temperature variation but also the warmth of spring and autumn, calculated following the equation: $KOI = 100 \times (T_{october}-T_{april})/ATR$.
3. Growing degree days at a base temperature of 5 °C (GDD5) were calculated by applying the daily temperature data following the equation: $(T_{max}+T_{min})/2-T_{base}$ (McMaster and Wilhelm, 1997); T_{base} equals 5 °C.
4. Ice conditions (number of ice-cover days): the number of ice-cover days was estimated using the ice-thickness dataset by summing the number of days with a minimum ice thickness > 0.

For lakes from the eastern Baltic dataset, water depth was measured simultaneously with coring from the ice; pH, oxygen concentrations, and water phosphorus content were measured in the following summer (Paper I). Lake water depth and pH for the rest of FBP TS were obtained from the original publications (Luoto, 2009; Kotrys et al., 2020). The lake-water depth, pH, and bedrock composition were determined simultaneously with summer coring for the Continentality Dataset (Paper II).

2.6 Data analysis

Chironomid count data were transformed into relative abundances (%). Only morphotypes with an abundance higher than 2% in at least one sample were included for statistical analysis to minimize the possible noise (Walker, 2001). Additional square-root transformation was applied to minimise variances among taxa for ordination analysis.

In Paper I, the FBP TS was divided into three biogeographic zones based on July air T: northern boreal (12.1–15.0 °C), southern boreal (15.0–17.0 °C), and temperate (17.0–19.2 °C). In Paper II, the Continentality Dataset was categorized into three KOI-based zones: continental (–10–0), transitional (0–10), and oceanic (10–20) (Stonevicius et al., 2018). FBP TS was divided by the ATR value to transitional (19–24 °C) and continental (24–28 °C) part. Analysis of Similarities (ANOSIM; Clarke & Green, 1988) was used to validate described divisions.

The Shapiro-Wilk test and Spearman correlations were used in Paper II to identify collinearity between environmental and climatic variables. Variables showing correlation coefficients > ±0.7 considered indistinguishable in their effects.

The detrended correspondence analysis (DCA; Hill & Gauch, 1980) was used to examine chironomid assemblages and compositional gradients in Papers I–II. In Paper I, redundancy analysis (RDA) and canonical correspondence analysis (CCA) were applied to chironomid assemblages data due to intermediate DCA axis lengths (3.1 and 2.4 SD; Birks & Birks, 1998; Lepš & Šmilauer, 2003). In Paper II, RDA was chosen for its shorter DCA axes (2.9 and 2 SD).

Generalized additive models (GAM; Wood, 2011) were applied to estimate the taxon-specific July air T/abundance relationships in the FBP TS (Paper I). Indicator species analysis (INDVAL; Dufrene & Legendre, 1997) was used to identify key morphotypes for the best-performing continentality variable in Paper II and Manuscript.

Weighted-average regression with inverse deshrinking (WA; Birks et al., 1997; Braak & Juggins, 1993) was used to estimate taxon-specific July air T and continentality optima in Papers I–II.

Weighted averaging-partial least squares (WA-PLS; Braak & Juggins, 1993) with bootstrapping (9999 permutations; Birks et al., 1997) was used to assess the feasibility of a chironomid-based TSs in Papers I–II and conduct the chironomid-inferred palaeoclimate reconstruction in Paper III and Manuscript. The best transfer function was selected based at minimized cross-validated root mean square error of prediction (RMSEP), with statistical significance set at $p \leq 0.05$. RMSE (root mean square error), bias, and R^2 were taken to consideration while discussing the reliability of the results.

Analyses were conducted in R (v4.1.1; Wickham et al., 2019; R Core Team, 2021) using packages: 'ggplot2' for visualization in Papers I–III and Manuscript (Wickham et al., 2019), 'dplyr' for general data processing in Papers I–III and Manuscript (Wickham et al., 2022), 'vegan' for ordination and ANOSIM in Papers I–II (Oksanen et al., 2022), 'rioja' for WA-PLS and stratigraphic plotting in Papers I–II (Juggins, 2022), 'indicspecies' for performing INDVAL on the Continentality Dataset in Paper II (De Cáceres & Legendre, 2009), 'mgcv' for performing the GAMs in Paper I (Wood, 2017). The C2 program (Juggins, 2003) was used to perform pollen-based and chironomid-based reconstructions. Stratigraphic diagrams for Manuscript were prepared in Tilia 3.0.1 software.

3 Results

3.1 Modern chironomid assemblages distribution

This section includes the key results on the modern chironomid distribution patterns across longitudinal and latitudinal gradients, presented in Papers I–II.

3.1.1 Chironomid taxonomic composition and distribution

The taxonomic composition of chironomid assemblages of the eastern Baltic area (Figure 3) included *Psectroclasdius sordidellus*-type (8.6% average abundance), *Chironomus plumosus*-type (8.6%), *Dicrotendipes nervosus*-type (6.8%), *Neozavrelia* (6.8%), *Polypedilum nubeculosum*-type (5.28%), *Glyptotendipes pallens*-type (4.8%), *Microtendipes pedellus*-type (4.6%) and *Corynoneura ambigua*-type (4.1%) as the most abundant ones. The most abundant taxa in the whole FBP TS were *Psectrocladius sordidellus*-type (15.6%), *Chironomus plumosus*-type (7.3%), *Ablabesmyia* (7.2%), *Procladius* (7%), *Microtendipes pedellus*-type (6.8%), *Cladotanytarsus mancus*-type (6.1%) and *Zalutschia zalutschicola*-type (5.7%).

The most abundant morphotypes in the Continentality Dataset (Figure 4) were *Chironomus plumosus*-type (9.6%), *Psectrocladius sordidellus*-type (7.4%), *Dicrotendipens* (4.6%), and *Tanytarsus pallidicornis*-type (3.5%). The presence of *Chironomus anthracinus*-type, *Heteratanytarsus*, *Heterotrissocladius marcidus*-type, *Sergentia coracina*-type, and *Zalutschia* characterises the transitional and oceanic parts of the dataset. These taxa are either absent or present in low quantities in continental lakes. Transitional lakes are further differentiated from oceanic ones by the presence of *Paratanytarsus penicillatus*-type, *Limnophyes*, and *Pseudorthocladius*, and higher abundances of *Heterotrissocladius marcidus*-type, *Tanytarsus mendax*-type, *Tanytarsus pallidicornis*-type, *Cricotopus intersectus*/*laricomalis*-type (marked as *Cricotopus*; Figure 4), and *Microtendipes pedellus*-type.

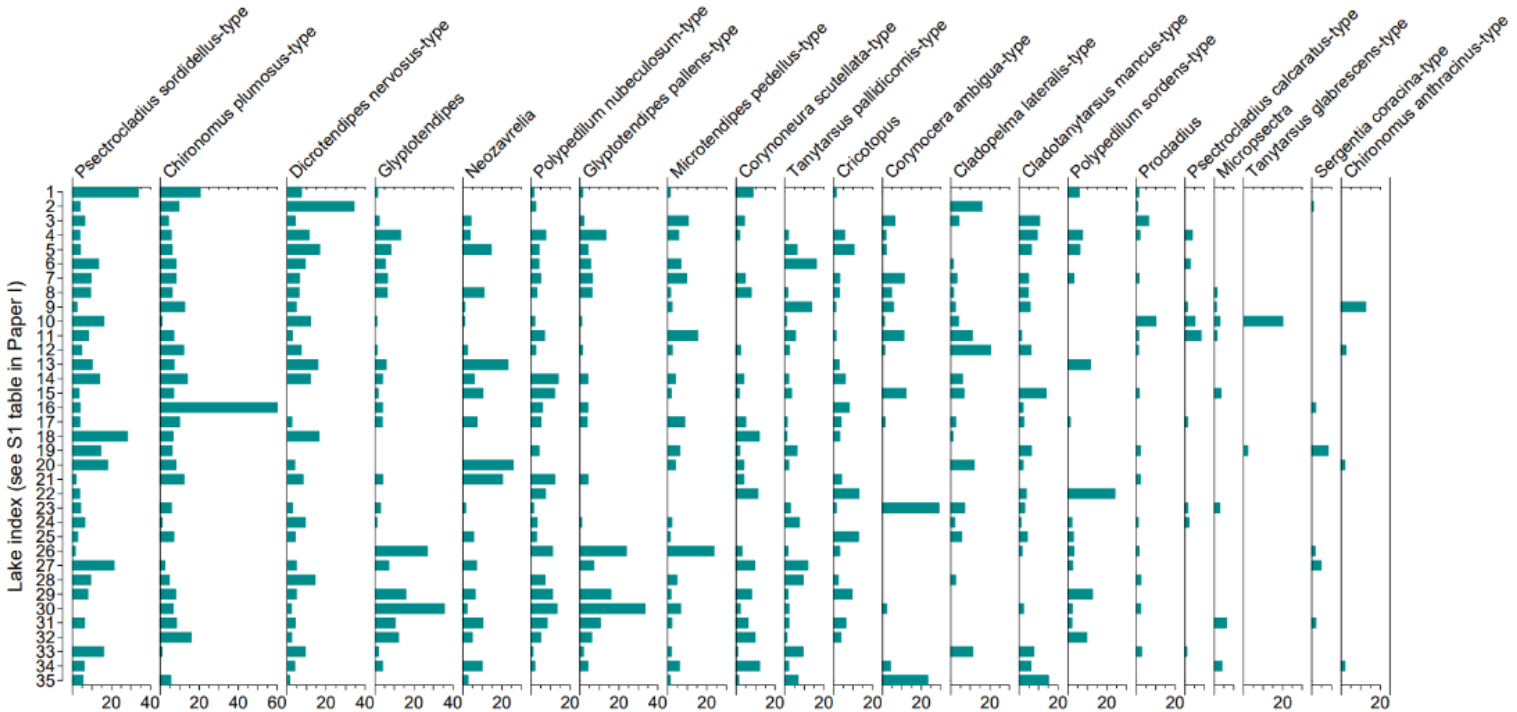

Figure 3 *Selected eastern Baltic (temperate climate zone) chironomid morphotypes from the lake surface sediment layer (0–2 cm) included in the FBP TS. Lake indices are ordered according to decreasing latitude. Morphotypes are organized according to the decreasing abundances in the eastern Baltic dataset.*

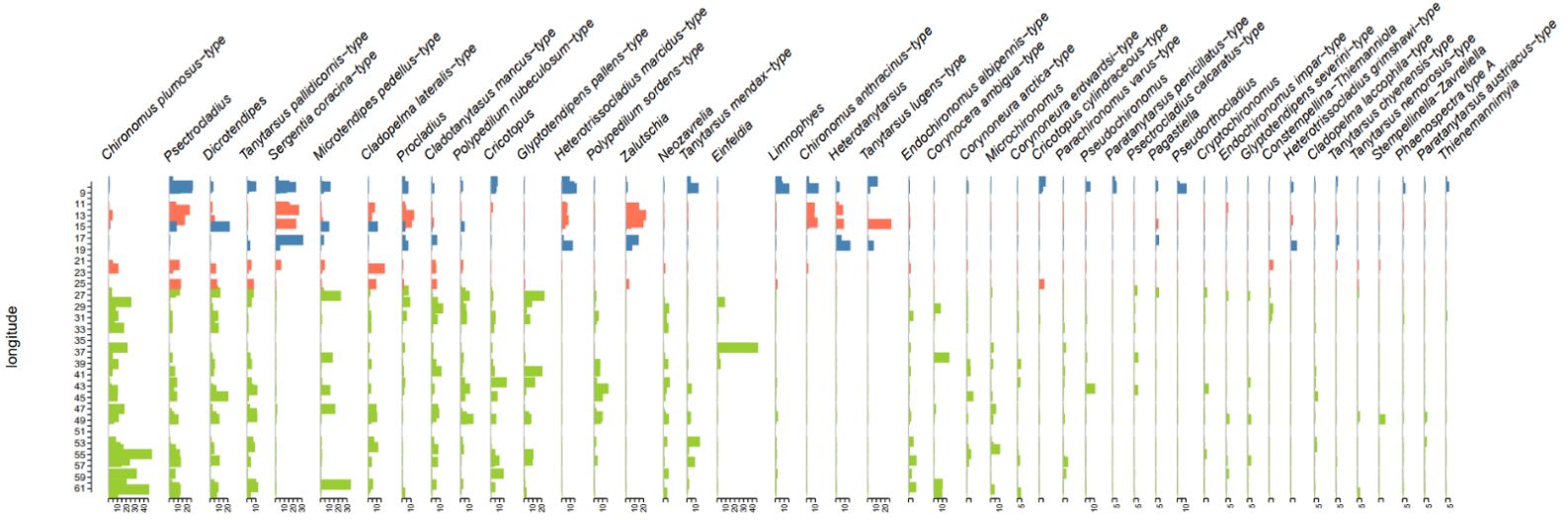

Figure 4 *Continentality Dataset chironomid morphotypes with abundances at least 2% in one sample (Paper II). Morphotypes are organized according to the longitudinal gradient. Continental sites have a KOI of –10 to 0, transitional sites range from 0 to 10, and oceanic sites from 10 to 20.*

3.1.2 Distribution of the TSs sites in respect to the climate and environmental variables

The variance gradient of DCA calculated for eastern Baltic chironomid assemblages equals 2.4 SD and 2.0 SD for Axis 1 and Axis 2, respectively. The DCA variance gradient for the FBP TS was 3.1 SD and 2.4 SD units for Axis 1 and 2, respectively (Figure 5A). The Continentality Dataset (Paper II) DCA variance gradient was 2.9 SD and 2 SD units for Axis 1 and 2, respectively (Figure 5B). Thus, while the distribution of the sites from FBP TS is relatively smooth, the gap between Russian-Latvian and Swedish-Norwegian parts is observed in the Continental Dataset.

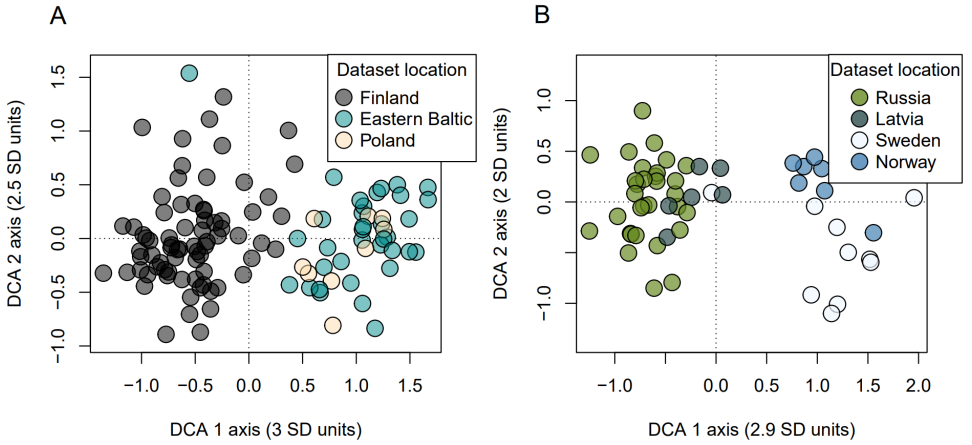

Figure 5 (A) *DCA ordination diagram for the chironomid assemblages from the FBP TS;* ***(B)*** *DCA ordination diagram for the chironomid assemblages from the Continentality Dataset.*

3.1.3 Influence of climate and environment factors on chironomid assemblages

RDA of the eastern Baltic dataset identified July air T, ATR and water phosphorus content as the only significant predictors of chironomid distribution (Table 2).

RDA and CCA of the FBP TS showed that all examined variables were significant. July air T explained 9.1% (CCA) / 14.4% (RDA) of variance, followed by ATR (7.3% / 10.9%), pH (7.2% / 11.5%), dissolved oxygen (4.5% / 7.5%), sampling depth (3.0% / 3.9%) and KOI (1.9% / 2.5%) (Table 3, Figure 8). July air T had the highest explanatory power based on the λ1:λ2 ratio (1.4 CCA / 1.3 RDA), indicating a strong relationship between July air T and chironomid assemblage data (Vilar et al., 2018). However, the horseshoe effect visible in the CCA plot (Figure 6) may have influenced the results.

In the Continentality Dataset KOI explained more chironomid assemblage variation (18.4%) than ATR (15%) (Table 2), both with λ1:λ2 >1. GDD5 and July air T each explained ~17% of the variation, outperforming April (4%) and October (14.2%) air T. However, the April air T was the only variable aligned with RDA Axis 2 (Figure 7). Ice-cover days had a significant impact, explaining 15.5% of the variation. Bedrock explained 16.8%, lake-water pH 12.3%, and lake depth 8.3% (Table 2, Figure 7).

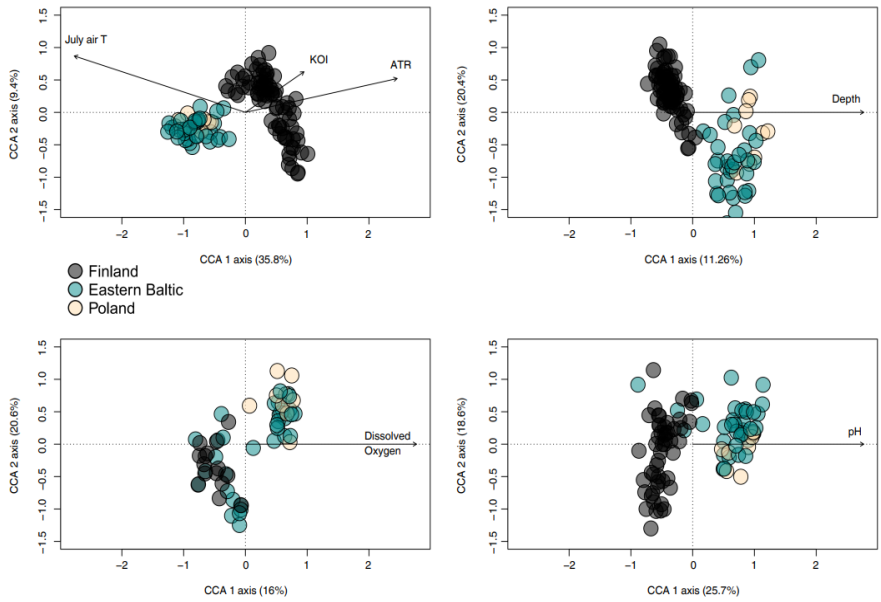

Figure 6 *CCA biplots for the lakes from the FBP TS with July air T, KOI, ATR, sampling depth, dissolved oxygen and pH as explanatory variables. The eigenvalues of the CCA1 and CCA2 axes are 0.3191 and 0.0569, respectively.*

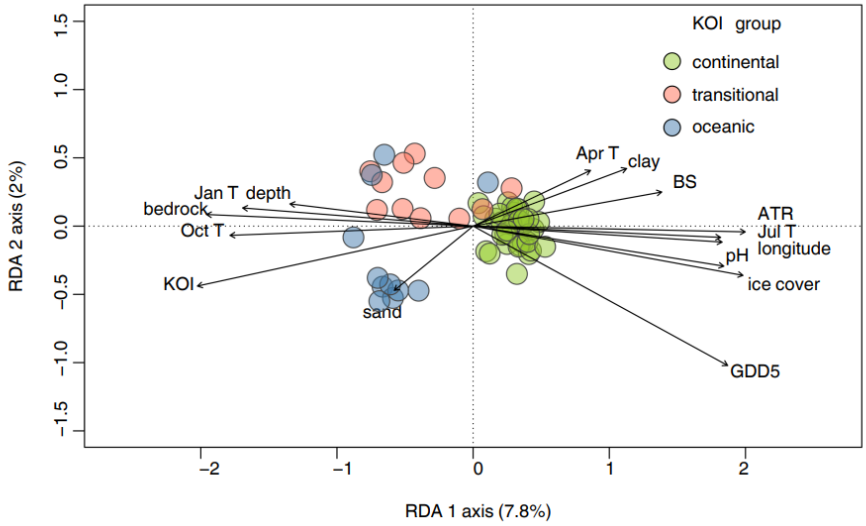

Figure 7 *RDA plot for the lakes from the Continentality Dataset with lake-water depth; longitude; lake water pH; bedrock type; soil base saturation (BS); soil clay content (clay); soil sand content (sand); July (Jul T), October (Oct T), and April (Apr T) mean air T (°C); lake-ice-cover (days); GDD5; KOI and ATR. Variables explain 44.6% of the variation in total with a p-value of 0.001. Continental sites have a KOI of –10 to 0, transitional sites range from 0 to 10, and oceanic sites from 10 to 20.*

Table 2 *The ordination tests output for the eastern Baltic dataset, FBP TS, and Continentality Dataset (Papers I–II). For eastern Baltic and Continentality datasets the percentage of variability explained is based on RDA. For FBP TS, the percentage of variability explained is presented as CCA/RDA results.*

Variable	Number of sites	% of variability explained	λ1:λ2	p-value
eastern Baltic dataset				
July air T	35	5.4	0.4	0.048
ATR	35	5	0.6	0.01
KOI	35	-	-	0.08
Water depth	35	-	-	0.1
pH	31	-	-	0.2
Dissolved oxygen	29	-	-	0.1
Total phosphorus	29	5.6	0.3	0.047
Finno-Baltic-Polish TS				
July air T	121	9.1/14.4	1.4/1.3	0.001/0.001
ATR	121	7.3/11	1.2/1.1	0.001/0.001
KOI	121	2/2.5	0.2/0.1	0.001/0.001
Water depth	121	3/4	0.3/0.23	0.001/0.001
pH	79	7.2/11.5	1/1	0.001/0.001
Dissolved oxygen	56	4.5/7.5	0.5/0.4	0.001/0.001
Continentality Dataset				
GDD5	51	17.2	1.5	0.001
October air T	51	14.2	1.2	0.001
April air T	51	4	0.2	0.045
July air T	51	17.4	1.3	0.001
Ice-cover	51	15.5	1.1	0.001
ATR	51	15	1.3	0.001
KOI	51	18.4	1.6	0.001
Bedrock	51	16.8	1.1	0.001
pH	51	12.3	1	0.001
Soil base saturation	51	8	0.5	0.002
Soil clay content	51	10	0.7	0.001
Soil sand content	51	4.7	0.2	0.013
Water depth	51	8.3	0.5	0.001
Longitude	51	13.1	0.8	0.001

3.1.4 Distribution of chironomids in respect to July air T

The ANOSIM test justified the significancy (p = 0.001) of division of FBP TS chironomid assemblages into 3 groups based on July air T – northern boreal (12.1–15.0 °C), southern boreal (15.0–17.0 °C), and temperate (17.0–19.2 °C) – with $R^2 = 0.54$.

GAM analysis across the entire FBP TS (Paper I) revealed that the taxa most strongly dependent on July air T were *Psectrocladius septentrionalis*-type (51.6% variance explained), *Psectrocladius calcaratus*-type (47.6%), *Micropsectra insignilobus*-type (43.7%), *Tanytarsus mendax*-type (39.4%), *Ablabesmyia* (35.6%), *Procladius* (33.7%), *Dicrotendipes pulsus*-type (32%), and *Chironomus plumosus*-type (28.3%). In contrast, *Psectrocladius sordidellus*-type, *Microtendipes pedellus*-type, and *Corynoneura lobata*-type showed no July air T dependence. *Psectrocladius septentrionalis*-type, *Tanytarsus lugens*-type, *Psectrocladius calcaratus*-type revealed July air T WA-calculated optimum in the northern boreal zone (Figure 8). 18 morphotypes within the group of the most abundant taxa, including *Ablabesmyia, Chironomus anthracinus*-type, and *Tanytarsus mendax*-type, were assigned to the southern boreal zone. 11 morphotypes, including *Chironomus plumosus*-type, *Dicrotendipes* and *Corynoneura scutellata*-type, revealed optimum in the temperate climate zone.

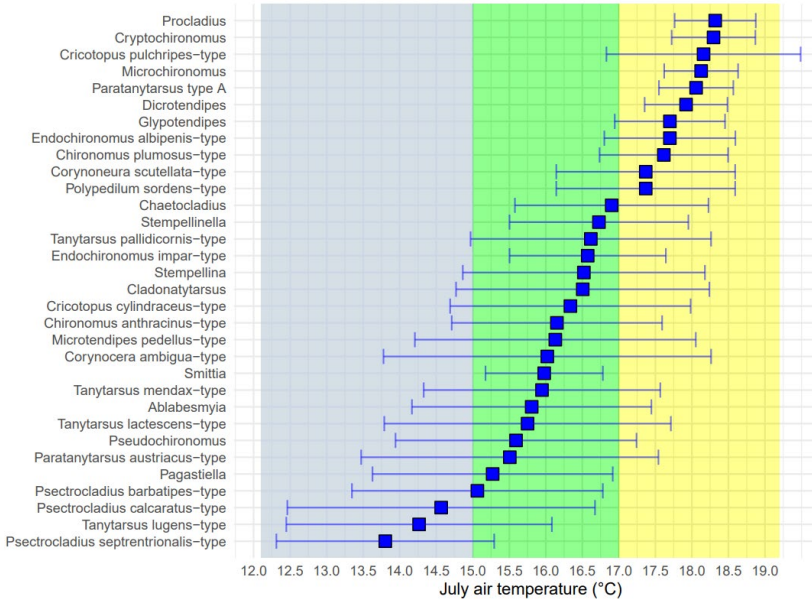

Figure 8 *WA based July air T optima and tolerances for the morphotypes in FBP TS with the abundances at least 5% in one sample. The background is coloured according to the July air T: blue represents northern boreal (12.1–15.0 °C), green represents southern boreal (15.0–17.0 °C), and yellow represents temperate (17.0–19.2 °C) climate.*

3.1.5 Distribution of chironomids in respect to continentality

ANOSIM test of FBP TS revealed that the division into two continentality groups – continental (ATR > 24 °C) and transitional (ATR < 24 °C) – is significant (p = 0.0001). An R-value of 0.4 indicated moderate separation between groups. While there is some overlap in taxonomic composition, the groups still show notable differences. 27 taxa were identified as continental climate-related ones (Figure 9), with *Protanypus*, *Heterotrissocladius marcidus*-type, and *Hydrobaenus* type explicated the smallest error in ATR optima of estimation. 17 morphotypes were identified as characteristic for the transitional part of the TS, where *Dicrotendipes notatus*-type, *Cryptochironomus* and *Ablabesmyia* revealed the smallest error in ATR optima of estimation.

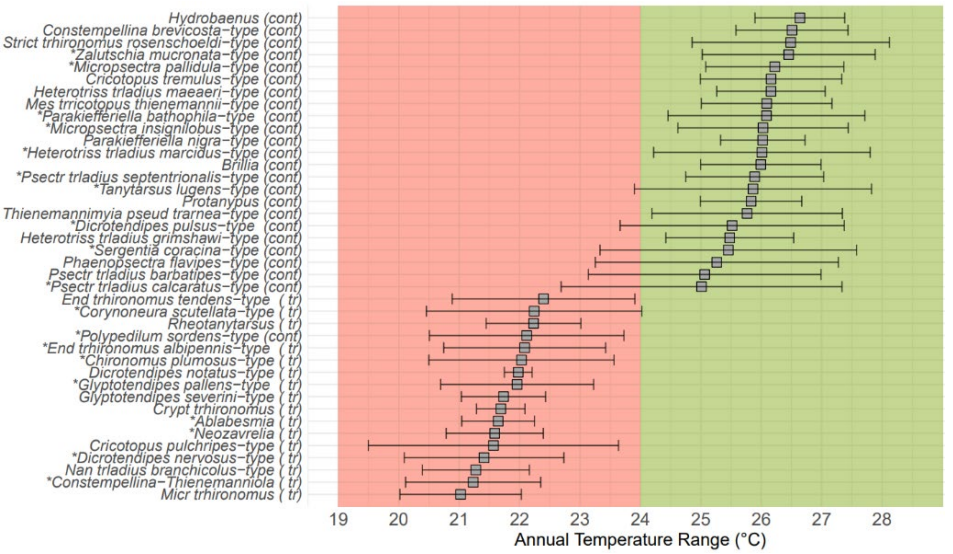

Figure 9 *WA based ATR optima and tolerances for morphotypes in FBP TS revealed as indicators by INDVAL. The continentality group affiliation identified by INDVAL is marked in brackets: tr – transitional, cont – continental; all taxa revealed statistical significance in the corresponding zone based on INDVAL. The star sign means revealed dependency in the July air T GAM models (Paper I). The background is coloured according to the ATR: continental (orange) for ATR < 24 °C, transitional (green) for ATR > 24 °C.*

In the case of the Continentality Dataset, ANOSIM revealed that the chironomid assemblages could be significantly divided by KOI (p = 0.007) into continental (–10–0), transitional (0–10), and oceanic (10–20) groups. R-value of 0.24 is indicative of some overlap in taxonomic composition between continental, transitional, and continental sites. Continental sites are indicated by the presence of *Glyptotendipes pallens*-type, *Neozavrelia*, *Polypedilum sordens*-type, and *Microchironomus* (Figure 10). The continental-transitional morphotype is *Chironomus plumosus*-type. Oceanic sites are characterised by *Paratanytarsus penicillatus*-type, *Pseudorthocladius*, *Thienemannimyia*, and *Limnophyes*. Oceanic-transitional morphotypes are *Procladius*, *Heterotrissocladius marcidus*-type, *Sergentia coracina*-type, *Zalutschia*, *Chironomus anthracinus*-type, *Heterotanytarsus*, and *Tanytarsus chinyensis*-type. One morphotype (*Cricotopus*) is assigned to the continental-oceanic group. Weighted-average regression revealed that the smallest tolerances are shown by *Microchironomus* and *Glyptotendipes pallens*-type, both from the continental part of the dataset (Figure 10).

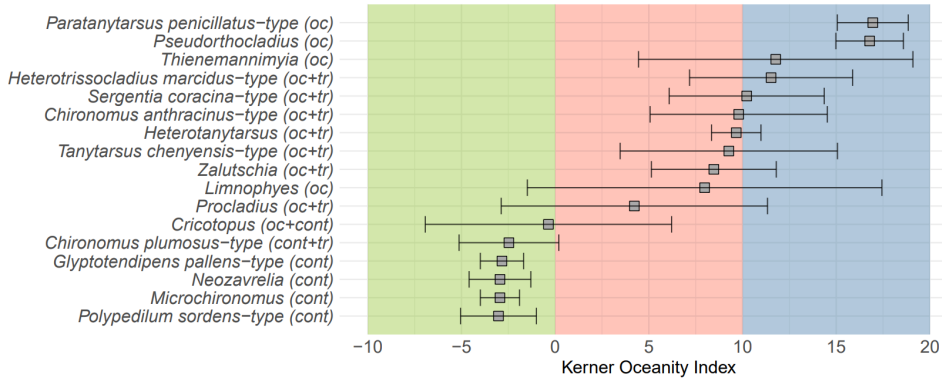

Figure 10 *WA based KOI optima and tolerances for morphotypes revealed as indicators by INDVAL. The continentality group affiliation identified by INDVAL is marked in brackets: oc – oceanic, tr – transitional, cont – continental; all taxa revealed statistical significance in the corresponding zone based on INDVAL. The background is coloured according to the KOI: continental (green) for KOI < 0, transitional (coral) for KOI 0–10, oceanic (blue) for KOI > 10.*

3.2 Chironomid-based inference models

This section includes results of FBP TS-based (1) July air T (Paper I) and (2) ATR (Manuscript) WA-PLS models building process, as well as the KOI WA-PLS model based on the Continentality Dataset (Paper II).

3.2.1 Inference model for July temperature reconstruction

The FBP TS-based two-component WA-PLS July air T inference model revealed the $RMSEP_{boot}$ of 0.7 and the R^2_{boot} of 0.9, suggesting reliable performance compared to Swiss-Norwegian TS (Table 3; Heiri et al., 2011). The scatterplot of cross-validated predicted vs. observed July air T (Figure 10) aligns closely with a 1:1 relationship. However, July air T below 13 °C tends to be overestimated, suggesting a slight positive bias at the colder end of the temperature gradient.

Table 3 *Error statistics of WA-PLS models based on the FBP and Swiss-Norwegian TSs and Continentality Dataset from which taxa with max abundance under 2% were excluded. Values are based on bootstrapping with 9999 cycles.*

Training set	Climate variable	$RMSE_{boot}$ (°C)	R^2_{boot}	Average $Bias_{boot}$ (°C)	Maximum $Bias_{boot}$ (°C)
Swiss-Norwegian (Heiri et al., 2011)	July air T	1.5	0.9	-0.02	1.5
Finno-Baltic-Polish (Paper I)	July air T	0.7	0.9	0.01	0.4
Finno-Baltic-Polish (Manuscript)	ATR	1.6	0.8	0.01	2.2
Continentality Dataset (Paper II)	KOI	5.1	0.7	-0.1	14.6

3.2.2 Inference models for continentality reconstruction

The KOI-based two-component WA-PLS inference model for the Continentality Dataset resulted in an $RMSEP_{boot}$ of 5.1 and an R^2_{boot} of 0.72 (Table 3). The ATR-based two-component WA-PLS inference model for the FBP TS revealed $RMSEP_{boot}$ of 1.6 and R^2_{boot} of 0.8 (Table 3). The scatterplots of cross-validated predicted vs. observed values followed the 1:1 relationship for both models (Figure 11B, C). Models revealed the increased error trend at the ends of the gradient. Thus, the FBP TS can be suggested to underestimate the high continental climates and overestimate the climates closer to the oceanic ones.

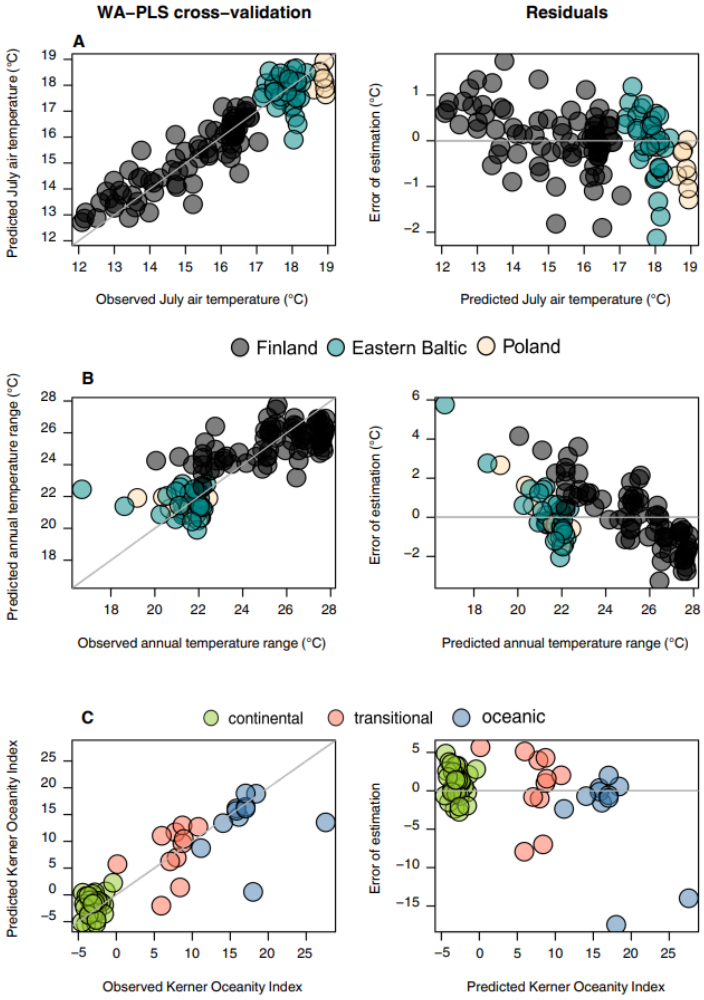

Figure 11 *Diagnostic plots of cross-validated estimates and prediction residuals compared with observed values of* ***(A)*** *July air T-based and* ***(B)*** *ATR-based two-component WA-PLS models for the FBP TS, and* ***(C)*** *KOI-based two-component WA-PLS model for the Continentality Dataset.*

3.3 Palaeoclimate reconstructions

This section includes the results of the palaeoclimate and environment reconstructions for Lakes Nakri and Petrovskoe, presented in Paper III and Manuscript.

3.3.1 Lake Nakri fossil chironomid assemblages

On average, 44 chironomid head capsules were counted per sample, with the count range 30–127, and 155 chironomid taxa identified in total (Figure 12). The late glacial period was characterized by the dominance of widely distributed *Microtendipes pedellus*-type and *Tanytarsus mendax*-type, both classified as cool-related taxa. *Chironomus anthracinus*-type, which also exhibited a broad distribution, was more closely associated with temperate-related taxa. Cold-related taxa, including *Tanytarsus lugens*-type, *Psectrocladius septentrionalis*-type, *Micropsectra insignilobus*-type, and *Heterotrissocladius grimshawi*-type, dominated between 14.5–13.5 ka cal BP. Additionally, taxa not directly linked to climate, such as *Procladius*, *Psectrocladius sordidellus*-type, and *Cricotopus intersectus*-type, were present during this period.

During the Early Holocene, temperate-related taxa, including *Dicrotendipes nervosus*-type, *Chironomus plumosus*-type, *Cladopelma lateralis*-type, and *Corynoneura scutellata*-type, were recorded, alongside generalist taxa like *Psectrocladius sordidellus*-type and *Cricotopus intersectus*-type. Cold-related *Tanytarsus penicillatus*-type and *Tanytarsus lugens*-type appeared only at the onset of this period. Temperate-related taxa such as *Glyptotendipes pallens*-type, *Neozavrelia*, and *Endochironomus albipennis*-type became dominant from 10 ka cal BP onward. Not climate dependent *Micropsectra contracta*-type, *Procladius*, and *Limnophyes-Paralymnophyes* first appeared at approximately 10.5 ka, 9.5 ka, and 8.5 ka cal BP, respectively.

The Middle Holocene assemblages largely resembled the Early Holocene ones. Still, they exhibited increased abundances of temperate-related *Cladotanytarsus mancus*-type and *Polypedilum sordens*-type, as well as climate-independent *Lauterborniella* and *Nanocladius rectinervis*-type. Cold-related taxa, including *Sergentia coracina*-type and *Micropsectra insignilobus*-type, reappeared during this period.

Peaks in temperate-related Chironomus plumosus-type, Neozavrelia, Cladopelma lateralis-type, Cladotanytarsus mancus-type, and Tanytarsus pallidicornis-type marked the Late Holocene. *Polypedilum nubeculosum*-type, a taxon associated with moderate conditions, showed overwhelming dominance around 0.5 ka cal BP. Cold-related taxa were nearly absent in this period, while climate-independent *Psectrocladius sordidellus*-type and *Cricotopus intersectus*-type increased in abundance.

3.3.2 Lake Petrovskoe fossil chironomid assemblages

Early Holocene was characterized by dominance of cold-related *Sergentia coracina*-type, *Stempellinella*, *Tanytarsus mendax*-type, *Cladotanytarsus*, and *Tanytarsus pallidicornis*-type. Warm-related taxa (*Dicrotendipes nervosus*-type, *Corynoneura scutellata*-type, *Chironomus plumosus*-type) increased toward the end of this period. Acidification indicators (*Cladotanytarsus*, *Pagastiella*) and taxa linked to submerged vegetation (*Lauterborniella*, *Gymnimetriocnemus-Bryophaenocladius*, *Polypedilum sordens*-type) were presented (Figure 13).

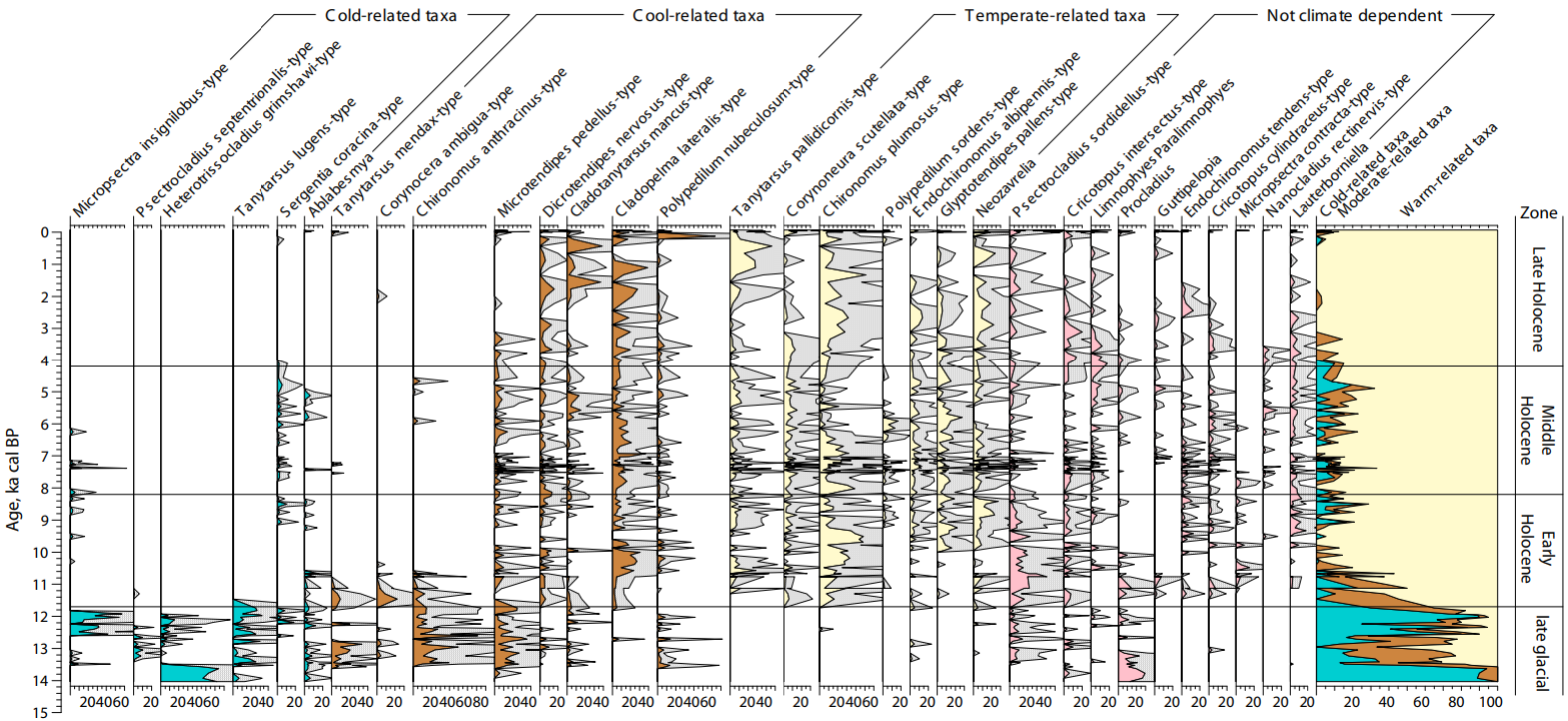

Figure 12 *Chironomid morphotypes diagram of the selected taxa from Lake Nakri sediments (Manuscript).*

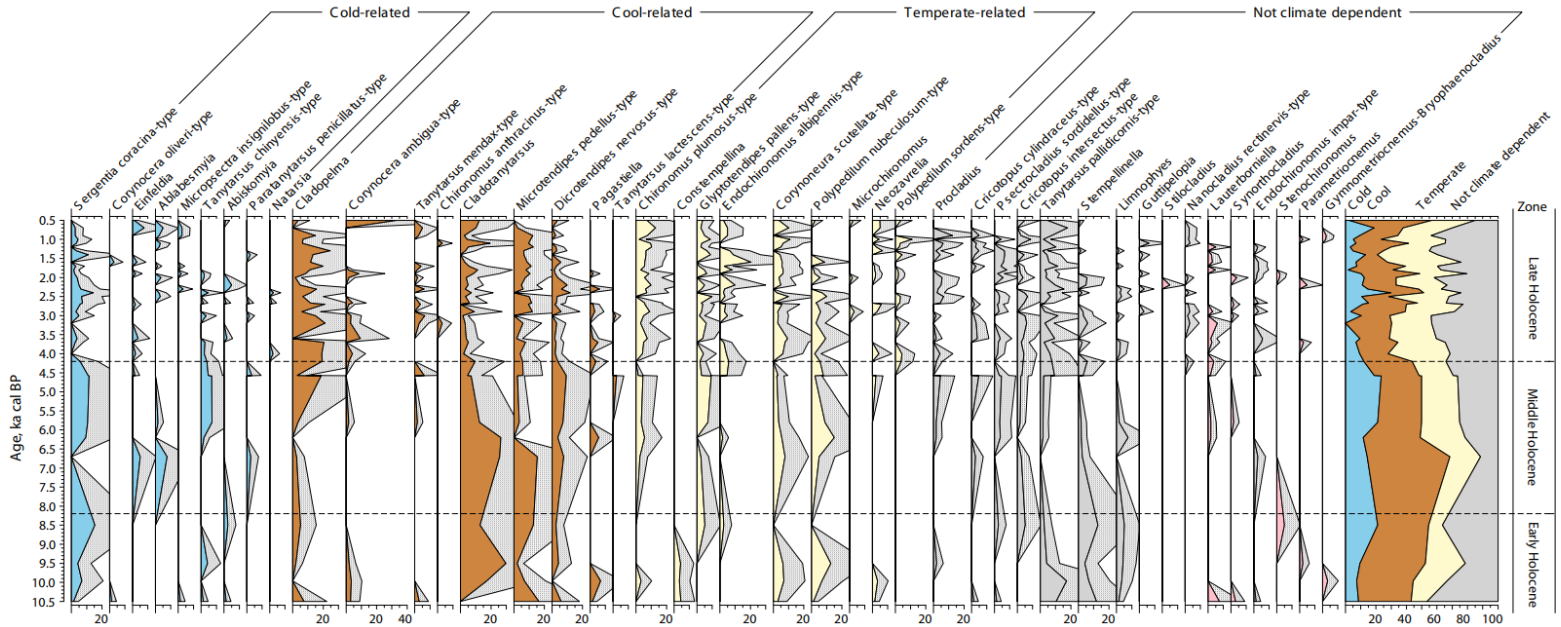

Figure 13 *Chironomid morphotypes diagram of the selected taxa from Lake Petrovskoe (Paper III). Chironomid morphotypes with abundances in the dataset of at least 2% in one sample were included. The pink colour indicated erosion and submerged wood indicative morphotypes.*

The Middle Holocene started with increased abundance of cold-related taxa *(Sergentia coracina*-type, *Stempellinella*). The presence of *Stenochironomus* indicated submerged vegetation or dead wood habitats. Cold-adapted taxa (*Sergentia coracina-Tanytarsus mendax*-type, *Tanytarsus chinensis*-type, *Stempellinella*) were gradually replaced by warm-related ones as *Cladopelma*, *Dicrotendipes nervosus*-type, *Nanocladius rectinervis*-type, and *Endochironomus albipennis*-type. Indicators of alkalization (*Guttipelopia*, *Endochironomus impar*-type) and taxa associated with submerged vegetation (*Cricotopus cylindraceus*-type, *Nanocladius rectinervis*-type, *Paratanytarsus penicillatus*-type) were also present, reflecting shifts in lake productivity and habitat conditions.

Late Holocene was characterized by a stable coexistence of temperate and cool-related taxa without clear dominance. Submerged wood indicators (*Synorthocladius, Gymnimetriocnemus-Bryophaenocladius*) and macrophyte-associated taxa increased. Throughout 0.8-0.5 ka cal BP, acidification (*Psectrocladius sordidellus*-type, *Cladotanytarsus*) and eutrophication indicators (*Micropsectra insignilobus*-type, *Neozavrelia*) increased. Warm-adapted taxa, including *Chironomus plumosus*-type, *Corynoneura scutellata*-type, *Einfeldia*, and *Microchironomus*, dominated at the very end of the sediment core.

3.3.3 Models performance

The chironomid-based July air T reconstruction of Lake Nakri exhibited comparable trends and performance values using FBP and Swiss-Norwegian TSs (Figure 14, Table 4). The FBP TS yielded the lowest reconstruction error (RMSEPboot = 0.7 °C). The chironomid-based ATR reconstruction using this TS resulted in an RMSEPboot of 1.4 °C and an R^2boot value of 0.8. The pollen-based July air T reconstruction for the Lake Nakri sequence demonstrated overall performance values similar to those of the chironomid-based reconstruction with the FBP TS. The only notable difference was a significantly larger estimate of maximum bias in the pollen-based reconstruction.

Table 4 *Error statistics of WA-PLS chironomid-based and pollen-based TSs cross-validation and reconstructions outcome.*

Training set	Climate variable	RMSEP $_{boot}$ (°C)	R^2_{boot}	Average $Bias_{boot}$ (°C)	Maximum $Bias_{boot}$ (°C)
Nakri (Manuscript)					
Finno-Baltic-Polish	July air T	0.7	0.9	0.02	0.7
Finno-Baltic-Polish	ATR	1.4	0.8	0.04	3.1
Swiss-Norwegian	July air T	1.5	0.9	–0.03	1
Pollen-based	July air T	0.7	0.8	–0.03	2.9
Petrovskoe					
Finno-Baltic-Polish (Paper III)	July air T	0.8	0.9	0.01	0.5
Finno-Baltic-Polish	ATR	1.6	0.8	0.02	2.2

The chironomid-based July air T reconstruction of Lake Petrovskoe using FBP TS exhibited similar performance values and climate trends as Lake Nakri (Table 4). The ATR reconstruction of Lake Petrovskoe was lower than the modern ATR value of the site (Figure 14B; dotted line). Thus, the mean reconstructed Holocene ATR value of 22 °C is the same for both produced reconstructions.

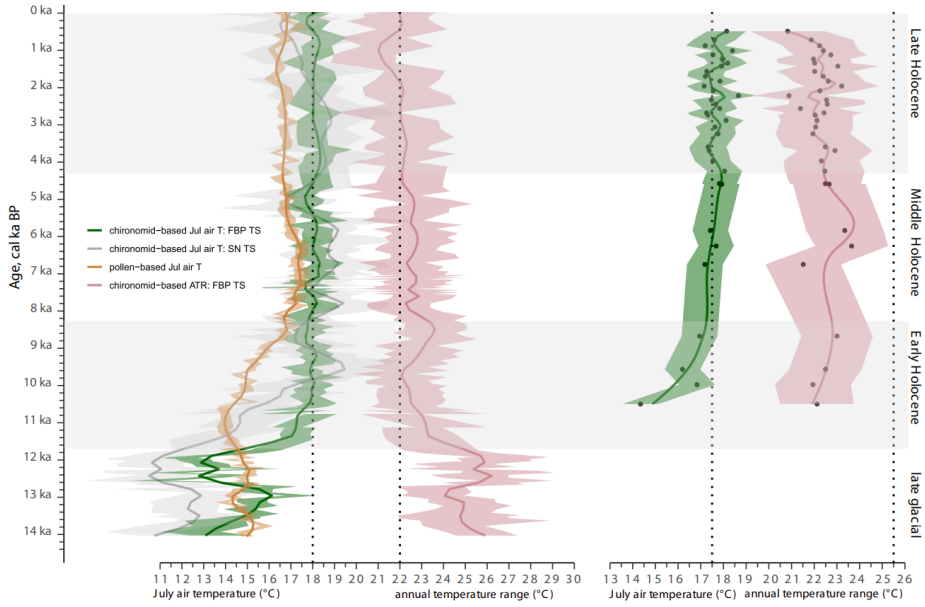

Figure 14 *WA-PLS July air T (°C) and annual temperature range (°C) reconstructions from* ***(A)*** *Lakes Nakri and* ***(B)*** *Petrovskoe. Dotted line indicates modern values. Orange line indicates pollen-based July air T reconstruction; grey line indicates chironomid-inferred July air T reconstruction based on Swiss-Norwegian training set (SN TS); green line indicates July air T chironomid-inferred reconstruction based on FBP TS; pink line indicates ATR range reconstruction based on FBP TS.*

4 Discussion

This part summarizes the results of Papers I-III and Manuscript and puts it in a broader context of already published literature.

Climate is widely recognized as one of the primary drivers shaping the regional distribution of chironomid assemblages (Luoto, 2009; Heiri et al., 2011; Kotrys et al., 2020). It influences chironomid life cycles both directly – by regulating reproductive processes – and indirectly by altering the characteristics of the warm, productive season and affecting key aspects of lake water chemistry, such as oxygen and phosphorus levels and trophic status (Brodersen & Anderson, 2002; Brodersen & Quinlan, 2006; Eggermont & Heiri, 2012). As shown in Papers I–II, July air T is one of the most important climatic variables that shape chironomid assemblages. However, it was revealed that chironomids are also significantly dependent on GDD5, October and April air T, and ice-cover duration. All these climate variables are connected to the term continentality and support the statistical outcomes that KOI (Paper II) and ATR (Manuscript) significantly influence chironomid assemblages.

However, it should be kept in mind that under stable climatic conditions, macroinvertebrate communities, including chironomids, tend to be more strongly governed by local environmental factors such as organic carbon availability and trophic state (Brodersen & Anderson, 2002; Velle et al., 2005; Luoto & Ojala, 2018).

4.1 Impact of environmental variables on chironomid assemblages

4.1.1 Water depth

In the FBP TS, the explanatory power of lake-water depth is 4%, whereas in the Continentality Dataset, it is notably higher – 8.3%. In both cases, sites sampling strategy was designed to minimize variations in water depth to enhance the climate signal. However, in the Continentality Dataset, the limited availability of lakes in the forest-steppe region near the Urals made it impossible to completely exclude deeper lakes from sampling.

The stronger explanatory power of lake-water depth in the Continentality Dataset compared to previous studies (Luoto, 2009; Kotrys et al., 2020) is likely due to the broad depth range represented in the dataset (1–45 m). However, a study of the Fennoscandian chironomid modern assemblages demonstrated that water depth can account for up to 10.2% of variation, despite the narrower depth range (0.85–27.0 m) (Korhola et al., 2000). The pronounced influence of water depth in the local dataset of northern Finland can be attributed to the rapid cooling and freezing of the epilimnion in autumn, which results in higher winter water temperatures in the north compared to the south (Kuusisto, 1981). Furthermore, northern lakes tend to warm more gradually during summer and often maintain an extended hypolimnetic storage of cold water (Walker & MacDonald, 1995). In contrast, within the Continentality Dataset and FBP TS, the processes of lake warming and freezing are more closely linked to the geographical position of the lake, which determines the duration of the cold season rather than to the water depth itself. This suggests that while water depth can significantly influence chironomid assemblages in certain climatic regions, its role may be modulated by broader geographical and climatic factors.

4.1.2 pH

In the eastern Baltic region, where alkaline lake waters are predominant, no significant influence of pH on chironomid assemblages was detected. However, the influence of pH recorded in the FBP TS and the Continentality Dataset (11.5% and 12.3%, respectively; RDA) is higher than in previous studies, where it generally explained up to 4% of the variation (Self et al., 2011; Kotrys et al., 2020). The most probable reason for this difference is a broad range of bedrock types brought by the greater geographical scale of these datasets. Thus, while Fennoscandian bedrock is mainly composed of acidic granites, the alkaline limestones prevail in the eastern Baltic region and the European part of Russia, and neutral to alkaline sandstones near the Ural Mountains.

4.1.3 Total phosphorus and dissolved oxygen

Total phosphorus concentration was the only significant environmental variable identified for lakes in the eastern Baltic region. This finding has important implications for contemporary lake ecology, highlighting that the effects of total phosphorus variations on the lake invertebrate communities are detectable even within a small subset of relatively undisturbed natural lakes. It was demonstrated that climate warming increases lake total phosphorus concentrations (Jeppesen et al., 2009; Lucas et al., 2023). This linkage suggests a heightened sensitivity of lake ecosystems, and invertebrate bottom communities in particular, to ongoing climate-driven phosphorus dynamics.

In the FBP TS, oxygen accounted for 7.5% of the variation in RDA analysis, which is higher than the 4.6% explained in the Finnish dataset alone (Luoto, 2009). This discrepancy can primarily be attributed to differences in the number and variety of study sites across the TSs. Verbruggen et al. (2011) reported that oxygen can explain up to 11% of the variation in a dataset focusing on deep, stratified lakes, concluding that deep-water oxygenation is a key factor influencing chironomid assemblages in such systems. However, the FBP TS includes a considerable proportion of shallow lakes, where hypolimnetic oxygen conditions have less influence on chironomid distributions.

4.1.4 Soil properties and bedrock

Soil properties are rarely discussed in the context of chironomid research. However, the findings of Paper II suggest their significant ecological importance. In the Continentality Dataset, soil base saturation, as well as sand and clay content, were found to significantly influence chironomid assemblages.

Barbiero et al. (2008) highlighted that variations in soil properties can lead to the formation of lakes with different chemical characteristics, even under identical climatic conditions. In general, the presence of a thick soil layer has a strong impact on water chemistry (Kamenik et al., 2001; Kopáček et al., 2004).

The influence of soils in the lake catchment on water chemistry is primarily attributed to alterations in the quantity and quality of terrestrial inputs (Bertolet et al., 2018), particularly the organic carbon content in lake water (Nelson et al., 1990; Kortelainen, 1993; Brodersen & Anderson, 2002; Larsen et al., 2017). Also, soils may influence water chemistry through erosion processes. It has been shown that soil erosion caused by deforestation can dramatically reduce chironomid biodiversity (Zhang, Tang, et al., 2013). In addition, soil parameters (base saturation, sand and clay content) influence a lake's ability to buffer acid deposition, thereby affecting pH values (Kähkönen, 1996; Stumm et al., 1996; Houle et al., 2006; Larsen et al., 2017). In turn, the structure and total biomass of chironomid communities are closely linked to the organic content in both lake

water and sediments (Nyman et al., 2005; Jyväsjärvi et al., 2013; Luoto et al., 2016) and pH, which is a well-known factor determining the distribution of chironomids (Orendt, 1999; Luoto, 2009).

Bedrock composition, though also seldom used in chironomid-focused studies, can significantly influence a lake's acid-neutralizing capacity (Brousseau et al., 1985; Kopáček et al., 2004). Additionally, bedrock influences pelagic phosphorus availability, carbon cycling, and metal concentrations (Hamilton et al., 2001) – all of which are factors to which chironomids are highly sensitive, as discussed in the Chironomidae Ecology chapter.

Therefore, soil properties and bedrock composition can indirectly shape chironomid community structure by modulating water chemistry. Incorporating these environmental variables may be especially valuable in ecological studies where extensive limnological chemistry data are unavailable. In the case of the Continentality Dataset (Paper II), the relatively lower importance of the soil and bedrock data compared to July air T, ATR, or KOI supports the hypothesis that chironomid distribution in this regional context is primarily driven by climatic factors.

4.2 Chironomid assemblages distribution in respect to climate

4.2.1 July air T

All tested modern chironomid datasets – the Continentality Dataset (Paper II), the eastern Baltic dataset and the FBP TS (Paper I) – demonstrated a clear dependence on July air T. Notably, even in the datasets with short temperature gradient, such as those in the eastern Baltic and Continentality Datasets, the distribution of chironomid assemblages was significantly explained by the July air T gradient. In the FBP TS, July air T emerged as the primary explanatory variable, with explanatory power comparable to previously published chironomid-based calibration sets (Larocque et al., 2001; Heiri et al., 2011; Kotrys et al., 2020).

The taxon-specific July air T optima estimated for the FBP TS (Figure 7) were generally consistent with those derived from the Swiss-Norwegian TS (Paper I). However, some taxa exhibited warmer optima than Swiss-Norwegian ones. Discrepancies in temperature optima estimation have also been observed in comparisons among Icelandic, Norwegian, Polish, and Finnish TSs (Holmes et al., 2016; Luoto et al., 2019). Potential explanations for these differences include: (1) the inability to distinguish certain taxa based solely on larval head capsule morphology, which may lead to grouping species with varying ecological preferences under a single morphotype (Brooks et al., 2007); (2) biogeographical effects that influence chironomid communities by limiting species dispersal, reducing competition, or promoting ecological isolation (Holmes et al., 2011); and (3) bottleneck effects resulting from specific environmental conditions or disturbance events (van Kleef et al., 2015).

Due to such complexities, the application of TSs beyond their regional boundaries is generally discouraged (Juggins, 2013; Medeiros et al., 2022). Nevertheless, extra-regional applications are common in practice. For instance, the Swiss-Norwegian inference model has been applied to sites in Estonia (Heiri et al., 2014), Lithuania (Šeirienė et al., 2021), Slovakia (Hájková et al., 2016), and Germany (Bolland et al., 2022). Similarly, the Swedish chironomid TS (Larocque et al., 2001) has been used to reconstruct past temperatures in Russian lakes (Andreev et al., 2005; E. A. Ilyashuk et al., 2005), while both North American and Swedish TSs have informed reconstructions from sites in Italy (Larocque & Finsinger,

2008) and Switzerland (Larocque-Tobler, 2010). Mostly, these reconstructions correspond well with other palaeoclimatic proxy data, such as ice cores, pollen, and macrofossils.

To improve calibration set performance and extend their geographical applicability, merging local and regional TSs is a commonly used approach (Holmes et al., 2011; T. Luoto et al., 2019; Kotrys et al., 2020). Accordingly, the development of the merged FBP TS in Paper I represents a critical step toward producing robust chironomid-based temperature reconstructions for the eastern Baltic region.

The performance statistics of the FBP inference model compare well with existing models (Larocque et al., 2001; Luoto, 2009; Heiri et al., 2011; Kotrys et al., 2020). However, the absence of representation at the colder end of the July air T gradient (< 12 °C) limits the model's usage for reconstructing the colder phases of the late glacial period. This shortcoming could be addressed by incorporating colder calibration sites, such as those from northern Norway. Nonetheless, a key strength of the FBP TS lies in its improved coverage of the warm end of the July air T gradient, thereby overcoming a known limitation of the Finnish TS and enhancing the accuracy of reconstructions for warm intervals of the Middle and Late Holocene, as well as for estimating past rates of July air T change for comparison with modern trends.

4.2.2 Continentality and growing season duration

The chironomid assemblages from the Continentality Dataset revealed significant dependency on GDD5, October and April air T, and ice-cover duration. Together with the strong performance of July air T, it supports the interpretation of the incredible importance of growing season warmth and duration for chironomid assemblages composition. Previous studies showed that GDD5 significantly influences chironomid assemblages (Lotter et al., 1997; Dieffenbacher-Krall et al., 2007). Also, it was shown that interannual variations in spring warming (Lindegaard & Brodersen, 2000) together with GDDs, can significantly affect swarming behaviour and the overall chironomid biomass emerging from lakes (Hodkinson et al., 1996). Likewise, the relatively high explanatory power of October air T implies that autumn processes such as water column mixing may also shape chironomid communities.

In Paper II, positive correlation between GDD5 and ice-cover duration was revealed. This pattern can be explained by the geographic alignment of the sites along a narrow latitudinal band following the ATR gradient. In this configuration, warmer summers are typically associated with colder winters, resulting in extended periods of ice-cover. Ice-cover has been shown to reduce dissolved oxygen concentrations in lakes, particularly depending on the lake's thermal regime (Golosov et al., 2007; Zdorovennova et al., 2021) and lake productivity – in productive lakes, chironomids tend to experience more severe hypoxia during colder periods with prolonged ice-cover (Lotter et al., 2002; Quinlan & Smol, 2002; Heiri & Lotter, 2003; Brodersen & Quinlan, 2006). Thus, chironomid assemblages revealed the response to ice-cover duration variations in previous studies (Quinlan et al., 2005; Ilyashuk et al., 2015). In the study of (Granados & Toro, 2000) the higher relative abundances of *Chironomus* were observed during colder years, as extended ice-cover led to increased hypoxic stress that favoured *Chironomus* over other chironomid taxa. Thus, the effect of continentality on chironomid assemblages can be indirect through other climate factors, which affect the limnological characteristics of the waterbody.

The main driver of chironomid communities change in the longitudinally distributed Continentality Dataset was KOI, which was calculated based on ATR, October and April

air T. Presence of the October and April air T in the formula highlights the importance of the start and end of the growing season. The WA-PLS model performance was relatively good, compared to the total KOI range in the Continentality Dataset (Paper II). However, the WA-PLS plot (Figure 11) reveals the gap between continental and transitional-oceanic sites, indicating the need to equalize the proportion of each group. Also, the number of sites in the Continentality Dataset (56) is comparably small to the vast geographic area it spread across (Figure 2). Thus, to use the Continentality Dataset for creating inference model for KOI reconstructions, its robustness needs to be increased by densifying the dataset.

The FBP TS, spread across wide latitudinal space (Figure 2), also revealed a considerable continentality gradient. However, the KOI gradient was much smaller than the ATR one. Thus, this dataset's continentality changes reflect more latitudinal winter and summer temperature changes than the start and end of the growing season. The number of taxa that were identified by INDVAL as characteristic for different continentality groups in FBP TS is much higher than in the Continentality Dataset (Figure 9, 10). In the Continentality Dataset, *Glyptotendipes pallens*-type, *Neozavrelia*, and *Microchironomus* are placed in the continental group, while in the FBP TS, they appear in the transitional group. This can be explained by the difference in datasets design in terms of geographical span and usage of different continentality indexes. Thus, taxa identified based on ATR in FBP TS are still very dependable on the July air T, while the ones based on KOI in the Continentality Dataset are also influenced by the start and end of the growing season. However, 23 taxa out of 42 ones identified as characteristic for ATR groups in FBP TS, were not dependent on July air T (GAM-based, Paper I). The model performance of ATR in FBP TS is close to that of July air T inference model. Thus, in the absence of the specifically designed continentality-related TS, FBP TS can be used to produce test reconstructions of ATR.

4.3 Validation of Lakes Nakri and Petrovskoe reconstructions

All conducted chironomid-based July air T reconstructions using WA-PLS and the FBP and Swiss–Norwegian TSs showed similar performance (Table 2) and broadly reflected the same climate patterns, including alignment with the GRIP (Rasmussen et al., 2023) or GISP2 (Kobashi et al., 2011) ice core records.

Cladocerans and chironomids stored in Lake Nakri sediments revealed minor environmental changes, which are not expected to shift the reconstructed July air T and ATR values (Manuscript). The Lake Petrovskoe FBP TS-based reconstruction of July air T can be disturbed by the natural and anthropogenic causes, which were indicated by the increased proportions of submerged wood and vegetation and soil erosion chironomid markers (*Gymnometriocnemus*, *Parametriocnemus*, *Synorthocladius*, *Stenochironomus*, *Stylocladius*) in Late and Early Holocene. Pollen analysis of Lake Petrovskoe indicated the enhance of anthropogenic activities, since 4.2 ka cal BP (Paper III). Also, the sample density between 4 and 10 ka cal BP in Lake Petrovskoe is low, which limits the interpretation of specific climate events of this part of the core and allows only for the identification of general trends.

The Swiss-Norwegian TS-based Lake Nakri reconstruction showed lower temperatures and greater variability during the late glacial and Early Holocene than FBP TS-based one. Such differences are well documented (Engels et al., 2014; Luoto et al., 2019) and are mainly due to regional variation in chironomid temperature optima and identification resolution differences. The Swiss-Norwegian TS includes a high number of cold climate

related analogues and some morphotypes that are grouped to genera level (e.g., *Dicrotendipes*, *Endochironomus*, *Cladopelma*), while the FBP set separates them into sub-genera groups. Though finer resolution increases misidentification risk, it can improve model performance if consistently applied (Heiri & Lotter, 2010). However, as both modern and fossil samples were identified using consistent keys and expert comparison, the risks were minimized. Therefore, prioritizing the FBP TS-based model for the Baltic lowlands due to its regional relevance is recommended.

Pollen-based reconstruction of Lake Nakri showed similar statistical performance as chironomid-based but differed in late glacial and early Holocene, showing diverging trends and timing – indicating warmer late glacial and delayed Early Holocene warming. This likely reflects delayed terrestrial vegetation migration to formerly glaciated areas of northern Europe (Väliranta et al., 2015; Rao et al., 2022; Zani et al., 2023) and the lack of modern analogues for late glacial landcover in the present-day ecosystems (Magny et al., 2000).

ATR reconstruction of Lakes Nakri and Petrovskoe using the FBP set yielded $RMSEP_{boot}$ of 1.4 °C and 1.6 °C, respectively, which is a reasonable performance compared to the given dataset's range (18.6–27.7 °C). The reconstructed values in the case of both lakes are similar, even though the modern ATR value of Lake Petrovskoe is higher (more continental). Such discrepancy can be explained by the underrepresentation of the continental sites in the FBP TS and underestimation of continental sites by the WA-PLS model (Figure 11B). Due to all the uncertainties that are still presented in chironomid-ATR relationships and in the absence of a specifically tailored TS, it is preferable to discuss reconstructed ATR curves as trends rather than absolute values.

4.4 Highlights on the postglacial climate history of the eastern Baltic area

4.4.1 Late glacial (14 ka – 11.7 ka cal BP)

Based on the previous studies, deglaciation of Estonia occurred approximately between 14.7 and 12.7 ka cal BP (Kalm et al., 2011; Lasberg & Kalm, 2013; Amon et al., 2016; Hughes et al., 2016). The oldest sediments in the Lake Nakri record date to approximately 14.5 ka cal BP, capturing the period since the early ice melting.

Previous pollen-based studies have identified two major late glacial climatic phases in the eastern Baltic region: the Bølling/Allerød warming and the subsequent Younger Dryas cooling (Seppä & Poska, 2004; Laumets et al., 2014). Chironomid-based reconstruction of Bølling/Allerød event in Lake Nakri exhibited temperatures around 16 °C, which was slightly colder than the one from the more southern location in Kaliningrad area (Druzinina et al., 2020). Thus, it is possible, that July air T during the Bølling/Allerød period exhibited an increasing trend from north to south and with greater distance from the ice sheet.

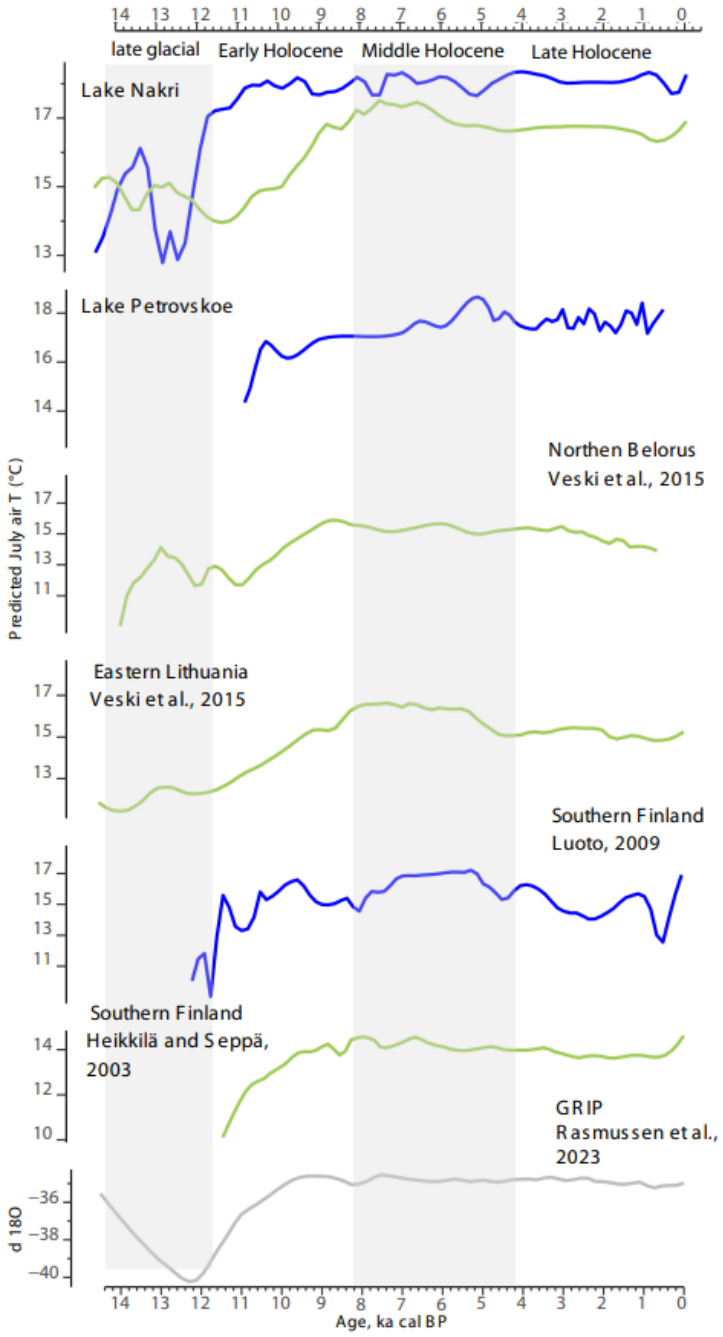

Figure 15 *July air T (°C) reconstructions of Lakes Nakri and Petrovskoe together with other records from the Baltic area and Greenland Ice Core Project (GRIP) isotopes curve. The green lines represent pollen-based reconstruction, the blue lines represent chironomid-based reconstruction, grey line represents isotopes.*

Pollen-based reconstructions from Lake Nakri and other parts of the eastern Baltic region (Veski et al., 2015) indicate a cool phase around 11.5–11 ka cal BP. However, other proxy-based climate reconstructions (Stivrins et al., 2016; Druzhinina et al., 2020; Šeirienė et al., 2021), as well as chironomid-based reconstruction of Lake Nakri, place the late glacial cooling episode between 12.7 and 11.7 ka cal BP. This discrepancy may be due to delayed responses in terrestrial vegetation migration and the absence of modern analogous, as discussed earlier.

Previously, the Younger Dryas was characterized mainly by cold winters, with summer temperatures comparable to present-day conditions according to pollen-based studies (Borisova, 1997; B. A. S. Davis et al., 2003). Theuerkauf & Joosten (2012) highlighted uncertainties regarding the extent of winter cooling and the degree of continentality during the Younger Dryas. The Younger Dryas period in Lake Nakri was marked by a drop in July air T down to 13 °C, which supports other chironomid-based reconstructions across Europe (Heiri et al., 2014). The chironomid-inferred ATR values in Lake Nakri exhibited an increase trend from Bølling/Allerød towards Younger Dryas. This agrees with cryogenic cave carbonate records from Great Britain (Töchterle et al., 2024), and climate model simulations of Younger Dryas conditions (e.g., Renssen et al., 2001). Also, there is evidence that the development of tundra biomes, typical for Younger Dryas in Norther Hemisphere, may have been promoted by the enhanced continentality (Sher et al., 2003; Kienast et al., 2008).

4.4.2 Early Holocene (11.7 ka – 8.2 ka cal BP)

Chironomid-based temperature reconstructions from Lake Nakri and Petrovskoe indicate that July air T during the Early Holocene reached approximately 17.5–18 °C, which is the same as today's values (Figure 14). The ATR fluctuations at that period were reconstructed as relatively small, exhibiting a steep decreasing trend from the previous Younger Dryas stage. These stable and warm climatic conditions facilitated the transition from tundra vegetation to boreal forest ecosystems, as reflected in the Lake Nakri and Petrovskoe pollen record and supported by similar findings across the eastern Baltic region (Amon et al., 2016; Poska et al., 2022). Around 8.5 ka cal BP, boreal forests were replaced with temperate broad-leaved forests (Saarse & Veski, 2001; Niinemets & Saarse, 2009; Poska et al., 2022). This transition was disrupted by the distinct cooling event around 8.2 ka cal BP, which is clearly registered in vegetation records from the eastern Baltic (Seppä & Poska, 2004; Niinemets & Saarse, 2009; Seppä et al., 2009; Veski et al., 2015).

The 8.2 ka event is also detected in the chironomid record from Lake Nakri as a temperature decline of roughly 1 °C between 9.0 and 8.0 ka cal BP and a more pronounced increase in ATR. In Lake Petrovskoe this event is almost not captured by the July air T curve, only by the ATR one. This can be explained by the low sampling density in Early Holocene part of the core as well as the special importance of ATR changes during 9.0–8.0 ka cal BP event.

Pollen-based reconstructions generally identify 8.2 ka event as a brief cooling episode (Heikkilä & Seppä, 2003; Veski et al., 2015), while chironomid records from southern Finland and central Poland suggest a more prolonged summer cooling period that began around 9.0 ka cal BP (T. P. Luoto et al., 2010; Płóciennik et al., 2011). Furthermore, Mayewski et al. (2004), drawing on global multi-proxy data, interpret the 9.0–8.0 ka cal BP interval as a partial climatic regression toward glacial conditions. This could lead to the regrowing of ice sheets, one of the causes of the increase in continentality

(Boulton & Hagdorn, 2006). Evidence from western Ireland, based on phosphorus levels in speleothem calcite, suggests a rise in temperature seasonality during the 8.2 ka event (Baldini et al., 2002). Additionally, studies have reported increased seasonal precipitation variability and pronounced dry events across the Northern Hemisphere between 9 and 8 ka cal BP (Shuman, 2012; N. Andersen et al., 2017). These climatic anomalies are believed to have been triggered by a weakened Atlantic Meridional Overturning Circulation, reduced summer insolation, and the cooling impact of volcanic aerosols (Mayewski et al., 2004; Carlson et al., 2008).

4.4.3 Middle Holocene (8.2 ka – 4.2 ka cal BP)

The Middle Holocene was marked by a generally warm and stable climate with the chironomid-inferred July air T of 17.5–18.5 °C both in Lakes Nakri and Petrovskoe. This period is often referred to as the Holocene Thermal Maximum, during which temperate broadleaved forests became well-established in the eastern Baltic region, as indicated by pollen records (Paper III, Manuscript). Despite this overall climatic stability, chironomid-based temperature reconstruction from Lake Nakri revealed minor summer cooling episodes of approximately 0.5–1 °C occurring around 7.5–7.0 ka and 6.5–5.5 ka cal BP, which coincide with slight ATR fluctuations. These episodes were not visible in the Lake Petrovskoe record due to the low density of the sampling; however, fluctuations in ATR, similar to Lake Nakri ones, were presented.

A cooling event around 7.5–7.0 ka cal BP is evident in chironomid data from southern Finland (Luoto et al., 2010; Figure 15), although this signal is not detected in local pollen-based reconstructions. Evidence from pollen records in Sweden points to winter cooling and an increase in continentality around 7.0 ka cal BP (Seppä et al., 2005), suggesting a possible seasonal asymmetry in climate change during this period.

The cooling interval between 6.5 and 5.5 ka cal BP is supported by both pollen and chironomid data from northern Belarus, eastern Latvia, and southern Finland (Luoto et al., 2010; Veski et al., 2015; Figure 15). Comparable cooling episodes have also been identified in marine and terrestrial records from the North Atlantic and central Europe (O'Brien et al., 1995; Oppo et al., 2003; Magny & Haas, 2004; Moros et al., 2004; Vollweiler et al., 2006). According to Marsicek et al. (2018), the average summer temperature decline around 5.5 ka across Europe and North America was estimated at a minimum of 0.5 °C.

The most plausible explanation for these cooling events is a reduction in solar activity, particularly a decline in summer insolation resulting from orbital forcing (Mayewski et al., 2004; Shuman, 2012). This decrease in insolation likely led to broader climate system responses, including reduced mid-latitude temperatures, altered El Niño-Southern Oscillation frequency, intensification of the westerlies over the North Atlantic and Siberia, glacier advances, treeline shifts in Scandinavia (Clement et al., 2000; Liu et al., 2000; Harrison et al., 2003; Braconnot et al., 2004; Mayewski et al., 2004; Shin et al., 2006; Liu et al., 2007). These climatic perturbations have been interpreted as a complex and hierarchical system response to peak rates of orbital insolation change (Shuman, 2012).

4.4.4 Late Holocene (4.2 – 0 ka cal BP)

The commonly accepted border of the Middle Holocene (4.2 ka cal BP) did not exhibit any specific climate of vegetation change events either in Lake Nakri or in Lake Petrovskoe. After approximately 4.0 ka cal BP, the eastern Baltic region underwent significant anthropogenic transformation, most notably through widespread deforestation. This land use facilitated the development of mixed boreal forests, replacing late-successional temperate tree species with early-successional taxa (Niinemets & Saarse, 2009; Poska et al., 2022). Chironomid-based reconstructions of Lakes Nakri and Petrovskoe indicate relatively stable July air T around 17–18 °C throughout the Late Holocene, with a slight warming of about 0.5 °C around 1.0 ka cal BP. This warming phase was followed by a subsequent cooling 0.5 °C, reflecting the climatic progression from the Medieval Warm Period to the Little Ice Age (Diaz et al., 2011; Płóciennik et al., 2011). Comparable climatic patterns are evident in pollen records from eastern Latvia and Southern Finland (Heikkilä & Seppä, 2003; Luoto et al., 2010; Veski et al., 2015; Figure 15).

The chironomid-inferred reduction of ATR was indicated since 2.0 until 0 ka cal BP, with Lake Petrovskoe exhibiting more drastic decrease than Lake Nakri. This is consistent with increased moisture availability in Southern Finland around 0.5 ka cal BP (Seppä et al., 2009) and general estimation of snowy winters and periodic cool, humid summers across Europe (Jones et al., 2014). These climatic shifts promoted positive glacier mass balances and widespread glacier advances across the Northern Hemisphere (Steiner et al., 2008; Solomina et al., 2015). The cooling during the Little Ice Age likely resulted from a combination of reduced summer insolation (Wanner et al., 2008) and frequent volcanic eruptions, which introduced aerosols into the atmosphere and suppressed summer temperatures (Owens et al., 2017). Additional contributing factors include increased surface albedo due to deforestation and enhanced sea-ice export from the Arctic, which may have further amplified regional cooling (Miles et al., 2020).

5 Conclusions

This thesis presents the first systematic study of modern chironomid assemblages from the eastern Baltic area and the eastern European part of Russia. The collected data formed the basis for developing a new regional FBP TS (Paper I) and a Continentality Dataset (Paper II). The FBP TS was used to reconstruct July air T and ATR throughout the entire postglacial period at two sites in the eastern Baltic area. The Continentality Dataset was used to examine the relationships between chironomid assemblages and continentality.

In the case of the latitudinally distributed FBP TS, July air T emerged as the primary factor influencing the distribution of chironomid assemblages. The strengths of the FBP TS include its geographic and climatic continuity, modern analogues covering the full range of expected postglacial temperature changes in the eastern Baltic region, and the representation of climatic and environmental conditions typical for eastern Baltic lowlands. The excellent WA-PLS performance values of the FBP inference model indicate that it currently provides the most reliable July air T reconstructions available for the Eastern Baltic region, adding an independent climate parameter and supporting the validity of chironomids as proxies for these environmental parameters.

In the longitudinally distributed Continentality Dataset, KOI explained the most variation within observed variables among tested continentality-related indexes. Performance of the Continentality Dataset within the KOI-based WA-PLS model suggests that chironomids hold potential as indicators of continentality. Paper II statistically confirmed that continentality, expressed in KOI, affects chironomid assemblages primarily through factors such as the timing and length of the growing season, the presence and duration of ice-cover, and the intensity of summer warmth. The Paper II findings emphasize the importance of developing targeted TSs tailored to specific environmental parameters to enable reliable reconstructions.

Chironomid assemblages from FBP TS also explicit dependency from continentality expressed as ATR, which increases from coastal areas towards inland in Finland and the eastern Baltic area. The number of sites included in FBP TS and performance statistics of the produced ATR inference model (Manuscript) allows for use in palaeoclimate reconstructions.

The chironomid-based reconstructions of July air T and ATR for Lakes Nakri and Petrovskoe (Paper III) correspond well with major event stratigraphy from previously published data. However, our results highlight the discrepancies between pollen- and chironomid-based reconstructions and differences arising from using different TS. Conducted reconstruction of Lakes Nakri (Manuscript) and Petrovskoe demonstrated that chironomid-based and pollen-based reconstructions of July air T during the Holocene generally exhibit consistent patterns. Nonetheless, notable discrepancies occur during the Younger Dryas and the early Holocene warming phases, likely due to the lack of modern analogues in modern vegetation communities. Chironomid-inferred July air T indicate relatively warm conditions during the Bølling-Allerød period, followed by a cooling phase during the Younger Dryas. An increase in ATR accompanied this cooling. During the Holocene, climate conditions appear to have been relatively stable in temperature and ATR reconstructions, punctuated by several minor cooling events of approximately 0.5–1 °C. These occurred around 8.0–9.0 ka cal BP, 7.0–7.5 ka, 6.5–5.5 ka cal BP, and around 0.5 ka cal BP. The ATR revealed an increase during the 8.0–9.0 ka cal BP cooling event and a decrease since 2.0 ka cal BP until nowadays.

The above-listed findings enhance our understanding of chironomid ecology and provide valuable insights into how ecosystems in the Eastern Baltic region have responded to past climate shifts in this previously understudied area. This knowledge helps to contextualize potential future environmental changes under ongoing global warming.

List of figures

List of tables

References

[1] Agasild, H., Kisand, A., Ainelo, E., Feldmann, T., Timm, H., Karus, K., Kisand, V., Jones, R. I., & Nõges, T. (2018). Chironomid incorporation of methane-derived carbon in plankton- and macrophyte-dominated habitats in a large shallow lake. *Freshwater Biology*, *63*(11), 1433–1445. https://doi.org/10.1111/fwb.13170

[2] Alexandrov, G. A., Ginzburg, A. S., & Golitsyn, G. S. (2019). Influence of North Atlantic Oscillation on Moscow Climate Continentality. *Izvestiya, Atmospheric and Oceanic Physics*, *55*(5), 407–411. https://doi.org/10.1134/S0001433819050025

[3] Amon, D. J., Ziegler, A. F., Dahlgren, T. G., Glover, A. G., Goineau, A., Gooday, A. J., Wiklund, H., & Smith, C. R. (2016). Insights into the abundance and diversity of abyssal megafauna in a polymetallic-nodule region in the eastern Clarion-Clipperton Zone. *Scientific Reports*, *6*(1), 30492. https://doi.org/10.1038/srep30492

[4] Andersen, N., Lauterbach, S., Erlenkeuser, H., Danielopol, D. L., Namiotko, T., Hüls, M., Belmecheri, S., Dulski, P., Nantke, C., Meyer, H., Chapligin, B., Von Grafenstein, U., & Brauer, A. (2017). Evidence for higher-than-average air temperatures after the 8.2 ka event provided by a Central European δ18O record. *Quaternary Science Reviews*, *172*, 96–108. https://doi.org/10.1016/j.quascirev.2017.08.001

[5] Andersen, T., Sæther, O., Cranston, P., & Epler, J. (2013). *The larvae of Orthocladiinae (Diptera: Chironomid) of the Holarctic region–Keys and diagnoses. Insect Systematics & Evolution.* (Vol. 66).

[6] Andreev, A. A., Tarasov, P. E., Ilyashuk, B. P., Ilyashuk, E. A., Cremer, H., Hermichen, W.-D., Wischer, F., & Hubberten, H.-W. (2005). Holocene environmental history recorded in Lake Lyadhej-To sediments, Polar Urals, Russia. *Palaeogeography, Palaeoclimatology, Palaeoecology*, *223*(3), 181–203. https://doi.org/10.1016/j.palaeo.2005.04.004

[7] Antczak-Orlewska, O., Płóciennik, M., Sobczyk, R., Okupny, D., Stachowicz-Rybka, R., Rzodkiewicz, M., Siciński, J., Mroczkowska, A., Krąpiec, M., Słowiński, M., & Kittel, P. (2021). Chironomid Morphological Types and Functional Feeding Groups as a Habitat Complexity Vestige. *Frontiers in Ecology and Evolution*, *8*. https://doi.org/10.3389/fevo.2020.583831

[8] Armitage, P. D., Cranston, P. S., & Pinder, L. C. V. (Eds.). (1995). *The Chironomid*. Springer Netherlands. https://doi.org/10.1007/978-94-011-0715-0

[9] Baldini, J. U. L., McDermott, F., & Fairchild, I. J. (2002). Structure of the 8200-Year Cold Event Revealed by a Speleothem Trace Element Record. *Science*, *296*(5576), 2203–2206. https://doi.org/10.1126/science.1071776

[10] Barbiero, L., Filho, A. R., Furquim, S. A. C., Furian, S., Sakamoto, A. Y., Valles, V., Graham, R. C., Fort, M., Ferreira, R. P. D., & Neto, J. P. Q. (2008). Soil morphological control on saline and freshwater lake hydrogeochemistry in the Pantanal of Nhecolândia, Brazil. *Geoderma*, *148*(1), 91–106. https://doi.org/10.1016/j.geoderma.2008.09.010

[11] Barley, E. M., Walker, I. R., Kurek, J., Cwynar, L. C., Mathewes, R. W., Gajewski, K., & Finney, B. P. (2006). A northwest North American training set: Distribution of freshwater midges in relation to air temperature and lake depth. *Journal of Paleolimnology*, *36*(3), 295–314. https://doi.org/10.1007/s10933-006-0014-6

[12] Battarbee, R. W. (2000). Palaeolimnological approaches to climate change, with special regard to the biological record. *Quaternary Science Reviews*, *19*(1), 107–124. https://doi.org/10.1016/S0277-3791(99)00057-8

[13] Berezina, N. A. (2001). Influence of Ambient pH on Freshwater Invertebrates under Experimental Conditions. *Russian Journal of Ecology*, *32*(5), 343–351. https://doi.org/10.1023/A:1011978311733

[14] Berglund, B. E., & Ralska-Jasiewiczowa, M. (1991). *Handbook of Holocene palaeoecology and palaeohydrology*. J. Wiley and sons.

[15] Bertolet, B. L., Corman, J. R., Casson, N. J., Sebestyen, S. D., Kolka, R. K., & Stanley, E. H. (2018). Influence of soil temperature and moisture on the dissolved carbon, nitrogen, and phosphorus in organic matter entering lake ecosystems. *Biogeochemistry*, *139*(3), 293–305. https://doi.org/10.1007/s10533-018-0469-3

[16] Birks, H. J. B. (2010). Numerical methods for the analysis of diatom assemblage data. In J. P. Smol & E. F. Stoermer (Eds.), *The Diatoms* (2nd ed., pp. 23–54). Cambridge University Press. https://doi.org/10.1017/CBO9780511763175.004

[17] Birks, H. J. B., & Birks, H. J. B. (1998). D.G. Frey and E.S. Deevey Review 1: Numerical tools in palaeolimnology – Progress, potentialities, and problems. *Journal of Paleolimnology*, *20*(4), 307–332. https://doi.org/10.1023/A:1008038808690

[18] Birks, H. j. b., Braak, C. j. f. T., Line, J. M., Juggins, S., Stevenson, A. C., Battarbee, R. W., Mason, B. J., Renberg, I., & Talling, J. F. (1997). Diatoms and pH reconstruction. *Philosophical Transactions of the Royal Society of London. B, Biological Sciences*, *327*(1240), 263–278. https://doi.org/10.1098/rstb.1990.0062

[19] Biswas, J. K., Rana, S., Bhakta, J. N., & Jana, B. B. (2009). Bioturbation potential of chironomid larvae for the sediment–water phosphorus exchange in simulated pond systems of varied nutrient enrichment. *Ecological Engineering*, *35*(10), 1444–1453. https://doi.org/10.1016/j.ecoleng.2009.06.004

[20] Bolland, A., Kern, O. A., Koutsodendris, A., Pross, J., & Heiri, O. (2022). Chironomid-inferred summer temperature development during the late Rissian glacial, Eemian interglacial and earliest Würmian glacial at Füramoos, southern Germany. *Boreas*, *51*(2), 496–516. https://doi.org/10.1111/bor.12567

[21] Borisova, O. K. (1997). Younger Dryas landscape and climate in Northern Eurasia and North America. *Quaternary International*, *41–42*, 103–109. https://doi.org/10.1016/S1040-6182(96)00041-9

[22] Boulton, G., & Hagdorn, M. (2006). Glaciology of the British Isles Ice Sheet during the last glacial cycle: Form, flow, streams and lobes. *Quaternary Science Reviews*, *25*(23), 3359–3390. https://doi.org/10.1016/j.quascirev.2006.10.013

[23] Braconnot, P., Harrison, S. P., Joussaume, S., Hewitt, C. D., Kitoch, A., Kutzbach, J. E., Liu, Z., Otto-Bliesner, B., Syktus, J., & Weber, S. L. (2004). Evaluation of PMIP coupled ocean-atmosphere simulations of the Mid-Holocene. In R. W. Battarbee, F. Gasse, & C. E. Stickley (Eds.), *Past Climate Variability through Europe and Africa* (Vol. 6, pp. 515–533). Springer Netherlands. https://doi.org/10.1007/978-1-4020-2121-3_24

[24] Brodersen, K. P., & Anderson, N. J. (2002). Distribution of chironomids (Diptera) in low arctic West Greenland lakes: Trophic conditions, temperature and environmental reconstruction. *Freshwater Biology*, *47*(6), 1137–1157. https://doi.org/10.1046/j.1365-2427.2002.00831.x

[25] Brodersen, K. P., & Lindegaard, C. (1999). Classification, assessment and trophic reconstruction of Danish lakes using chironomids. *Freshwater Biology*, *42*(1), 143–157. https://doi.org/10.1046/j.1365-2427.1999.00457.x

[26] Brodersen, K. P., & Quinlan, R. (2006). Midges as palaeoindicators of lake productivity, eutrophication and hypolimnetic oxygen. *Quaternary Science Reviews*, *25*(15), 1995–2012. https://doi.org/10.1016/j.quascirev.2005.03.020

[27] Brodin, Y.-W., & Gransberg, M. (1993). Responses of insects, especially Chironomid (Diptera), and mites to 130 years of acidification in a Scottish lake. *Hydrobiologia*, *250*(3), 201–212. https://doi.org/10.1007/BF00008590

[28] Brooks, S. J., Bennion, H., & Birks, H. J. B. (2001). Tracing lake trophic history with a chironomid–total phosphorus inference model. *Freshwater Biology*, *46*(4), 513–533. https://doi.org/10.1046/j.1365-2427.2001.00684.x

[29] Brooks, S. J., & Birks, H. J. B. (2000). Chironomid-inferred late-glacial and early-Holocene mean July air temperatures for Kråkenes Lake, western Norway. *Journal of Paleolimnology*, *23*(1), 77–89. https://doi.org/10.1023/A:1008044211484

[30] Brooks, S. J., Langdon, P. G., & Heiri, O. (2007). The identification and use of Palaearctic Chironomid larvae in palaeoecology. *Quaternary Research Association Technical Guide*, *10*, Article 10.

[31] Brousseau, C. S., Baccante, D., & Maki, L. W. (1985). Role of Bedrock and Surficial Geology in Determining the Sensitivity of Thunder Bay Area Lakes to Acidification. *Journal of Great Lakes Research*, *11*(4), 501–507. https://doi.org/10.1016/S0380-1330(85)71793-5

[32] Bryce, D., & Hobart, A. (1972). *The Biology and Identification of the Larvae of the Chironomid (diptera): Introduction and Key to Subfamilies* (Vol. 23). Classey.

[33] Butcher, J. B., Nover, D., Johnson, T. E., & Clark, C. M. (2015). Sensitivity of lake thermal and mixing dynamics to climate change. *Climatic Change*, *129*(1), 295–305. https://doi.org/10.1007/s10584-015-1326-1

[34] Cao, Y., Zhang, E., Chen, X., John Anderson, N., & Shen, J. (2012). Spatial distribution of subfossil Chironomid in surface sediments of a large, shallow and hypertrophic lake (Taihu, SE China). *Hydrobiologia*, *691*(1), 59–70. https://doi.org/10.1007/s10750-012-1030-3

[35] Carlson, A. E., LeGrande, A. N., Oppo, D. W., Came, R. E., Schmidt, G. A., Anslow, F. S., Licciardi, J. M., & Obbink, E. A. (2008). Rapid early Holocene deglaciation of the Laurentide ice sheet. *Nature Geoscience*, *1*(9), 620–624. https://doi.org/10.1038/ngeo285

[36] Chamutiová, T., Hamerlík, L., & Bitušík, P. (2020). Subfossil chironomids (Diptera, Chironomid) of lakes in the Tatra Mountains: An illustrated guide. *Zootaxa*, *4819*(2). https://doi.org/10.11646/zootaxa.4819.2.2

[37] Chen, J., Zhang, E., Brooks, S. J., Huang, X., Wang, H., Liu, J., & Chen, F. (2014). Relationships between chironomids and water depth in Bosten Lake, Xinjiang, northwest China. *Journal of Paleolimnology*, *51*(2), 313–323. https://doi.org/10.1007/s10933-013-9727-5

[38] Clarke, K. R., & Green, R. H. (1988). Statistical design and analysis for a "biological effects" study. *Marine Ecology Progress Series*, *46*(1/3), 213–226.

[39] Clement, A. C., Seager, R., & Cane, M. A. (2000). Suppression of El Niño during the Mid-Holocene by changes in the Earth's orbit. *Paleoceanography*, *15*(6), 731–737. https://doi.org/10.1029/1999PA000466

[40] Cohen, J., Saito, K., & Entekhabi, D. (2001). The role of the Siberian high in northern hemisphere climate variability. *Geophysical Research Letters*, *28*(2), 299–302. https://doi.org/10.1029/2000GL011927

[41] Cortelezzi, A., Paggi, A. C., Rodríguez, M., & Capítulo, A. R. (2011). Taxonomic and nontaxonomic responses to ecological changes in an urban lowland stream through the use of Chironomid (Diptera) larvae. *Science of The Total Environment*, *409*(7), 1344–1350. https://doi.org/10.1016/j.scitotenv.2011.01.002

[42] Davis, B. A. S., Brewer, S., Stevenson, A. C., & Guiot, J. (2003). The temperature of Europe during the Holocene reconstructed from pollen data. *Quaternary Science Reviews*, *22*(15–17), 1701–1716. https://doi.org/10.1016/S0277-3791(03)00173-2

[43] Davis, J. C. (1975). Minimal Dissolved Oxygen Requirements of Aquatic Life with Emphasis on Canadian Species: A Review. *Journal of the Fisheries Research Board of Canada*, *32*(12), 2295–2332. https://doi.org/10.1139/f75-268

[44] De Bisthoven, L. J., Gerhardt, A., & Soares, A. M. V. M. (2005). Chironomid larvae as bioindicators of an acid mine drainage in Portugal. *Hydrobiologia*, *532*(1), 181–191. https://doi.org/10.1007/s10750-004-1387-z

[45] De Cáceres, M., & Legendre, P. (2009). *Associations between species and groups of sites: Indices and statistical inference*. *90*, 3566–3574. https://doi.org/doi:10.1890/08-1823.1

[46] Di Veroli, A., Santoro, F., Pallottini, M., Selvaggi, R., Scardazza, F., Cappelletti, D., & Goretti, E. (2014). Deformities of chironomid larvae and heavy metal pollution: From laboratory to field studies. *Chemosphere*, *112*, 9–17. https://doi.org/10.1016/j.chemosphere.2014.03.053

[47] Diaz, H. F., Trigo, R., Hughes, M. K., Mann, M. E., Xoplaki, E., & Barriopedro, D. (2011). Spatial and Temporal Characteristics of Climate in Medieval Times Revisited. *Bulletin of the American Meteorological Society*, *92*(11), 1487–1500. https://doi.org/10.1175/BAMS-D-10-05003.1

[48] Dieffenbacher-Krall, A., Vandergoes, M., & Denton, G. (2007). *An inference model for mean summer air temperatures in the Southern Alps, New Zealand, using subfossil chironomids*. *26(19-21)*, 2487–2504. https://doi.org/doi:10.1016/j.quascirev.2007.06.016

[49] Druzhinina, O., Kublitskiy, Y., Stančikaitė, M., Nazarova, L., Syrykh, L., Gedminienė, L., Uogintas, D., Skipityte, R., Arslanov, K., Vaikutienė, G., Kulkova, M., & Subetto, D. (2020). The Late Pleistocene–Early Holocene palaeoenvironmental evolution in the SE Baltic region: A new approach based on chironomid, geochemical and isotopic data from Kamyshovoye Lake, Russia. *Boreas*, *49*(3), 544–561. https://doi.org/10.1111/bor.12438

[50] Dufrene, M., & Legendre, P. (1997). Species Assemblages and Indicator Species: The Need for a Flexible Asymmetrical Approach. *Ecological Monographs*, *67*(3), 345–366. https://doi.org/10.2307/2963459

[51] Edvardsson, J., Corona, C., Mažeika, J., Pukienė, R., & Stoffel, M. (2016). Recent advances in long-term climate and moisture reconstructions from the Baltic region: Exploring the potential for a new multi-millennial tree-ring chronology. *Quaternary Science Reviews*, *131*, 118–126. https://doi.org/10.1016/j.quascirev.2015.11.005

[52] Eggermont, H., & Heiri, O. (2012). The chironomid-temperature relationship: Expression in nature and palaeoenvironmental implications. *Biological Reviews*, *87*(2), 430–456. https://doi.org/10.1111/j.1469-185X.2011.00206.x

[53] Engels, S., & Cwynar, L. C. (2011). Changes in fossil chironomid remains along a depth gradient: Evidence for common faunal thresholds within lakes. *Hydrobiologia*, *665*(1), 15–38. https://doi.org/10.1007/s10750-011-0601-z

[54] Engels, S., Cwynar, L. C., Rees, A. B. H., & Shuman, B. N. (2012). Chironomid-based water depth reconstructions: An independent evaluation of site-specific and local inference models. *Journal of Paleolimnology*, *48*(4), 693–709. https://doi.org/10.1007/s10933-012-9638-x

[55] Engels, S., Self, A., Luoto, T., Brooks, S., & Helmens, K. (2014). *A comparison of three Eurasian chironomid–climate calibration datasets on a W–E continentality gradient and the implications for quantitative temperature reconstructions*. *51*, 529–547. https://doi.org/10.1007/s10933-014-9772-8

[56] Fortin, M.-C., Medeiros, A. S., Gajewski, K., Barley, E. M., Larocque-Tobler, I., Porinchu, D. F., & Wilson, S. E. (2015). Chironomid-environment relations in northern North America. *Journal of Paleolimnology*, *54*(2), 223–237. https://doi.org/10.1007/s10933-015-9848-0

[57] Frey, D. (1986). Cladocera Analysis. In *Berglund, B. E. (ed.),Handbook of Holocene Palaeoecology and Palaeohydrology* (pp. 667–692). John Wiley & Sons Ltd.

[58] Fu, C. (1992). Transitional Climate Zones and Biome Boundaries: A Case Study from China. In A. J. Hansen & F. di Castri (Eds.), *Landscape Boundaries: Consequences for Biotic Diversity and Ecological Flows* (pp. 394–402). Springer. https://doi.org/10.1007/978-1-4612-2804-2_20

[59] Giesecke, T., Bjune, A. E., Chiverrell, R. C., Seppä, H., Ojala, A. E. K., & Birks, H. J. B. (2008). Exploring Holocene continentality changes in Fennoscandia using present and past tree distributions. *Quaternary Science Reviews*, *27*(13), 1296–1308. https://doi.org/10.1016/j.quascirev.2008.03.008

[60] Golosov, S., Maher, O. A., Schipunova, E., Terzhevik, A., Zdorovennova, G., & Kirillin, G. (2007). Physical background of the development of oxygen depletion in ice-covered lakes. *Oecologia*, *151*(2), 331–340. https://doi.org/10.1007/s00442-006-0543-8

[61] Gonzales, L. M., & Grimm, E. C. (2009). Synchronization of late-glacial vegetation changes at Crystal Lake, Illinois, USA with the North Atlantic Event Stratigraphy. *Quaternary Research*, *72*(2), 234–245. https://doi.org/10.1016/j.yqres.2009.05.001

[62] Gorczyński., L. (1920). Sur Le Calcul Du Degré Du Continentalisme Et Son Application Dans La Climatologie. *Geografiska Annaler*, *2*(4), 324–331.

[63] Granados, I., & Toro, M. (2000). Recent warming in a high mountain lake (Laguna Cimera, Central Spain) inferred by means of fossil chironomids. *Journal of Limnology*, *59*(1s), 109. https://doi.org/10.4081/jlimnol.2000.s1.109

[64] Hájková, P., Pařil, P., Petr, L., Chattová, B., Matys Grygar, T., & Heiri, O. (2016). A first chironomid-based summer temperature reconstruction (13–5 ka BP) around 49°N in inland Europe compared with local lake development. *Quaternary Science Reviews*, *141*, 94–111. https://doi.org/10.1016/j.quascirev.2016.04.001

[65] Hamilton, P. B., Gajewski, K., Atkinson, D. E., & Lean, D. R. S. (2001). Physical and chemical limnology of 204 lakes from the Canadian Arctic Archipelago. *Hydrobiologia*, *457*(1), 133–148. https://doi.org/10.1023/A:1012275316543

[66] Harrison, S. P., Kutzbach, J. E., Liu, Z., Bartlein, P. J., Otto-Bliesner, B., Muhs, D., Prentice, I. C., & Thompson, R. S. (2003). Mid-Holocene climates of the Americas: A dynamical response to changed seasonality. *Climate Dynamics*, *20*(7), 663–688. https://doi.org/10.1007/s00382-002-0300-6

[67] Heikkilä, M., & Seppä, H. (2003). A 11,000 yr palaeotemperature reconstruction from the southern boreal zone in Finland. *Quaternary Science Reviews*, *22*(5), 541–554. https://doi.org/10.1016/S0277-3791(02)00189-0

[68] Heiri, O. (2004). Within-lake variability of subfossil chironomid assemblages in shallow Norwegian lakes. *Journal of Paleolimnology*, *32*(1), 67–84. https://doi.org/10.1023/B:JOPL.0000025289.30038.e9

[69] Heiri, O., Brooks, S. J., Birks, H. J. B., & Lotter, A. F. (2011). A 274-lake calibration data-set and inference model for chironomid-based summer air temperature reconstruction in Europe. *Quaternary Science Reviews*, *30*(23), 3445–3456. https://doi.org/10.1016/j.quascirev.2011.09.006

[70] Heiri, O., Brooks, S. J., Renssen, H., Bedford, A., Hazekamp, M., Ilyashuk, B., Jeffers, E. S., Lang, B., Kirilova, E., Kuiper, S., Millet, L., Samartin, S., Toth, M., Verbruggen, F., Watson, J. E., van Asch, N., Lammertsma, E., Amon, L., Birks, H. H., … Lotter, A. F. (2014). Validation of climate model-inferred regional temperature change for late-glacial Europe. *Nature Communications*, *5*(1), 4914. https://doi.org/10.1038/ncomms5914

[71] Heiri, O., & Lotter, A. F. (2003). 9000 years of chironomid assemblage dynamics in an Alpine lake: Long-term trends, sensitivity to disturbance, and resilience of the fauna. *Journal of Paleolimnology*, *30*(3), 273–289. https://doi.org/10.1023/A:1026036930059

[72] Heiri, O., Lotter, A. F., & Lemcke, G. (2001). Loss on ignition as a method for estimating organic and carbonate content in sediments: Reproducibility and comparability of results. *Journal of Paleolimnology*, *25*(1), 101–110. https://doi.org/10.1023/A:1008119611481

[73] Hersbach, H., Bell, B., Berrisford, P., Hirahara, S., Horányi, A., Muñoz-Sabater, J., Nicolas, J., Peubey, C., Radu, R., Schepers, D., Simmons, A., Soci, C., Abdalla, S., Abellan, X., Balsamo, G., Bechtold, P., Biavati, G., Bidlot, J., Bonavita, M., … Thépaut, J.-N. (2020). The ERA5 global reanalysis. *Quarterly Journal of the Royal Meteorological Society*, *146*(730), 1999–2049. https://doi.org/10.1002/qj.3803

[74] Hill, M. O., & Gauch, H. G. (1980). Detrended correspondence analysis: An improved ordination technique. *Vegetatio*, *42*(1), 47–58. https://doi.org/10.1007/BF00048870

[75] Holmes, N., Langdon, P. G., Caseldine, C., Brooks, S. J., & Birks, H. J. B. (2011). Merging chironomid training sets: Implications for palaeoclimate reconstructions. *Quaternary Science Reviews*, *30*(19), 2793–2804. https://doi.org/10.1016/j.quascirev.2011.06.013

[76] Holmes, N., Langdon, P. G., Caseldine, C. J., Wastegård, S., Leng, M. J., Croudace, I. W., & Davies, S. M. (2016). Climatic variability during the last millennium in Western Iceland from lake sediment records. *The Holocene*, *26*(5), 756–771. https://doi.org/10.1177/0959683615618260

[77] Houle, D., Ouimet, R., Couture, S., & Gagnon, C. (2006). Base cation reservoirs in soil control the buffering capacity of lakes in forested catchments. *Canadian Journal of Fisheries and Aquatic Sciences*, *63*(3), 471–474. https://doi.org/10.1139/f06-007

[78] Hughes, A. L. C., Gyllencreutz, R., Lohne, Ø. S., Mangerud, J., & Svendsen, J. I. (2016). The last Eurasian ice sheets – a chronological database and time-slice reconstruction, DATED-1. *Boreas*, *45*(1), 1–45. https://doi.org/10.1111/bor.12142

[79] Hupfer, M., Jordan, S., Herzog, C., Ebeling, C., Ladwig, R., Rothe, M., & Lewandowski, J. (2019). Chironomid larvae enhance phosphorus burial in lake sediments: Insights from long-term and short-term experiments. *Science of The Total Environment*, *663*, 254–264. https://doi.org/10.1016/j.scitotenv.2019.01.274

[80] Ilyashuk, B., Gobet, E., Heiri, O., Lotter, A. F., van Leeuwen, J. F. N., van der Knaap, W. O., Ilyashuk, E., Oberli, F., & Ammann, B. (2009). Lateglacial environmental and climatic changes at the Maloja Pass, Central Swiss Alps, as recorded by chironomids and pollen. *Quaternary Science Reviews*, *28*(13), 1340–1353. https://doi.org/10.1016/j.quascirev.2009.01.007

[81] Ilyashuk, B., Ilyashuk, E., & Dauvalter, V. (2003). Chironomid responses to long-term metal contamination: A paleolimnological study in two bays of Lake Imandra, Kola Peninsula, northern Russia. *Journal of Paleolimnology*, *30*(2), 217–230. https://doi.org/10.1023/A:1025528605002

[82] Ilyashuk, E. A., Ilyashuk, B. P., Hammarlund, D., & Larocque, I. (2005). Holocene climatic and environmental changes inferred from midge records (Diptera: Chironomid, Chaoboridae, Ceratopogonidae) at Lake Berkut, southern Kola Peninsula, Russia. *The Holocene*, *15*(6), 897–914. https://doi.org/10.1191/0959683605hl865ra

[83] Ilyashuk, E. A., Ilyashuk, B. P., Tylmann, W., Koinig, K. A., & Psenner, R. (2015). Biodiversity dynamics of chironomid midges in high-altitude lakes of the Alps over the past two millennia. *Insect Conservation and Diversity*, *8*(6), 547–561. https://doi.org/10.1111/icad.12137

[84] Jeppesen, E., Kronvang, B., Meerhoff, M., Søndergaard, M., Hansen, K. M., Andersen, H. E., Lauridsen, T. L., Liboriussen, L., Beklioglu, M., Özen, A., & Olesen, J. E. (2009). Climate Change Effects on Runoff, Catchment Phosphorus Loading and Lake Ecological State, and Potential Adaptations. *Journal of Environmental Quality*, *38*(5), 1930–1941. https://doi.org/10.2134/jeq2008.0113

[85] Jiménez-Moreno, G., Heiri, O., García-Alix, A., Anderson, R. S., Jiménez-Espejo, F. J., López-Blanco, C., Jiménez, L., Pérez-Martínez, C., Rodrigo-Gámiz, M., López-Avilés, A., & Camuera, J. (2023). Holocene summer temperature reconstruction based on a chironomid record from Sierra Nevada, southern Spain. *Quaternary Science Reviews*, *319*, 108343. https://doi.org/10.1016/j.quascirev.2023.108343

[86] Jones, P. D., Harpham, C., & Vinther, B. M. (2014). Winter-responding proxy temperature reconstructions and the North Atlantic Oscillation. *Journal of Geophysical Research: Atmospheres*, *119*(11), 6497–6505. https://doi.org/10.1002/2014JD021561

[87] Juggins, S. (2003). *Software for ecological and palaeoecological data analysis and visualisation*. University of Newcastle.

[88] Juggins, S. (2013). Quantitative reconstructions in palaeolimnology: New paradigm or sick science? *Quaternary Science Reviews*, *15*(64), 20–32.

[89] Juggins, S. (2022). *rioja: Analysis of Quaternary science data, R package version (1.0-5)*. https://cran.r-project. org/web/packages/rioja/rioja.pdf

[90] Jyväsjärvi, J., Boros, G., Jones, R. I., & Hämäläinen, H. (2013). The importance of sedimenting organic matter, relative to oxygen and temperature, in structuring lake profundal macroinvertebrate assemblages. *Hydrobiologia*, *709*(1), 55–72. https://doi.org/10.1007/s10750-012-1434-0

[91] Kähkönen, A.-M. (1996). Soil geochemistry in relation to water chemistry and sensitivity to acid deposition in Finnish Lapland. *Water, Air, and Soil Pollution*, *87*(1), 311–327. https://doi.org/10.1007/BF00696844

[92] Kall, T., Oja, T., & Tänavsuu, K. (2014). Postglacial land uplift in Estonia based on four precise levelings. *Tectonophysics*, *610*, 25–38. https://doi.org/10.1016/j.tecto.2013.10.002

[93] Kalm, V., Raukas, A., Rattas, M., & Lasberg, K. (2011). Pleistocene Glaciations in Estonia. In *Developments in Quaternary Sciences* (Vol. 15, pp. 95–104). Elsevier. https://doi.org/10.1016/B978-0-444-53447-7.00008-8

[94] Kamenik, C., Schmidt ,Roland, Kum ,Georg, & and Psenner, R. (2001). The Influence of Catchment Characteristics on the Water Chemistry of Mountain Lakes. *Arctic, Antarctic, and Alpine Research*, *33*(4), 404–409. https://doi.org/10.1080/15230430.2001.12003448

[95] Kansanen, P. H. (1985). *Assessment of Pollution History from Recent Sediments in Lake Vanajavesi, Southern Finland. II. Changes in the Chironomid, Chaoboridae and Ceratopogonidae (Diptera) Fauna*. *22*(1), 57–90.

[96] Karima, Z. (2021). Chironomid: Biology, ecology and systematics. In *The Wonders of Diptera: Characteristics, Diversity, and Significance for the World's Ecosystems* (p. 188). IntechOpen.

[97] Kaufman, D., McKay, N., Routson, C., Erb, M., Davis, B., Heiri, O., Jaccard, S., Tierney, J., Dätwyler, C., Axford, Y., Brussel, T., Cartapanis, O., Chase, B., Dawson, A., De Vernal, A., Engels, S., Jonkers, L., Marsicek, J., Moffa-Sánchez, P., … Zhilich, S. (2020). A global database of Holocene paleotemperature records. *Scientific Data*, *7*(1), 115. https://doi.org/10.1038/s41597-020-0445-3

[98] Kienast, F., Tarasov, P., Schirrmeister, L., Grosse, G., & Andreev, A. A. (2008). Continental climate in the East Siberian Arctic during the last interglacial: Implications from palaeobotanical records. *Global and Planetary Change*, *60*(3), 535–562. https://doi.org/10.1016/j.gloplacha.2007.07.004

[99] Klaus PeterBrodersen, K. P., Pedersen, O., Lindegaard, C., & Hamburger, K. (2004). Chironomids (Diptera) and oxy-regulatory capacity: An experimental approach to paleolimnological interpretation. *Limnology and Oceanography*, *49*(5), 1549–1559. https://doi.org/10.4319/lo.2004.49.5.1549

[100] Klink, A., & Pillot, H. (2003). *Chironomid Larvae: Key to the Higher Taxa and Species of the Lowlands of Northwestern Europe*. Expert-Center for Taxonomic Identification. https://www.nhbs.com/chironomid-larvae

[101] Kopáček, J., Kaňa, J., Šantrůčková, H., Picek, T., & Stuchlík, E. (2004). Chemical and Biochemical Characteristics of Alpine Soils in the Tatra Mountains and their Correlation with Lake Water Quality. *Water, Air, and Soil Pollution*, *153*(1), 307–328. https://doi.org/10.1023/B:WATE.0000019948.23456.14

[102] Korhola, A., Olander, H., & Blom, T. (2000). Cladoceran and chironomid assemblages as qualitative indicators of water depth in subarctic Fennoscandian lakes. *Journal of Paleolimnology*, *24*(1), 43–54. https://doi.org/10.1023/A:1008165732542

[103] Kortelainen, P. (1993). Content of Total Organic Carbon in Finnish Lakes and Its Relationship to Catchment Characteristics. *Canadian Journal of Fisheries and Aquatic Sciences*, *50*(7), 1477–1483. https://doi.org/10.1139/f93-168

[104] Kotrys, B., Płóciennik, M., Sydor, P., & Brooks, S. (2020). Expanding the Swiss-Norwegian chironomid training set with Polish data. *Boreas*, *49*(1), 89–107. https://doi.org/10.1111/bor.12406

[105] Krantzberg, G., & Stokes, P. M. (1988). The importance of surface adsorption and pH in metal accumulation by chironomids. *Environmental Toxicology and Chemistry*, *7*(8), 653–670. https://doi.org/10.1002/etc.5620070807

[106] Kurek, J., & Cwynar, L. (2009). The potential of site-specific and local chironomid-based inference models for reconstructing past lake levels. *Journal of Paleolimnology*, *42*, 37–50. https://doi.org/10.1007/s10933-008-9246-y

[107] Kuusisto, E. (1981). Water temperatures of lakes and rivers in Finland in the period 1961-1975. *Publications of the Water Research Institute (Finland)*, *44*, 40.

[108] Langdon, P. G., Holmes, N., & Caseldine, C. J. (2008). Environmental controls on modern chironomid faunas from NW Iceland and implications for reconstructing climate change. *Journal of Paleolimnology*, *40*(1), 273–293. https://doi.org/10.1007/s10933-007-9157-3

[109] Langdon, P. G., Ruiz, Z., Brodersen, K. P., & Foster, I. D. L. (2006). Assessing lake eutrophication using chironomids: Understanding the nature of community response in different lake types. *Freshwater Biology*, *51*(3), 562–577. https://doi.org/10.1111/j.1365-2427.2005.01500.x

[110] Larocque, I., & Finsinger, W. (2008). Late-glacial chironomid-based temperature reconstructions for Lago Piccolo di Avigliana in the southwestern Alps (Italy). *Palaeogeography, Palaeoclimatology, Palaeoecology*, *257*(1), 207–223. https://doi.org/10.1016/j.palaeo.2007.10.021

[111] Larocque, I., Hall, R. I., & Grahn, E. (2001). Chironomids as indicators of climate change: A 100-lake training set from a subarctic region of northern Sweden (Lapland). *Journal of Paleolimnology*, *26*(3), 307–322. https://doi.org/10.1023/A:1017524101783

[112] Larocque-Tobler, I. (2010). Reconstructing temperature at Egelsee, Switzerland, using North American and Swedish chironomid transfer functions: Potential and pitfalls. *Journal of Paleolimnology*, *44*(1), 243–251. https://doi.org/10.1007/s10933-009-9400-1

[113] Larocque-Tobler, I. (2014). The Polish sub-fossil chironomids. *Palaeontologia Electronica*, *17*(1;3A), 28. https://doi.org/10.26879/391

[114] Larsen, A. S., O'Donnell, J. A., Schmidt, J. H., Kristenson, H. J., & Swanson, D. K. (2017). Physical and chemical characteristics of lakes across heterogeneous landscapes in arctic and subarctic Alaska. *Journal of Geophysical Research: Biogeosciences*, *122*(4), 989–1008. https://doi.org/10.1002/2016JG003729

[115] Lasberg, K., & Kalm, V. (2013). Chronology of Late Weichselian glaciation in the western part of the East European Plain. *Boreas*, *42*(4), 995–1007. https://doi.org/10.1111/bor.12016

[116] Laumets, L., Kalm, V., Poska, A., Kele, S., Lasberg, K., & Amon, L. (2014). Palaeoclimate inferred from δ18O and palaeobotanical indicators in freshwater tufa of Lake Äntu Sinijärv, Estonia. *Journal of Paleolimnology*, *51*(1), 99–111. https://doi.org/10.1007/s10933-013-9758-y

[117] Lepš, J., & Šmilauer, P. (2003). *Multivariate Analysis of Ecological Data using CANOCO*. Cambridge University Press. https://doi.org/10.1017/CBO9780511615146

[118] Little, J. L., & Smol, J. P. (2001). A chironomid-based model for inferring late-summer hypolimnetic oxygen in southeastern Ontario lakes. *Journal of Paleolimnology*, *26*(3), 259–270. https://doi.org/10.1023/A:1017562703986

[119] Liu, Z., Kutzbach, J., & Wu, L. (2000). Modeling climate shift of El Nino variability in the Holocene. *Geophysical Research Letters*, *27*(15), 2265–2268. https://doi.org/10.1029/2000GL011452

[120] Liu, Z., Wang, Y., Gallimore, R., Gasse, F., Johnson, T., deMenocal, P., Adkins, J., Notaro, M., Prentice, I. C., Kutzbach, J., Jacob, R., Behling, P., Wang, L., & Ong, E. (2007). Simulating the transient evolution and abrupt change of Northern Africa atmosphere–ocean–terrestrial ecosystem in the Holocene. *Quaternary Science Reviews*, *26*(13), 1818–1837. https://doi.org/10.1016/j.quascirev.2007.03.002

[121] Lotter, A. F., Appleby, P. G., Bindler, R., Dearing, J. A., Grytnes, J.-A., Hofmann, W., Kamenik, C., Lami, A., Livingstone, D. M., Ohlendorf, C., Rose, N., & Sturm, M. (2002). The sediment record of the past 200 years in a Swiss high-alpine lake: Hagelseewli (2339 m a.s.l.). *Journal of Paleolimnology*, *28*(1), 111–127. https://doi.org/10.1023/A:1020328119961

[122] Lotter, A. F., Sturm, M., Teranes, J. L., & Wehrli, B. (1997). Varve formation since 1885 and high-resolution varve analyses in hypertrophic Baldeggersee (Switzerland). *Aquatic Sciences*, *59*(4), 304–325. https://doi.org/10.1007/BF02522361

[123] Lucas, E., Kennedy, B., Roswall, T., Burgis, C., & Toor, G. S. (2023). Climate Change Effects on Phosphorus Loss from Agricultural Land to Water: A Review. *Current Pollution Reports*, *9*(4), 623–645. https://doi.org/10.1007/s40726-023-00282-7

[124] Luoto, T., Kotrys, B., & Płóciennik, M. (2019). East European chironomid-based calibration model for past summer temperature reconstructions. *Climate Research*, *77*(1), 63–76. https://doi.org/10.3354/cr01543

[125] Luoto, (2009). Subfossil Chironomid (Insecta: Diptera) along a latitudinal gradient in Finland: development of a new temperature inference model. *Journal of Quaternary Science*, *24*(2), 150–158. https://doi.org/10.1002/jqs.1191

[126] Luoto, (2011). The relationship between water quality and chironomid distribution in Finland—A new assemblage-based tool for assessments of long-term nutrient dynamics. *Ecological Indicators*, *11*(2), 255–262. https://doi.org/10.1016/j.ecolind.2010.05.002

[127] Luoto, , Kultti, S., Nevalainen, L., & Sarmaja-Korjonen, K. (2010). Temperature and effective moisture variability in southern Finland during the Holocene quantified with midge-based calibration models. *Journal of Quaternary Science*, *25*(8), 1317–1326. https://doi.org/10.1002/jqs.1417

[128] Luoto, , & Ojala, A. E. K. (2018). Controls of climate, catchment erosion and biological production on long-term community and functional changes of chironomids in High Arctic lakes (Svalbard). *Palaeogeography, Palaeoclimatology, Palaeoecology*, *505*, 63–72. https://doi.org/10.1016/j.palaeo.2018.05.026

[129] Luoto, , Rantala, M. V., Galkin, A., Rautio, M., & Nevalainen, L. (2016). Environmental determinants of chironomid communities in remote northern lakes across the treeline – Implications for climate change assessments. *Ecological Indicators*, *61*, 991–999. https://doi.org/10.1016/j.ecolind.2015.10.057

[130] Luoto, , & Salonen, V. P. (2010). Fossil midge larvae (Diptera: Chironomid) as quantitative indicators of late-winter hypolimnetic oxygen in southern Finland: A calibration model, case studies and potentialities. *Boreal Environment Research*, *15*, 1–18.

[131] Magny, M., Guiot, J., & Schoellammer, P. (2001). Quantitative Reconstruction of Younger Dryas to Mid-Holocene Paleoclimates at Le Locle, Swiss Jura, Using Pollen and Lake-Level Data. *Quaternary Research*, *56*(2), 170–180. https://doi.org/10.1006/qres.2001.2257

[132] Magny, M., & Haas, J. N. (2004). A major widespread climatic change around 5300 cal Yr BP at the time of the Alpine Iceman. *Journal of Quaternary Science*, *19*(5), 423–430. https://doi.org/10.1002/jqs.850

[133] Marsicek, J., Shuman, B. N., Bartlein, P. J., Shafer, S. L., & Brewer, S. (2018). Reconciling divergent trends and millennial variations in Holocene temperatures. *Nature*, *554*(7690), 92–96. https://doi.org/10.1038/nature25464

[134] Martel-Cea, A., Astorga, G. A., Hernández, M., Caputo, L., & Abarzúa, A. M. (2021). Modern chironomids (Diptera: Chironomid) and the environmental variables that influence their distribution in the Araucanian lakes, south-central Chile. *Hydrobiologia*, *848*(10), 2551–2568. https://doi.org/10.1007/s10750-021-04575-0

[135] Mayewski, P. A., Rohling, E. E., Curt Stager, J., Karlén, W., Maasch, K. A., Meeker, L. D., Meyerson, E. A., Gasse, F., Van Kreveld, S., Holmgren, K., Lee-Thorp, J., Rosqvist, G., Rack, F., Staubwasser, M., Schneider, R. R., & Steig, E. J. (2004). Holocene climate variability. *Quaternary Research*, *62*(3), 243–255. https://doi.org/10.1016/j.yqres.2004.07.001

[136] Medeiros, A., Chipman, M., Francis, D., Hamerlík, L., Langdon, P., Puleo, P., Schellinger, G., Steigleder, R., Walker, I., Woodroffe, S., & Axford, Y. (2022). A continental-scale chironomid training set for reconstructing Arctic temperatures. *Quaternary Science Reviews*, *15*(294), 107728.

[137] Meier, H. E. M., Kniebusch, M., Dieterich, C., Gröger, M., Zorita, E., Elmgren, R., Myrberg, K., Ahola, M. P., Bartosova, A., Bonsdorff, E., Börgel, F., Capell, R., Carlén, I., Carlund, T., Carstensen, J., Christensen, O. B., Dierschke, V., Frauen, C., Frederiksen, M., … Zhang, W. (2022). Climate change in the Baltic Sea region: A summary. *Earth System Dynamics*, *13*(1), 457–593. https://doi.org/10.5194/esd-13-457-2022

[138] Miles, M. W., Andresen, C. S., & Dylmer, C. V. (2020). Evidence for extreme export of Arctic sea ice leading the abrupt onset of the Little Ice Age. *Science Advances*, *6*(38), eaba4320. https://doi.org/10.1126/sciadv.aba4320

[139] Mooney, S. D., & Tinner, W. (2011). The analysis of charcoal in peat and organic sediments. *Mires and Peat*, *7*, 09.

[140] Moore, P. D., Webb, J. A., & Collinson, M. E. (1991). *Pollen analysis*. Blackwell.

[141] Moros, M., Emeis, K., Risebrobakken, B., Snowball, I., Kuijpers, A., McManus, J., & Jansen, E. (2004). Sea surface temperatures and ice rafting in the Holocene North Atlantic: Climate influences on northern Europe and Greenland. *Quaternary Science Reviews*, *23*(20), 2113–2126. https://doi.org/10.1016/j.quascirev.2004.08.003

[142] Mousavi, S. K. (2002). *Boreal chironomid communities and their relations to environmental factors—The impact of lake depth, size and acidity. 7*, 63–75.

[143] Nazarova, L., Syrykh, L., Grekov, I., Sapelko, T., Krasheninnikov, A., & Solovieva, N. (2023). *Chironomid-Based Modern Summer Temperature Data Set and Inference Model for the Northwest European Part of Russia*. *15(5)*, 976. https://doi.org/10.3390/w15050976

[144] Nelson, P. N., Cotsaris, E., Oades, J. M., & Bursill, D. B. (1990). Influence of soil clay content on dissolved organic matter in stream waters. *Marine and Freshwater Research*, *41*(6), 761–774. https://doi.org/10.1071/mf9900761

[145] Ni, Z., Zhang, E., Meng, X., Sun, W., & Ning, D. (2023). Chironomid-based reconstruction of 500-year water-level changes in Daihai Lake, northern China. *CATENA*, *227*, 107122. https://doi.org/10.1016/j.catena.2023.107122

[146] Niinemets, E., & Saarse, L. (2009). Holocene vegetation and land-use dynamics of south-eastern Estonia. *Quaternary International*, *207*(1–2), 104–116. https://doi.org/10.1016/j.quaint.2008.11.015

[147] Nishimura, P., & Laroque, C. (2011). Observed continentality in radial growth–climate relationships in a twelve site network in western Labrador, Canada. *Dendrochronologia*, *29*(1), 17–23.

[148] Nyman, M., Korhola, A., & Brooks, S. J. (2005). The distribution and diversity of Chironomid (Insecta: Diptera) in western Finnish Lapland, with special emphasis on shallow lakes. *Global Ecology and Biogeography*, *14*(2), 137–153. https://doi.org/10.1111/j.1466-822X.2005.00148.x

[149] O'Brien, S. R., Mayewski, P. A., Meeker, L. D., Meese, D. A., Twickler, M. S., & Whitlow, S. I. (1995). Complexity of Holocene Climate as Reconstructed from a Greenland Ice Core. *Science*, *270*(5244), 1962–1964. https://doi.org/10.1126/science.270.5244.1962

[150] Oksanen, J., Simpson, G., Blanchet, F., Kindt, R., Legendre, P., Minchin, P., O'Hara, R., Solymos, P., Stevens, M., Szoecs, E., Wagner, H., Barbour, M., Bedward, M., Bolker, B., Borcard, D., Carvalho, G., Chirico, M., De Caceres, M., Durand, S., … Weedon, J. (2022). *Vegan: Community ecology package. R package version 2.6-4*. https://CRAN.R-project. org/package=vegan

[151] Oppo, D. W., McManus, J. F., & Cullen, J. L. (2003). Deepwater variability in the Holocene epoch. *Nature*, *422*(6929), 277–277. https://doi.org/10.1038/422277b

[152] Orendt, C. (1999). Chironomids as Bioindicators in Acidified Streams: A Contribution to the Acidity Tolerance of Chironomid Species with a Classification in Sensitivity Classes. *International Review of Hydrobiology*, *84*(5), 439–449. https://doi.org/10.1002/iroh.199900038

[153] Owens, M. J., Lockwood, M., Hawkins, E., Usoskin, I., Jones, G. S., Barnard, L., Schurer, A., & Fasullo, J. (2017). The Maunder minimum and the Little Ice Age: An update from recent reconstructions and climate simulations. *Journal of Space Weather and Space Climate*, *7*, A33. https://doi.org/10.1051/swsc/2017034

[154] Pegler, S., Simmatis, B., Labaj, A. L., Meyer-Jacob, C., & Smol, J. P. (2020). Long-Term Changes in Chironomid Assemblages Linked to Lake Liming and Fertilization in Previously Acidified Middle Lake (Sudbury, Canada). *Water, Air, & Soil Pollution*, *231*(8), 410. https://doi.org/10.1007/s11270-020-04780-y

[155] Pinder, L. C. V. (1992). Biology of epiphytic Chironomid (Diptera:Nematocera) in chalk streams. *Hydrobiologia*, *248*(1), 39–51. https://doi.org/10.1007/BF00008884

[156] Płóciennik, M., Self, A., Birks, H. J. B., & Brooks, S. J. (2011). Chironomid (Insecta: Diptera) succession in Żabieniec bog and its palaeo-lake (central Poland) through the Late Weichselian and Holocene. *Palaeogeography, Palaeoclimatology, Palaeoecology*, *307*(1), 150–167. https://doi.org/10.1016/j.palaeo.2011.05.010

[157] Poska, A., Väli, V., Vassiljev, J., Alliksaar, T., & Saarse, L. (2022). Timing and drivers of local to regional scale land-cover changes in the hemiboreal forest zone during the Holocene: A pollen-based study from South Estonia. *Quaternary Science Reviews*, *277*, 107351. https://doi.org/10.1016/j.quascirev.2021.107351

[158] Preston, D., Caine, N., McKnight, D., Williams, M., Hell, K., Miller, M., Hart, S., & Johnson, P. (2016). Climate regulates alpine lake ice-cover phenology and aquatic ecosystem structure. *Geophysical Research Letters*, *43*(10), 5353–5360. https://doi.org/10.1002/2016GL069036

[159] Quinlan, R., Douglas, M. S. V., & Smol, J. P. (2005). Food web changes in arctic ecosystems related to climate warming. *Global Change Biology*, *11*(8), 1381–1386. https://doi.org/10.1111/j.1365-2486.2005.00981.x

[160] Quinlan, R., & Smol, J. P. (2002). Regional assessment of long-term hypolimnetic oxygen changes in Ontario (Canada) shield lakes using subfossil chironomids. *Journal of Paleolimnology*, *27*(2), 249–260. https://doi.org/10.1023/A:1014219629845

[161] Quinlan, R., Smol, J. P., & Hall, R. I. (1998). Quantitative inferences of past hypolimnetic anoxia in south-central Ontario lakes using fossil midges (Diptera: Chironomid). *Canadian Journal of Fisheries and Aquatic Sciences*, *55*(3), 587–596. https://doi.org/10.1139/f97-279

[162] Rao, Z., Tian, Y., Guang, K., Wei, S., Guo, H., Feng, Z., Zhao, L., & Li, Y. (2022). Pollen Data as a Temperature Indicator in the Late Holocene: A Review of Results on Regional, Continental and Global Scales. *Frontiers in Earth Science*, *10*, 845650. https://doi.org/10.3389/feart.2022.845650

[163] Rasmussen, S. O., Dahl-Jensen, D., Fischer, H., Fuhrer, K., Hansen, S. B., Hansson, M., Hvidberg, C. S., Jonsell, U., Kipfstuhl, S., Ruth, U., Schwander, J., Siggaard-Andersen, M.-L., Sinnl, G., Steffensen, J. P., Svensson, A. M., & Vinther, B. M. (2023). Ice-core data used for the construction of the Greenland Ice-Core Chronology 2005 and 2021 (GICC05 and GICC21). *Earth System Science Data*, *15*(8), 3351–3364. https://doi.org/10.5194/essd-15-3351-2023

[164] Raukas, A., & Teedumäe, A. (1997). *Geology and Mineral Resources of Estonia*. Estonian Academy Publishers.

[165] Rees, A. B. H., Cwynar, L. C., & Cranston, P. S. (2008). Midges (Chironomid, Ceratopogonidae, Chaoboridae) as a temperature proxy: A training set from Tasmania, Australia. *Journal of Paleolimnology*, *40*(4), 1159–1178. https://doi.org/10.1007/s10933-008-9222-6

[166] Renssen, H., Isarin, R. F. B., Jacob, D., Podzun, R., & Vandenberghe, J. (2001). Simulation of the Younger Dryas climate in Europe using a regional climate model nested in an AGCM: Preliminary results. *Global and Planetary Change*, *30*(1–2), 41–57. https://doi.org/10.1016/S0921-8181(01)00076-5

[167] Rigterink, S., Krahn, K. J., Kotrys, B., Urban, B., Heiri, O., Turner, F., Pannes, A., & Schwalb, A. (2024). Summer temperatures from the Middle Pleistocene site Schöningen 13, northern Germany, determined from subfossil chironomid assemblages. *Boreas*, *53*(4), 525–542. https://doi.org/10.1111/bor.12658

[168] Roosa, S., Prygiel, E., Lesven, L., Wattiez, R., Gillan, D., Ferrari, B. J. D., Criquet, J., & Billon, G. (2016). On the bioavailability of trace metals in surface sediments: A combined geochemical and biological approach. *Environmental Science and Pollution Research*, *23*(11), 10679–10692. https://doi.org/10.1007/s11356-016-6198-z

[169] Ruse, L. P., Ruse, L. R., Herrmann, S. J., & Sublette, J. E. (2000). Chironomid (diptera) Species Distribution Related to Environmental Characteristics of the Metal-Polluted Arkansas River, Colorado. *Western North American Naturalist*, *60*(1), 34–56.

[170] Saarse, L., & Veski, S. (2001). Spread of broad-leaved trees in Estonia. *Proceedings of the Estonian Academy of Sciences, Geology*, *50*(1), 51–65.

[171] Sæther, O. A. (2000). Zoogeographical patterns in Chironomid (Diptera). *SIL Proceedings, 1922-2010*, *27*(1), 290–302. https://doi.org/10.1080/03680770.1998.11901242

[172] Salonen, J. S., Seppä, H., Luoto, M., Bjune, A. E., & Birks, H. J. B. (2012). A North European pollen–climate calibration set: Analysing the climatic responses of a biological proxy using novel regression tree methods. *Quaternary Science Reviews*, *45*, 95–110. https://doi.org/10.1016/j.quascirev.2012.05.003

[173] Salonen, V.-P., Alhonen, P., Itkonen, A., & Olander, Heikki. (1993). *The trophic history of Enajarvi, SW Finland, with special reference to its restoration problems*. *268*, 147–162.

[174] Schütz, S. A., & Füreder, L. (2019). Egg development and hatching success in alpine chironomids. *Freshwater Biology*, *64*(4), 685–696. https://doi.org/10.1111/fwb.13254

[175] Seire, A., & Pall, P. (2000). *Chironomid larvae(Diptera, Chironomid) as indicators of water quality in Estonian streams*. *49*(4), 307–316.

[176] Šeirienė, V., Gastevičienė, N., Luoto, , Gedminienė, L., & Stančikaitė, M. (2021). The Lateglacial and early Holocene climate variability and vegetation dynamics derived from chironomid and pollen records of Lieporiai palaeolake, North Lithuania. *Quaternary International*, *605–606*, 55–64. https://doi.org/10.1016/j.quaint.2020.12.017

[177] Self, A., Brooks, S., Birks, H., Nazarova, L., Porinchu, D., Odland, A., Yang, H., & Jones, V. (2011). *The distribution and abundance of chironomids in high-latitude Eurasian lakes with respect to temperature and continentality: Development and application of new chironomid-based climate-inference models in northern Russia*. *30(9-10)*. https://doi.org/10.1016/j.quascirev.2011.01.022

[178] Seppä, H., Bjune, A. E., Telford, R. J., Birks, H. J. B., & Veski, S. (2009). Last nine-thousand years of temperature variability in Northern Europe. *Climate of the Past*, *5*(3), 523–535. https://doi.org/10.5194/cp-5-523-2009

[179] Seppä, H., Hammarlund, D., & Antonsson, K. (2005). Low-frequency and high-frequency changes in temperature and effective humidity during the Holocene in south-central Sweden: Implications for atmospheric and oceanic forcings of climate. *Climate Dynamics*, *25*(2–3), 285–297. https://doi.org/10.1007/s00382-005-0024-5

[180] Seppä, H., & Poska, A. (2004). Holocene annual mean temperature changes in Estonia and their relationship to solar insolation and atmospheric circulation patterns. *Quaternary Research*, *61*(1), 22–31. https://doi.org/10.1016/j.yqres.2003.08.005

[181] Sher, A., Kuzmina, S., Kiseyov, S., & Lister, A. (2003). *Tundra-steppe environment in Arctic Siberia and the evolution of the woolly mammoth*. 136–142.

[182] Shin, S.-I., Sardeshmukh, P. D., Webb, R. S., Oglesby, R. J., & Barsugli, J. J. (2006). Understanding the Mid-Holocene Climate. *Journal of Climate*, *19*(12), 2801–2817. https://doi.org/10.1175/JCLI3733.1

[183] Shuman, B. (2012). Patterns, processes, and impacts of abrupt climate change in a warm world: The past 11,700 years. *WIREs Climate Change*, *3*(1), 19–43. https://doi.org/10.1002/wcc.152

[184] Solomina, O. N., Bradley, R. S., Hodgson, D. A., Ivy-Ochs, S., Jomelli, V., Mackintosh, A. N., Nesje, A., Owen, L. A., Wanner, H., Wiles, G. C., & Young, N. E. (2015). Holocene glacier fluctuations. *Quaternary Science Reviews*, *111*, 9–34. https://doi.org/10.1016/j.quascirev.2014.11.018

[185] Stansell, N. D., Klein, E. S., Finkenbinder, M. S., Fortney, C. S., Dodd, J. P., Terasmaa, J., & Nelson, D. B. (2017). A stable isotope record of Holocene precipitation dynamics in the Baltic region from Lake Nuudsaku, Estonia. *Quaternary Science Reviews*, *175*, 73–84. https://doi.org/10.1016/j.quascirev.2017.09.013

[186] Steiner, D., Pauling, A., Nussbaumer, S. U., Nesje, A., Luterbacher, J., Wanner, H., & Zumbühl, H. J. (2008). Sensitivity of European glaciers to precipitation and temperature – two case studies. *Climatic Change*, *90*(4), 413–441. https://doi.org/10.1007/s10584-008-9393-1

[187] Stivrins, N., Belle, S., Trasune, L., Blaus, A., & Salonen, S. (2021). Food availability and temperature optima shaped functional composition of chironomid assemblages during the Late Glacial–Holocene transition in Northern Europe. *Quaternary Science Reviews*, *266*, 107083. https://doi.org/10.1016/j.quascirev.2021.107083

[188] Stivrins, N., Soininen, J., Amon, L., Fontana, S. L., Gryguc, G., Heikkilä, M., Heiri, O., Kisielienė, D., Reitalu, T., Stančikaitė, M., Veski, S., & Seppä, H. (2016). Biotic turnover rates during the Pleistocene-Holocene transition. *Quaternary Science Reviews*, *151*, 100–110. https://doi.org/10.1016/j.quascirev.2016.09.008

[189] Stonevicius, E., Stankunavicius, G., & Rimkus, E. (2018). Continentality and Oceanity in the Mid and High Latitudes of the Northern Hemisphere and Their Links to Atmospheric Circulation. *Advances in Meteorology*, *1*, 5746191. https://doi.org/10.1155/2018/5746191

[190] Stralberg, D., Arseneault, D., Baltzer, J. L., Barber, Q. E., Bayne, E. M., Boulanger, Y., Brown, C. D., Cooke, H. A., Devito, K., Edwards, J., Estevo, C. A., Flynn, N., Frelich, L. E., Hogg, E. H., Johnston, M., Logan, T., Matsuoka, S. M., Moore, P., Morelli, T. L., … Whitman, E. (2020). Climate-change refugia in boreal North America: What, where, and for how long? *Frontiers in Ecology and the Environment*, *18*(5), 261–270. https://doi.org/10.1002/fee.2188

[191] Stumm, W., Morgan, J. J., & Drever, J. I. (1996). Aquatic chemistry. *Journal of Environmental Quality*, *25*(5), 1162.

[192] Suranyi, T., Talbot, J., Francis, D., Feussom Tcheumeleu, A., Grondin, P., Rius, D., Ali, A. A., Bergeron, Y., & Millet, L. (2025). Chironomid assemblages in surface sediments from 182 lakes across New England and Eastern Canada: Development and validation of a new summer temperature transfer function. *Quaternary Science Reviews*, *357*, 109333. https://doi.org/10.1016/j.quascirev.2025.109333

[193] Takahashi, M. A., Higuti, J., Bagatini, M., Zviejkovski, I. P., & Velho, L. F. M. (2008). *Composition and biomass of larval chironomid (Insecta, Diptera) as potential indicator of trophic conditions in southern Brazil reservoirs*. *20*(1), 5–13.

[194] ter Braak, C. J. F., & Juggins, S. (1993). Weighted averaging partial least squares regression (WA-PLS): An improved method for reconstructing environmental variables from species assemblages. *Hydrobiologia*, *269*(1), 485–502. https://doi.org/10.1007/BF00028046

[195] Theuerkauf, M., & Joosten, H. (2012). Younger Dryas cold stage vegetation patterns of central Europe–climate, soil and relief controls. *Boreas*, *41*(3), 391–407. https://doi.org/10.1111/j.1502-3885.2011.00240.x

[196] Töchterle, P., Baldo, A., Murton, J. B., Schenk, F., Edwards, R. L., Koltai, G., & Moseley, G. E. (2024). Reconstructing Younger Dryas ground temperature and snow thickness from cave deposits. *Climate of the Past*, *20*(7), 1521–1535. https://doi.org/10.5194/cp-20-1521-2024

[197] Tóth, M., Magyari, E. K., Buczkó, K., Braun, M., Panagiotopoulos, K., & Heiri, O. (2015). Chironomid-inferred Holocene temperature changes in the South Carpathians (Romania). *The Holocene*, *25*(4), 569–582. https://doi.org/10.1177/0959683614565953

[198] Väliranta, M., Salonen, J. S., Heikkilä, M., Amon, L., Helmens, K., Klimaschewski, A., Kuhry, P., Kultti, S., Poska, A., Shala, S., Veski, S., & Birks, H. H. (2015). Plant macrofossil evidence for an early onset of the Holocene summer thermal maximum in northernmost Europe. *Nature Communications*, *6*(1), 6809. https://doi.org/10.1038/ncomms7809

[199] van Kleef, H., Verberk, W. C. E. P., Kimenai, F. F. P., van der Velde, G., & Leuven, R. S. E. W. (2015). Natural recovery and restoration of acidified shallow soft-water lakes: Successes and bottlenecks revealed by assessing life-history strategies of chironomid larvae. *Basic and Applied Ecology*, *16*(4), 325–334. https://doi.org/10.1016/j.baae.2015.02.007

[200] Velle, G., Brodersen, K. P., Birks, H. J. B., & Willassen, E. (2010). Midges as quantitative temperature indicator species: Lessons for palaeoecology. *The Holocene*, *20*(6), 989–1002. https://doi.org/10.1177/0959683610365933

[201] Velle, G., Brooks, S. J., Birks, H. J. B., & Willassen, E. (2005). Chironomids as a tool for inferring Holocene climate: An assessment based on six sites in southern Scandinavia. *Quaternary Science Reviews*, *24*(12), 1429–1462. https://doi.org/10.1016/j.quascirev.2004.10.010

[202] Verbruggen, F., Heiri, O., Meriläinen, J., & Lotter, A. (2011). Subfossil chironomid assemblages in deep, stratified European lakes: Relationships with temperature, trophic state and oxygen. *Freshwater Biology*, *56*(3), 407–423. https://doi.org/10.1111/j.1365-2427.2010.02508.x

[203] Verschuren, D., & Eggermont, H. (2006). Quaternary paleoecology of aquatic Diptera in tropical and Southern Hemisphere regions, with special reference to the Chironomid. *Quaternary Science Reviews*, *25*(15), 1926–1947. https://doi.org/10.1016/j.quascirev.2006.01.008

[204] Veski, S., Seppä, H., Stančikaitė, M., Zernitskaya, V., Reitalu, T., Gryguc, G., Heinsalu, A., Stivrins, N., Amon, L., Vassiljev, J., & Heiri, O. (2015). Quantitative summer and winter temperature reconstructions from pollen and chironomid data between 15 and 8 ka BP in the Baltic–Belarus area. *Quaternary International*, *19*(388), 4–11.

[205] Vilar, A. G., Donders, T., Cvetkoska, A., & Wagner-Cremer, F. (2018). Seasonality modulates the predictive skills of diatom based salinity transfer functions. *PLOS ONE*, *13*(11), e0199343. https://doi.org/10.1371/journal.pone.0199343

[206] Vollweiler, N., Scholz, D., Mühlinghaus, C., Mangini, A., & Spötl, C. (2006). A precisely dated climate record for the last 9 kyr from three high alpine stalagmites, Spannagel Cave, Austria. *Geophysical Research Letters*, *33*(20), 2006GL027662. https://doi.org/10.1029/2006GL027662

[207] Walker, I. R. (1987). Chironomid (Diptera) in paleoecology. *Quaternary Science Reviews*, *6*(1), 29–40. https://doi.org/10.1016/0277-3791(87)90014-X

[208] Walker, I. R. (2001). Midges: Chironomid and Related Diptera. In J. P. Smol, H. J. B. Birks, & W. M. Last (Eds.), *Tracking Environmental Change Using Lake Sediments* (Vol. 4, pp. 43–66). Springer Netherlands. https://doi.org/10.1007/0-306-47671-1_3

[209] Walker, I. R., & MacDonald, G. M. (1995). Distributions of Chironomid (Insecta: Diptera) and other Freshwater Midges with Respect to Treeline, Northwest Territories, Canada. *Arctic and Alpine Research*, *27*(3), 258–263. https://doi.org/10.1080/00040851.1995.12003120

[210] Walker, I. R., & Mathewes, R. W. (1987). Chironomid (Diptera) and Postglacial Climate at Marion Lake, British Columbia, Canada. *Quaternary Research*, *27*(1), 89–102. https://doi.org/10.1016/0033-5894(87)90052-4

[211] Wanner, H., Beer, J., Bütikofer, J., Crowley, T. J., Cubasch, U., Flückiger, J., Goosse, H., Grosjean, M., Joos, F., Kaplan, J. O., Küttel, M., Müller, S. A., Prentice, I. C., Solomina, O., Stocker, T. F., Tarasov, P., Wagner, M., & Widmann, M. (2008). Mid- to Late Holocene climate change: An overview. *Quaternary Science Reviews*, *27*(19), 1791–1828. https://doi.org/10.1016/j.quascirev.2008.06.013

[212] Wickham, H., Averick, M., Bryan, J., Chang, W., McGowan, L. D., François, R., Grolemund, G., Hayes, A., Henry, L., Hester, J., Kuhn, M., Pedersen, T. L., Miller, E., Bache, S. M., Müller, K., Ooms, J., Robinson, D., Seidel, D. P., Spinu, V., … Yutani, H. (2019). Welcome to the Tidyverse. *Journal of Open Source Software*, *4*(43), 1686. https://doi.org/10.21105/joss.01686

[213] Wickham, H., Francois, R., Henry, L., & Muller, K. (2022). *Dplyr: A grammar of data manipulation. R package version 1.0.10*.

[214] Williams, J., Jackson, S., & Kutzbach, J. (2007). Projected distributions of novel and disappearing climates by 2100 AD. *Proceedings of the National Academy of Sciences*, *104*(14), 5738–5742. https://doi.org/doi.org//pnas.0606292104

[215] Wood, S. N. (2011). Fast stable restricted maximum likelihood and marginal likelihood estimation of semiparametric generalized linear models. *Journal of the Royal Statistical Society: Series B (Statistical Methodology)*, *73*(1), 3–36. https://doi.org/10.1111/j.1467-9868.2010.00749.x

[216] Wood, S. N. (2017). *Generalized Additive Models: An Introduction with R* (2nd ed.). Chapman and Hall/CRC. https://doi.org/10.1201/9781315370279

[217] Woodcock, T., Longcore, J., McAuley, D., Mingo, T., Bennatti, C. R., & Stromborg, K. (2005). The role of pH in structuring communities of maine wetland macrophytes and chironomid larvae (Diptera). *Wetlands*, *25*(2), 306–316. https://doi.org/10.1672/7

[218] Zambakas, J. (1992). *General climatology*. Department of Geology, National & Kapodistrian University of Athens, Greece.

[219] Zani, D., Lischke, H., & Lehsten, V. (2023). Climate and dispersal limitation drive tree species range shifts in post-glacial Europe: Results from dynamic simulations. *Frontiers in Ecology and Evolution*, *11*, 1321104. https://doi.org/10.3389/fevo.2023.1321104

[220] Zdorovennova, G., Zdorovennov, R., & Terzhevik, A. (2021). Dissolved Oxygen in a Shallow Ice-Covered Lake in Winter: Effect of Changes in Light, Thermal and Ice Regimes. *Water*, *13*(17), 2435. https://doi.org/10.3390/w13172435

[221] Zhang, E., Cao, Y., Langdon, P., Wang, Q., Shen, J., & Yang, X. (2013). Within-lake variability of subfossil chironomid assemblage in a large, deep subtropical lake (Lugu lake, southwest China). *Journal of Limnology*, *72*(1), 10. https://doi.org/10.4081/jlimol.2013.e10

[222] Zhang, E., Tang, H., Cao, Y., Langdon, P., Wang, R., Yang, X., & Shen, J. (2013). The effects of soil erosion on chironomid assemblages in Lugu Lake over the past 120 years. *International Review of Hydrobiology*, *98*(3), 165–172. https://doi.org/10.1002/iroh.201301468

Acknowledgements

My PhD experience has been both challenging and exciting – a true adventure filled with opportunities to grow as a scientist and as a person. I would like to express my sincere appreciations to the many people who made this journey possible.

I extend my heartfelt gratitude to my supervisor, Prof. Siim Veski, for his unwavering support, expert guidance, and patience throughout these years. Thank you for helping me navigate both scientific and organizational challenges, for your countless valuable insights, and for laying the foundation of the papers through your experience, ideas and vision. The guidance you provided has shaped my development as both a researcher and an individual.

A very special thank you to my co-supervisor, Dr. Anneli Poska. I am forever grateful that your announcement about this PhD opportunity reached me four and a half years ago. Thank you for your incredible dedication – spending countless hours guiding me through data analysis, scientific writing, and, especially, for your emotional support throughout this entire journey.

I am also thankful to my co-supervisor, Dr. Simon Belle, for introducing me to the method of chironomid analysis and for providing me an expertise and a comprehensive overview of the methodology from multiple perspectives. This learning was incredibly important.

My sincere thanks to all the colleagues I met at conferences and workshops – your feedback and advice were truly invaluable. I especially thank Prof. Oliver Heiri and Prof. Mateusz Płóciennik for hosting me in their laboratories during internships and for their continued scientific support afterward.

I would also like to acknowledge my colleagues at Tallinn University of Technology. Atko Heinsalu, Jüri Vassiljev, Merlin Liiv have been incredibly helpful with both scientific and organizational matters. My appreciation to Olle Hints for being an outstanding head of department, and to Helle Pohl-Raidla for her tireless support in the daily life of the department.

To my fellow PhD students – thank you for the conversations, collaboration, and shared experiences that helped make the journey more manageable. I would especially like to thank my office mates, Ivan, Anna, and Eliise, for the friendship, warm-heartedness and support over the years.

To my spouse, Yurii – there's no short way to express how much your support has meant to me over these years, so I will simply say that I am grateful we went through it together. To my friends and family, thank you for staying in touch, maintaining our bonds, and cheering me on. I am especially grateful to my mum, Marina, my little sister, Alexandra, and my grandmother, Valentina, for their help during fieldwork in Russia and for their constant encouragement throughout my PhD journey.

Finally, I want to acknowledge my grandfather, Vladimir. Although he could not witness this moment, his support played a key role in shaping my path. From taking me to natural history museums in my early childhood to providing everything I needed during my university years; he always encouraged me to follow my dreams and pursue a life in science.

This work was supported by the Estonian Research Council grants PRG1993 and TK215; Doctoral School of Earth Sciences and Ecology, supported by the European Union, European Regional Development Fund (ASTRA "TTÜ arenguprogramm aastateks 2016–2022"); Kristjan Jaak scholarship; Dora Plus scholarship.

Abstract

Postglacial climate change in Eastern Europe: focus on Chironomid-based reconstruction of summer temperatures and continentality

The current PhD thesis investigates the use of fossil Chironomidae (non-biting midges) as bioindicators for reconstructing past climatic conditions, specifically mean July air temperature (T) and continentality. In the scope of the thesis, two chironomid-based inference models were developed and applied to two palaeosediment sequences in the understated in terms of Eastern Baltic and nearby areas to enhance our understanding of late Quaternary climate variability and ecosystem responses.

The first component of the study introduces a new Finno-Baltic-Polish (FBP) chironomid training set (121 lakes), extending the geographic and climatic coverage of July air T-based reconstructions into the eastern Baltic lowlands. Canonical correspondence analysis revealed the strong influence of July air temperature 9.1% on chironomid assemblages distribution. Cross-correlated weighted averaging-partial least squares chironomid-July air T inference model revealed the robust performance values with $RMSEP_{boot}$ = 0.7 °C, thus reinforcing the reliability of chironomid-based temperature reconstructions in previously underrepresented regions.

Further, the ecological relevance of continentality as a driver of modern chironomid distribution was evaluated across longitudinally distributed 51 lakes in the East European Plain and southern Scandinavia, as well as in the FBP training set. The results demonstrate that chironomid assemblages exhibit clear responses to continentality gradients. Notably, the Kerner Oceanity Index revealed the highest explanatory power (18.4%) in the longitudinal continental dataset, whereas the annual temperature range (ATR) was the most critical continentality-related variable in the FBP training set (11%).

The final component of the thesis includes the application of the July air T and ATR chironomid-inferred models on the late glacial and Holocene fossil chironomid assemblages of the Lake Nakri in southern Estonia (14.5 ka years-long record) and Lake Petrovskoe in western Russia (10 ka years-long record). The results identify major climate events such as the Younger Dryas, as well as minor ones, e.g., 9.0–8.0 ka, 7–7.5 ka, and 5–5.5 ka cold events.

Together, these studies advance the methodology and spatial applicability of chironomid-based palaeoclimatic reconstructions. The findings contribute to a deeper understanding of long-term climate dynamics in Eastern Europe and offer valuable tools for future assessments of climate change impacts in sensitive freshwater ecosystems.

Lühikokkuvõte

Pärastjääaja kliimamuutus Ida-Euroopas: fookus Hironomiidide-põhisele suvetemperatuuride ja kontinentaalsuse rekonstruktsioonile

Käesolev doktoritöö uurib subfossiilsete hironomiidide (Chironomidae e. surusääsklased) kasutamist bioindikaatoritena mineviku kliimatingimuste, eriti juuli keskmise õhutemperatuuri (MJAT) ja kontinentaalsuse rekonstrueerimisel. Töö raames töötati välja kaks surusääskedel põhinevat järeldus-mudelit mida saab rakendatada seni paleoökoloogiliselt väheuuritud aladel Baltimaades ja Ida-Euroopa lauskmaa lääneosas. Et parandada meie arusaamist nende alade pärastjääaegse kliima muutlikkusest rakendati neid mudeleid kahe pärastjääaegse settejärjestuse põhjal kliimaparameetrite rekonstrueerimiseks.

Uurimistöö esimene osa tutvustab uut Soome-Balti-Poola (FBP) surusääskede andmebaasi (121 järve sette pinnaproovid), mis laiendab MJAT-i (juuli keskmine õhutemperatuur) rekonstruktsioonide geograafilist ja klimaatilist katvust Baltimaadesse ja nende lähiümbrusesse. Kanooniline korrespondentsanalüüs näitas juuli õhutemperatuuri tugevat mõju (9,1%) surusääskede koosluste jaotusele. Kaalutud keskmistamise osalise vähimruutude meetodil koostatud surusääskede põhise MJAT-järeldus-mudeli statistiline veahinnang oli madal ($RMSEP_{boot}$ = 0,7 °C), kinnitades seega surusääskedel põhinevate temperatuurirekonstruktsioonide suurt statistilist usaldusväärsust ka selles varem vähemuuritud piirkonnas.

Kontinentaalsuse ökoloogilist tähtsust kaasaegsete surusääskede koosluste kujundajana hinnati nii piki Ida-Euroopa lauskmaad ja Skandinaavia lõunaosa paikeval ida-läänesuunalisel transektil 51 järvest kogutud andmete, kui ka eelkirjeldatud FBP andmebaasi põhjal. Tulemused näitavad, et surusääskede kooslused reageerivad selgelt kontinentaalsuse muutustele. Kerneri okeaansusindeks oli ida-läänesuunalises andmestikus suurim muutuste selgitusjõud (18,4%), samas kui FBP andmebaasis oli kõige olulisem kontinentaalsusega seotud muutuja aastane temperatuurivahemik (ATR) (11%).

Töö viimane osa hõlmab surusääskedel põhinevate mudelite rakendamist MJAT ja ATR rekonstrueerimiseks hilisjääaja ja Holotseeni fossiilsete surusääskede kooslustele Lõuna-Eestis asuvas Nakri järves (viimased 14,5 tuhat aastat) ja Lääne-Venemaal asuvas Petrovskoe järves (viimased 10 tuhat aastat). Tulemused näitavad nii suuremaid kliimasündmusi nagu noorema Drüüase aegne jahenemine, aga ka väiksemaid sündmusi, näiteks 9–8, 7–7,5 ja 5–5,5 tuhat aastat tagasi esinenud külmemad perioodid.

Kokkuvõttes arendavad need uuringud surusääskedel põhinevate paleokliima rekonstruktsioonide metoodikat ja ruumilist rakendatavust. Tulemused aitavad süvendada arusaamist Ida-Euroopa pikaajalisest kliimadünaamikast ning annavad väärtusliku tööriista tulevaste kliimamuutuste mõju hindamiseks tundlikes magevee ökosüsteemides.

Appendix 1 (Paper I)

Bakumenko, V., Poska, A., Płóciennik, M., Gasteviciene, N., Kotrys, B., Luoto, T.P., Belle, S. and Veski, S. (2024). Chironomid-based inference model for mean July air temperature reconstructions in the eastern Baltic area. Boreas, 53(3), pp. 401–414. doi: 10.1111/bor.12655

BOREAS An international journal of Quaternary research

Chironomidae-based inference model for mean July air temperature reconstructions in the eastern Baltic area

VARVARA BAKUMENKO, ANNELI POSKA, MATEUSZ PŁÓCIENNIK, NERINGA GASTEVICIENE, BARTOSZ KOTRYS, TOMI P. LUOTO, SIMON BELLE AND SIIM VESKI

BOREAS

Bakumenko, V., Poska, A., Płóciennik, M., Gasteviciene, N., Kotrys, B., Luoto, T. P., Belle, S. & Veski, S. 2024 (July): Chironomidae-based inference model for mean July air temperature reconstructions in the eastern Baltic area. *Boreas*, Vol. 53, pp. 401–414. https://doi.org/10.1111/bor.12655. ISSN 0300-9483.

Here we present a new eastern Baltic Chironomidae training set (TS) containing 35 sites that was collected and merged with neighbouring published Finnish (82 lakes) and northern part of the Polish (nine lakes) TSs. Chironomidae, non-biting midges, are known to be strongly responsive to the July air temperature and are widely used to infer palaeotemperature. Several modern analogue-based TSs necessary for calibrating the relationships between mean July air temperature (MJAT) and chironomids are available for Europe. However, none of these is representative of the transitional climate typical for eastern Baltic (Estonia, Latvia, Lithuania). The Finno–Baltic–Polish TS contains 121 sites and covers a geographically continuous 70–50°N latitudinal and 7 °C (12.1–19.2 °C) MJAT gradient. Canonical correspondence analysis revealed that, among the tested environmental variables (pH, water depth, dissolved oxygen, MJAT), the MJAT explains the highest amount of variation, both for the eastern Baltic separately and the Finno–Baltic–Polish TSs. The weighted averaging–partial least squares-based cross-validation test reveals that the Finno–Baltic–Polish TS has a low root mean square error of prediction (0.7 °C) confirming the high reliability of the TS. The temperature optima of the taxa included in the new Finno–Baltic–Polish TS and widely used Swiss–Norwegian TS were examined. The observed dissimilarities can be attributed to the differences in the temperature ranges represented by the TS, the taxonomic identification level, the general cosmopolitan taxa distribution patterns and the influence of TS-specific geographic position, climatic or environmental conditions. The new Finno–Baltic–Polish TS adds to the knowledge on the modern distribution of Chironomidae taxa and widens the geographical area of reliable Chironomid-based MJAT reconstructions into the eastern European lowland.

Varvara Bakumenko (varvara.bakumenko@taltech.ee) and Siim Veski, Department of Geology, Tallinn University of Technology, Ehitajate tee 5, 19086 Tallinn, Estonia; Anneli Poska, Department of Geology, Tallinn University of Technology, Ehitajate tee 5, 19086 Tallinn, Estonia and Department of Physical Geography and Ecosystem Science, Lund University, SE-221 00 Lund, Sweden; Mateusz Płóciennik, Department of Invertebrate Zoology and Hydrology, University of Lodz, Prezydenta Gabriela Narutowicza 68, 90-136 Łódź, Poland; Neringa Gasteviciene, Laboratory of Quaternary Research, Nature Research Centre, Akademijos str. 2, LT-08412 Vilnius, Lithuania; Bartosz Kotrys, Polish Geological Institute, National Research Institute, Pomeranian Branch in Szczecin, ul. Wieniawskiego 20, 71-130 Szczecin, Poland; Tomi P. Luoto, Faculty of Biological and Environmental Sciences, Ecosystems and Environment Research Programme, University of Helsinki, Yliopistonkatu 4, 00100 Helsinki, Finland; Simon Belle, Department of Aquatic Sciences and Assessment, Swedish University of Agricultural Sciences, SE-750 07 Uppsala, Sweden; *received 17th October 2023, accepted 3rd March 2024.*

Accurate climate reconstructions are important in investigating ecosystem response to climate changes in eastern Europe. Presently available climate reconstructions are based on a variety proxy (Kaufman *et al.* 2020), where pollen-based reconstructions make the biggest contribution in eastern Europe (Feurdean *et al.* 2014). However, considerable migration delays of the terrestrial vegetation during the Lateglacial and Early Holocene and substantial anthropogenic land cover change during the Late Holocene can influence the quality of the pollen-based reconstructions, especially in northern and eastern Europe (Väliranta *et al.* 2015; Rao *et al.* 2022). Thus, there is a need for an independent proxy to increase the reliability of the climate reconstructions in the eastern Baltic (Estonia, Latvia, Lithuania).

The Chironomidae, non-biting midges from the Diptera family, are widely distributed in freshwaters, and chitinous remains of larvae that are morphologically well preserved in Quaternary lake sediments allowing their identification to the morphotype level (Brooks *et al.* 2007) are often used as an independent and reliable climate proxy. Chironomid community composition in Holarctic lakes has been reported to be strongly associated with the mean July air and water temperatures (Walker & Mathewes 1987; Barley *et al.* 2006; Heiri *et al.* 2011; Kotrys *et al.* 2020; Nazarova *et al.* 2023). Subfossils of Chironomidae larvae deposited in lake sediments are widely used to reconstruct July air temperature during the Quaternary (Eggermont & Heiri 2012; Gouw-Bouman *et al.* 2019; Plikk *et al.* 2019). However, they can be influenced by other environmental factors such as trophic state (Brooks *et al.* 2001; Luoto 2011) and deepwater oxygen concentrations (Brooks *et al.* 2001; Quinlan & Smol 2001; Verbruggen *et al.* 2011; Ursenbacher *et al.* 2020), but also pH, heavy metal concentration and lake water depth (Heiri 2004; Rees *et al.* 2008; Nazarova *et al.* 2011; Ruse *et al.* 2018; Pegler *et al.* 2020; Ni *et al.* 2023).

Relationships between chironomid assemblages and temperature can be explored using calibration training sets (TSs) that describe the distribution and abundance of

DOI 10.1111/bor.12655

chironomid taxa across a temperature gradient (Eggermont & Heiri 2012). TSs are produced by collecting sediment samples from a large number of lakes across geographic or elevation gradients and by analysing the chironomid remains contained in these sediments (Lotter *et al.* 1997), thus providing an estimate of the composition of the modern chironomid fauna of these lakes (Heiri *et al.* 2011). Numerical inference models (transfer/calibration functions) (Birks 1998; Birks *et al.* 2010) can then be applied to determine chironomid–temperature correlation and to infer July temperature values. Inference models using chironomids as a proxy are based on a range of different numerical approaches, i.e. weighted averaging-partial least square regression, maximum likelihood regression and modern analogue technique (Heiri *et al.* 2011; Self *et al.* 2011; Medeiros *et al.* 2022), and allow the estimation of inferred July temperatures with a prediction error ranging from less than 2 °C (Kaufman *et al.* 2020). Existing chironomid–July temperature calibration TSs and inference models in Europe have been developed in Switzerland (Lotter *et al.* 1997), Norway (Brooks & Birks 2000), northern Sweden (Larocque *et al.* 2001), Finland (Luoto 2009), Poland (Kotrys *et al.* 2020), Slovakia (Chamutiova *et al.* 2020) and N and NE Russia (Nazarova *et al.* 2023). While these TSs represent a wide range of biogeographical conditions, a considerable part of the sites are from highlands and none from the eastern Baltic.

The eastern Baltic area, which is a part of the European Plain, is located in the transitional zone between maritime and continental climates. The border areas separating continental-scale climatic zones exhibit significant variations in climate factors (temperature, humidity, wind speed, etc.) and climatic instability (Fu 1992). Thus, the eastern Baltic area reveals heightened sensitivity to changes in northern Europe's air circulation patterns (Giesecke *et al.* 2008; Seppä *et al.* 2009), which could result in the emergence of unique Chironomidae assemblages. The eastern Baltic Chironomidae fauna is understudied, and no local TS has been developed so far. The Swiss–Norwegian and Finnish TSs have been used for the reconstruction of summer temperatures during glacial and Early Holocene climate events in the eastern Baltic (Heiri *et al.* 2014; Šeirienė *et al.* 2021). On one hand, the Finnish TS lacks the warmer analogues that could correspond to the modern mean July air temperature (MJAT) range in the eastern Baltic region. In addition, the diverse bedrock composition, with acidic bedrock in Finland and carbonate in the Eastern Baltic, can be expected to result in varying water chemistry, which affects chironomid assemblages (Eggermont & Heiri 2012). On the other hand, the Swiss–Norwegian–Polish (Kotrys *et al.* 2020) and north European TSs (Larocque *et al.* 2001; Luoto 2009) have a spatial gap of calibration sites and lack modern analogues of Chironomidae communities reflecting the combination of the mild maritime climate and carbonate bedrock that is typical for the eastern Baltic. This complicates the use of regression-based methods for temperature reconstruction since they rely on the even spacing of samples along environmental gradients.

Another issue is that the multiple Chironomidae species with different ecological preferences belong to the same morphotype. Furthermore, the same morphotypes can represent different species in different regions, introducing additional bias into transfer functions (Velle *et al.* 2010; Juggins 2013; Medeiros *et al.* 2015). Calibration functions perform best in the geographical region in which the calibration TSs were developed, and the absence of the local TS could influence the reliability of the reconstruction (Heiri *et al.* 2011; Plikk *et al.* 2019; Płóciennik *et al.* 2022).

The objectives of this work are: (i) to compile a new chironomid TS representative of environmental conditions of the eastern Baltic; and (ii) to build a comprehensive TS representative of low-elevation areas of northern Europe and cover the temperature range expected for post-glacial conditions by merging eastern Baltic TS with samples from Finnish (Luoto 2009) and Polish TSs (Kotrys *et al.* 2020).

Material and methods

Chironomid training sets

The eastern Baltic TS consists of Chironomidae assemblage data and the corresponding MJAT for 35 lakes from Estonia, Latvia and Lithuania (Fig. 1A). Chosen lakes in the eastern Baltic TS have characteristic water chemistry for the region (Tables 1, S1, Fig. S1) and low anthropogenic impact on their surroundings. The region is located at the transition from the temperate to the boreal domains and between maritime and continental climates. The weather changes here frequently depending on the domination of the western zonal flow or continental high-pressure conditions (Johannessen 1970). The highest peak in the area is 318 m a.s.l. The bedrock in the eastern Baltic consists mainly of limestones and sandstones, thus the pH of the lakes is mostly alkaline. The surroundings of lakes chosen for sampling consist of coniferous, broad-leaved and mixed forests and low-intensity agricultural activity. Lakes were sampled in a transect along the MJAT gradient (17.2–18.4 °C).

The Finnish 110-site TS (Luoto 2009) and nine sites from the Polish TS (Kotrys *et al.* 2020) were merged (see below, section 'Chironomidae identification and TSs harmonisation') with the eastern Baltic TS. The resulting Finno–Baltic–Polish TS (Fig. 1B, Table 1) covers an MJAT range of 12.1–19.2 °C and a latitudinal range of 69.44–53.9°N.

Detailed information about Finnish and Polish sampling sites and their Chironomidae assemblages can be found in the original publications (Luoto 2009; Kotrys *et al.* 2020).

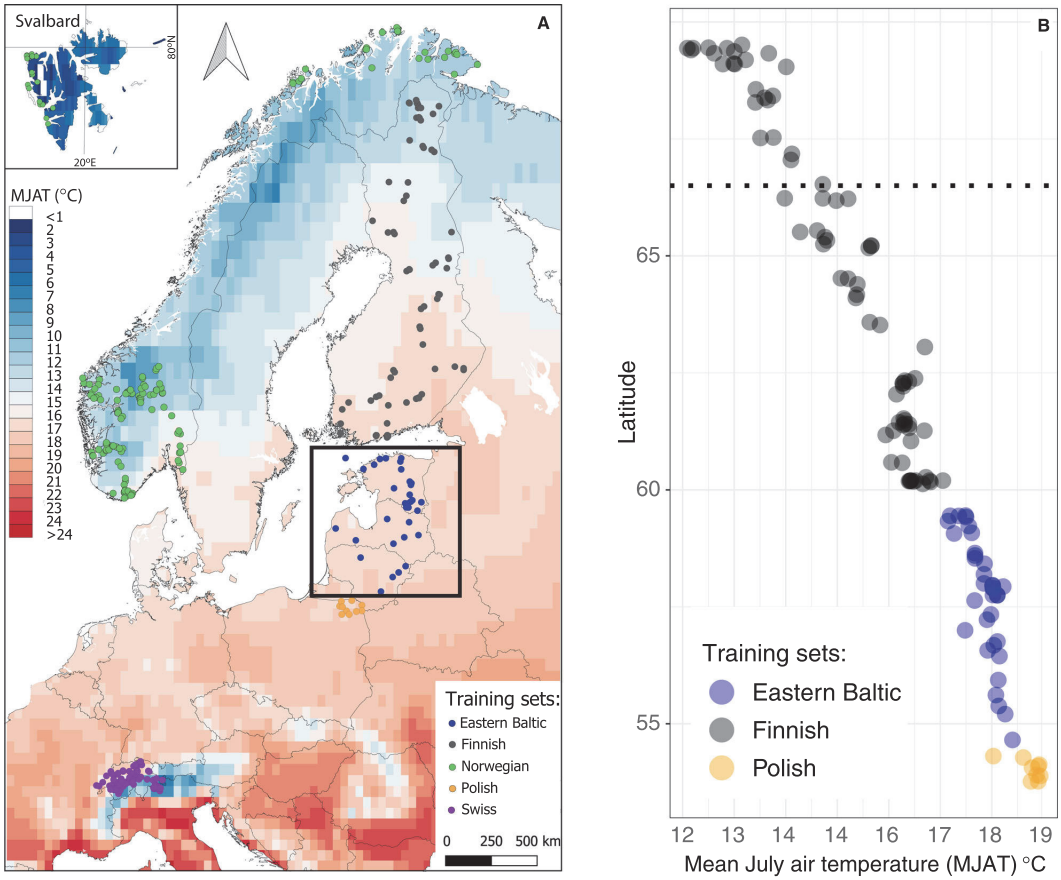

Fig. 1. Location of the sites (A) included in the Finno–Baltic–Polish and Swiss–Norwegian training sets (TSs) and the distribution of the Finno–Baltic–Polish TS sites, where the grey frame indicates new eastern Baltic sites (B) along the mean July air temperature (MJAT) and latitudinal gradient. The dotted black line represents the polar circle 66.5°N boundary.

The Swiss–Norwegian TS (Heiri *et al.* 2011) and supplementary environmental data were downloaded from the National Oceanic and Atmospheric Administration website. It covers a broad MJAT and latitudinal range (Table 1) in central and northern Europe. The Swiss–Norwegian TS was used without excluding any outliers.

Sampling and laboratory procedures

The eastern Baltic TS is based on surface sediment samples of 35 medium-sized natural lakes. The samples were collected from the deepest part of the analysed lakes using a gravity corer. During the sampling, the topmost 2 cm of sediment was taken and later analysed in the laboratory. Sampling in Estonia was carried out in 2021 (February), in Latvia in 2019–2021 (February) and in Lithuania in 2022 (February) (Table S1). The water chemistry data were collected during the summers of 2021 and 2022. The sediment samples were water-sieved with a 100 µm mesh size sieve to remove fine sediment. The deflocculation in 10% KOH, which had been applied in samples processing of Finnish (Luoto 2009) and Polish (Kotrys *et al.* 2020) TSs, was skipped owing to the generally loose and watery sediment structure. Each sample was thereafter transferred into a Petri dish, and Chironomidae head capsules were collected with fine forceps under a stereomicroscope at 25× magnification. The obtained head capsules were air-dried and mounted in Aquatex® mounting medium. Taxonomic identification was conducted under the microscope at 100–400× magnification. The average number of head capsules collected per sample was 65, with counts ranging from 42 to 125.

Table 1. Environmental data for different subsets of the Finno–Baltic–Polish and Swiss–Norwegian training sets (TSs).

Training set	Finnish	Eastern Baltic	Polish	Swiss–Norwegian
Number of lakes	82	35	9	265
Latitude (°N)	60.13–69.44	54.65–59.45	53.9–54.3	46.15–79.8
Longitude (°E)	22.0–30.13	24.2–27.34	22.06–23.48	5–31.04
Sampling water depth range (m)	0.5–9.0	1.4–21.8	3.3–15.0	–
July air temperature (°C)	12.1–17.5	17.2–18.4	18.4–19.2	3.5–18.4
pH	4.4–9.3	4.48–9.5	7.81–8.73	–
Dissolved oxygen (g L^{-1})	0.5–11.8	6.4–16.6	–	–
Water phosphorus content (g mL^{-1})	–	0.007–0.169	–	–

The laboratory procedures for the Finnish, Swiss–Norwegian, and Polish TSs samples are described in the original papers (Luoto 2009; Heiri *et al*. 2011; Kotrys *et al*. 2020).

Chironomidae identification and TSs harmonization

Chironomid head capsules from the Eastern Baltic TS were identified according to Schmid (1993), Klink and Pillot (2003), Brooks *et al*. (2007), Larocque-Tobler (2014) and Andersen *et al*. (2013). The eastern Baltic TS Chironomidae collection is stored and available in the Department of Geology at Tallinn University of Technology, Tallinn, Estonia.

The taxonomic resolution of Eastern Baltic TS and all of the used published TSs (Finnish (Luoto 2009), Polish (Kotrys *et al*. 2020) and Swiss–Norwegian (Heiri *et al*. 2011)) is based on that described in Brooks *et al*. (2007). The taxonomic harmonization between TSs was done on the count data. The few apparent taxonomic differences were handled as follows:

- Head capsules that lacked identifying features and were only identified to the genus or subfamily taxonomic level (Tanytarsini, *Tanytarsus* spp., *Paratanytarsus* spp., Tanypodinae, Chironomini, Orthocladinae) were excluded from the Finno–Baltic–Polish TS owing to the possibility of introducing bias into the inference model by including groups containing taxa representing different spectra of ecological conditions.
- The *Cricotopus intersectus* type was merged with the *Cricotopus laricomalis* type into one type owing to the high chance of misidentification of these morphotypes.
- *Ablabesmyia* spp. was merged with *Ablabesmyia monilis* type, *Ablabesmyia longistyla* type and *Ablabesmyia phatta* type owing to the absence of identification features in the eastern Baltic and Polish TSs.
- The *Corynoneura scutellata* type was merged with *Corynoneura edwardsi* type and *Corynoneura arctica* type following the identifications used in the Finnish TS (Luoto 2009).

Following the above-described taxonomic harmonization, the relative abundances were recalculated.

Water chemistry, lake depth and climate data

For the eastern Baltic TS, lake depth was measured during lake sampling using a mechanical tape; the pH and oxygen concentration were measured in the field with the YSI ProDSS probe at 30–40 cm above the sediment surface of the lake; and the water phosphorus was determined in the laboratory from the top water layer samples using a HACH LKC349 analysis kit and Hach Lange DR 2800 spectrophotometer by Anna Lanka (unpublished data). Some additional water chemistry information was obtained from lake monitoring centres (Latvian Environment, Geology and Meteorology Center and the Lithuanian Environmental Protection Agency under the Ministry of the Environment). The pH data for Eastern Baltic TS are available for 33 lakes and dissolved oxygen and water phosphorus data are available for 29 lakes from the eastern Baltic TS. The dissolved oxygen for eastern Baltic sites was measured in July and August, whereas for Finnish lakes it was measured between February and April; thus, joining these data series could be unrepresentative of environmental conditions. For the Finnish, Polish and Swiss–Norwegian TSs the water chemistry and lake water depth were derived from the original publications (Luoto 2009; Heiri *et al*. 2011; Kotrys *et al*. 2020). The MJAT for each lake in Eastern Baltic TS was estimated using 30-year gridded (0.1 × 0.1°) observational data (1991–2020), obtained from the E-OBS TS (Cornes *et al*. 2018) downloaded from the Copernicus Climate Data Store. The same approach interpolating the meteorological stations' observations and calculating 30 year means was used for the Finnish, Polish and Swiss–Norwegian TSs (Luoto 2009; Heiri *et al*. 2011; Kotrys *et al*. 2020).

Data analysis

For the statistical analysis, chironomid assemblage data of Finno–Baltic–Polish TS were transformed into relative abundances (%). Only taxa with an abundance of at least 2% in one sample were considered during numerical analysis and square root transformation was applied to equalize variances among taxa.

Chironomidae assemblages were analysed using detrended correspondence analysis (DCA; Hill & Gauch 1980) to examine the general distribution of communities

and the compositional gradient lengths along the first two DCA axes. The length of DCA Ax1 and Ax2 (3.1 and 2.4 standard deviation (SD) units, respectively) falls into the intermediate category, for which the use of both redundancy analysis (RDA) and canonical correspondence analysis (CCA) has been recommended (Birks 1998; Lepš & Šmilauer 2003). We have used RDA and CCA for Finno–Baltic–Polish TS to produce results comparable with earlier studies (Luoto 2009; Kotrys *et al*. 2020). The CCA was applied to evaluate the significance of the environmental variables that explain significant variation in the chironomid data. Owing to a different number of observations for each variable the CCAs were run with only one environmental variable at a time (Table 1). The statistical significance of each selected variable was tested by a Monte Carlo permutation test (9999 unrestricted permutations) (Ter Braak 1992; Ter Braak & Verdonschot 1995). To choose the most relevant explanatory variables, $\lambda 1{:}\lambda 2$ ratios were also calculated, where $\lambda 1$ is the eigenvalue of the first constrained CCA axis and $\lambda 2$ is the eigenvalue of the second unconstrained axis. RDA was applied on eastern Baltic TS owing to the shorter length of DCA Ax1 and Ax2 (2.4 and 2.0 SD units, respectively).

The MJAT optima for individual taxa across the Finno–Baltic–Polish TS were estimated based on weighted-average regression with inverse deshrinking (Ter Braak & Juggins 1993). The generalized additive models (GAMs) (Wood 2011) in the whole Finno–Baltic–Polish TS were applied to estimate the taxon-specific MJAT–abundance relationships. For taxa for which a significant relationship with MJAT was revealed, the variance was calculated. To study the temperature-related distribution of taxa, the TS was divided into three biogeographic zones based on MJAT intervals: northern boreal (12.1–15.0 °C), southern boreal (15.0–17.0 °C) and temperate (17.0–19.2 °C) (Fig. 1B). Linear regression was applied to the taxa presented within the biogeographic zones to ensure that they reveal significant dependency in the same biogeographical zone where their weighted averaging-based optima are situated. For some understudied taxa, additional GAMs for estimating the dependency between their abundances and dissolved oxygen level, water phosphorus, sampling depth and pH values were calculated.

The Chironomid-inferred MJAT model building

The Finno–Baltic–Polish inference model was built using cross-correlated weighted averaging–partial least squares (WA-PLS) regression and calibration (Ter Braak & Juggins 1993). The best transfer functions were selected as those producing the lowest cross-validated root mean squared error of prediction (RMSEP). The components were accepted as statistically significant at the $p \leq 0.05$ level. Bootstrapping techniques (9999 permutations; Birks *et al*. 1990; Birks 1998) were used to calculate cross-validated error and performance statistics for the WA-PLS inference model, such as the RMSEP, the maximum bias, the mean bias and the coefficient of determination (R^2) between inferred and predicted values within the individual calibration TSs (Finnish, Finno–Baltic–Polish and Swiss–Norwegian TSs). July air optima and tolerance of the individual taxa were estimated based on the WA regression (Ter Braak & Juggins 1993).

Numerical analysis and plots were performed with the free software program R version 4.1.1. using the following packages: 'tidyverse' for data restructuring and visualizing (Wickham *et al*. 2019), 'dplyr' for data restructuring and basic calculations (Wickham *et al*. 2022), 'vegan' for ordination (Oksanen *et al*. 2022), 'rioja' for performing the WA-PLS analysis and plotting the stratigraphic diagram (Juggins 2022) and 'mgcv' for performing the GAMs (Wood 2017).

Results

Composition of Chironomidae assemblages

A total of 112 Chironomidae morphotypes were identified in 35 lakes from the eastern Baltic region, of which 30 morphotypes were not present at the Finnish and Polish sites. The most abundant taxa (Fig. 2) in the eastern Baltic TS are *Psectrocladius sordidellus* type (8.6%), *Chironomus plumosus* type (8.6%), *Dicrotendipes nervosus* type (6.8%), *Neozavrelia* (6.8%), *Polypedilum nubeculosum* type (5.28%), *Glyptotendipes pallens* type (4.8%), *Microtendipes pedellus* type (4.6%) and *Corynoneura ambigua* type (4.1%).

The merged Finno–Baltic–Polish TS after deleting species with abundances less than 2% contains 106 taxa and 121 sites. Following Luoto (2009), five sites from the Finnish TS were considered outliers and excluded from the MJAT inference model. The most abundant taxa in the final TS were *P. sordidellus* type (average abundance 15.6%), *C. plumosus* type (7.3%), *Ablabesmyia* (7.2%), *Procladius* (7%), *M. pedellus* type (6.8%), *Cladotanytarsus mancus* type (6.1%) and *Zalutschia zalutschicola* type (5.7%).

Ordination analysis

The variance gradient of DCA calculated for eastern Baltic Chironomidae assemblages equals 2.4 SD and 2.0 SD for Ax1 and Ax2, respectively, whereas the Finno–Baltic–Polish TS DCA variance gradient equals 3.1 SD and 2.4 SD, respectively (Fig. 3).

The RDAs of the 35 eastern Baltic sites revealed that MJAT and water phosphorus content were the only environmental variables that explain the Chironomidae community distribution significantly (Table 2). In contrast, the RDAs and CCAs of the Finno–Baltic–Polish TS revealed that each of the examined

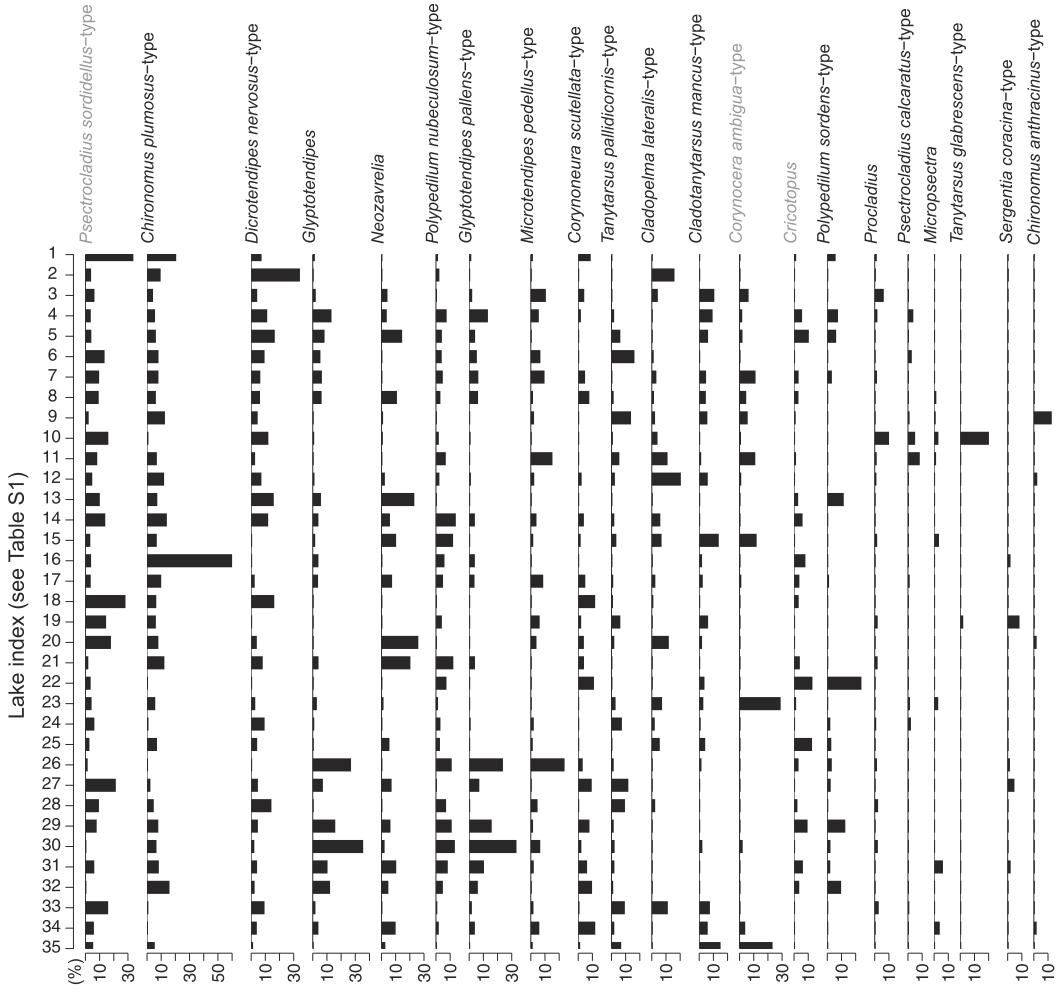

Fig. 2. Selected eastern Baltic chironomid morphotypes from the lake surface sediment layer ((0–2)–2 cm) included in the Finno–Baltic–Polish TS. Lake indices are ordered according to decreasing latitude (Table S1). Species are organized according to the decreasing abundances in the eastern Baltic TS; taxa with MJAT dependency are marked with grey.

environmental variables explains the Chironomidae assemblages significantly. The MJAT explains the 9.1% CCA-based (14.4% RDA-based) Chironomidae assemblage variance followed by pH (7.2% (CCA), 11.5 (RDA)), dissolved oxygen (4.5% (CCA), 7.5% (RDA)) and sampling depth (3.0% (CCA), 3.9% (RDA)) (Table 3, Fig. 4). The strongest explanatory variable for the Chironomidae community according to the $\lambda 1{:}\lambda 2$ ratio was MJAT (1.4 CCA-based, 1.3 RDA-based; Table 3). Training sets with ratios $\lambda 1{:}\lambda 2 > 1$ are characterized by strong relationships between the examined environmental variable and the assemblage data relative to the remaining variance in the TS and are therefore suitable for developing inference models (Goldenberg Vilar *et al*. 2018). However, it must be kept in mind that the CCA plot demonstrating the dependency of chironomid assemblages from MJAT exhibits the horseshoe effect, which could affect the results.

To assess the relationship between MJAT and chironomid assemblages in different parts of the Finno–Baltic–Polish TS, CCA with MJAT as an explanatory variable for different subsets was performed (Table 4). The variance explained by the MJAT in Finno–Baltic–Polish TS is 9.1% (CCA-based), which is almost the same as in only the Finnish TS (9.6%). The ratio of the unique taxa in the TS (Table 4) was calculated as a percentage of taxa

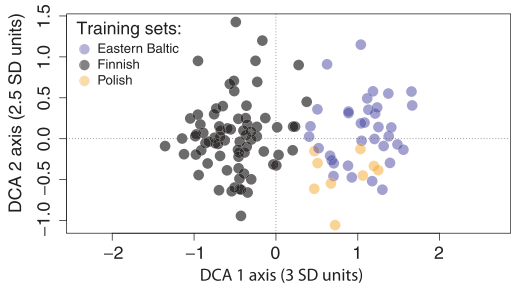

Fig. 3. Detrended correspondence analysis (DCA) ordination diagram for the lakes from the Finno–Baltic–Polish TS.

observed only in a particular TS. This ratio is almost equal for the Polish–Baltic area and the Finnish one.

Species–MJAT relations analysis

The linear regression analyses (Table S2) indicated that the most MJAT-dependent taxa in the different biogeographic zones of the Finno–Baltic–Polish TS were *Micropsectra insignilobus* type (35.5% of variance explained), *Zalutschia mucronata* type (16%), *Psectrocladius septentrionalis* type (15.3%), *Tanytarsus lugens* type (14.8%) and *Psectrocladius calcaratus* type (12.3%) for the northern boreal part of the TS; *Procladius* (23.1%), *Tanytasus mendax* type (21.6%), *C. scutellata* type (20.8%), *Chironomus anthracinus* type (18.9%) and *Ablabesmyia* (11.9%) for the southern boreal part; and *D. nervosus* type (35.5%), *Ablabesmyia* (33.13%), *C. arctica* type (25.6%), *C. plumosus* type (21.2%) and *Neozavrelia* (20.2%) in the temperate part of the gradient. The taxa whose distribution revealed the strongest MJAT dependence based on GAM over the entire Finno–Baltic–Polish TS (Fig. 5) were *P. septentrionalis* type (51.6% of variation explained by the MJAT), *P. calcaratus* type (47.6%), *M. insignilobus* type (43.7%), *T. mendax* type (39.4%), *Ablabesmyia* (35.6%), *Procladius* (33.7%), *Dicrotendipes pulsus* type (32%) and *C. plumosus* type (28.3%). In contrast, *P. sordidellus* type, *M. pedellus* type and *Corynoneura lobata* type did not reveal any MJAT dependency at all. *Limnophyes* and *C. ambigua* type morphotypes had MJAT dependency only within one biogeographical zone but not across the entire gradient. The average variation explained by MJAT for the different taxa was 9.2% less within individual zones than in the GAM-based estimations for the whole Finno–Baltic–Polish TS. The July air temperature optima for each taxon are situated in the same biogeographic zones, where they reveal significant distribution (Table S2).

Inference model for Chironomid-inferred July air temperature reconstructions

The Finnish and Finno–Baltic–Polish TSs WA-PLS cross-validation models both demonstrated the smallest RMSEP value with the two-component model with 0.8 and 0.7 °C, respectively (Table 5). The bootstrapped maximum bias was 1.1 and 0.4 °C, and R^2 was 0.9 for Finnish and Finno–Baltic–Polish TSs. Thus, the performance of the new TS is comparably similar to that of the Finnish TS. Scatterplots of cross-validated predicted vs. observed MJATs in the Finno–Baltic–Polish cross-validation model generally follow a 1:1 relationship (Fig. 6). However, observed MJATs below 13 °C are consistently overestimated by the model, suggesting a minor bias on the colder end of the temperature gradient.

Discussion

The DCA revealed that eastern Baltic and Polish TSs form a separate group from Finnish TS sites, whereas samples from Poland are closer and partially embedded into the eastern Baltic sample space (Fig. 3). Even though 30 taxa were different from the Finnish or Polish Chironomidae communities, only seven of them reached an abundance of 2% at least in one sample and were included in the Finno–Baltic–Polish TS. These seven unique taxa account for 9.1% of the whole Finno–Baltic–Polish TS Chironomidae taxa composition (Table 4). Thus, the eastern Baltic and Polish samples provide new information about species communities and give new modern analogues to the Finno–Baltic–Polish TS.

Chironomidae assemblages' sensitivity to the environmental parameters

Most MJAT relationships were studied on a wide regional or climatological scale with a gradient length greater than

Table 2. The results of RDA of the eastern Baltic TS using only one environmental variable. The number of sites with the respective environmental variable measured, the amount of variability explained, *p*-values and the $\lambda 1{:}\lambda 2$ ratio are provided.

Name of the measured variable	Mean July air temperature	Water depth	Dissolved oxygen	pH	Water phosphorus content
Number of sites	35	35	29	31	29
Percentage of variability explained	5.4	–	–	–	5.6
p-Value	0.048	0.1	0.2	0.1	0.047
$\lambda 1{:}\lambda 2$	0.37	–	–	–	0.34

Table 3. The results of canonical correspondence analysis (CCA) and RDA of the Finno–Baltic–Polish TS using only one environmental variable. The number of sites with the respective environmental variable measured, the amount of variability explained, *p*-values and the $\lambda 1$:$\lambda 2$ ratio are provided.

Name of the measured variable	Mean July air temperature	Water depth	Dissolved oxygen	pH
Number of sites	121	121	56	79
Ordination method	CCA/RDA	CCA/RDA	CCA/RDA	CCA/RDA
Percentage of variability explained	9.1/14.4	3.0/3.9	4.5/7.5	7.2/11.5
p-Value	0.001/0.001	0.001/0.001	0.001/0.001	0.001/0.001
$\lambda 1$:$\lambda 2$	1.4/1.3	0.3/0.23	0.5/0.4	1/1

5 °C (Larocque *et al.* 2001; Luoto 2009); however, the minimal gradient length requirements are unknown. In the eastern Baltic TS, the MJAT explains a significant proportion (5.4% RDA-based) of the Chironomidae assemblage composition, suggesting that a MJAT range of approximately 2 °C as in the eastern Baltic TS is already enough to find significant MJAT–Chironomidae relationships. The RDA and CCA of the Finno–Baltic–Polish TS revealed that all observed environmental variables had a significant influence on the chironomid communities, with the MJAT explaining the highest amount of distribution (9.1% CCA-based) and having the highest $\lambda 1$:$\lambda 2$ ratio (1.4) of the studied ones. This agrees with other chironomid calibration TSs from Europe: 6.2% for the Swiss–Norwegian TS (Heiri *et al.* 2011), 7.7% for the northern Sweden TS (Larocque *et al.* 2001) and 9.6% for the Swiss–Norwegian–Polish TS (Kotrys *et al.* 2020) TSs.

The pH, water depth and oxygen level in the eastern Baltic TS (Table 2) were non-significant and this might be explained by the short gradient range and generally stable environmental conditions. The water phosphorus content has been recorded to have a significant influence on the Chironomidae communities (Brooks *et al.* 2001; Luoto 2011). In contrast to the eastern Baltic TS the statistically significant secondary factors in the Finno–Baltic–Polish TS are pH gradient (7.2% (CCA), 11.5% (RDA) of distribution explained), dissolved oxygen (4.5% (CCA), 7.5% (RDA)) and sampling depth (3.0% (CCA), 3.9% (RDA)). The pH is known to be an influential factor in the limnology of aquatic environments and the distribution of chironomids (Orendt 1999;

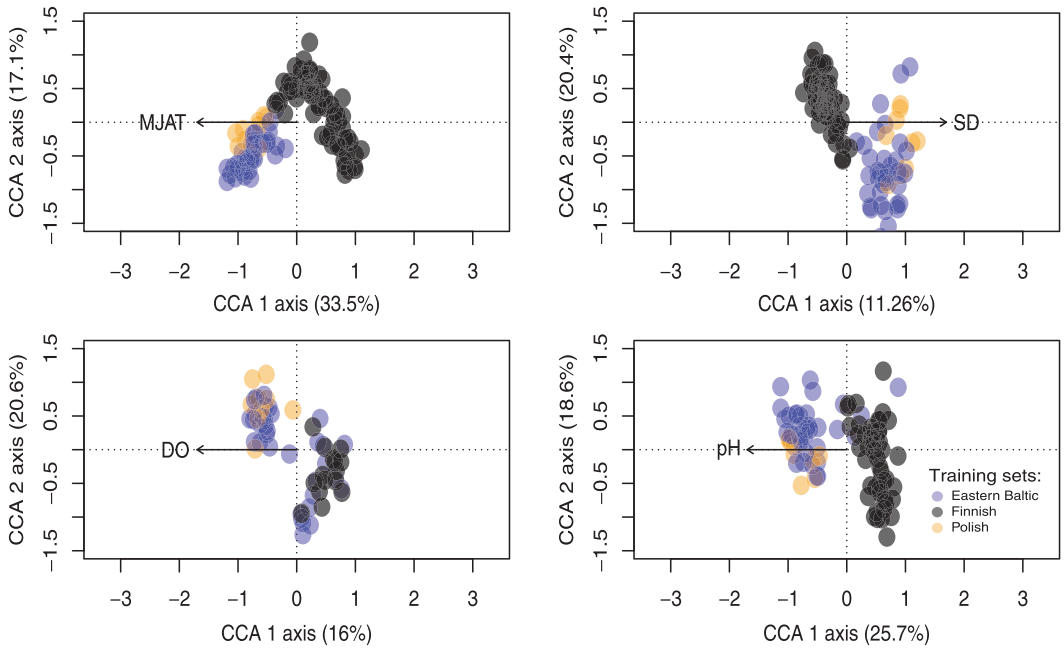

Fig. 4. The canonical correspondence analysis (CCA) biplots for the lakes from the Finno–Baltic–Polish TS with MJAT, sampling depth (SD), dissolved oxygen (DO) and pH as explanatory variables. The eigenvalues of the CCA1 and CCA2 axes are 0.3191 and 0.0569, respectively.

Table 4. Results of CCAs of the different parts of the Finno–Baltic–Polish and Swiss–Norwegian full dataset (Heiri *et al.* 2011) TSs set with mean July air temperature as an explanatory variable. The number of sites, variability explained by the environmental factor, *p*-values and $\lambda 1{:}\lambda 2$ ratio are provided for each subset and combinations of these. MJAT = mean July air temperature.

	Training set			
	Polish–Baltic (Polish; Baltic)	Finnish	Finno–Baltic–Polish	Swiss–Norwegian
Number of sites	44 (9; 35)	77	121	265
Total taxa included	82 (53; 77)	79	101	154
Unique taxa for the component (%)	26.8 (0; 9.1)	24.0	–	100
Variance explained by MJAT (°C) (%)	6.3 (–; 5.4)[1]	9.6	9.1	5.6
p-Value	0.001 (0.45; 0.048)	0.001	0.001	0.001
$\lambda 1{:}\lambda 2$	0.39 (–; 0.37)	1.37	1.37	1.13
MJAT (°C)	17.2–19.2 (18.4–19.2; 17.2–18.4)	12.1–17.5	12.1–19.2	3.5–18.4

[1]RDA-based.

Brooks *et al.* 2007). For instance, in the Swiss–Norwegian–Polish TS (Kotrys *et al.* 2020), it explains 3.85%, and in the TS from Russia (Self *et al.* 2011), it explains 3.8%. In the Finno–Baltic–Polish TS, pH is the second most significant factor, although in the eastern Baltic part of the TS, pH does not explain the

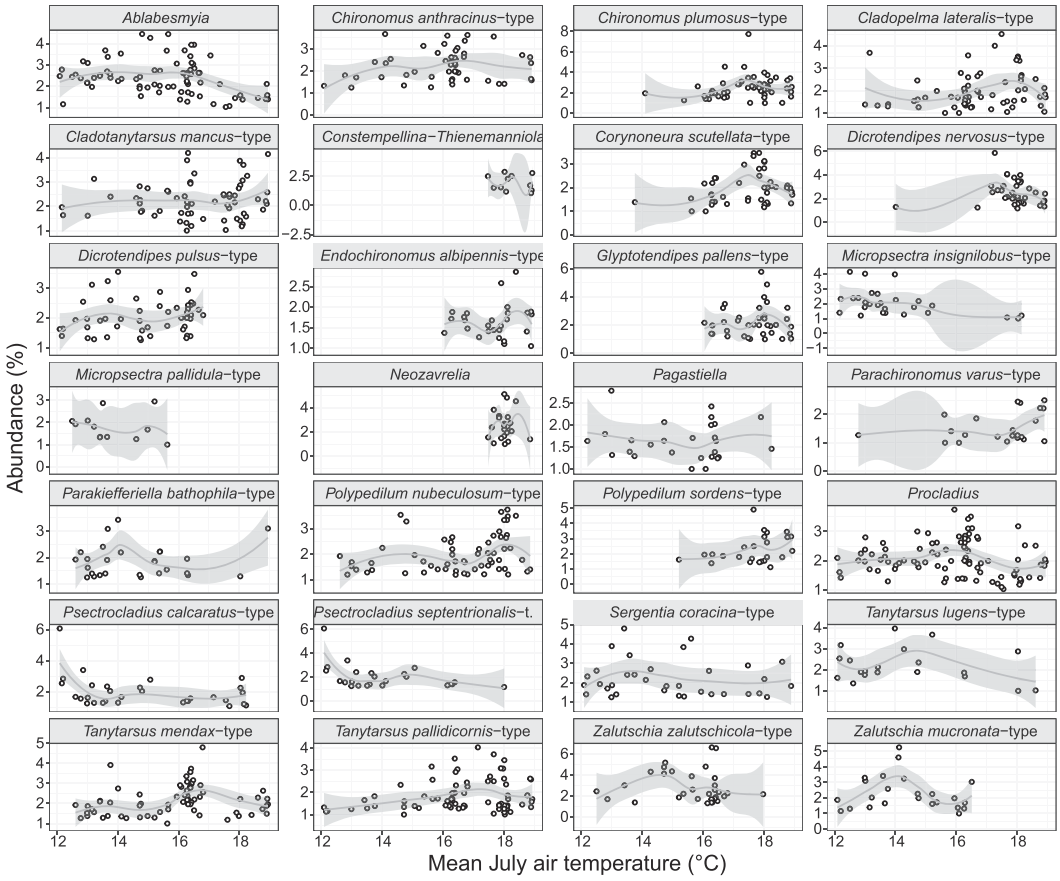

Fig. 5. Distribution of taxa with a significant relationship with temperature and abundances >2% in the Finno–Baltic–Polish TS. The lines are calculated by loess smoothing over the whole TS.

Table 5. Weighted averaging–partial least squares cross-validated models based on the Finnish and Finno–Baltic–Polish TS error statistics. Values are based on bootstrapping with 9999 bootstrap cycles except for the RMSE, which represents non-cross-validated values. Outliers and the least abundant taxa (max abundance under 2%) were excluded before calculating the inference model. RMSE = root mean square error; RMSEP = root mean square error of prediction; WA-PLS = weighted averaging–partial least squares.

Training set	Finnish			Finno–Baltic–Polish		
WA-PLS components	1	2	3	1	2	3
RMSE (°C)	0.6	0.5	0.4	0.8	0.6	0.4
RMSEP (°C)	0.8	0.8	0.8	0.9	0.7	0.7
Maximum bias (°C)	0.8	1.1	0.4	1.2	0.4	0.3
Average bias (°C)	0.02	0.01	0.00	0.00	0.01	−0.01
R^2	0.8	0.9	0.9	0.8	0.9	0.9

chironomids distribution significantly. The pH ranges between 4.5 and 8.9 in the eastern Baltic lakes, with only three lakes having pH values lower than 7 and 32 lakes having pH values of 7–8.9. Thus, eastern Baltic Chironomidae communities reflect the changes within 1.9 pH units; however, adding the alkaline eastern Baltic sites to the more acidic Finnish ones increases the influence of the pH variable from 2.4% (CCA-based; Luoto 2009) to 7.2% (CCA-based). Sampling depth explained 2.4% of the variation in the Finnish TS and increased to 3.0% after merging with eastern Baltic and Polish lakes. The increase in the explanatory power is the result of adding lakes with depths of 10–21 m, whereas the deepest lake in the Finnish TS is 9 m.

Based on the GAM, among 44 taxa that had a mean abundance higher than 2% in the northern boreal, southern boreal or temperate parts of the TS (Table S2), 30 morphotypes revealed significant MJAT dependency (Fig. 5). Thus, the estimated taxa groups and their proportions can be considered characteristic features for the corresponding biogeographical zones.

Dominant MJAT-dependent taxa in the eastern Baltic and Polish sites (17.5–19.2 °C) (*C. plumosus* type, *D. nervosus* type, *Tanytarsus pallidicornis* type, *Polypedilum sordens* type, *Cladopelma lateralis* type, *G. pallens* type, *P. nubeculosum* type, *C. mancus* type, *C. lateralis* type and *Constempellina–Thienemanniola*) were also considered warm-related in the Polish, Swiss–Norwegian, Canadian and northern America TSs (Walker *et al.* 1997; Heiri *et al.* 2011; Kotrys *et al.* 2020; Medeiros *et al.* 2022). *Chironomus plumosus* type, *C. lateralis* type, *P. sordens* type and *G. pallens* type have rare findings in the northern boreal part of the TS; however, they increase their abundance when the MJAT is warmer than 16 °C. *Dicrotendipes nervosus* increases its abundances above 17 °C. *Tanytarsus pallidicornis* type as well as *C. mancus* type appear in all parts of the Finno–Baltic–Polish TS, although they tend to increase in abundance from 16 to 19.1 °C. *Polypedilum nubeculosum* type, which has always been reported as a warm-related taxon (Heiri *et al.* 2011; Medeiros *et al.* 2022), has two peaks of distribution according to GAM (Fig. 5)–one at approximately 14.5 °C and another at approximately 18 °C – which could be explained by the occurrence of different species included in the type or by the presence of compensatory ecological factors in the northern boreal zone of the Finno–Baltic–Polish TS. Also, the *P. nubeculosum* type includes many species, whose subfossils cannot be separated from each other; it is possible that peaks represent two different species – one dominating in the northern boreal zone of MJAT gradient and another dominating in the temperate Baltic–Polish range of the TS. The *Constempellina–Thienemanniola* morphotype revealed MJAT optima of approximately 18.3 °C, with 16.2% variance explained, thus the type can be considered as warm-adapted in the Finno–Baltic–Polish TS. This is confirmed by the Swiss–Norwegian–Polish TS when it appears in many warm lakes of northern Poland. *Neozavrelia* has been described as a stenotherm taxon distributed in calcareous waters

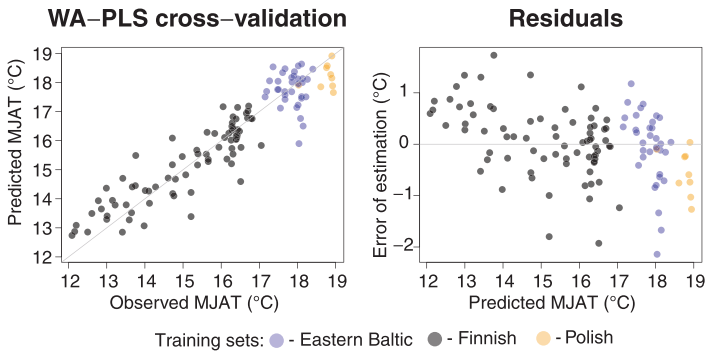

Fig. 6. Diagnostic plots of cross-validated estimates and prediction residuals compared with observed values of the Finno–Baltic–Polish TS calculated with a WA-PLS-based model based on two components.

(Ekrem 2006; Brooks *et al*. 2007). In the Finno–Baltic–Polish TS, *Neozavrelia* shows a strong positive relationship with MJAT and is mainly found in calcareous waters, which is in good agreement with Brooks *et al*. (2007). *Procladius* appears over the whole Finno–Baltic–Polish TS, with a broad distribution, which can be explained by the low identification resolution and the existence of regional morphotypes with different climatic optimums. The same observation was made within the study from Russia (Self *et al*. 2011), where *Procladius* had been considered a cosmopolitan taxon. *Chironomus plumosus* type, *C. lateralis* type and *T. glabrescens* type, although present in the temperate and southern boreal biogeographical zones, have significant positive correlations with a MJAT only in the temperate part of the Finno–Baltic–Polish TS. These taxa also seem to be related to secondary environmental variables along their distribution. For example, *C. plumosus* type has a strong negative relationship with dissolved oxygen concentrations, which agrees with studies by Little & Smol (2000) with ecological data that indicate that the taxon is related to low oxygen concentrations. *Limnophyes* and *C. ambigua* type revealed MJAT dependency in the southern and northern boreal zones respectively but not on the scale of the whole Finno–Baltic–Polish TS. *Limnophyes* has a significant MJAT relationship in the southern boreal zone of the TS and does not have any dependencies with secondary environmental gradients, so the pattern of its distribution must be clarified in future research. Previously, *Limnophyes* was described as a MJAT-related species and a possible indicator of water level fluctuations (Brooks *et al*. 2007), and a negative correlation with water depth was found (Self *et al*. 2011). The distribution of *C. ambigua* type revealed two MJAT optima in the Swiss–Norwegian–Polish TS (Kotrys *et al*. 2020), which together with findings in the current study, can be the basis for considering the presence of different cryptic species inside the type.

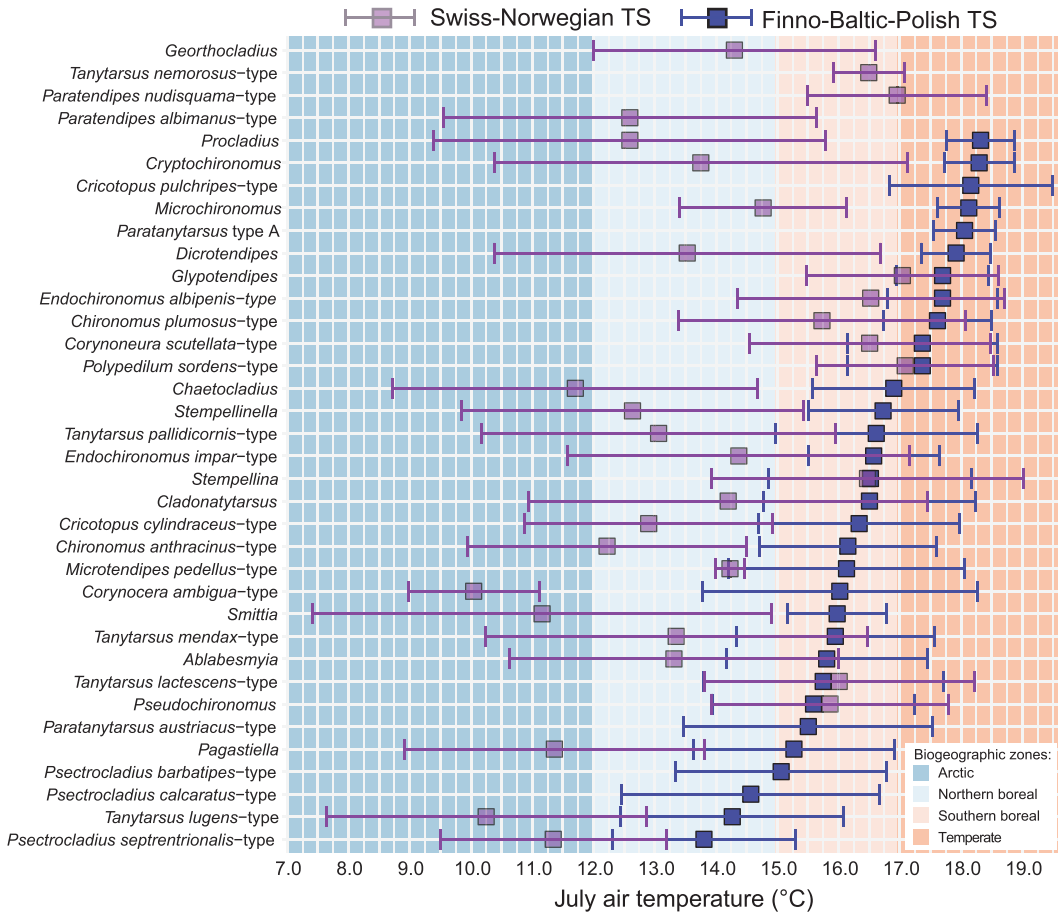

Fig. 7. The WA-based July taxa optima calculated in Finno–Baltic–Polish and Swiss–Norwegian TSs.

Inference model cross-validation and taxa MJAT optima estimations

The cross-validation performance of the Finno–Baltic–Polish TS is slightly better compared with the Finnish TS (Table 5; 0.7 and 0.8 of RMSEP (°C) respectively). Furthermore, the RMSEP, obtained from the Finno–Baltic–Polish WA-PLS model is comparably smaller than some of the other widely used TSs. For instance, the North American TS exhibited an RMSEP of 1.93 (Fortin *et al*. 2015) and the Swiss–Norwegian TS revealed an RMSEP of 1.4 (Heiri *et al*. 2011).

For most WA-based morphotypes, their MJAT optima are situated in the biogeographic zones, where their distribution is significant. Thus the calculated optima values are expected to be reliable. Generally, optima for the same taxa, calculated based on the Finno–Baltic–Polish TS, are warmer than those calculated using the Swiss–Norwegian TS (Fig. 7). Some taxa revealed the same MJAT optima regardless of TS origin (*Glyptotendipes*, *P. sordens* type, *Stempellina*, *Tanytarsus lactescens* type, *Pseudochironomus*). *Endochironomus albipennis* type, *C. plumosus* type and *C. scutellata* type MJAT optima in Finno–Baltic–Polish TS are within the error bars of those in the Swiss–Norwegian TS, e.g. exhibiting similar but narrower distribution areas. These morphotypes have a very low abundance or are absent in the Finno–Baltic–Polish TS sites with MJAT <16 °C. However, the same taxa revealed a more cold-adapted distribution pattern, appearing in sites with <14 °C MJAT in the Swiss–Norwegian TS, especially in the Swiss part of it (Heiri *et al*. 2011). The broader difference can be related to geographic position-, climate- or environment-driven differences (elevation, bedrock acidity, climate continentality, etc.) in the Swiss Alps and Finno–Baltic–Polish areas. *Endochironomus impar* type, *P. septentrionalis* type, *T. lugens* type, *Pagastiella* and *Ablabesmyia* exhibited optima with the intersecting error bars in the tested TSs. Considering that in the Finno–Baltic–Polish TS these taxa revealed quite a cosmopolitical distribution pattern (Fig. 5), we conclude that the same pattern is apparent in the Swiss–Norwegian TS. The most pronounced differences in optima are observed for taxa that were identified on a lower taxonomic level (e.g. *Procladius*, *Dicrotendipens*, *Chaetocladius*, *Microchironomus*, *Stempellinella*, *Smittia*) and can include species with different climatic preferences, thus leading to the mismatch of the optima in two tested TSs even within the error bars. This aligns well with the study of Heiri & Lotter (2010), which stated that the chironomid-based TSs with the high taxonomic resolution have the smallest RMSEP.

The absence of the cold (<12 °C) part of the MJAT gradient in the Finno–Baltic–Polish TS makes it impossible to reconstruct the colder phases of the Lateglacial climate. This could be handled by further adding colder sites, e.g. northern Norwegian ones. The advantage of the new Fino–Baltic–Polish TS is in providing warmer modern analogues, which fixes the issue of the warm end of the gradient in the Finnish TS. This statistical issue mentioned previously (Heiri *et al*. 2011) appears because of the lack of warm analogues and results in inferred July temperature overestimation. Having adequate warm analogues from the eastern Baltic is beneficial in reconstructions of the warm periods of the Middle and Late Holocene along with estimations of the previous July temperature change rates, which can be compared and discussed with modern ones.

Conclusions

The eastern Baltic TS contributes new information about Chironomidae taxa distribution patterns in the understudied Baltic region. The modern assemblages improve considerably the statistical performance of the inference model of July temperature when merged with other TSs from the region. Thus, building the Chironomidae TS representative of the environmental conditions of the study area is an important prerequisite for high-quality chironomid-based palaeoenvironmental reconstructions. The advantages of the Finno–Baltic–Polish TS are geographic and climatic continuity and the presence of warm modern analogues.

The MJAT and water phosphorus content were the only statistically significant environmental variables among the other tested ones (pH, water depth and dissolved oxygen level) which explained a Chironomidae distribution in the eastern Baltic TS. Thus, the MJAT range of approximately 2 °C as in the eastern Baltic TS is already sufficient to find significant MJAT–Chironomidae relationships. The MJAT had the highest explanatory power in the regional Finno–Baltic–Polish TS.

The differences in estimated Chironomidae distribution–MJAT optima in the Finno–Baltic–Polish and Swiss–Norwegian TSs highlight the importance of the TS selection. The differences can be attributed to the temperature range represented by the TS, taxonomic identification level, general cosmopolitan taxa distribution pattern and the influence of geographic position-, climate- or environment-driven differences. These results suggest that further tests are needed to investigate the impact of Chironomidae TS taxonomic composition and biogeographic origin on palaeotemperature reconstructions.

Acknowledgements. – This study was financially supported by the Estonian Research Council grant PRG323 and PRG1993. Varvara Bakumenko was supported by the Doctoral School of Earth Sciences and Ecology, supported by the European Union, European Regional Development Fund (ASTRA 'TTÜ arenguprogramm aastateks 2016–2022'). The water chemistry data were collected by Anna Lanka (Tallinn University of Technology). Special gratitude goes to Oliver Heiri for chironomid identification help and scientific guidance. The three journal reviewers are gratefully acknowledged for their valuable suggestions. We express our gratitude to Jan A. Piotrowski, the Editor-

in-Chief, for his diligent corrections and editorial management. None of the authors has any competing interests.

Author contributions. – Conceptualization: VB, SV, AP; Laboratory analysis/sample collection: VB, SV, MP, BK, TPL; Supervision – SV, SB; Writing – original draft: VB; Writing – review and editing: VB, AP, SV, SB, MP, NG.

Data availability statement. – Data available on request.

References

Andersen, T., Sæther, O. A., Cranston, P. S. & Epler, J. H. 2013: The larvae of Orthocladiinae (Diptera: Chironomidae) of the Holarctic region-keys and diagnoses. *Insect Systematics & Evolution 66*, 189–385.

Barley, E. M., Walker, I. R., Kurek, J., Cwynar, L. C., Mathewes, R. W., Gajewski, K. & Finney, B. P. 2006: A northwest North American training set: distribution of freshwater midges in relation to air temperature and lake depth. *Journal of Paleolimnology 36*, 295–314.

Birks, H. J. B. 1998: D.G. Frey and E.S. Deevey review 1: numerical tools in palaeolimnology – progress, potentialities, and problems. *Journal of Paleolimnology 20*, 307–332.

Birks, H. J. B., Braak, C. T., Line, J. M., Juggins, S. & Stevenson, A. C. 1990: Diatoms and pH reconstruction. *Philosophical Transactions of the Royal Society of London. Series B: Biological Sciences 327*, 263–278.

Birks, H. J. B., Heiri, O., Seppä, H. & Bjune, A. E. 2010: Strengths and weaknesses of quantitative climate reconstructions based on Late-Quaternary. *The Open Ecology Journal 3*, 68–100.

Brooks, S. J. & Birks, H. J. B. 2000: Chironomid-inferred late-glacial and early-Holocene mean July air temperatures for Kråkenes Lake, western Norway. *Journal of Paleolimnology 23*, 77–89.

Brooks, S. J., Bennion, H. & Birks, H. J. B. 2001: Tracing lake trophic history with a chironomid–total phosphorus inference model. *Freshwater Biology 46*, 513–533.

Brooks, S. J., Langdon, P. G. & Heiri, O. 2007: The identification and use of Palaearctic Chironomidae larvae in palaeoecology. *Quaternary Research Association Technical Guide 10*, i–vi.

Chamutiova, T., Hamerlik, L. & BituŠÍk, P. 2020: Subfossil chironomids (Diptera, Chironomidae) of lakes in the Tatra Mountains: an illustrated guide. *Zootaxa 4819*, 216–264.

Cornes, R. C., van der Schrier, G., van den Besselaar, E. J. & Jones, P. D. 2018: An ensemble version of the E-OBS temperature and precipitation data sets. *Journal of Geophysical Research: Atmospheres 123*, 9391–9409.

Eggermont, H. & Heiri, O. 2012: The chironomid-temperature relationship: expression in nature and palaeoenvironmental implications. *Biological Reviews 87*, 430–456.

Ekrem, T. 2006: A redescription of *Neozavrelia cuneipennis* (Edwards) comb. nov., with a checklist of *Neozavrelia* species of the world (Diptera: Chironomidae). *Zootaxa 1153*, 1–16.

Feurdean, A., Perşoiu, A., Tanţău, I., Stevens, T., Magyari, E. K., Onac, B. P., Marković, S., Andrič, M., Connor, S., Färcaş, S. & Gałka, M. 2014: Climate variability and associated vegetation response throughout Central and Eastern Europe (CEE) between 60 and 8 ka. *Quaternary Science Reviews 106*, 206–224.

Fortin, M. C., Medeiros, A. S., Gajewski, K., Barley, E. M., Larocque-Tobler, I., Porinchu, D. F. & Wilson, S. E. 2015: Chironomid-environment relations in northern North America. *Journal of Paleolimnology 54*, 223–237.

Fu, C. 1992: Transitional climate zones and biome boundaries: a case study from China. *In* Hansen, A. J. & di Castri, F. (eds.): *Landscape Boundaries. Ecological Studies 92*, 394–402. Springer, New York.

Giesecke, T. A. E. B., Bjune, A. E., Chiverrell, R. C., Seppä, H., Ojala, A. E. K. & Birks, H. J. B. 2008: Exploring Holocene continentality changes in Fennoscandia using present and past tree distributions. *Quaternary Science Reviews 27*, 1296–1308.

Goldenberg Vilar, A., Donders, T., Cvetkoska, A. & Wagner-Cremer, F. 2018: Seasonality modulates the predictive skills of diatom based salinity transfer functions. *PLoS One 13*, e0199343, https://doi.org/10.1371/journal.pone.0199343.

Gouw-Bouman, M. T. I. J., Van Asch, N., Engels, S. & Hoek, W. Z. 2019: Late Holocene ecological shifts and chironomid-inferred summer temperature changes reconstructed from Lake Uddelermeer, the Netherlands. *Palaeogeography, Palaeoclimatology, Palaeoecology 535*, 109366, https://doi.org/10.1016/j.palaeo.2019.109366.

Heiri, O. 2004: Within-lake variability of subfossil chironomid assemblages in shallow Norwegian lakes. *Journal of Paleolimnology 32*, 67–84.

Heiri, O. & Lotter, A. F. 2010: How does taxonomic resolution affect chironomid-based temperature reconstruction? *Journal of Paleolimnology 44*, 589–601.

Heiri, O., Brooks, S. J., Birks, H. J. B. & Lotter, A. F. 2011: A 274-lake calibration data-set and inference model for chironomid-based summer air temperature reconstruction in Europe. *Quaternary Science Reviews 30*, 3445–3456.

Heiri, O., Brooks, S. J., Renssen, H., Bedford, A., Hazekamp, M., Ilyashuk, B., Jeffers, E. S., Lang, B., Kirilova, E., Kuiper, S. & Millet, L. 2014: Validation of climate model-inferred regional temperature change for late-glacial Europe. *Nature Communications 5*, 4914, https://doi.org/10.1038/ncomms5914.

Hill, M. O. & Gauch, H. G. 1980: Detrended correspondence analysis: an improved ordination technique. *Vegetatio 42*, 47–58.

Johannessen, O. M. 1970: Note on some vertical profiles below ice floes in the Gulf of St. Lawrence and near the North Pole. *Journal of Geophysical Research 75*, 2857–2861.

Juggins, S. 2013: Quantitative reconstructions in palaeolimnology: new paradigm or sick science? *Quaternary Science Reviews 64*, 20–32.

Juggins, S. 2022: *rioja: analysis of quaternary science data, R package version (1.0-5)*. Available at: https://cran.r-project.org/web/packages/rioja/rioja.pdf.

Kaufman, D., McKay, N., Routson, C., Erb, M., Davis, B., Heiri, O., Jaccard, S., Tierney, J., Dätwyler, C., Axford, Y. & Brussel, T. 2020: A global database of Holocene paleotemperature records. *Scientific Data 7*, 115, https://doi.org/10.1038/s41597-020-0445-3.

Klink, A. G. & Pillot, H. K. M. 2003: *Chironomidae Larvae: Key to the Higher Taxa and Species of the Lowlands of Northwestern Europe*. ETI 6338, Expert Center for Taxonomic Identification, University of Amsterdam, Amsterdam.

Kotrys, B., Płóciennik, M., Sydor, P. & Brooks, S. J. 2020: Expanding the Swiss–Norwegian chironomid training set with Polish data. *Boreas 49*, 89–107.

Larocque, I., Hall, R. I. & Grahn, E. 2001: Chironomids as indicators of climate change: a 100-lake training set from a subarctic region of northern Sweden (Lapland). *Journal of Paleolimnology 26*, 307–322.

Larocque-Tobler, I. 2014: The Polish sub-fossil chironomids. *Palaeontologia Electronica 17*, 1–28.

Lepš, J. & Šmilauer, P. 2003: *Multivariate Analysis of Ecological Data Using CANOCO*. 280 pp. Cambridge University Press, Cambridge, https://doi.org/10.1017/CBO9780511615146.

Little, J. L. & Smol, J. P. 2000: Changes in fossil midge (Chironomidae) assemblages in response to cultural activities in a shallow, polymictic lake. *Journal of Paleolimnology 23*, 207–212.

Lotter, A. F., Birks, H. J. B., Hofmann, W. & Marchetto, A. 1997: Modern diatom, cladocera, chironomid, and chrysophyte cyst assemblages as quantitative indicators for the reconstruction of past environmental conditions in the Alps. I. Climate. *Journal of Paleolimnology 18*, 395–420.

Luoto, T. P. 2009: Subfossil Chironomidae (Insecta: Diptera) along a latitudinal gradient in Finland: development of a new temperature inference model. *Journal of Quaternary Science 24*, 150–158.

Luoto, T. P. 2011: The relationship between water quality and chironomid distribution in Finland – a new assemblage-based tool for assessments of long-term nutrient dynamics. *Ecological Indicators 1*, 255–262.

Medeiros, A. S., Chipman, M. L., Francis, D. R., Hamerlík, L., Langdon, P., Puleo, P. J., Schellinger, G., Steigleder, R., Walker, I. R., Woodroffe, S. & Axford, Y. 2022: A continental-scale chironomid training set for reconstructing Arctic temperatures. *Quaternary Science Reviews 294*, 107728, https://doi.org/10.1016/j.quascirev.2022.107728.

Medeiros, A. S., Gajewski, K., Porinchu, D. F., Vermaire, J. C. & Wolfe, B. B. 2015: Detecting the influence of secondary environmental gradients on chironomid-inferred paleotemperature reconstructions in northern North America. *Quaternary Science Reviews 124*, 265–274.

Nazarova, L., Herzschuh, U., Wetterich, S., Kumke, T. & Pestryakova, L. 2011: Chironomid-based inference models for estimating mean July air temperature and water depth from lakes in Yakutia, northeastern Russia. *Journal of Paleolimnology 45*, 57–71.

Nazarova, L., Syrykh, L., Grekov, I., Sapelko, T., Krasheninnikov, A. B. & Solovieva, N. 2023: Chironomid-based modern summer temperature data set and inference model for the northwest European part of Russia. *Water 15*, 976, https://doi.org/10.3390/w15050976.

Ni, Z., Zhang, E., Meng, X., Sun, W. & Ning, D. 2023: Chironomid-based reconstruction of 500-year water-level changes in Daihai Lake, northern China. *Catena 227*, 107122, https://doi.org/10.1016/j.catena.2023.107122.

Oksanen, J. and 32 others 2022: *vegan: community ecology package. R package version 2.6-4*. Available at: https://CRAN.R-project.org/package=vegan.

Orendt, C. 1999: Chironomids as bioindicators in acidified streams: a contribution to the acidity tolerance of chironomid species with a classification in sensitivity classes. *International Review of Hydrobiology 84*, 439–449.

Pegler, S., Simmatis, B., Labaj, A. L., Meyer-Jacob, C. & Smol, J. P. 2020: Long-term changes in chironomid assemblages linked to lake liming and fertilization in previously acidified middle lake (Sudbury, Canada). *Water, Air, & Soil Pollution 231*, 410, https://doi.org/10.1007/s11270-020-04780-y.

Plikk, A., Engels, S., Luoto, T. P., Nazarova, L., Salonen, J. S. & Helmens, K. F. 2019: Chironomid-based temperature reconstruction for the Eemian interglacial (MIS 5e) at Sokli, northeast Finland. *Journal of Paleolimnology 61*, 355–371.

Płóciennik, M., Mroczkowska, A., Pawłowski, D., Wieckowska-Lüth, M., Kurzawska, A., Rzodkiewicz, M., Okupny, D., Szmańda, J., Mazurkevich, A., Dolbunova, E. & Luoto, T. P. 2022: Summer temperature drives the lake ecosystem during the Late Weichselian and Holocene in Eastern Europe: a case study from East European Plain. *Catena 214*, 106206, https://doi.org/10.1016/j.catena.2022.106206.

Quinlan, R. & Smol, J. P. 2001: Setting minimum head capsule abundance and taxa deletion criteria in chironomid-based inference models. *Journal of Paleolimnology 26*, 327–342.

Rao, Z., Tian, Y., Guang, K., Wei, S., Guo, H., Feng, Z., Zhao, L. & Li, Y. 2022: Pollen data as a temperature indicator in the late Holocene: a review of results on regional, continental and global scales. *Frontiers in Earth Science 10*, 84565, https://doi.org/10.3389/feart.2022.845650.

Rees, A. B., Cwynar, L. C. & Cranston, P. S. 2008: Midges (Chironomidae, Ceratopogonidae, Chaoboridae) as a temperature proxy: a training set from Tasmania, Australia. *Journal of Paleolimnology 40*, 1159–1178.

Ruse, L. P., Greaves, H. M., Sayer, C. D. & Axmacher, J. C. 2018: Consequences of pond management for chironomid assemblages and diversity in English farmland ponds. *Journal of Limnology 77*, 160–168, https://doi.org/10.4081/jlimnol.2018.1789.

Schmid, P. E. 1993: *A Key to the Larval Chironomidae and Their Instars from Austrian Danube Region Streams and Rivers. Part 1: Diamesinae, Prodiamesinae and Orthocladiinae*. 512 pp. Federal Institute for Water Quality, Vienna.

Šeirienė, V., Gastevičienė, N., Luoto, T. P., Gedminienė, L. & Stančikaitė, M. 2021: The Lateglacial and early Holocene climate variability and vegetation dynamics derived from chironomid and pollen records of Lieporiai palaeolake, North Lithuania. *Quaternary International 605*, 55–64.

Self, A. E., Brooks, S. J., Birks, H. J. B., Nazarova, L., Porinchu, D., Odland, A., Yang, H. & Jones, V. J. 2011: The distribution and abundance of chironomids in high-latitude Eurasian lakes with respect to temperature and continentality: development and application of new chironomid-based climate-inference models in northern Russia. *Quaternary Science Reviews 30*, 1122–1141.

Seppä, H., Bjune, A. E., Telford, R. J., Birks, H. J. B. & Veski, S. 2009: Last nine-thousand years of temperature variability in Northern Europe. *Climate of the Past 5*, 523–535.

Ter Braak, C. J. 1992: Permutation versus bootstrap significance tests in multiple regression and ANOVA. *In Bootstrapping and Related Techniques: Proceedings of an International Conference, Held in Trier, FRG, June 4–8, 1990*, 79–85. Springer, Berlin.

Ter Braak, C. J. & Juggins, S. 1993: Weighted averaging partial least squares regression (WA-PLS): an improved method for reconstructing environmental variables from species assemblages. *In Proceedings of the Twelfth International Diatom Symposium, Renesse, the Netherlands*, 485–502. Springer, Dordrecht.

Ter Braak, C. J. & Verdonschot, P. F. 1995: Canonical correspondence analysis and related multivariate methods in aquatic ecology. *Aquatic Sciences 57*, 255–289.

Ursenbacher, S., Stötter, T. & Heiri, O. 2020: Chitinous aquatic invertebrate assemblages in Quaternary lake sediments as indicators of past deepwater oxygen concentration. *Quaternary Science Reviews 231*, 106203, https://doi.org/10.1016/j.quascirev.2020.106203.

Väliranta, M., Salonen, J. S., Heikkilä, M., Amon, L., Helmens, K., Klimaschewski, A., Kuhry, P., Kultti, S., Poska, A., Shala, S. & Veski, S. 2015: Plant macrofossil evidence for an early onset of the Holocene summer thermal maximum in northernmost Europe. *Nature Communications 6*, 6809, https://doi.org/10.1038/ncomms7809.

Velle, G., Brodersen, K. P., Birks, H. J. B. & Willassen, E. 2010: Midges as quantitative temperature indicator species: lessons for palaeoecology. *The Holocene 20*, 989–1002.

Verbruggen, F., Heiri, O., Meriläinen, J. J. & Lotter, A. F. 2011: Subfossil chironomid assemblages in deep, stratified European lakes: relationships with temperature, trophic state and oxygen. *Freshwater Biology 56*, 407–423.

Walker, I. R. & Mathewes, R. W. 1987: Chironomids, lake trophic status, and climate. *Quaternary Research 28*, 431–437.

Walker, I. R., Levesque, A. J., Cwynar, L. C. & Lotter, A. F. 1997: An expanded surface-water palaeotemperature inference model for use with fossil midges from eastern Canada. *Journal of Paleolimnology 18*, 165–178.

Wickham, H., Averick, M., Bryan, J., Chang, W., McGowan, L. D., François, R., Grolemund, G., Hayes, A., Henry, L., Hester, J., Kuhn, M., Pedersen, T. L., Miller, E., Bache, S. M., Müller, K., Ooms, J., Robinson, D., Seidel, D. P., Spinu, V., Takahashi, K., Vaughan, D., Wilke, C., Woo, K. & Yutani, H. 2019: Welcome to the tidyverse. *Journal of Open Source Software 4*, 1686, https://doi.org/10.21105/joss.01686.

Wickham, H., François, R., Henry, L. & Müller, K. 2022: *Dplyr: a grammar of data manipulation. R package version 1.0.10*. Available at: https://CRAN.R-project.org/package=dplyr.

Wood, S. N. 2011: Fast stable restricted maximum likelihood and marginal likelihood estimation of semiparametric generalized linear models. *Journal of the Royal Statistical Society Series B: Statistical Methodology 73*, 3–36.

Wood, S. N. 2017: *Generalized Additive Models: An Introduction with R*. 496 pp. Chapman and Hall/CRC, Boca Raton.

Supporting Information

Additional Supporting Information to this article is available at http://www.boreas.dk.

Fig. S1. Distribution of environmental variables in lakes of the Eastern Baltic training set.

Table S1. Environmental and geographical data of Eastern Baltic lakes.

Table S2. Linear regression and general additive models of species with mean abundance >1% with the mean July air temperature (MJAT) as an explanatory variable.

Appendix 2 (Paper II)

Bakumenko, V., Poska, A., Birks, H. J. B., Huser, B., & Veski, S. (2025). Chironomid-climate continentality conundrum. PLOS One, 20(8), e0327780. https://doi.org/10.1371/journal.pone.0327780

RESEARCH ARTICLE

Chironomid-climate continentality conundrum

Varvara Bakumenko[1], **Anneli Poska**[1,2*], **H. John B. Birks**[3], **Brian Huser**[4], **Siim Veski**[1]

1 Department of Geology, Tallinn University of Technology, Tallinn, Estonia, **2** Department of Physical Geography and Ecosystem Science, Lund University, Sweden, **3** Department of Biological Sciences and Bjerknes Centre for Climate Research, University of Bergen, Norway; Environmental Change Research Centre, University College London, London, United Kingdom, **4** Department of Aquatic Sciences and Assessment, Swedish University of Agricultural Sciences, Uppsala, Sweden

* anneli.poska@nateko.lu.se

Abstract

It is predicted that continentality, a climate parameter representative of a region's annual temperature and precipitation range, will undergo significant changes in the future. The lack of past continentality reconstructions makes it impossible to decipher any long-term patterns of continentality changes. Here, we investigate the extent to which continentality influences modern chironomid assemblages and evaluate their ecological relevance for palaeolimnological data-based reconstructions of past continentality. We selected 53 lakes along a longitudinal gradient covering the East European Plain (Western part of Russia, Estonia, Latvia) and southern Scandinavia (Sweden and Norway). We analysed the dependency of chironomid assemblages on a variety of environmental parameters including two continentality indices (annual temperature range (ATR) and the Kerner Oceanity Index (KOI)), growing degree days at base temperature 5 °C, mean air temperatures of July, April, and October, number of ice-cover days, lake-water pH, loss-of-ignition and water depth using redundancy analysis. Correlations between all variables were tested to check for possible confounding effects. KOI had the highest explanatory power of 18.4% in the dataset and an absence of collinearity (correlation index < 0.7) with all the other tested variables. Further, we estimated weighted average optima to investigate the distribution of the morphotypes along the continentality gradient in the dataset. *Glyptotendipes pallens*-type, *Neozavrelia*, *Polypedilum sordens*-type, and *Microchironomus* showed a preference for a continental climate, while *Paratanytarsus penicillatus*-type, *Pseudorthocladius*, *Thienemannimyia*, and *Limnophyes* were found mainly in samples from oceanic areas. Weighted averaging-partial least squares regression was used for a trial test of the data, resulting in a promising KOI-based model performance with $R^2 = 0.73$ and RMSEP = 5.1. Despite the relatively small dataset, our study suggests that chironomid data have the potential for further development as a tool for reconstructing palaeocontinentality.

OPEN ACCESS

Citation: Bakumenko V, Poska A, Birks HJB, Huser B, Veski S (2025) Chironomid-climate continentality conundrum. PLoS One 20(8): e0327780. https://doi.org/10.1371/journal.pone.0327780

Editor: Walter Finsinger, Centre National de la Recherche Scientifique, FRANCE

Received: December 2, 2024

Accepted: June 20, 2025

Published: August 5, 2025

Data availability statement: All relevant data are within the paper and its Supporting Information files.

Funding: : This study was financially supported by the Estonian Research Council grants PRG1993 and TK215. Varvara Bakumenko was supported by the Doctoral School of Earth Sciences and Ecology, supported by

the European Union, European Regional Development Fund (ASTRA "TTÜ arengupro-gramm aastateks 2016–2022"). Anneli Poska was supported by Swedish strategic research area BECC (Biodiversity and Ecosystem Services in a Changing Climate); MERGE (ModElling the Regional and Global Earth system at Lund University).

Competing interests: The authors have declared that no competing interests exist.

Introduction

Continentality, a climate parameter that combines information on annual variation in temperature and precipitation, has changed in the past and is predicted to change in the future [1,2]. Continentality of a region depends on the distance from the ocean and the prevailing atmospheric circulation patterns [2]. While the annual temperature range (ATR, calculated as the difference between the coldest and the warmest months) is the simplest and most used metric to estimate continentality, several other indices have been proven relevant to describe the continentality gradient in nature. These include the Gorzynski [3] continentality index, which includes latitude in the index, and the Kerner Oceanity Index (KOI; [4]), which includes October and April air temperatures.

Continentality has significantly changed over the last century [2,5], resulting in an increase in Northern Europe, most of North America and East Asia [2], and a decrease in the Eastern Baltic countries (Estonia, Latvia, Lithuania) [6]. These changes are expected to continue in the context of ongoing climate change [6,7]. Continentality variations may occur due to changes in solar radiation, and variations in atmospheric circulation and ocean heat transportation [8]. These changes affect various natural processes, such as permafrost degradation [9], ecosystem productivity [10], biodiversity distribution [11], tree bimodality growth [12]. Continentality can affect the aquatic zoobenthos by inducing variations in the start, duration, and heat accumulation of the growing season [13] as well as the timing of lake turnover [14]. It can also influence the formation and duration of the ice-cover at mid and high latitudes, leading to changes in water pH [15] and dissolved oxygen concentration [16]. Northern and eastern Europe, and the Baltic area in particular, are situated in a transitional zone between continental and oceanic climates, making this region highly suited for studies of long-term changes in continentality. Furthermore, a marked increase in continentality (annual temperature range) has been observed in the eastern Baltic area during recent decades (−1.7 KOI values per decade; [2]), highlighting the urgent need for past continentality-related knowledge, which could assist in making realistic, evidence-based continentality predictions. Understanding long-term continentality is essential for accurate climate modelling, ecosystem management, climate change adaptation, land-use planning, and unravelling the Earth's geological history. It provides a framework for interpreting both past and future climate dynamics, especially in regions where the influence of landmasses dominates over oceanic moderation.

Long-term reconstructions of past changes in climate parameters are often used to determine and predict their impacts on ecosystems (e.g., [17–22]). Only a few reconstructions of palaeocontinentality have been published [23–27]. For instance, increased seasonality has been inferred from cryogenic cave carbonates in Great Britain during the Younger Dryas period event. [28], and from phosphorus concentrations changes in stalagmite calcite in western Ireland during the 8.2 ka cooling [29]. Other attempts to develop a continentality reconstruction have been based on tree rings or ice wedges data [25,27]. However, tree-ring data are confounded by too many intertwined environmental and climate factors, while ice wedges are limited to the few regions that historically had permafrost. Thus, not much is known about continentality changes in the past and their impact on ecosystems.

Larvae of chironomids, non-biting midges from the family Chironomidae, are recognised as one of the most reliable palaeoclimate proxies [30]. The taxonomic composition of subfossil chironomid assemblages is known to be responsive to environmental conditions [31,32], such as lake water trophic state [33,34], dissolved oxygen concentrations [35,36], pH [34,37], and depth [37,38]; warm season temperatures [39–42], and heat accumulation expressed as growing degree days (GDD; [43]). Chironomids are often assumed to be non-responsive directly to changes in winter temperatures as they experience diapause during the winter season in temperate and boreal climate zones [44]. However, several studies have shown a significant dependency of chironomid assemblages on winter temperatures [30,45]. An indirect impact of winter temperatures has been observed in several recent studies, showing that chironomid assemblages from boreal and temperate zones can be affected by the duration of ice cover, which is inversely correlated with dissolved oxygen levels and the warm season duration [24,46], as well as with continentality [47]. Self et al. [24] show that chironomid assemblages in northern Russia are influenced by continentality (Gorzynski continentality index), which is thought to have an indirect effect through variations in ice-cover period length. It is commonly recommended to use chironomid training sets only within the biogeographic area from which they originated [48,49]. Therefore, the training set developed by Self et al. [24] is applicable only in northern Russia.

To expand our understanding of the relationship between chironomids and continentality in areas with transitional climates in northern and eastern Europe, we have assembled a new chironomid dataset that represents a wide range of climatic and environmental variations along a longitudinal continentality gradient (Fig 1) in northern and eastern Europe – from the oceanic Norwegian coast to the continental Ural Mountains. The objectives of our study are to determine (1) possible confounding factors to continentality environmental variables; (2) the potential influence of continentality and related climate variables on chironomid assemblages; and (3) the indicator taxa representative of different parts of the continentality gradient. This paper aims to serve as a prerequisite and justification for the increased use of chironomids as a continentality proxy and as a starting point for developing a more extensive training set applicable in northern and eastern Europe. Data derived from continentality reconstructions will enhance our understanding of how continentality varies over time and how it impacts natural ecosystems.

Materials and methods

Climate data

Hourly temperature (°C) and lake ice-thickness (mm) data for each lake were extracted from the ERA5 dataset with hourly temporal and 0.25° x 0.25°spatial resolution [50], which was downloaded from the Copernicus Climate Data Store. Using the downloaded climatic data, the following variables were calculated based on a 30-year mean:

(1) Mean January, April, July and October temperatures (°C).

(2) Continentality indices: annual temperature range (ATR; the difference between the warmest month's mean temperature (July for all sites) and the coldest month's mean temperature (January for all sites)); Kerner Oceanity Index (KOI; [4]), reflecting not only annual temperature variation, but also the warmth of spring and autumn, calculated following the equation: KOI = 100×(To-Ta)/ATR, where To is the mean October air temperature (°C), Ta is the mean April air temperature (°C), and ATR is the annual air temperature range (°C)).

(3) Annual sum of Growing Degree Days at a base temperature of 5 °C (GDD5) was calculated by applying the daily temperature data following the equation [51]: $\sum_{i=1}^{365} \frac{Tmin+Tmax}{2} - Tbase$, where T_{base} equals 5 °C and i refers to day of the year.

(4) Ice conditions (number of ice-cover days): the number of ice-cover days was estimated using the ice-thickness dataset by summing the number of days with a minimum ice thickness across the lake > 0 mm.

Based on the above-listed datasets a set of thematic maps covering Northern and Eastern Europe was created. The dataset design strategy was guided by the longitudinal (east to west) continentality (ATR) gradient observed in northern Europe (Fig 1).

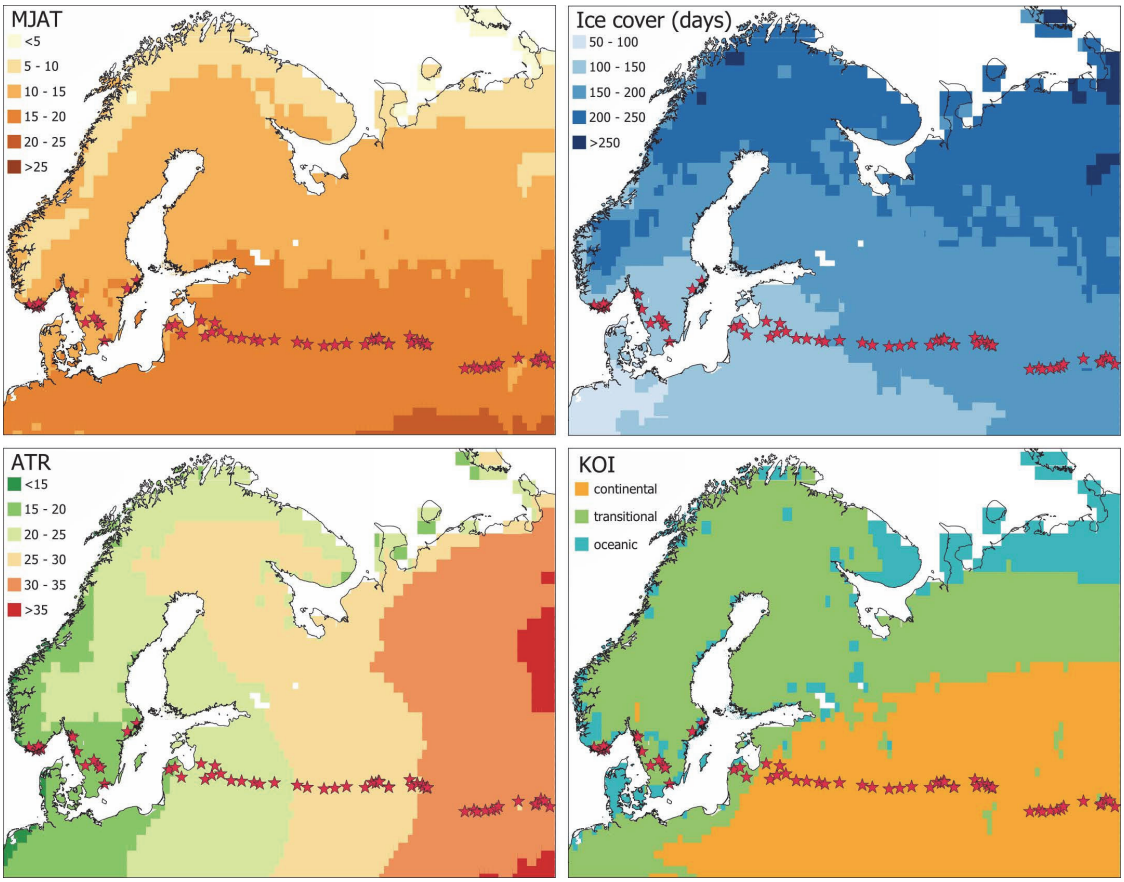

Fig 1. Map of sampled lakes with respect to mean July air temperature (MJAT; °C), ice-cover duration (days), annual temperature range (ATR; °C), and Kerner Oceanity Index (KOI; continental area (orange) is KOI −10 - 0, transitional (green) is KOI = 0–10, and oceanic (blue) is KOI 10-20).

https://doi.org/10.1371/journal.pone.0327780.g001

Site selection

The following sets of sites (Table 1) were used to compile the training set:

(1) six oceanic sites from Norway (part of the Swiss-Norwegian training set collected in 1995–1999 by Heiri et al. [39]; the data were downloaded from the National Centre of Environmental Information online storage);

(2) seven intermediate continentality sites from Latvia (part of the Finno-Baltic-Polish training set collected in 2019–2021 by Bakumenko et al. [42]);

(3) thirty-one intermediate to continental sites from western Russia collected for this study in 2021;

(4) nine oceanic to intermediate continentality sites from Sweden (Huser, unpublished) collected in 2014 were added to fill the biogeographical gap between the Norwegian and Latvian-Russian parts of the dataset (Fig 1).

Table 1. Environmental and climate gradients covered by the new combined dataset. Growing degree days and ice-cover represents sum annual variables.

Dataset origin	Norway	Sweden	Latvia	Russia
Number of sites	6	9	7	31
Latitude (°N)	58.02–58.25	57.2–59.5	56.4–57.3	54.5–56.2
Longitude (°E)	7.0–8.2	11.5–18.3	21.7–27.1	28.2–61.7
Distance to sea (km)	3.2–20.2	2–110	41.2–176	255–1568
Elevation (m, above the sea level)	24–251	28–238	51–108	57–391
July air temperature (°C)	14.6–16.8	16.0–17.3	18.0–20.0	17.8–20.2
Annual temperature range (°C)	14.4–16.7	17–19.4	19.8–22.7	23.0–33.3
Kerner Oceanity Index	15.8–27.5	6–11.3	−2.4–8.4	−4.5 – −1.6
Growing degree days 5 (°C)	1200–1511	939–1088	1599–1729	1497–1880
Ice-cover period (days)	35–83	43–65	91–126	126–196
Sampling water depth (m)	5.2–19.5	6.5–45	2.8–20	0.7–12.5
Lake-water pH	5.1–7	6–7.2	6.8–8.6	7.5–10.8

https://doi.org/10.1371/journal.pone.0327780.t001

Thus, the final dataset consists of 53 lake sediment surface samples along the longitudinal gradient 7–61.7 °E, between 54.5 and 59.5 °N latitude (Fig 1, Table 1). The dataset covers a broad range of environmental and climatic gradients. Most of the lakes are situated in low-elevation areas with fully vegetated catchments (Table 1). The surrounding biomes range from temperate steppe in the east to hemiboreal and temperate mixed in the central regions, and coniferous forests in the west. Bedrock includes sandstone in the eastern part of the dataset, limestone in the middle, and gneiss/granitoid in the western part (southern Norway and Sweden).

Environmental data

The basic environmental variables (lake-water depth and pH, sediment loss-of-ignition (LOI), and catchment soil and bedrock composition) were included to assess their influence on the Chironomidae assemblages and to examine potential confounding effects with the climatic variables.

In connection with the surface-sediment sampling, lake-water depth and pH (at 30–40 cm above the sediment surface) were measured in the field. LOI was measured only for Russian and Latvian samples using the standard procedure [52]. The underlying bedrock type was identified using a bedrock map of Europe (Commission of the Geological Map of the World Subcommission for Europe; CGMW). Soil composition data (sand, clay, and soil base saturation) were extracted from the FAO Digital Soil Map of the World (2003). While a multitude of other environmental parameters could affect the chironomid assemblages, we selected those that are most commonly used and consistently available across the entire dataset.

Sediment sample collection and laboratory processing

Surface-sediment samples for all parts of the dataset were collected using a gravity corer from the deepest part of each lake. The upper 2 cm of lake sediment were taken for analysis. Sampling did not involve endangered or protected species and was done following legal acts of the corresponding countries. In the laboratory, sediment samples of 5 cm^3 were water-sieved with a 100-µm mesh to remove fine sediment. Each sample was then transferred to a Petri dish from which chironomid head capsules were extracted with fine forceps under a stereomicroscope at 25x magnification. The head capsules were air-dried and mounted in Aquatex® or Euparal® mounting medium. Taxonomic identification was conducted under a light microscope at 100–400X magnification.

Taxonomic identification and dataset harmonisation

For all four parts of the dataset (Norwegian, Swedish, Latvian, Russian), identification of the chironomid head capsules was done following the taxonomic approach of Brooks et al. [53]. Chironomid assemblages from the Latvian, Russian

(analysed by Varvara Bakumenko), and Swedish (analysed by Simon Belle) parts were identified using keys by Klink and Pillot [54], Brooks et al. [53], Larocque-Tobler [55], and Andersen et al. [56]. On average, 69 chironomid head capsules were identified per sample, with a range of 47–139 (S1 File).Final taxonomic harmonisation was done after merging all the above-described datasets. All identifications at genus or subfamily taxonomic level (Tanytarsini, *Tanytarsus* spp., *Paratanytarsus* spp., Tanypodinae, Chironomini, Orthocladinae) were excluded from the merged dataset to avoid including broad groups of Chironomidae species with a wide range of ecological preferences. The excluded taxa made up less than 10% of the total head capsules count in the dataset and no more than 8% in any individual sample. *Cricotopus intersectus*-type was merged with *Cricotopus laricomalis*-type into one type due to the likelihood of misidentification of these morphotypes. Morphotype-level identifications from *Einfeldia (Einfeldia dissidens*-type), *Zalutschia (Zalutschia zalutschicola*-type), *Eukieferiella* (*Eukiefferiella coerulescens*-type), and *Dicrotendipes (Dicrotendipes nervosus*-type and *Dicrotendipes notatus*-type) were merged into corresponding genera level groups due to the differences in identification resolution in parts of the dataset. Harmonisation was done before transforming the data into relative abundances.

Numerical analysis

The harmonized chironomid count data was transformed into relative abundances, and thereafter square-root transformed. To remove rare taxa, only morphotypes with an abundance higher than 2% in at least one sample were included for numerical analysis to improve performance of the inference model [57]. Based on KOI, the dataset was divided into 3 parts: continental with KOI −10–0, transitional with KOI 0–10, and oceanic with KOI 10–20 [2]. Analysis of similarities (ANOSIM; [58]) was applied to justify the KOI-based division of the chironomid assemblages. Bedrock data were grouped in 4 groups (sand-containing, clay-containing, carbonates-containing, granits/granitoids) and coded as numbers (1–4) for the numerical analyses.

Principal component analysis (PCA) was applied to the environmental and climate data of the dataset to investigate their gradients length. The Shapiro-Wilcox test and Spearman correlations were used to test for collinearity between environmental and climatic variables. Variables with correlation coefficient $> \pm 0.7$ were considered highly correlated and their effect on chironomid assemblages could not be distinguished from each other.

Detrended correspondence analysis (DCA; [59]) was applied to the chironomid assemblages data to examine the distribution of taxa and the compositional gradient lengths along the first two DCA axes. Redundancy analysis (RDA) was chosen based on the length of DCA axis-1 and axis-2 of the dataset (2.9 and 2 SD units, respectively; [60,61]). RDA was applied to determine which environmental variables explain significant compositional variation in the chironomid data. Weighted averaging-partial least squares (WA-PLS; [62]) was performed to evaluate the idea of developing a chironomid-based training set applicable to the reconstructions of continentality. The continentality related variable which showed the strongest relationship to the chironomid assemblages and had a $\lambda 1{:}\lambda 2$ ratio of more than 1 in RDA was used. The strongest transfer function was determined as the one producing the lowest cross-validated root mean square error of prediction (RMSEP). The relevant components were accepted as statistically significant at the $p \leq 0.05$ level. Bootstrapping techniques (9999 permutations; [60,63]) were used to estimate cross-validated error and performance statistics for the WA-PLS inference model, such as RMSEP, maximum and mean bias, and the coefficient of determination (R^2) between inferred and predicted values.

Indicator species analysis (INDVAL; [64]) was applied to reveal characteristic morphotypes for the best performing continentality related variable according to the RDA results. Weighted-average regression with inverse deshrinking ([62]) was applied to the taxa that were determined as potential indicators to estimate taxon-specific continentality optima.

The software program R version 4.1.1. (R Core Team, 2021) was used to perform numerical analyses and create plots. The following packages were used: 'tidyverse' for data visualisation [65], 'dplyr' for data restructuring and basic calculations [66], 'vegan' for ordination and ANOSIM [67], 'rioja' for WA-PLS and WA and plotting the stratigraphic diagram [68], and 'indicspecies' for performing the INDVAL [69].

Results

Climatic and environmental setting of the dataset

PCA of the environmental and climate data indicated that GDD5 and ice-cover had the longest gradients (Fig 2A). Most tested variables, except for ATR, KOI, January and October mean temperatures, aligned with the first PCA axis, hence the explanatory power of the axis was high (25.8%). Among the climatic variables, GDD5, KOI, ATR, October and July air temperatures were significantly correlated with one another and with most of the remaining climatic variables. April air temperatures were correlated with only two climatic variables: KOI and ice-cover. January air temperatures explicit no significant correlations with other variables (Fig 2B). Environmental variables (water depth, pH, soil base saturation, sand and clay content) generally had correlation values of <± 0.7 with climatic variables (GDD5, ice-cover, July, April, and October mean air temperatures, ATR, KOI) except for bedrock which was highly correlated (>0.8) with ice-cover, ATR, and October mean air temperature.

Chironomidae assemblage composition and distribution

The harmonized dataset includes on average 63 head capsules per sample with counts ranging from 42 head capsules to 139 head capsules. The dataset includes 51 lakes and 73 morphotypes (Fig 3; S1 File). The most abundant morphotypes are *Chironomus plumosus*-type (0.8–49.1% per sample), *Psectrocladius sordidellus*-type (0.7–26.9%), *Dicrotendipens* (0.7–22.2%), and *Tanytarsus pallidicornis*-type (0.7–12.8%). The presence of *Chironomus anthracinus*-type, *Heteratanytarsus*, *Heterotrissocladius marcidus*-type, *Sergentia coracina*-type, and *Zalutschia* characterises the transitional and oceanic parts of the dataset. These taxa are either absent or present in lower quantities in more continental lakes. Transitional lakes are further differentiated from oceanic ones by the presence of *Psecrocladius penicillatus*-type and *Pseudorthocladius*, and higher abundances of *Heterotrissocladius marcidus*-type, *Tanytarsus pallidicornis*-type and *Microtendipes pedellus*-type.

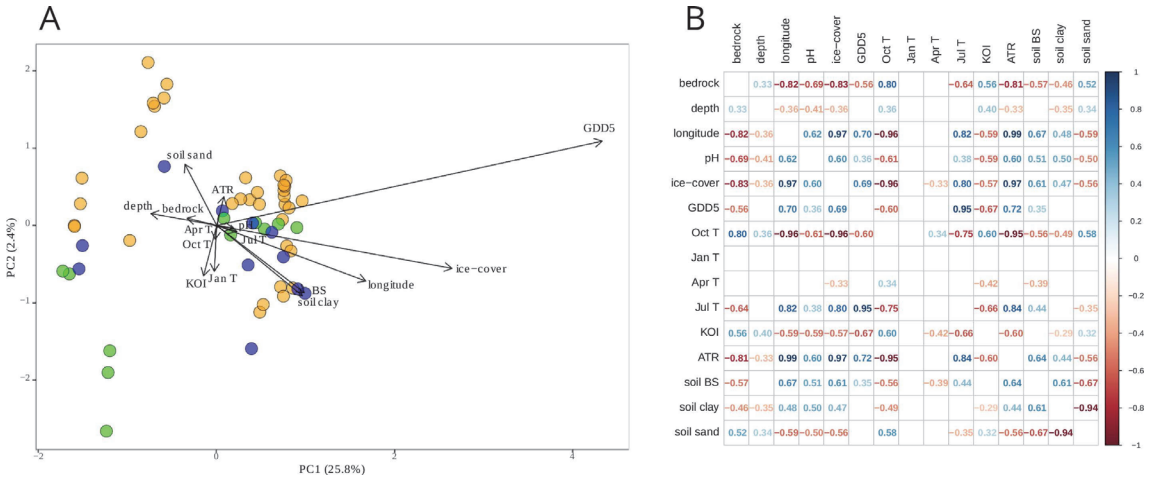

Fig 2. (A) Principal component analysis (PCA) with total variation of 27.6% and (B) Spearman correlation matrix of the climatic and environmental variables in the dataset: bedrock type; lake-water depth (m); longitude; lake-water pH; lake ice-cover (days); growing degree days with base temperature 5°C (GDD5); October (Oct T), January (Jan T), April (Apr T) and July (Jul T) mean air temperatures (°C); Kerner Oceanity Index (KOI); and annual temperature range (ATR); soil base saturation (soil BS); soil clay content (soil clay); soil sand content (soil sand). Continental sites (orange) are KOI −10–0, transitional (green) are KOI = 0–10, and oceanic (blue) are KOI 10–20.

https://doi.org/10.1371/journal.pone.0327780.g002

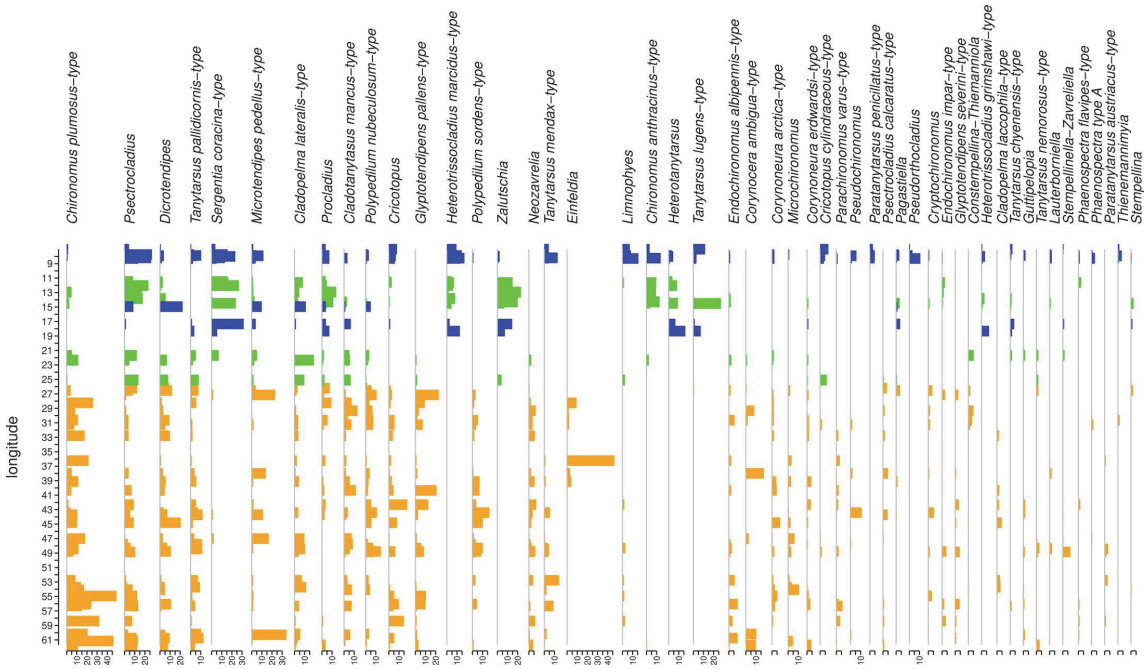

Fig 3. Chironomid morphotypes with abundances in the dataset of at least 2% in one sample. Species are arranged in abundance according to the longitudinal gradient. Continental sites (orange) are KOI −10–0, transitional (green) are KOI = 0–10, and oceanic (blue) are KOI 10–20.

https://doi.org/10.1371/journal.pone.0327780.g003

ANOSIM revealed that the chironomid assemblages can be significantly divided by KOI ($p = 0.007$) with an R-value of 0.24 indicative of some overlap in taxonomic composition between continental, transitional, and continental sites.

Redundancy analysis

For the two tested continentality indices, KOI explained more variation in the chironomid assemblages than ATR (18.4% and 15% respectively; Table 2) with a λ_1:λ_2 ratio greater than 1. GDD5 and July mean air temperature explained the same amount of chironomid assemblage variation (17.2% and 17.4%, respectively; Table 2) and both have a λ_1:λ_2 ratio >1 and a stronger explanatory power compared to April (4%), January (8%) and October (14.2%) mean air temperatures. April and January mean air temperatures are the only variables aligned with the second RDA axis. The number of ice-cover days shows a significant influence on the chironomid assemblages (Table 2) with 15.5% of the variation explained and a λ_1:λ_2 ratio >1.

Bedrock explained 16.8% of the chironomid-assemblage variation (Table 2; Fig 4). Lake-water pH accounted for 12.3%, and lake-water depth explained 8.3% of the variation in the chironomid assemblages. LOI did not reveal any significant influence on chironomid assemblages (Russian and Latvian parts).

Chironomid – Kerner Oceanity Index relationships

INDVAL revealed significant indicator morphotypes for the continental, oceanic, and transitional (continental-transitional and oceanic-transitional) groups (Fig 5; S3 File). Continental sites are indicated by the presence of *Glyptotendipes*

Table 2. Results of the redundancy analysis (RDA) of the dataset and tested environmental and climatic variables in the dataset: lake-water depth (m); longitude; lake-water pH; bedrock type; July (Jul T), October (Oct T), and April (Apr T) mean air temperatures (°C); lake ice-cover (days); growing degree days with base temperature of 5°C (GDD5); Kerner Oceanity Index (KOI); and annual temperature range (ATR). The proportion of chironomid-assemblage variation explained by each variable, *p*-values, and λ_1:λ_2 ratios are given.

Variable	% of variation explained	*p*-value	λ_1:λ_2
Longitude	13.1	0.001	0.8
Environment			
Bedrock	16.8	0.001	1.1
pH	12.3	0.001	1
Soil base saturation	8	0.002	0.5
Soil clay content	10	0.001	0.7
Soil sand content	4.7	0.013	0.2
LOI (Russian and Latvian samples)	–	0.6	–
Depth (m)	8.3	0.001	0.5
Climate			
GDD5	17.2	0.001	1.5
Oct T	14.2	0.001	1.2
Apr T	4	0.045	0.2
Jul T	17.4	0.001	1.3
Jan T	8	0.021	0.5
Ice-cover	15.5	0.001	1.1
ATR	15	0.001	1.3
KOI	18.4	0.001	1.6

https://doi.org/10.1371/journal.pone.0327780.t002

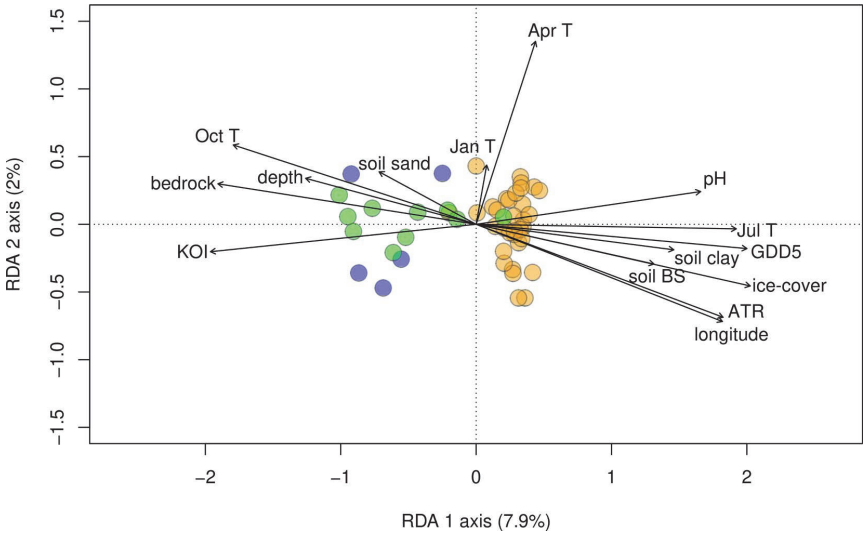

Fig 4. Redundancy analysis (RDA) plot showing the climate and environmental variables, revealed the significant dependency in the dataset: lake-water depth (m); longitude; lake water pH; bedrock type; soil base saturation (soil BS); soil clay content (soil clay); soil sand content (soil sand); July (Jul T), January (Jan T), October (Oct T), and April (Apr T) mean air temperatures (°C); lake-ice cover (days); growing degree days with base temperature of 5°C (GDD5); Kerner Oceanity Index (KOI); and annual temperature range (ATR). Variables explain 44.6% of variation in total with a *p*-value of 0.001. Continental sites (orange) correspond to −10–0 KOI, transitional sites (green) to 0–10 KOI, and oceanic sites (blue) to 10–20 KOI.

https://doi.org/10.1371/journal.pone.0327780.g004

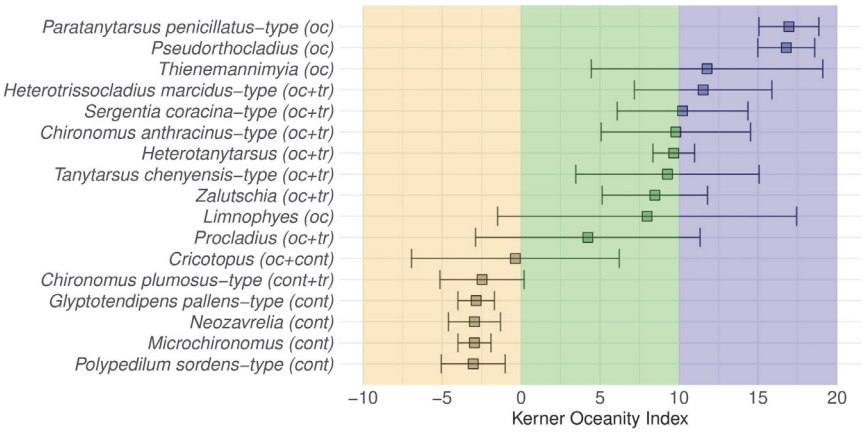

Fig 5. Weighted-average based Kerner Oceanity Index (KOI) optima and tolerances for morphotypes revealed as indicators by INDVAL. The continentality group affiliation identified by INDVAL is marked in brackets: oc – oceanic, tr – transitional, cont – continental; all taxa revealed statistical significance in the corresponding zone based on IndVal. The background is colored according to the KOI: continental (orange) for KOI < 0, transitional (green) for KOI 0–10, oceanic (blue) for KOI > 10.

https://doi.org/10.1371/journal.pone.0327780.g005

pallens-type, *Neozavrelia*, *Polypedilum sordens*-type, and *Microchironomus.* The continental-transitional morphotype is *Chironomus plumosus*-type. Oceanic sites are characterised by *Paratanytarsus penicillatus*-type, *Pseudorthocladius*, *Thienemannimyia*. Oceanic-transitional morphotypes are *Procladius*, *Heterotrissocladius marcidus*-type, *Sergentia coracina*-type, *Zalutschia*, *Chironomus anthracinus*-type, *Heterotanytarsus*, and *Tanytarsus chinyensis*-type. One morphotype (*Cricotopus)* is assigned to the continental-oceanic group.

Weighted-average regression (Fig 5; S4 File) reveals that the widest tolerance interval has morphotypes with optima in the transitional part of the dataset (*Procladius, Limnophyes, Tanytarsus chinyensis*-type) and *Thienemannimyia* from the oceanic part of the dataset. The smallest tolerances are shown by *Microchironomus* and *Glyptotendipes pallens*-type, both from the continental part of the dataset.

Inference model for continentality reconstructions

The KOI-based two-component WA-PLS inference model has an RMSEP of 5.1, RMSE of 4.3, R^2 of 0.72, average bias of −0.1, and maximum bias of 14.6. A scatterplot of the cross-validated predicted vs. observed KOI generally follows a 1:1 relationship (Fig 6A). The reconstruction errors (Fig 6B) indicate an increased error in the transitional and oceanic parts of the dataset.

Discussion

Effect of environmental and climate variables on the chironomid assemblages

July mean air temperature, GDD5, ice-cover are positively correlated with each other (correlation index >0.8; Fig 2B) and are arranged together along the first axis of both the PCA and RDA plots (Fig 2A and 4). Also, their explanatory powers are relatively similar (Table 2). Thus, July mean air temperature, GDD5, ice-cover reflect the longitudinal gradient, and hence, their individual effects on chironomid assemblages are difficult to distinguish reliably. The discussed variables are positively correlated with the first axis. The positive correlation between bedrock and October mean air temperature is most probably an artefact of the dataset design. The climate variables that did not reveal strong (>0.7) correlations are

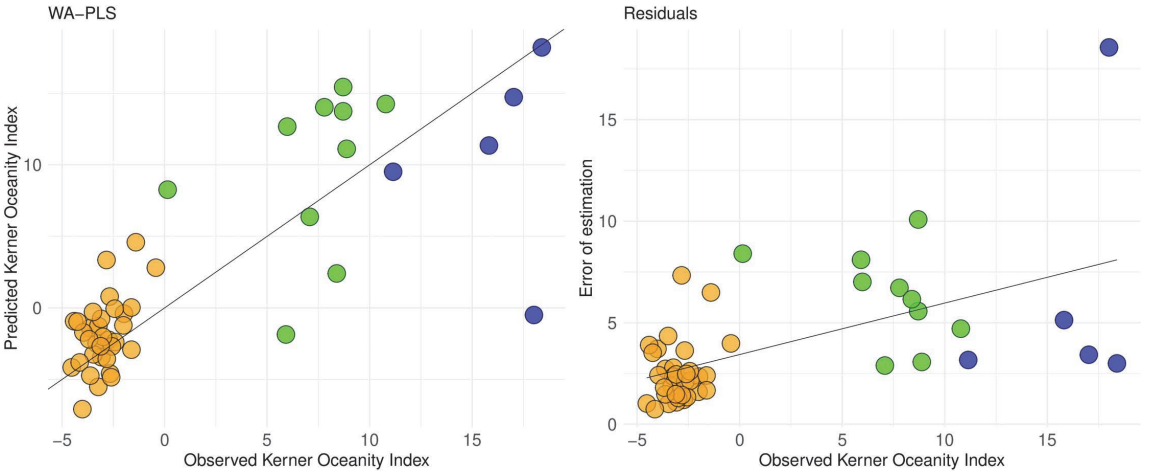

Fig 6. (A) Diagnostic plot of cross-validated estimates of the dataset compared with observed Kerner Oceanity Index (KOI) values and (B) residuals plot from a weighted-average partial least squares (WA-PLS) model based on two components. Continental sites (orange) correspond to −10–0 KOI, transitional sites (green) to 0–10 KOI, and oceanic sites (blue) to 10–20 KOI.

https://doi.org/10.1371/journal.pone.0327780.g006

lake-water pH, lake-water depth, April and January mean air temperature, and KOI. The independence of KOI can be explained by its formula: it includes October, January and April mean air temperatures. Further, KOI explains the highest amount of variation in the chironomid assemblages (18.4%; Table 2). Thus, KOI appears to be a key driver of change in the chironomid assemblages in the present dataset (Fig 4; Table 2). However, the chironomid assemblages from the dataset could be influenced by unmeasured environmental variables (e.g., water trophic state, conductivity, and oxygen content; catchment vegetation cover/type).

In our study, GDD5 has higher explanatory power (17.2%) than in previous studies: GDD5 explains 9% of the variation in Swiss Alps chironomid assemblages [70] and 9.7% in New Zealand Alps assemblages [71]. This could be due to the wide spatial spread of our sampling sites combined with the long GDD5 gradient in our dataset (Fig 2A) and suggests the importance of growing-season length for chironomid assemblages. The high performance of July, relatively high of October, and significant April mean air temperatures in the RDA, which are all related to growing season duration, also support this interpretation. Furthermore, April mean air temperature, while having the lowest explanatory power (4%) among the tested climatic variables, is aligned with the second RDA axis, together with January mean air temperatures suggesting the distinctive impact of the growing-season start on the chironomid assemblages. While, the relationship of chironomid assemblages and October air temperatures has not been studied before, its relatively high explanatory power suggests that the time of the autumn water column mixing may also influence chironomid assemblages. January mean air temperature has been found to impact chironomid assemblages and explained 5.2% in Swedish chironomid training set [45]. The higher influence of January mean air temperatures on the studied dataset (8%) is explained by a high range of this climate variable: from −14 °C in Urals to −1−0 °C in coastal Baltic area.

Ice cover is known to cause depletion in the dissolved oxygen content of lake water [16,72]. Thus, the importance of ice cover can be explained by affecting dissolved oxygen changes, to which chironomids are known to be sensitive [35,36,73,74]. Warmer air temperature combined with shorter ice-cover duration have been shown to increase lake water pH [75] over a longer period of time. Our dataset covers a long gradient of ice-cover duration (35−196 days) and ATR,

which may explain why lake-water pH has a higher explanatory power in our dataset compared to other chironomid datasets [21,42]. The strong negative correlation between ice-cover and bedrock type ($r = -0.83$) suggests that variations in bedrock may also influence the water pH, in addition to the direct effects of ice-cover.

The high explanatory power of bedrock type (16.8% variation in chironomid assemblages) can be explained by the fact that bedrock influences water chemistry, soil, terrestrial vegetation type, productivity of the ecosystem, and catchment erosion processes [76–84]. The explanatory power of lake-water depth (8.3%) is considerably stronger than in other studies [21,42,85]. This may be due to the broad depth range in our dataset (1–45 m), whereas the datasets referenced above did not include lakes deeper than 21 m. Water depth influences chironomids via variations in water temperature, oxygen concentration, habitat structure, macrophytes presence and food quality and availability [37,86]. The properties of surrounding soils (base saturation, sand and clay content) most probably have an indirect effect on chironomid assemblages through changing the limnological conditions by regulating the drainage of organic and inorganic components and during catchment erosion processes [87–93]. The independence of lake-water depth and pH, as well as soil properties from climatic variables makes it possible to separate the effect of local environmental factors from regional climate factors on the chironomid assemblages.

Morphotype-specific relationships with kerner oceanity index

Chironomid taxa identified as characteristic of the continental group (Fig. 5) are commonly identified as warm summer-related ones [21,39,42]. Our study indicates that a preference for warm summer temperatures is accompanied by a tolerance for a short growing season in these taxa. The only exception is *Neozavrelia*, which was previously considered as a cold stenothermic taxon [53]. However, according to recent findings from central, eastern, and northern Europe [21,42] it appears to be a warm-related one. The modern distribution of *Neozavrelia* taxon includes both extreme oceanic climates (Norway, Russian Far East, Japan) as well as highly continental ones (Eastern Siberia) [53,94]. *Glyptotendipes pallens*-type has been observed to tolerate severe winter conditions [95], which probably helps it to survive in continental climates. *Microchironomus*, *Polypedilum sordens*-type, and *Glyptotendipes* have been recorded emerging in March and April, even beneath the snow/ice or through ice cracks [96]. Such behaviour can be considered as an adaptation to cold winters [97]. Also, in continental conditions of rapid seasonal change and hot summers, the emergence in early spring helps to avoid extreme air heat during mating. *Chironomus plumosus*-type, identified as a continental to transitional morphotype, reveals another survival strategy: during winter diapause nearly all the larvae are in the fourth instar and start the active emergence in June in Russia [98]. Also, a study by Self et al. [24] found that *Chironomus plumosus*-type show significant responses to continentality. From a morphological perspective, a small body size (*Microchironomus, Naeozavrelia*) and pigmentation (*Glyptotendipes pallens*-type, *Chironomus plumosus*-type*, Polypedilum sordens*-type*, Neozavrelia*) can help to survive cold winter conditions [97].

Most of the oceanic and oceanic-transitional morphotypes reveal a cool summer-related distribution [21,39,42]. Preference of a longer growing season is suggested by our data. Self et al. [24] identified *Heterotrissocladius marcidus*-type, *Heterotanytarsus*, *Sergentia coracina*-type, *Pseudorthocladius*, and *Thienemannimyia* as low continentality (oceanity) dependent taxa, which aligns well with our results. Also, these authors explain the distribution of *Pseudorthocladius* and *Thienemannimyia* in oceanic sites with their terrestrial and splash zones habitats where melting, refreezing, or wind removal can expose the chironomids to cellular damage from repeated freeze-thaw cycles. Terrestrial chironomids have adapted to such disturbances through behavioral and physiological mechanisms, including hibernation and the ability to lower their body's freezing point [97]. Terrestrial *Limnophyes*, which is oceanic climate related in our dataset, is expected to have the same adaptations. *Heterotrissocladius marcidus*-type [99], *Sergentia coracina*-type [100], *Chironomus anthracinus*-type, *Procladius* [95], and *Tanytarsus chinyensis*-type [101] emerge in mid-summer and in autumn (September-October), and are thus adapted to oceanic cool springs, mild summers, and warm autumns.

Creating a kerner oceanity index-based model

Two continentality indices (ATR, KOI) were tested in this study. ATR is calculated as the difference between the coldest and the warmest months, while the KOI calculation uses the ATR value and incorporates spring (April) and autumn (October) temperatures. A previous chironomid-continentality study [24] used the Gorzynski continentality index, which is also ATR-based, but includes latitude. However, as our dataset is constrained to a narrow latitudinal band (Fig 1, Table 1), it is assumed that any impact of latitude would not be detectable. Furthermore, the Gorczynski continentality index is not applicable to oceanic sites [102] and cannot therefore be used for coastal areas of the eastern Baltic and southern Scandinavia.

The RMSEP of the chironomid-inferred WA-PLS KOI model is 5.1. Considering that the RMSEP covers about 15% of KOI gradient length in the dataset (−4.5–27.5; Table 1), this seems to be a very promising variable. However, no KOI-based model has been published so far. In Self et al. [24], where the Gorzynski continentality index was used, the reported R^2 value was 0.73, which is the same as in our model. The prediction errors (Fig 6) tend to increase from the continental to oceanic part of the dataset; a pattern also seen in Self et al. [24]. The issue could be because our dataset is relatively small but covers a large geographical area, which is reflected in the species occurrence pattern, with only 66% of the species occurring in at least five sediment samples (10% of the investigated dataset). Also, the higher proportion of continental than transitional and oceanic sites, increases the robustness of the continental part of the model. An increase in the number of sites, especially transitional and oceanic ones, and in the density of the training set may improve the model's accuracy.

July air temperature has previously been considered as the main driver to explain chironomid assemblage distribution [21,39,42,85]. The high amount of variation explained by July air temperature in our dataset, where the summer temperature gradient was intentionally reduced by the sampling design, highlights its importance for chironomid assemblages in the selected study area. However, the performance of the current dataset in the statistical tests indicates that chironomids may be used as a continentality proxy. Development of specialised training sets dedicated to specific parameters are an essential prerequisite for successful reconstructions of different palaeoenvironmental variables.

Conclusions

Summer temperatures are commonly considered to be a key driver of chironomid assemblage patterns. However, in our dataset, collected along a transect from the oceanic Atlantic coast to the continental central Russia, July air temperature is the second strongest explanatory variable and a part of a general longitude-related group of variables, which also includes annual temperature range, ice-cover duration, and growing degree days (GDD5). The Kerner Oceanity Index (KOI) represents a distinct gradient in the dataset. It explains the highest variation in the chironomid assemblages and is independent of the other tested variables. Therefore, KOI is a comprehensive continentality metric in our dataset, accounting for both the annual temperature range and the spring and autumn air temperatures.

Despite the dataset being relatively small for creating a robust palaeoclimate continentality reconstruction, the WA-PLS model performance for KOI shows promising results with an $R^2 = 0.73$ and RMSEP of 5.1. We conclude, therefore, that further investigation of chironomid-continentality relationships and the creation of a larger continentality-based chironomid training set are justified.

Supporting information

S1 File. Chironomidae assemblages composition of the continentality dataset.
(CSV)

S2 File. Environmental data.
(CSV)

S3 File. IndVal performance values for the taxa revealed significancy.
(DOCX)

S4 File. Weighted average regression based estimated optima for Chironomidae morphotypes revealed significancy in IndVal.
(CSV)

Acknowledgments

We express our gratitude to Simon Belle, Angela Self, and Steve Brooks for scientific advice.

Author contributions

Conceptualization: Anneli Poska, Siim Veski.

Data curation: Varvara Bakumenko, Anneli Poska.

Formal analysis: Varvara Bakumenko.

Funding acquisition: Siim Veski.

Investigation: Varvara Bakumenko, Brian Huser.

Methodology: Varvara Bakumenko, Anneli Poska.

Project administration: Siim Veski.

Resources: Siim Veski.

Supervision: Anneli Poska, H. John B. Birks, Siim Veski.

Validation: Anneli Poska.

Visualization: Varvara Bakumenko, Anneli Poska.

Writing – original draft: Varvara Bakumenko.

Writing – review & editing: Anneli Poska, H. John B. Birks, Siim Veski.

References

1. Jones VJ, Solovieva N, Self AE, McGowan S, Rosén P, Salonen JS, et al. The influence of Holocene tree-line advance and retreat on an arctic lake ecosystem: a multi-proxy study from Kharinei Lake, North Eastern European Russia. J Paleolimnol. 2011;46(1):123–37. https://doi.org/10.1007/s10933-011-9528-7
2. Stonevicius E, Stankunavicius G, Rimkus E. Continentality and Oceanity in the Mid and High Latitudes of the Northern Hemisphere and Their Links to Atmospheric Circulation. Advances in Meteorology. 2018;2018:1–12. https://doi.org/10.1155/2018/5746191
3. Gorczyński L. Sur Le Calcul Du Degré Du Continentalisme Et Son Application Dans La Climatologie. Geografiska Annaler. 1920;2: 324–31.
4. Zambakas J. General climatology. Greece: Department of Geology, National & Kapodistrian University of Athens. 1992.
5. Alexandrov GA, Ginzburg AS, Golitsyn GS. Influence of North Atlantic Oscillation on Moscow Climate Continentality. Izv Atmos Ocean Phys. 2019;55(5):407–11. https://doi.org/10.1134/s0001433819050025
6. Bethere L, Sennikovs J, Bethers U. Climate indices for the Baltic states from principal component analysis. Earth Syst Dynam. 2017;8(4):951–62. https://doi.org/10.5194/esd-8-951-2017
7. Williams JW, Jackson ST, Kutzbach JE. Projected distributions of novel and disappearing climates by 2100 AD. Proc Natl Acad Sci U S A. 2007;104(14):5738–42. https://doi.org/10.1073/pnas.0606292104 PMID: 17389402
8. Driscoll DM, Fong JMY. Continentality: A basic climatic parameter re-examined. Intl Journal of Climatology. 1992;12(2):185–92. https://doi.org/10.1002/joc.3370120207
9. Hamm A, Magnússon RÍ, Khattak AJ, Frampton A. Continentality determines warming or cooling impact of heavy rainfall events on permafrost. Nat Commun. 2023;14(1):3578. https://doi.org/10.1038/s41467-023-39325-4 PMID: 37328462
10. Molchanova NP, Letuchy AV, Morozova SV, Kondakov KS, Shcherbakova NA. The influence of the degree of climate continentality on the productivity of agricultural production. IOP Conf Ser: Earth Environ Sci. 2022;1010(1):012156. https://doi.org/10.1088/1755-1315/1010/1/012156

11. Shiryaev AG. Climate continentality increases the beta diversity of macrofungal communities. Bot Pac. 2020;9(2). https://doi.org/10.17581/bp.2020.09216
12. Valeriano C, Gutiérrez E, Colangelo M, Gazol A, Sánchez-Salguero R, Tumajer J, et al. Seasonal precipitation and continentality drive bimodal growth in Mediterranean forests. Dendrochronologia. 2023;78:126057. https://doi.org/10.1016/j.dendro.2023.126057
13. Nishimura P, Laroque C. Observed continentality in radial growth–climate relationships in a twelve site network in western Labrador, Canada. Dendrochronologia. 2011;29:17–23.
14. Butcher JB, Nover D, Johnson TE, Clark CM. Sensitivity of lake thermal and mixing dynamics to climate change. Climatic Change. 2015;129(1–2):295–305. https://doi.org/10.1007/s10584-015-1326-1
15. Preston DL, Caine N, McKnight DM, Williams MW, Hell K, Miller MP, et al. Climate regulates alpine lake ice cover phenology and aquatic ecosystem structure. Geophysical Research Letters. 2016;43(10):5353–60. https://doi.org/10.1002/2016gl069036
16. Zdorovennova G, Palshin N, Golosov S, Efremova T, Belashev B, Bogdanov S, et al. Dissolved Oxygen in a Shallow Ice-Covered Lake in Winter: Effect of Changes in Light, Thermal and Ice Regimes. Water. 2021;13(17):2435. https://doi.org/10.3390/w13172435
17. Heikkilä M, Seppä H. A 11,000 yr palaeotemperature reconstruction from the southern boreal zone in Finland. Quaternary Science Reviews. 2003;25:541–54.
18. Heiri O, Brooks SJ, Renssen H, Bedford A, Hazekamp M, Ilyashuk B, et al. Validation of climate model-inferred regional temperature change for late-glacial Europe. Nat Commun. 2014;5:4914. https://doi.org/10.1038/ncomms5914 PMID: 25208610
19. Veski S, Seppä H, Stančikaitė M, Zernitskaya V, Reitalu T, Gryguc G. Quantitative summer and winter temperature reconstructions from pollen and chironomid data between 15 and 8 ka BP in the Baltic–Belarus area. Quaternary Int. 2015;19:4–11.
20. Marsicek J, Shuman BN, Bartlein PJ, Shafer SL, Brewer S. Reconciling divergent trends and millennial variations in Holocene temperatures. Nature. 2018;554(7690):92–6. https://doi.org/10.1038/nature25464 PMID: 29388952
21. Kotrys B, Płóciennik M, Sydor P, Brooks SJ. Expanding the Swiss-Norwegian chironomid training set with Polish data. Boreas. 2019;49(1):89–107. https://doi.org/10.1111/bor.12406
22. Schmidhauser NRMM, Finsinger W, Cagliero E, Heiri O. Holocene ecosystem and temperature development inferred from invertebrate remains in Zminje Jezero (Dinaric Alps, Montenegro). J Paleolimnol. 2024;72(3):343–61. https://doi.org/10.1007/s10933-024-00334-y PMID: 39329145
23. Tarasov P, Granoszewski W, Bezrukova E, Brewer S, Nita M, Abzaeva A, et al. Quantitative reconstruction of the last interglacial vegetation and climate based on the pollen record from Lake Baikal, Russia. Climate Dynamics. 2005;25(6):625–37. https://doi.org/10.1007/s00382-005-0045-0
24. Self AE, Brooks SJ, Birks HJB, Nazarova L, Porinchu D, Odland A, et al. The distribution and abundance of chironomids in high-latitude Eurasian lakes with respect to temperature and continentality: development and application of new chironomid-based climate-inference models in northern Russia. Quaternary Science Reviews. 2011;30(9–10):1122–41. https://doi.org/10.1016/j.quascirev.2011.01.022
25. Opel T, Murton JB, Wetterich S, Meyer H, Ashastina K, Günther F, et al. Past climate and continentality inferred from ice wedges at Batagay megaslump in the Northern Hemisphere's most continental region, Yana Highlands, interior Yakutia. Clim Past. 2019;15(4):1443–61. https://doi.org/10.5194/cp-15-1443-2019
26. González-Sampériz P, Gil-Romera G, García-Prieto E, Aranbarri J, Moreno A, Morellón M, et al. Strong continentality and effective moisture drove unforeseen vegetation dynamics since the last interglacial at inland Mediterranean areas: The Villarquemado sequence in NE Iberia. Quaternary Science Reviews. 2020;242:106425. https://doi.org/10.1016/j.quascirev.2020.106425
27. Giesecke T, Bjune AE, Chiverrell RC, Seppä H, Ojala AEK, Birks HJB. Exploring Holocene continentality changes in Fennoscandia using present and past tree distributions. Quaternary Science Rev. 2008;27(13–14):1296–308. https://doi.org/10.1016/j.quascirev.2008.03.008
28. Töchterle P, Baldo A, Murton JB, Schenk F, Edwards RL, Koltai G, et al. Reconstructing Younger Dryas ground temperature and snow thickness from cave deposits. Clim Past. 2024;20(7):1521–35. https://doi.org/10.5194/cp-20-1521-2024
29. Baldini JUL, McDermott F, Fairchild IJ. Structure of the 8200-year cold event revealed by a speleothem trace element record. Science. 2002;296(5576):2203–6. https://doi.org/10.1126/science.1071776 PMID: 12077412
30. Eggermont H, Heiri O. The chironomid-temperature relationship: expression in nature and palaeoenvironmental implications. Biol Rev Camb Philos Soc. 2012;87(2):430–56. https://doi.org/10.1111/j.1469-185X.2011.00206.x PMID: 22032243
31. Walker IR, Fernando CH, Paterson CG. The chironomid fauna of four shallow, humic lakes and their representation by subfossil assemblages in the surficial sediments. Hydrobiologia. 1984;112(1):61–7. https://doi.org/10.1007/bf00007667
32. Brooks SJ. Fossil midges (Diptera: Chironomidae) as palaeoclimatic indicators for the Eurasian region. Quaternary Science Reviews. 2006;25(15–16):1894–910. https://doi.org/10.1016/j.quascirev.2005.03.021
33. Brodersen KP, Lindegaard C. Classification, assessment and trophic reconstruction of Danish lakes using chironomids. Freshwater Biology. 1999;42(1):143–57. https://doi.org/10.1046/j.1365-2427.1999.00457.x
34. Luoto TP. The relationship between water quality and chironomid distribution in Finland—A new assemblage-based tool for assessments of long-term nutrient dynamics. Ecological Indicators. 2011;11(2):255–62. https://doi.org/10.1016/j.ecolind.2010.05.002
35. Verbruggen F, Heiri O, Meriläinen JJ, Lotter AF. Subfossil chironomid assemblages in deep, stratified European lakes: relationships with temperature, trophic state and oxygen. Freshwater Biology. 2010;56(3):407–23. https://doi.org/10.1111/j.1365-2427.2010.02508.x
36. Ursenbacher S, Stötter T, Heiri O. Chitinous aquatic invertebrate assemblages in Quaternary lake sediments as indicators of past deepwater oxygen concentration. Quaternary Science Reviews. 2020;231:106203. https://doi.org/10.1016/j.quascirev.2020.106203

37. Heiri O. Within-lake variability of subfossil chironomid assemblages in shallow Norwegian lakes. Journal of Paleolimnology. 2004;32(1):67–84. https://doi.org/10.1023/b:jopl.0000025289.30038.e9
38. Ni Z, Zhang E, Meng X, Sun W, Ning D. Chironomid-based reconstruction of 500-year water-level changes in Daihai Lake, northern China. CATENA. 2023;227:107122. https://doi.org/10.1016/j.catena.2023.107122
39. Heiri O, Brooks SJ, Birks HJB, Lotter AF. A 274-lake calibration data-set and inference model for chironomid-based summer air temperature reconstruction in Europe. Quaternary Science Reviews. 2011;30(23–24):3445–56. https://doi.org/10.1016/j.quascirev.2011.09.006
40. Fortin M-C, Medeiros AS, Gajewski K, Barley EM, Larocque-Tobler I, Porinchu DF, et al. Chironomid-environment relations in northern North America. J Paleolimnol. 2015;54(2–3):223–37. https://doi.org/10.1007/s10933-015-9848-0
41. Nazarova L, Syrykh L, Grekov I, Sapelko T, Krasheninnikov AB, Solovieva N. Chironomid-Based Modern Summer Temperature Data Set and Inference Model for the Northwest European Part of Russia. Water. 2023;15(5):976. https://doi.org/10.3390/w15050976
42. Bakumenko V, Poska A, Płóciennik M, Gasteviciene N, Kotrys B, Luoto TP, et al. Chironomidae-based inference model for mean July air temperature reconstructions in the eastern Baltic area. Boreas. 2024;53(3):401–14. https://doi.org/10.1111/bor.12655
43. Velle G, Brodersen KP, Birks HJB, Willassen E. Midges as quantitative temperature indicator species: Lessons for palaeoecology. The Holocene. 2010;20(6):989–1002. https://doi.org/10.1177/0959683610365933
44. Armitage PD, Cranston PS, Pinder LCV. The Chironomidae. Springer Netherlands. 1995. https://doi.org/10.1007/978-94-011-0715-0
45. Larocque I, Hall RI, Grahn E. Journal of Paleolimnology. 2001;26(3):307–22. https://doi.org/10.1023/a:1017524101783
46. Nazarova LB, Self AE, Brooks SJ, Solovieva N, Syrykh LS, Dauvalter VA. Chironomid fauna of the lakes from the Pechora river basin (east of European part of Russian Arctic): Ecology and reconstruction of recent ecological changes in the region. Contemp Probl Ecol. 2017;10(4):350–62. https://doi.org/10.1134/s1995425517040059
47. Engels S, Self AE, Luoto TP, Brooks SJ, Helmens KF. A comparison of three Eurasian chironomid–climate calibration datasets on a W–E continentality gradient and the implications for quantitative temperature reconstructions. J Paleolimnol. 2014;51(4):529–47. https://doi.org/10.1007/s10933-014-9772-8
48. Juggins S. Quantitative reconstructions in palaeolimnology: new paradigm or sick science?. Quaternary Science Reviews. 2013;15:20–32.
49. Medeiros A, Chipman M, Francis D, Hamerlík L, Langdon P, Puleo P. A continental-scale chironomid training set for reconstructing Arctic temperatures. Quaternary Science Reviews. 2022;15:107728.
50. Hersbach H, Bell B, Berrisford P, Hirahara S, Horányi A, Muñoz-Sabater J, et al. The ERA5 global reanalysis. Quart J Royal Meteoro Soc. 2020;146(730):1999–2049. https://doi.org/10.1002/qj.3803
51. Mcmaster G. Growing degree-days: one equation, two interpretations. Agricultural Forest Meteorol. 1997;87(4):291–300. https://doi.org/10.1016/s0168-1923(97)00027-0
52. Heiri O, Lotter AF, Lemcke G. Loss on ignition as a method for estimating organic and carbonate content in sediments: reproducibility and comparability of results. J Paleolimnol. 2001;25(1):101–10. https://doi.org/10.1023/a:1008119611481
53. Brooks SJ, Langdon PG, Heiri O. The identification and use of Palaearctic Chironomidae larvae in palaeoecology. 2007.
54. Klink A, Pillot H. Chironomidae larvae: key to the higher taxa and species of the lowlands of northwestern Europe. Expert-Center for Taxonomic Identification. 2003.
55. Larocque-Tobler I. The Polish sub-fossil chironomids. Palaeontologia Electronica. 2014;17: 28. https://doi.org/10.26879/391
56. Andersen T, Sæther O, Cranston P, Epler J. The larvae of Orthocladiinae (Diptera: Chironomidae) of the Holarctic region–keys and diagnoses. Insect Systematics & Evolution. 2013.
57. Walker IR. Midges: Chironomidae and Related Diptera. Developments in Paleoenvironmental Res. Springer Netherlands. 2001. p. 43–66. https://doi.org/10.1007/0-306-47671-1_3
58. Clarke KR, Green RH. Statistical design and analysis for a “biological effects” study. Marine Ecology Progress Series. 1988;46:213–26.
59. Hill MO, Gauch HG Jr. Detrended correspondence analysis: An improved ordination technique. Vegetatio. 1980;42(1–3):47–58. https://doi.org/10.1007/bf00048870
60. Birks HJB, Birks HJB. D.G. Frey and E.S. Deevey Review 1: Numerical tools in palaeolimnology – Progress, potentialities, and problems. J Paleolimnol. 1998;20(4):307–32. https://doi.org/10.1023/a:1008038808690
61. Lepš J, Šmilauer P. Multivariate Analysis of Ecological Data using CANOCO. Cambridge University Press. 2003. https://doi.org/10.1017/cbo9780511615146
62. ter Braak CJF, Juggins S. Weighted averaging partial least squares regression (WA-PLS): an improved method for reconstructing environmental variables from species assemblages. Hydrobiologia. 1993;269–270(1):485–502. https://doi.org/10.1007/bf00028046
63. Diatoms and pH reconstruction. Phil Trans R Soc Lond B. 1990;327(1240):263–78. https://doi.org/10.1098/rstb.1990.0062
64. Dufrene M, Legendre P. Species Assemblages and Indicator Species: The Need for a Flexible Asymmetrical Approach. Ecological Monographs. 1997;67(3):345. https://doi.org/10.2307/2963459
65. Wickham H, Averick M, Bryan J, Chang W, McGowan L, François R, et al. Welcome to the Tidyverse. JOSS. 2019;4(43):1686. https://doi.org/10.21105/joss.01686

66. Wickham H, Francois R, Henry L, Muller K. Dplyr: a grammar of data manipulation. 2022.
67. Oksanen J, Simpson G, Blanchet F, Kindt R, Legendre P, Minchin P. Vegan: community ecology package. 2022.
68. Juggins S. Rioja: analysis of Quaternary science data, R package version (1.0-5). 2022.
69. De Cáceres M, Legendre P. Associations between species and groups of sites: indices and statistical inference. Ecology. 2009;90(12):3566–74. https://doi.org/10.1890/08-1823.1 PMID: 20120823
70. Lotter AF, Sturm M, Teranes JL, Wehrli B. Varve formation since 1885 and high-resolution varve analyses in hypertrophic Baldeggersee (Switzerland). Aquatic Sci 1997;59(4):304–25. https://doi.org/10.1007/bf02522361
71. Dieffenbacher-Krall AC, Vandergoes MJ, Denton GH. An inference model for mean summer air temperatures in the Southern Alps, New Zealand, using subfossil chironomids. Quaternary Science Reviews. 2007;26(19–21):2487–504. https://doi.org/10.1016/j.quascirev.2007.06.016
72. Golosov S, Maher OA, Schipunova E, Terzhevik A, Zdorovennova G, Kirillin G. Physical background of the development of oxygen depletion in ice-covered lakes. Oecologia. 2007;151(2):331–40. https://doi.org/10.1007/s00442-006-0543-8 PMID: 17115190
73. Brooks SJ, Birks HJB. Chironomid-inferred air temperatures from Lateglacial and Holocene sites in north-west Europe: progress and problems. Quaternary Sci Rev. 2001;20(16–17):1723–41. https://doi.org/10.1016/s0277-3791(01)00038-5
74. Quinlan R, Smol JP. J Paleolimnol. 2001;26(3):327–42. https://doi.org/10.1023/a:1017546821591
75. Schreder S, Sommaruga R, Psenner R, Chimani B, Ganekind M, Koinig KA. Changes in air temperature, but not in precipitation, determine long-term trends in water chemistry of high mountain lakes of the Alps with and without rock glacier influence. Sci Total Environ. 2023;905:167750. https://doi.org/10.1016/j.scitotenv.2023.167750 PMID: 37838057
76. Marchetto A, Mosello R, Psenner R, Bendetta G, Boggero A, Tait D, et al. Factors affecting water chemistry of alpine lakes. Aquatic Sci. 1995;57(1):81–9. https://doi.org/10.1007/bf00878028
77. Probst A, Probst JL, Massabuau JC, Fritz B. Surface Water Acidification in the Vosges Mountains: Relation to Bedrock and Vegetation Cover. Forest Decline and Atmospheric Deposition Effects in the French Mountains. Berlin, Heidelberg: Springer. 1995. p. 371–86. https://doi.org/10.1007/978-3-642-79535-0_18
78. Witty JH, Graham RC, Hubbert KR, Doolittle JA, Wald JA. Contributions of water supply from the weathered bedrock zone to forest soil quality. Geoderma. 2003;114(3–4):389–400. https://doi.org/10.1016/s0016-7061(03)00051-x
79. Alexander EB. RATES OF SOIL FORMATION FROM BEDROCK OR CONSOLIDATED SEDIMENTS. Physical Geography. 1985;6(1):25–42. https://doi.org/10.1080/02723646.1985.10642261
80. Searcy KB, Wilson BF, Fownes JH. Influence of Bedrock and Aspect on Soils and Plant Distribution in the Holyoke Range, Massachusetts. J Torrey Botanical Society. 2003;130(3):158. https://doi.org/10.2307/3557551
81. Dong X, Martin JB, Cohen MJ, Tu T. Bedrock mediates responses of ecosystem productivity to climate variability. Commun Earth Environ. 2023;4(1). https://doi.org/10.1038/s43247-023-00773-x
82. Hahm WJ, Riebe CS, Lukens CE, Araki S. Bedrock composition regulates mountain ecosystems and landscape evolution. Proc Natl Acad Sci U S A. 2014;111(9):3338–43. https://doi.org/10.1073/pnas.1315667111 PMID: 24516144
83. Gan F, Shi H, Gou J, Zhang L, Dai Q, Yan Y. Responses of soil aggregate stability and soil erosion resistance to different bedrock strata dip and land use types in the karst trough valley of Southwest China. International Soil and Water Conservation Research. 2024;12(3):684–96. https://doi.org/10.1016/j.iswcr.2023.09.002
84. Ao L, Wu Y, Xu Q, Zhou Y, Chen X, Liang P, et al. The Role of Bedrock Topography in the Runoff Process and Soil Erosion on Karst Steep Slopes. Land Degrad Dev. 2024;36(2):533–44. https://doi.org/10.1002/ldr.5377
85. Luoto TP. Subfossil Chironomidae (Insecta: Diptera) along a latitudinal gradient in Finland: development of a new temperature inference model. J Quaternary Science. 2008;24(2):150–8. https://doi.org/10.1002/jqs.1191
86. Kurek J, Cwynar LC. The potential of site-specific and local chironomid-based inference models for reconstructing past lake levels. J Paleolimnol. 2008;42(1):37–50. https://doi.org/10.1007/s10933-008-9246-y
87. Kopáček J, Kaňa J, Šantrůčková H, Picek T, Stuchlík E. Chemical and Biochemical Characteristics of Alpine Soils in the Tatra Mountains and their Correlation with Lake Water Quality. Water, Air, & Soil Pollution. 2004;153(1–4):307–28. https://doi.org/10.1023/b:wate.0000019948.23456.14
88. Bertolet BL, Corman JR, Casson NJ, Sebestyen SD, Kolka RK, Stanley EH. Influence of soil temperature and moisture on the dissolved carbon, nitrogen, and phosphorus in organic matter entering lake ecosystems. Biogeochemistry. 2018;139(3):293–305. https://doi.org/10.1007/s10533-018-0469-3
89. Barbiero L, Filho AR, Furquim SAC, Furian S, Sakamoto AY, Valles V, et al. Soil morphological control on saline and freshwater lake hydrogeochemistry in the Pantanal of Nhecolândia, Brazil. Geoderma. 2008;148(1):91–106. https://doi.org/10.1016/j.geoderma.2008.09.010
90. Eggermont H, Verschuren D. Impact of soil erosion in disturbed tributary drainages on the benthic invertebrate fauna of Lake Tanganyika, East Africa. Biological Conservation. 2003;113(1):99–109. https://doi.org/10.1016/s0006-3207(02)00353-1
91. Houle D, Ouimet R, Couture S, Gagnon C. Base cation reservoirs in soil control the buffering capacity of lakes in forested catchments. Can J Fish Aquat Sci. 2006;63(3):471–4. https://doi.org/10.1139/f06-007
92. Kähkönen A-M. Soil geochemistry in relation to water chemistry and sensitivity to acid deposition in Finnish Lapland. Water Air Soil Pollut. 1996;87(1–4):311–27. https://doi.org/10.1007/bf00696844

93. Nelson P, Cotsaris E, Oades J, Bursill D. Influence of soil clay content on dissolved organic matter in stream waters. Mar Freshwater Res. 1990;41(6):761. https://doi.org/10.1071/mf9900761
94. Orel OV. Revision of the genus Neozavrelia Goetghebuer, Thienemann, 1941 (Diptera: Chironomidae) from Eastern Siberia and the Russian Far East, with the description of new species. Zootaxa. 2021;4938(3):zootaxa.4938.3.1. https://doi.org/10.11646/zootaxa.4938.3.1 PMID: 33756972
95. Pillot H. Chironomidae larvae, vol. 3: Orthocladiinae: biology and ecology of the aquatic Orthocladiinae. Brill Academic Publishers.
96. Danks HV. Life cycles in polar arthropods - flexible or programmed?. Eur J Entomol. 2013;96:83–102.
97. Lencioni V. Survival strategies of freshwater insects in cold environments. J Limnol. 2004;63(1s):45. https://doi.org/10.4081/jlimnol.2004.s1.45
98. Sokolova N. Chironomus plumosus L. (Diptera, Chironomidae). Systematics, morphology. Ecology, production. 1983.
99. Goffová K, Bitušik P, Čiamporová-Zaťovičová Z, Bukvová D, Hamerlík L. Seasonal dynamics and life cycle of Heterotrissocladius marcidus (Diptera: Chironomidae) in high altitude lakes (High Tatra Mts, Slovakia). Biologia. 2015;70(7):943–7. https://doi.org/10.1515/biolog-2015-0103
100. Shcherbina G. Ecology and production of monocyclic species of Chironomidae (Diptera) from Lake Vishtynetskoe of the Kaliningrad region (USSR). Acta Biol Debr Oecol Hung. 1989;3:295–303.
101. Tokeshi M. Production ecology. The Chironomidae. Springer Netherlands. 1995. p. 269–96. https://doi.org/10.1007/978-94-011-0715-0_11
102. Ciaranek D. Variability of the thermal continentality index in Central Europe. Components of the Environment. 2014;307–13.

Appendix 3 (Paper III)

Nosova, M.B., Zakharov, A.L., Lavrenov, N.G., Zaretskaya, N.E., Mazei, N.G., Kupriyanov, D.A., Pastukhova, Y.A., **Bakumenko, V.O.**, Severova, E.E. and Konstantinov, E.A. (2025). A multi-proxy centennial-resolution paleoecological record of Holocene lake sediments in the marginal zone of Last Scandinavian Glaciation (Tver Region, Russia). Quaternary International, 729, p. 109778. doi: 10.1016/j.quaint.2025.109778

Quaternary International 729 (2025) 109778

Contents lists available at ScienceDirect

Quaternary International

journal homepage: www.elsevier.com/locate/quaint

A multi-proxy centennial-resolution paleoecological record of Holocene lake sediments in the marginal zone of Last Scandinavian Glaciation (Tver Region, Russia)

M.B. Nosova [a,b,*], A.L. Zakharov [b], N.G. Lavrenov [a], N.E. Zaretskaya [b], N.G. Mazei [c], D.A. Kupriyanov [b], Yu.A. Pastukhova [c], V.O. Bakumenko [b,d], E.E. Severova [e,f], E.A. Konstantinov [b]

[a] Main Botanical Garden, Russian Academy of Sciences, 4 Botanicheskaya Street, Moscow, 127276, Russia
[b] Institute of Geography, Russian Academy of Sciences, 29 Staromonetniy Lane, Moscow, 119017, Russia
[c] Faculty of Geography, Lomonosov Moscow State University, 1 Leninskie Gory, Moscow, 119991, Russia
[d] Department of Geology, Tallinn University of Technology, Ehitajate tee 5, 19086, Tallinn, Estonia
[e] Biological Faculty, Lomonosov Moscow State University, 1 Leninskie Gory, 119991, Moscow, Russia
[f] Faculty of Biology, Shenzhen MSU -BIT University, Shenzhen, 518172, China

ARTICLE INFO

Keywords:
Paleolimnology
Multiproxy
Biomisation
Paleoecology
Holocene

ABSTRACT

This paper presents a new centennial-resolution multi-proxy record of the Holocene environmental changes obtained from the small Petrovskoe Lake in the former marginal zone of the Last Scandinavian (Valdai) Glaciation. The series of analyses of the lacustrine deposits includes grain size, loss on ignition, magnetic susceptibility, pollen, macrofossils, cladoceran, chironomids and macrocharcoals, were conducted on a 16.35 m-long sediment core. Based on the data obtained, mass accumulation rate was calculated and the stages of vegetation change were determined using biomisation method. The stages of the reservoir development were identified. It was revealed that during the initial stage of development (11000–10200 cal yr BP), a *Sphagnum* mire formed on a buried block of dead ice, which was subsequently flooded, resulting in the formation of a kettle hole lake. In the period from 11000 to 10000 cal yr BP, "cold" biomes with dominance of *Betula* and *Pinus* prevailed. The periods of most active erosion during the early Holocene correspond to 10200–9400 cal yr BP. The further development of the lake followed a path of steadily increasing trophicity and sedimentation rate. A rapid increase in broad-leaved taxa led to the emergence of *warm mixed forests* biome already 9500 cal yr BP. A long warm period, characterized by the dominance of broadleaved species (*Tilia, Quercus, Fraxinus, Ulmus*), lasted until 4200 cal yr BP when *taiga* and *cold deciduous forests* biomes began to replace the *warm mixed forests*. Key moments of anthropogenic impact that influenced the progressive degradation of primary forests and their replacement by secondary stands began at the time of 4200, 2900, 2200, 1500, 1200 and 800 cal yr BP that coincide with archaeological cultural shifts, short-term episodes of erosion and correlates well with fire activity.

1. Introduction

The Last Termination (the end of the Late Pleistocene) and its transition to the modern interglacial – the Holocene – was marked by significant environmental transformations due to rapid degradation of the last glaciation and abrupt climate changes.

The northwestern part of the East European Plain, which was covered with the southeastern lobe of the last Scandinavian (Valdai) glaciation, was strongly modified in landforms, hydrographic system and vegetation cover (Chebotareva and Makarycheva, 1974; Khotinskiy, 1977; Velichko, 2009; Novenko, 2016), especially within its marginal zone. This zone crosses the Smolensk, Tver, Yaroslavl and Vologda regions in the European part of Russia (Svendsen et al., 2004), and the processes of landscape formation and further development within it differed fundamentally from those outside it (Sudakova and Antonov, 2021), consisting of several interacting paleoenvironmental factors such as geomorphological structure, climate and anthropogenic transformation.

* Corresponding author. Main Botanical Garden, Russian Academy of Sciences, 4 Botanicheskaya Street, Moscow, 127276, Russia.
E-mail address: mashanosova@mail.ru (M.B. Nosova).

https://doi.org/10.1016/j.quaint.2025.109778
Received 10 December 2024; Received in revised form 25 March 2025; Accepted 31 March 2025
Available online 18 April 2025

The last glaciation has been studied from a paleogeographic point of view by various authors and in different aspects. These researches took place in Fennoscandia, the Northern European and Baltic sectors of the Scandinavian Glaciation (Elovicheva and Bogdel, 1987; Błaszkiewicz, 2011; Marks, 2015; Rdzany and Frydrych, 2018; Stivrins et al., 2017a), as well as in Eurasia as a whole (Velitchko et al., 1989; Velichko, 2009; Patton et al., 2017). Paleoecological studies concerning the features of landscape and vegetation development in the marginal glaciation zone are more concentrated in the Northern, Western and Baltic parts of Europe and less widespread in the vast area of the East European Plain (Khomutova, 1982; Novenko et al., 2009; Novenko and Olchev, 2015; Borisova, 2021). Very few studies included high resolution data, which allowed us to see not only millennial trends, but also recognize centennial fluctuations and even short-term events at the early stages of local vegetation development (Birks and Birks, 2006).

The area of our interest lying within the southeastern marginal zone of the Last Glaciation, is located in the Tver Region of Russia (Fig. 1) within the interfluve area between Zapadnaya Dvina and Lovat Rivers. Paleoecological studies in the temperate mixed forest (broadleaved-coniferous forests or sub-taiga) zone have been ongoing for over 100 years, resulting in representative sequences (Kremenetski et al., 2000; Davydova et al., 2001; Elovicheva, 2001; Wohlfarth et al., 2006; Novenko et al., 2009, 2015, 2016; Nosova et al., 2017, 2019; Borisova, 2019; Mazei et al., 2020; Konstantinov et al., 2021; Tishkov et al., 2023; Sapelko et al., 2019, 2022; Lavrenov et al., 2024). However, the data coverage is still insufficient, and the time resolution is too low for high-quality spatial and temporal correlation of paleoecological events. On the scale of the Zapadnaya Dvina-Lovat interfluve the paleoecological studies have been conducted previously (Gunova and Sirin, 1996; Kozharinov et al., 2003; Eremeev et al., 2009; Eremeev and Dzjuba, 2010), but these studies lacked sufficient chronometric support. In recent decades, the dynamics of Holocene vegetation have been investigated in the upper reaches of Zapadnaya Dvina (south of Pskov Region), particularly in relation to archaeological excavations from various periods, including Neolithic pile dwellings. Well-dated sequences were obtained from several mires in this area (Tarasov et al., 2019, 2022). The application of various methods, with particular attention to early indicators of anthropogenic impact in general and of subsistence economies in particular, enabled the authors mentioned above to reconstruct the conditions of early landscape development and human impact, unfortunately with low time resolution in the top part of the cores.

The presented study aims to reconstruct the paleoenvironmental setting in the former marginal zone of the last glaciation based on a detailed paleoecological study of a natural archive with rapidly accumulated sediments. This work is part of the development of a reference network of high-quality sedimentary records on the East European Plain. Precise ^{14}C dating and centennial-scaled data allow us to establish a detailed reference sequence for the southeastern sector of the Last Scandinavian Ice Sheet and to contextualize our results in Eastern Europe.

2. Environmental settings

2.1. Geomorphology

We focused our studies in the sedimentary archive of small Petrovskoe Lake (56.72481 N, 31.57739 E; 181 m above sea level) which is a part of the larger Rucheiskoe lake system. It is situated on the western

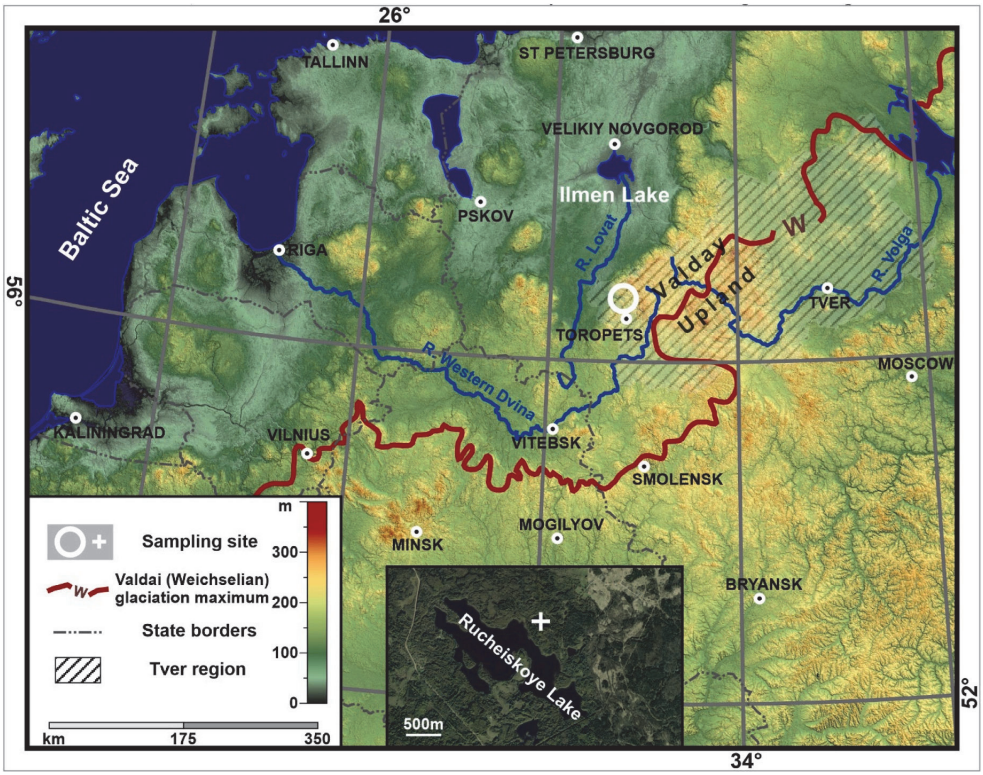

Fig. 1. Location and general view of the study site.

part of Tver Region, 23 km north from Toropets town in the west of the East European Plain (Fig. 1). It belongs to the Lovat-Ilmen basin connecting with it via a river Serezha. Several springs that feed the lake originate at the Zapadnaya Dvina-Lovat interfluve.

From the geomorphological point of view, the study area is located on the western edge of the Valdai Upland (Fig. 1). The relief of the territory is composed of end moraine ridges formed during the uneven degradation of the Valdai (Last Scandinavian) ice sheet (Malakhovsky and Sammet, 1982). The landforms consist of variously oriented hills, ridges and depressions.

The lake system includes Lake Rucheiskoye itself, which has a complex shape with bays and peninsulas, 2.7 km long and 1.2 km wide, and two small lakes: Petrovskoye in the north and Demidovskoye in the east (Fig. 1, insertion). The depth of the Rucheiskoe Lake is 28–30 m, the small lakes reach 5–6 m. The swampy lowlands and streams flowing through them connect all the lakes into the integrated system. Lake Petrovskoe (Fig. 2) has a roughly square shape with a diameter of approximately 150–200 m. The site was selected for drilling due to its low runoff, high sediment thickness and accessibility for sampling with a manual equipment.

According to many paleoenvironmental studies (Kvasov and Treshnikov, 1986; Chebotareva and Makarycheva, 1974; Strivins et al., 2017a), the origin of several lakes in the zone (including our object) of last glaciation is often associated with the trough of the glacial runoff and/or the buried blocks of dead ice inside it.

2.2. Climate and vegetation

The area is located in the zone of moderately continental climate, with temperatures $t_{Jan} = -5.9°C$, $t_{Jul} = +18.2°C$, $t_{min} = -42.2°C$ and $t_{max} = +36.5°C$. Mean annual precipitation is 758 mm, and evaporation is about 400 mm/yr (Pogoda i klimat.).

According to recent vegetation zonation, the western part of the Tver Region belongs to the subtaiga subzone (Safronova et al., 1999). Another point of view is that broadleaved-coniferous forests are the separate vegetation zone (Gribova et al., 1980). The modern vegetation of the investigated area is dominated by secondary mixed forests with *Pinus sylvestris, Betula pendula, B. alba, Populus tremula* and *Alnus incana* coexist, with patches of *Picea abies* and less abundant broadleaved forests at various stages of succession. The presence of broadleaved trees (*Quercus robur, Tilia cordata, Fraxinus excelsior, Ulmus laevis, U. glabra, Acer platanoides*) in the vegetation is currently increasing under the canopy of secondary forests. Wetlands in the area include different types of lakes with surrounding floodplains and various bog communities. Eutrophic swamps with *Betula* spp., *Alnus incana* and *Alnus glutinosa* occupy floodplains and forested bog margins.

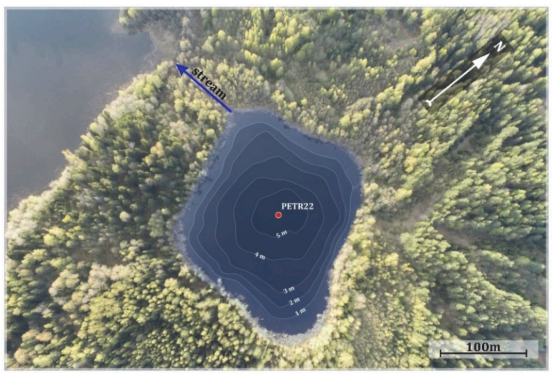

Fig. 2. Bathymetry and general view of Lake Petrovskoe.

2.3. Archaeology

The Zapadnaya Dvina-Lovat interfluve area is rich in explored but poorly examined archaeological records from the Late Mesolithic to the Middle Ages, mostly to the west of the area of our interest (Dolukhanov et al., 1989; Eremeev and Dzjuba, 2010). The first signs of small-scale human impact on vegetation of mixed-forests zone date back to the Neolithic period (Tarasov et al., 2022). Significant changes resulting from agricultural activity in temperate mixed forests date back to the Early Iron Age, 2800 BP–1500 BP (Nosova et al., 2017, 2019; Novenko et al., 2009, 2015; Tarasov et al., 2022). However, the question regarding the potential earlier emergence of agro-pastoral farming in the region remains unresolved (Lavrenov et al., 2021; Krenke et al., 2022; Ershova et al., 2022).

Directly along the shores of Lake Rucheiskoye system, two fortified hills of the Early Iron Age, two large burial mound groups of V–XI cent. CE and several Old-Russian settlements of VII–XI cent. CE (Stankevich, 1953; Eremeev and Dzjuba, 2010) were found, and, according to oral reports of archaeologist V.M. Vorobyov (Tver), Late Neolithic artefactual remains were discovered.

3. Methods

The text of the article contains the briefest descriptions of the methods. Detailed methods see in the Supplementary 1.

3.1. Bathymetry

The bathymetric survey was carried out using a compact two-beam echo sounder Deeper Pro+, controlled with the Fish Deeper software. The resulting data were visualized in the Global Mapper software in the form of a collage with aerial photography made in the Inkscape vector editor.

3.2. Sampling

Drilling of Lake Petrovskoye was carried out on March 12–13, 2022 using a 100 × 5 cm Livingstone piston sampler. Samples were collected from the ice in the dippest part of the lake (6m). The total core lenght was 16.35.

3.3. Grain-size analysis

Grain size measurements were carried out using a Malvern Mastersizer 3000 laser diffractometer. Sample preparation was based on recommendations of (Konert and Vandenberghe, 1997; Blott et al., 2004) and analyzer setup was based on (Özer et al., 2010).

3.4. Loss on ignition (LOI)

LOI at 550 °C were determined, according to Heiri et al. (2001).

3.5. Magnetic susceptibility

The magnetic susceptibility (χ) was measured using a ZH Instruments 150L device. The measurement technique was based on the recommendations described by Maher (1998).

3.6. Measurement of dry bulk density

The dry bulk density (D_b) is the ratio of the dry mass of the sample to the volume of the fresh sample. The mass of the sample is determined after drying to constant weight at 105 °C and the volume of the sample is determined using a plastic syringe (Blake, 1965).

3.7. Dating

The samples for radiocarbon LSC dating were collected during the drilling process at intervals of 1 or 2 m (Table 1). Radiocarbon dating of these samples (silty peat and gyttja) was carried out in the Laboratory of Radiocarbon Dating and Electron Microscopy, Institute of Geography, Russian Academy of Sciences (IG RAS) according to standard A-B-A procedure (Zaretskaya et al., 2012). The most of the samples (all the LSC samples) consist of highly decomposed gyttja (sapropel) thus we suppose that the sediment is quite uniform without significant bioturbations, long roots and other possible contaminations.

Six additional samples for AMS dating (total organic carbon - TOC) were pretreated using the procedure of organic matter extraction and target preparation (Zazovskaya et al., 2017a, 2017b). The measurements of AMS targets were performed at the Center for Applied Isotope Studies (CAIS) at the University of Georgia, USA. For calibration, we used the Calib v. 8.2 software and IntCal 2020 calibration curve (Reimer et al., 2020). The age-depth model was developed using the Bayesian-based software package "Rbacon" (Blaauw and Christen, 2011).

3.8. Calculation of mass accumulation rates

Mass accumulation rates (MAR) are defined as the product of dry bulk density and linear sedimentation rates, which are directly calculated from the age-depth model.

3.9. Pollen analysis

We processed and analyzed the samples for pollen at 10 cm intervals using standard procedures described in Moore et al. (1991). Pollen was counted of at least 500 pollen grains of tree species under the light microscope and was identified using published keys (Moore et al., 1991) and image databases (PalDat; The Global Pollen Project; Botany Collection MSU Russia). We use Tilia v. 1.7.16 and CONISS programs for calculation and visualization of the data (Grimm, 1987, 2011).

3.10. Quantitative biome reconstruction

Quantitative biome reconstruction, or biomisation, approximates major vegetation types (biomes) from fossil pollen spectra by assigning pollen taxa to biomes based on the modern ecology and distribution of pollen-producing plants. The method's accuracy for the study region was verified and modified by Tarasov et al. (1998). Affinity scores, calculated as the sum of the square roots of percentage fossil pollen data for biome-specific taxa, are used in the analysis. The taxa list is derived from Tarasov et al. (1998) and aligns with recent regional studies (Tarasov et al., 2022).

Data preparation and affinity score calculations were performed using Microsoft Excel. Results were visualized with Python's Matplotlib library (Hunter, 2007), applying the Savitzky–Golay smoothing filter (Savitzky and Golay, 1964) to enhance plot readability.

3.11. Macrofossil analysis

The samples of 2 cm^3 were taken at intervals of 5 or 10 cm and the only layers from the depth of 14–16.35 m were analyzed. The samples were washed with water using a sieve with 125 μm mesh size and examined using a ZEISS Primo Star microscope. Plant residues (leaves, roots and epidermis) were identified (Katz et al., 1977; Ignatov and Ignatova, 2003) and were expressed in absolute values.

3.12. Chironomidae analysis

Fossil Chironomidae communities in 35 sediment samples from Lake Petrovskoe core were analyzed. Samples of 5 cm^3 each were taken from the 0.6–15.55 m depth with an interval of 40 cm. Sediment processing followed standard procedure (Brooks et al., 2007). On average, 54 head capsules were collected for one sample; the count range was from 40 head capsules to 90. Brooks et al. (2007) approximated the taxonomic resolution of Chironomidae. Additionally, keys by Schmid (1993), Klink and Pillot (2003), Larocque-Tobler (2014) and Andersen et al. (2013) were used for head capsules identification. Chironomidae-based reconstruction was produced following Heiri et al. (2011) using Weighted Averaging-Partial Least Squares (WA-PLS; ter Braak and Juggins, 1993) regression calculation with bootstrapping (9999 permutations; Birks et al., 1998). Finno-Baltic-Polish (Bakumenko et al., 2024) training set was used for the July tempature reconstruction.

3.13. Cladocera analysis

Samples for cladoceran were analyzed according to a method proposed by Korhola and Rautio (2001) with modifications. A deflocculation with KOH was excluded from sample pretreatment due to potential destruction of some remains. Microscope slides were made by mixing wet sediment material with glycerol at the slide glass. Cladocera species were identified and counted by head shields, ephippia, postabdomens and shell using a Biomed-3 microscope at magnification × 100–400. The

Table 1
Results of radiocarbon dating of Petrovskoe Lake deposits. Dating fraction: bulk — bulk organic matter, TOC — no vegetation debris, total organic carbon in sediments.

#	Depth, m from bottom surface	Material	Dating fraction	Lab. No.	Method	Radiocarbon date (^{14}C yr BP ±1σ)	Calibrated age, cal yr BP
							1 σ (median probability) 2 σ
1	1.4	gyttja	TOC	IGAN 10817	AMS	1800 ± 20	1720–1630 (**1700**) 1740–1620
2	1.8–2.0	gyttja	bulk	IGAN 10657	LSC	1190 ± 70	1180–1050 (**1110**) 1180–960
3	3.8–4.0	gyttja	bulk	IGAN 10658	LSC	1570 ± 70	1520–1390 (**1460**)1590–1340
4	5.9	gyttja	TOC	IGAN 10818	AMS	2270 ± 25	2340–2210 (**2260**) 2350–2160
5	5.8–6.0	gyttja	bulk	IGAN 10659	LSC	1860 ± 60	1830–1710 (**1770**)1930–1610
6	7.8–8.0	gyttja	bulk	IGAN 10660	LSC	2360 ± 60	2490–2330 (**2410**)2700–2300
7	9.8–10.0	gyttja	bulk	IGAN 10661	LSC	3030 ± 60	3340–3160 (**3230**)3380–3060
8	10.8–11.0	gyttja	bulk	IGAN 10662	LSC	3760 ± 70	4240–3990 (**4130**)4305–3960
9	11.8–12.0	gyttja	bulk	IGAN 10663	LSC	4640 ± 70	5470–5305 (**5390**)5580–5270
10	12.8–13.0	gyttja	bulk	IGAN 10664	LSC	5560 ± 70	6400–6290 (**6360**) 6490–6270
11	13.9–14.1	gyttja	bulk	IGAN 10448	LSC	6020 ± 90	6960–6740 (**6870**) 7080–6670
12	13.95	gyttja	TOC	IGAN 10852	AMS	6985 ± 30	7920–7780 (**7820**)7930–7720
13	14.7–14.9	gyttja	bulk	IGAN 10449	LSC	9000 ± 90	10240–9960 (**10120**) 10310–9880
14	15.4	gyttja	TOC	IGAN 10819	AMS	8980 ± 30	10220–10160 (**10180**) 10230–10120
15	15.7	silty peat	TOC	IGAN 10820	AMS	9655 ± 30	11170–10890 (**11090**) 11190–10870
16	16.2	silt	TOC	IGAN 10821	AMS	9735 ± 30	11210–11170 (**11190**) 11230–11110

entire sample volume was analyzed under the microscope with the aim of the total count of 200 cladoceran remains whenever possible. Habitat preferences of cladoceran taxa were determined following Bjerring et al. (2009), Bledzki and Rybak (2016).

3.14. Macrocharcoal analysis

Macrocharcoal analysis (particle size >125 μm) was carried out according to the standard method (Mooney and Tinner, 2011) using samples of volume 1 cm^3. Long-term trend of background macrocharcoal accumulation rate and local fire episodes were identified based on tapas software (Finsinger and Bonnici, 2022), which is the modification of the CharAnalysis software (Higuera, 2009).

4. Results

4.1. Chronology

The results of radiocarbon dating and the age-depth model are presented in Table 1 and Fig. 3. A total of 16 LSC and AMS ^{14}C dates were used to construct the age-depth model. The model was calculated from 0.0 m to 16.2 m depth, with the ages (median) of 280 and 11190 cal yr BP. Due to the probable loss of the upper liquid sediment during sampling, the age of the top of core was estimated by extrapolating sedimentation rates. It should be noted that this approach makes the age calculation of the upper part of the sediment less reliable.

Two inversions were found in the date series — # 1 and 5 of Table 1. In general, the series of dates forms a smooth concave curve without steps. This indicates a constant sedimentation without large hiatuses. The Rbacon model fits the dates well, agreeing with most of them. Only two dates were completely discarded — # 1 and 11. The remaining dates intersect with the model with their confidence intervals. The relatively low agreement of dates with the model in the range from 2 to 4 ka can be explained by the Rbacon model algorithm, which tends to smooth out sharp changes in sedimentation rate. This effect could potentially shift age towards aging for the few hundred years.

4.2. Lithostratigraphy and MAR

The lithostratigraphy and composition of the sedimentary sequence is shown in Fig. 4 and Supplementary 2. Stratigraphy is based on a synthesis of the field description and laboratory lithological analyses. The sedimentary sequence with a thickness of 16.35 m is subdivided into 9 units:

1. 0.0–0.5 m (280–490 cal yr BP). Organic gyttja, black (Ox – dark brown), saturated with water, loose. Extremely low D_b (<0.05 g cm^{-3}), high LOI (>55 %).

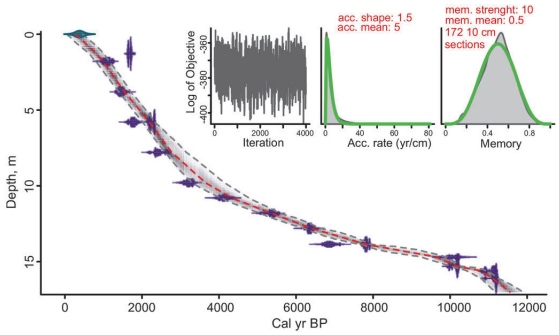

Fig. 3. Age-depth model of the Petrovskoe sedimentary sequence.

2. 0.5–2.2 m (490–1100 cal yr BP). Organic gyttja, dark gray-brown (Ox – dark brown), medium density, porous. Negative values of χ and extremely high of LOI (69.2 %), sharp local peak of sand (15 %, 590 cal yr BP).
3. 2.2–10.0 m (1100–3770 cal yr BP). Silty gyttja, black (Ox – dark brown), denser than the upper part. Sharp local peak of χ (up to $0.3*10^{-6}$, m^3 kg^{-1}, 1130–1240 cal yr BP), LOI values around 50 %, LOI local minimum 37.2 % (2910 cal yr BP), zone of high clay content (>14 %, 1820–2350 cal yr BP).
4. 10.0–14.6 m (3770–9480 cal yr BP). Laminated silty gyttja, black (Ox – dark brown), pyrite framboids. Relatively high χ between 4000 and 7000 cal yr BP, LOI 30–40 %, slight tendency for MGS to increase downwards, local peak of clay in the bottom of the unit.
5. 14.6–15.4 m (9480–10360 cal yr BP). Silty gyttja, dark gray-brown (Ox – gray-brown), pyrite framboids, wooden remains. Instability of unit composition, maximum of clay content (24 %) at 9560 cal yr BP.
6. 15.4–15.65 m (10360–10840 cal yr BP). Silty peat, black (Ox – dark brown), pyrite framboids, wooden remains.
7. 15.65–15.8 m (10840–10940 cal yr BP). Ferruginous silty peat, olive (Ox – red–brown), iron cutans, poor in plant remains. Extremely high χ ($0.71*10^{-6}$, m^3 kg^{-1}, 10870 cal yr BP).
8. 15.8–16.2 m (10940–11190 cal yr BP). Silty peat, dark gray-brown, wooden remains and charcoals.
9. 16.2–16.35 m (>1190 cal yr BP). Sandy clay silt with rare gravel, light gray-brown, high density. Maximum of sand content (29.7 %) and D_b (1.6 g cm^{-3}), minimum LOI (2 %).

The MAR graph shows significant variation along the core, from 0.006 to 0.076 g cm^{-2} yr^{-1}. High values (>0.04 g cm^{-2} yr^{-1}) are observed in the 2.6–7.8 m (1200–2700 cal yr BP). Minimum rates are found in the near-surface zone and at the beginning of the lacustrine deposition zone, which is situated above the peat interlayer. For the lower 15 cm of the core, rates were not calculated, as these sections belong to different accumulation types and are part of an extrapolated age model, meaning their age cannot be accurately determined and is likely older than the Pleistocene-Holocene boundary.

4.3. Pollen analysis

The results of pollen analysis are presented in Fig. 5:

Zone 1 (16.3–16.1 m, 11200–11100 cal yr BP): The lower two samples, composed of mineral matter and detrital material, belong to the very beginning of the Holocene. It is characterized by the presence of Chenopodiaceae, *Salix, Betula nana, Alnus, Pinus* and *Picea* in the spectra, as well as high values of *Lycopodium clavatum* and Polypodiaceae.

Zone 2 (16.1–15 m, 11100–9900 cal yr BP): *Picea* pollen content is minimal (1 percent), *Pinus* varies significantly (from 20 % to 75 %) and *Betula* is abundant (up to 61 %). Poaceae, Cyperaceae and *Artemisia* are also prominent. Cannabaceae, *Urtica*, *Filipendula* and *Thelypteris* appear, increasing their presence synchronously with *Ulmus*. The content of non-arboreal pollen (NAP) reaches up to 24 %. Although the deposit is composed of peat, pollen of wetland plants (*Potamogeton, Nymphaea, Nuphar, Equisetum*) is found.

Zone 3 (15–14.25 m, 9900–8660 cal yr BP): During this time *Betula* and *Pinus* gradually lose their dominance, while *Alnus* and broad-leaved pollen increase maintaining a significant presence of *Humulus* and *Urtica*. *Alnus* is likely a local origin along with *Humulus* and *Urtica* formed the vegetation of the lake floodplain, which developed as the dead ice melted. During this period, the content of *Quercus* and *Tilia* increases, *Betula nana* nearly disappears, and *Carpinus* emerges. The abundance of NAP decreases, with *Filipendula* and other wet meadow grasses becoming more prominent.

Zone 4 (14.25–12.00 m, 8660–5560 cal yr BP): In this time sedimentation continues at a similarly slow rate. The spectra from this period contain the maximum amount of tree pollen (90–97 %). *Alnus*

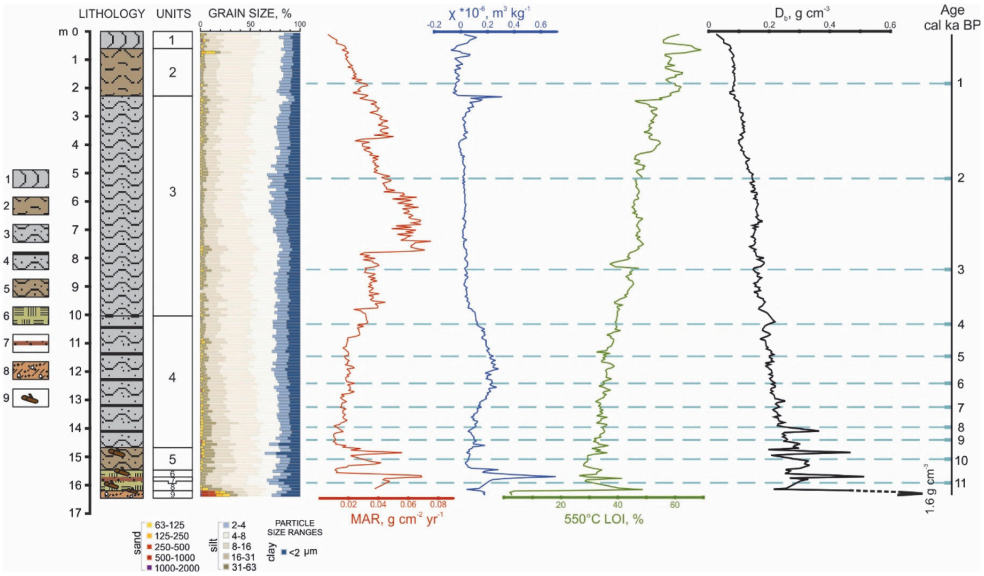

Fig. 4. Lithological properties of the Petrovskoe sediment core. Legend: 1 — loose organic gyttja, 2 — porous organic gyttja, 3 — silty gyttja, 4 — laminated silty gyttja, 5 — silty gyttja with wooden remains, 6 — silty peat, 7 — ferruginized silty peat, 8 — sandy clay silt with gravel, 9 — wooden remains. For more detailed lithological properties, see Supplementary 2.

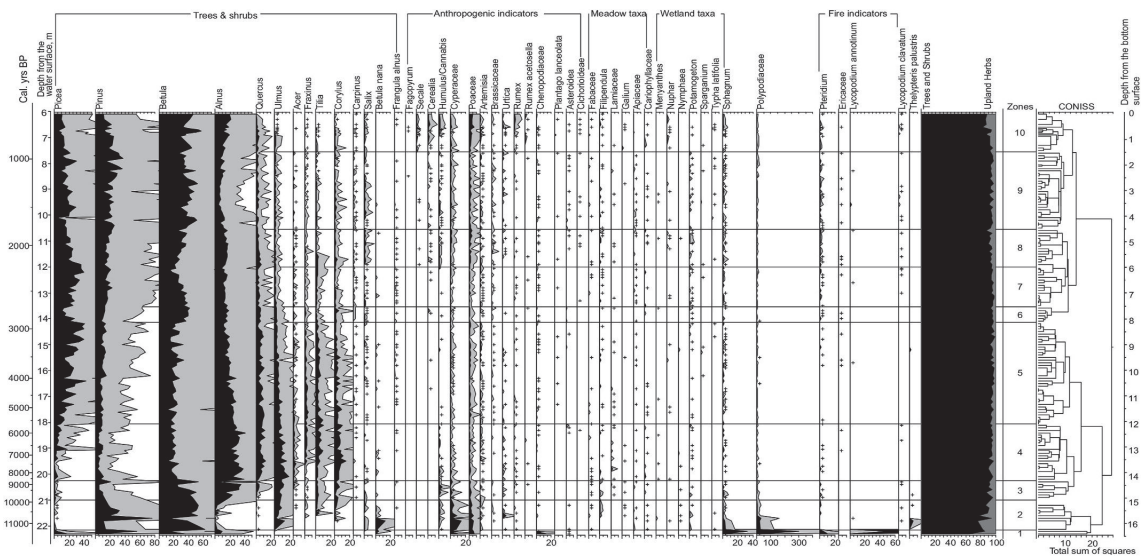

Fig. 5. Selective pollen percentage diagram of the Petrovskoe lacustrine sequence.

and broad-leaved species dominate, reaching their peak abundance here. *Betula* reduces its presence in the spectra to 10–26 %, *Pinus* to 3–11 %, while *Picea* increases slightly towards the end of the period. Alnus stands and pollen prevailed possibly due to the lake being surrounded by a young floodplain overgrown with a mire forest of alder and birch. The amount of NAP decreases to a minimum.

Zone 5 (12–8.15 m, 5560–2890 cal yr BP): This zone is characterized by a small and very gradual decrease in broad-leaved pollen, with a sharp decline towards the top of the zone. *Pinus* and *Betula* slightly increase their presence, while *Picea* shows a significant rise at the beginning of this period, reaching over 40 %. Around 4200 cal yr BP, the first pollen grain of Cerealia appears (at a depth of 10.7 m). From this point, *Alnus* begins to decline, and *Pinus* increases in the upper part of the zone to 13–14 %, occurring simultaneously with the appearance of Ericaceae, particularly *Calluna,* and *Pteridium* (after a long hiatus). Slightly earlier than Cerealia, *Plantago major* and *Plantago lanceolata* appear simultaneously.

Zone 6 (8.15–7.55 m, 2890–2650 cal yr BP): During this period, the

AP/NAP ratio remains unchanged, but significant changes occur in the composition of the pollen spectra. At the lower boundary of the zone, the percentage of broad-leaved species decreases and *Picea* sharply declines to 10–20 %, while *Betula* increases to 30–40 %. The content of *Pinus* increases only slightly, but from this point it begins to grow in sync with a noticeable strengthening of *Pteridium*, *Potamogeton* and Brassicaceae.

Zone 7 (7.55–5.95 m, 2650–2240 cal yr BP): Starting around 2600 cal yr BP, *Picea* increases again to 40 % by the end of the period, while *Betula* decreases in an antiphase. The presence of *Pinus* in the spectra gradually rises, and broadleaved trees continue to decrease (with *Ulmus* and *Quercus* declining the most and *Tilia* the least). At the beginning of this zone, there was a hiatus in Cerealia and *Urtica*. The amount of NAP decreases slightly, reaching as low as 2–3 % in some levels.

Zone 8 (5.95–4.55 m, 2240–1790 cal yr BP): In this zone, the percentage of *Picea* decreases, while *Betula, Pinus* and *Salix* increases. Cerealia, *Urtica* and Cannabaceae reappear and increase, and Brassicaceae, Poaceae, Cyperaceae and NAP in general increase. Simultaneously, the percentage of *Pteridium* increases, and *Secale* appears. Additionally, there is an increase in the presence of aquatic plants (*Potamogeton*, *Sparganium*, *Nuphar*) and weeds.

Zone 9 (4.55–1.55 m, 1790–910 cal yr BP): During this period, *Alnus* decreases from 13 % to 6 %, a phenomenon we attribute to the "*Alnus* decline." The content of *Picea* pollen drops sharply at the lower boundary of the zone, after which its percentage fluctuates between 10 and 30 %. The percentages of *Pinus* and *Betula* show significant fluctuations but with an overall upward trend. There is a continued decrease in the proportion of broad-leaved pollen. Near the top of the zone, *Picea* pollen reaches a local maximum for a short period. NAP and anthropogenic indicators remain sporadic but stable until this point, after which they decrease synchronously with *Picea*. Among herbaceous plants, Apiaceae and Brassicaceae, as well as *Pteridium* and *Lycopodium*, play a prominent role.

Zone 10 (1.55–0 m, 910–280 cal yr BP): *Alnus* and *Betula* increase here, while *Picea* and *Pinus* decrease. At ca. 800 cal yr BP, pollen of broadleaved trees nearly disappeared, whereas NAPs rose to a maximum, composed mainly of anthropogenic indicators such as Cerealia, *Secale*, *Rumex*, *Artemisia*, Cannabaceae, Poaceae, Brassicaceae and *Urtica*.

4.4. Quantitative biome reconstructions

The table of the resulting affinity scores is placed in the Supplementary File 3. The pollen-based biome reconstruction (Fig. 6) reveals that forest biomes consistently maintain higher affinity scores compared to non-forest biomes throughout the entire sequence. The gradual integration and sharp rise in the presence of deciduous tree species in forests led to the formation of *cool mixed forests* during the Holocene Climatic Optimum. *Quercus* sp. shows a significant rise in the pollen spectra since approximately 9500 cal yr BP, while *Fraxinus* sp. starts to affect biome scores around 7500 cal yr BP (Suppl. 3). These tree species indicate more temperate biomes compared to other broadleaf tree species. Subsequent climate aridisation and cooling caused a selective loss of broad-leaved species and an increase in the presence of taiga species. As a result, between 4200 and 3250 cal yr BP, *cool mixed forests of the modern type* were formed. However, the high scoring levels of non-forest biomes at the beginning (11100–9500 cal yr BP) and in the most recent period (3750 cal yr BP to present) are significant.

4.5. Macrofossil analysis

Above the brown-gray silt deposits, which contain very few plant remains, and transitional interbedded deposits, there is a layer of mineralized *Sphagnum* peat (approximately 50 cm thick), predominantly composed of the boreal species *Sphagnum teres*. At a depth of 15.7 m (approximately 10700 cal yr BP), the peat is interbedded with a highly mineralized ferruginous layer that contains few plant remains but a large quantity of framboids and idioblasts from plants of the Nymphaeaceae family. Below this layer, the peat contains sporangia of Polypodiales, as well as small quantities of Nymphaeaceae, *Menyanthes trifoliata* and *Rhynchospora alba*. Above this depth, the diversity of

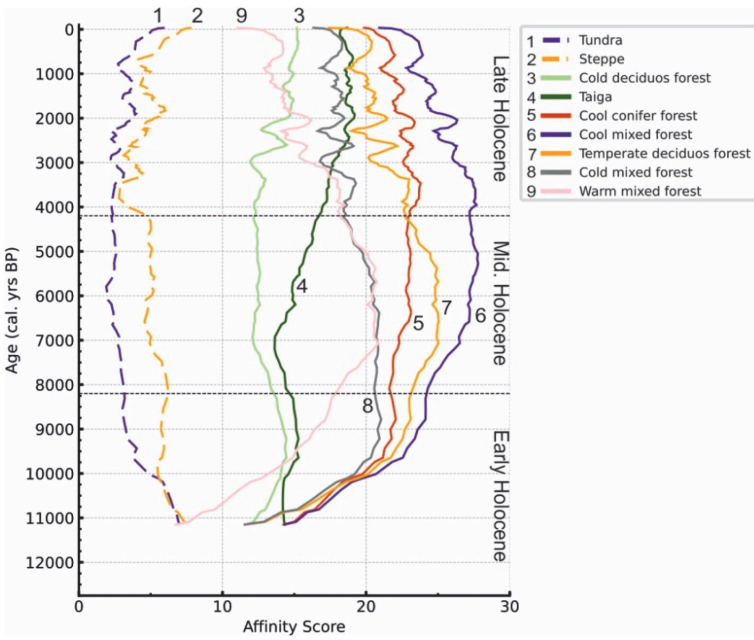

Fig. 6. Pollen-based quantitative biome reconstructions.

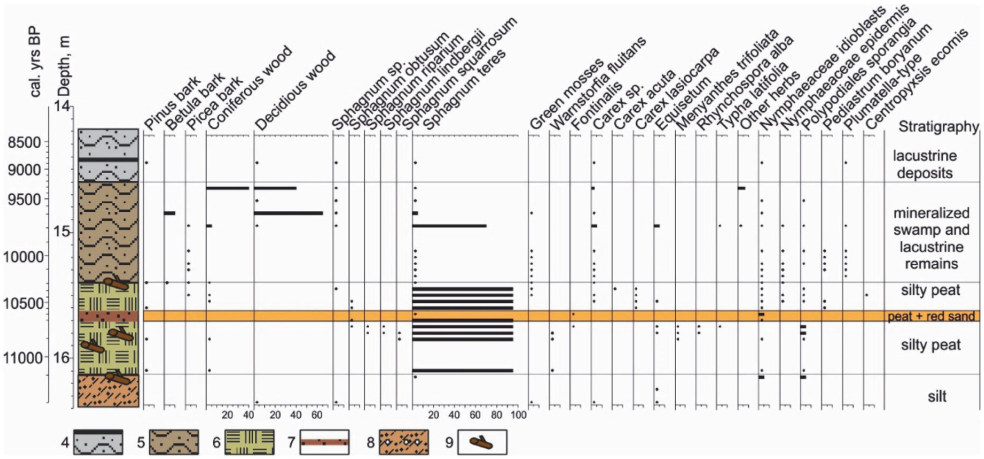

Fig. 7. Macrofossil diagram of the Petrovskoe Lake bottom sediments (Early Holocene). The lithology column and legend is inherited from Fig. 4. Legend: 4 — laminated silty gyttja, 5 — silty gyttja with wooden remains, 6 — silty peat, 7 — ferruginized silty peat, 8 — sandy clay silt with gravel, 9 — wooden remains.

macroremains increases, including wood remains, sedges, aquatic plants and green algae. Above the 15.5 m level (10300 cal yr BP), isolated recognizable plant remains include coniferous and deciduous wood, sedges, *Sphagnum* mosses and aquatic taxa.

4.6. Chironomidae analysis

73 fossil Chironomidae morphotypes were identified in Lake Petrovskoe (Fig. 8). The most abundant morphotypes along the core were *Cladopelma lateralis*-type, *Cladotanytarsus mancus*-type, *Sergentia coracina*-type and *Tanytarsus pallidicornis*-type. The two components Chironomidae-inferred WA-PLS-based July air temperature reconstruction was performed with RMSEP of 0.8, RMSE of 0.6, R^2 of 0.9, average bias of 0.01 and maximum bias of 0.9. Seven zones were identified using cluster analysis:

Seven zones were identified using cluster analysis:

Zone CH1 (15.50–14.65 m, 10478–9547 cal yr BP): it is characterized by the dominance of colder temperatures and oligotrophic morphotypes: *Sergentia coracina*-type, *Stempellinella*, *Tanytarsus mendax*-type, *Cladotanytarsus, Tanytarsus pallidicornis*-type. Further, some warm-related *taxa (Dicrotendipes nervosus*-type*, Coroneura scutellata-type, Chironomus plumosus*-type*)* increase their abundance by the end of the zone. Therefore, Chironomidae inferred July air temperature reconstruction indicates early Holocene warming from 13.3 °C to 14.6 °C at the end of the zone. The dominant abundances of *Cladotanytarsus* and the presence of *Pagastiella* morphotypes together identify the increase of the lake's productivity and acidification (Brooks et al., 2007). Further, presence of *Lauterborniella*, *Gymnimetriocnemus-Bryophaenocladius*, *Polypedilum sordens-type, Cricotopus cylindraceus-type* preferred submerged wood and vegetation habitat type and *Parametriocnemus*, which is mainly

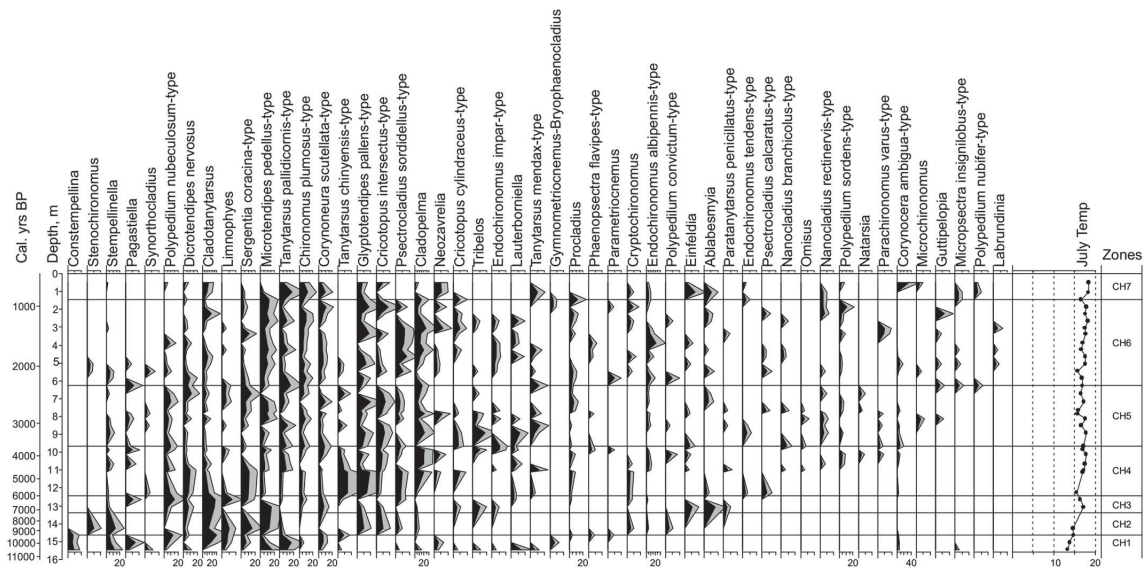

Fig. 8. Chironomidae fossil assemblages from the Petrovskoe lacustrine sequence.

represented by terrestrial species, indicates erosion processes in the lake.

Zone CH2 (14.65–13.05 m, 9547–6735 cal yr BP) is marked by increasing abundances of cold-related *Sergentia coracina*-type, *Stempellinella*. Also, the appearance of Stenochironomus indicates the presence of submerged vegetation or dead wood in the lake. The Chironomidae inferred temperature reconstruction indicates a cool stage of 14.4 °C followed by rapid warming up to 17 °C.

Zone CH3 13.4–12.65 m, 6735–6243 cal yr BP) is characterized by increasing warm-related *Polypedilum nubecolusum*-type, *Dicrotendipes nervosus*-type, *Corynoneura scutellata*-type, *Einfeldia* as well as appearance of *Cricotopus cylindraceus*-type, *Tribelus*, *Ablabesmyia*, *Paratanytarsus penicillatus*-type, which are indicators of macrophytes presence. The Chironomidae inferred July air temperature reconstruction suggests slight variation around 17.0° C–16.0 °C.

Zone CH4 (12.65–9.65 m, 6243–3585 cal yr BP) is marked by increasing of cold-related taxa (*Cladotanytarsus*, *Sergentia coracina*-type, *Tanytarsus mendax*-type, *Tanytarsus chinensis*-type, *Stempellinella*) and followed by dominance of warm-related morphotypes, such as *Cladopelma*, *Dicrotendipes nervosus*-type, *Nanocladius retinervis-type* and *Endochironomus albipennis*-type. The Chironomidae-inferred temperature reconstruction reveals 6000 BP anomaly cooling (Spurk et al., 2002) to 15.4 °C with subsequent warming up to 17.7 °C. Presence of *Guttipelopia* and *Endochironomus impar*-type indicates alkalization of the water. In addition, the fossil Chironomidae community suggests presence of submerged wood (*Gymnimetriocnemus-Bryophaenocladius*), slight erosion process (*Parametriocnemus*), water vegetation and macrophytes (*Cricotopus cylindraceus*-type, *Paratanytarsus penicillatus*-type, *Nanocladius rectinervis*-type) and general ecosystem disturbance (*Omisus*).

Zone CH5 (9.65–6.25 m, 3585–2327 cal yr BP) reveals relatively stable July air temperature conditions with general fluctuations around 16° C–17 °C and minor cooling event around 2710–2651 cal yr BP. The above-described groups of warm-related and cold-related taxa are presented in this zone without clear dominance of each group. Further, this zone is marked by the appearance and increase of various taxa related to the presence of submerged wood (*Synorthocladius*, *Gymnimetriocnemus-Bryophaenocladius*) and water vegetation.

Zone CH6 (6.25–1.45 m, 2327–872 cal yr BP) starts with 1°C cooling to 15.6 °C with subsequent warming up to 18.2 °C and ends with 1.6°C cooling, which corresponds to the Medieval climate event. Generally, the composition of fossil Chironomidae assemblage follows the pattern of the previous zone. The unique feature of this zone is pick of *Endochironomis albipennis*-type, a warm-related taxon, but also an indicator of vegetation in the water, stems in particular. Also, the appearance of *Criptochironomus* highlights the increase of nutrients in the water.

Zone CH7 (1.45–0.5 m, 872–485 cal yr BP) is marked by the rapid increase of *Psectrocladius sordidellius*-type and *Cladotanytarsus*, which were previously recognized as acidification markers (Brooks et al., 2007; Potito et al., 2014). *Micropsectra insignilobus*-type and *Neozavrelia* increase marks eutrophication of the water. The Chironomidae inferred July temperature reconstruction indicates warming towards the modern values — 18.3 °C. The fossil community of this zone includes various warm-related taxa, such as *Chironomus plumosus*-type, *Coroneura scutellata*-type, *Einfeldia, Microchironomus*.

4.7. Cladocera analysis

In total, 17 taxa of Cladocera were identified from the sediment samples of Lake Petrovskoe (Fig. 9). The most abundant taxa were the pelagic *Bosmina* sp. and *Daphnia* sp. and the eurytopic *Chydorus sphaericus* s.l. The water level has fluctuated throughout the lake's history. Based on these changes, eight zones can be distinguished.

Zone CL1 (15.50–13.75 m, 10600–7670 cal yr BP): The cladoceran taphocomplex is mainly represented by pelagic species *Bosmina* sp. and *Daphnia* sp. Their proportion is more than 90 % throughout the entire period, which indicates a large area of open pelagic zone.

Zone CL2 (13.75–13.15 m, 7670–6860 cal yr BP): In addition to

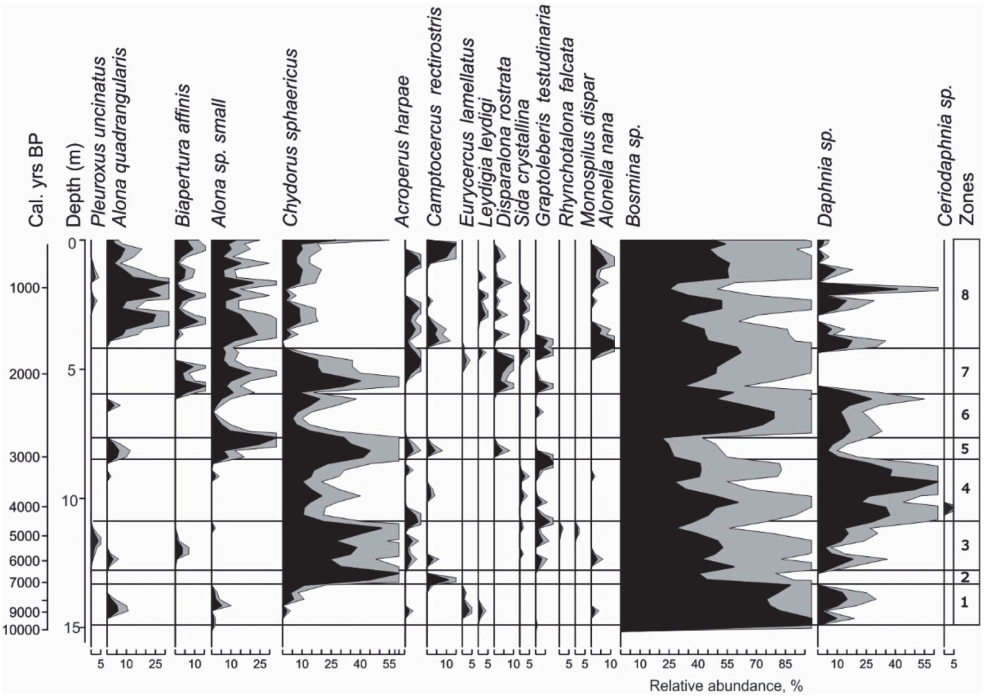

Fig. 9. Cladocera fossil assemblages from the Petrovskoe lacustrine sequence.

pelagic species, the dominant group includes a group of eurytopic species *Chydorus sphaericus* s.l. This could reflects eutrofication of the lake.

Zone CL3 (13.15–11.5 m, 6860–5060 cal yr BP): The species diversity in the cladoceran taphocomplex increases, phytophilic species (*Biapertura affinis, Acroperus harpae* and *Graptoleberis testudinaria*) appear in the taphocomplex. This indicates the development of aquatic vegetation and a more intense (compared to the previous zone) decrease in the water level.

Zone CL4 (11.50–19.00 m, 5060–3280 cal yr BP): Pelagic *Daphnia* sp. predominate in the taphocomplex of cladocerans, while the abundance of shallow-water (phytophilic and benthic) taxa decreases. This indicates an increase in the water level.

Zone CL5 (19.00–8.15 m, 3280–2880 cal yr BP): The abundance of phytophilic and benthic *Alona* sp. and the eurytopic *Chydorus sphaericus* s.l. increases among remains, while the proportion of pelagic species in the taphocomplex decreases. The benthic *Alona quadrangularis* has a significant proportion in the taphocomplex. This may indicate a decrease in the water level.

Zone CL6 (8.15–6.25 m, 2880–2320 cal yr BP): Pelagic species constituted 74–98 % of the taphocomplex of cladocerans. Shallow-water species almost disappeared, the exception is a few finds of phytophilic *Graptoleberis testudinaria* and benthic *Alona quadrangularis*. Also, at the beginning and at the end of this zone there are remains of *Alona* sp. and eurytopic *Chydorus sphaericus* s.l. During this period, the water level apparently increased significantly.

Zone CL7 (6.25–4.50 m, 2320–1770 cal yr BP): The composition of the remains of cladocerans became more even. The proportion of pelagic taxa decreased due to the increase in the proportion of *Chydorus sphaericus* s.l. and the appearance of shallow-water species in the taphocomplex: *Biapertura affinis, Acroperus harpae, Disparalona rostrata, Alona* sp. At the end of the zone remains of *Sida crystallina* appear. Probably, all this may indicate the shallowing of the lake and its overgrowing with aquatic plants.

Zone CL8 (4.50–0.60 m, 1770–530 cal yr BP): The benthic *Alona quadrangularis* occupies a significant proportion in the cladoceran taphocomplex, which indicates a significant decrease in the water level and an increase in the area of the littoral zone. However, the pelagic taxa *Bosmina* sp. and *Daphnia* sp. have a dominant position in the taphocomplex, which reflects the presence of a relatively large area of the pelagic zone. In addition, this zone was characterized by the presence of the acidophilic species *Alonella nana*, indicating acidic conditions in the reservoir.

4.8. Macrocharcoal analysis

Macrocharcoal accumulation rates (CHAR) during the Holocene were heterogeneous (Fig. 10). Four main periods of charcoal particle accumulation can be identified. The first interval (11100–9800 cal yr BP) is characterized by low background CHAR values (0–2 pieces $cm^{-2}yr^{-1}$). However, several peaks of interpolated CHAR are observed, with values reaching up to 30 pieces $cm^{-2}yr^{-1}$. Six local fire episodes are identified for this interval, with fire return intervals ranging from 30 to

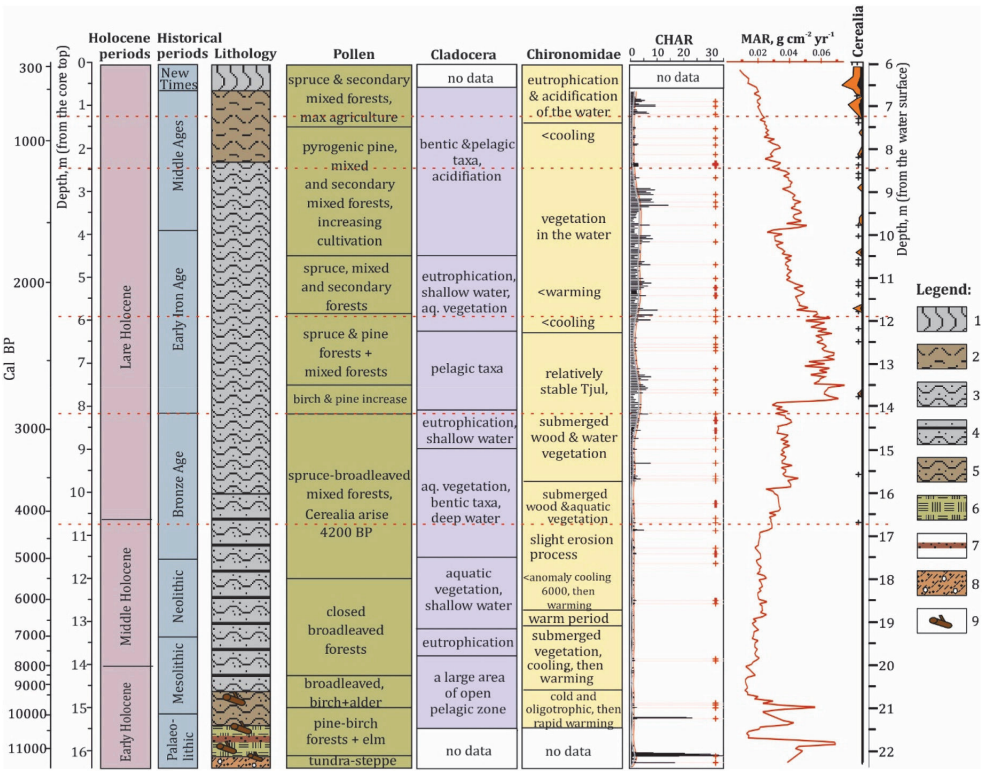

Fig. 10. Main stages of changes in proxies. More details on the dynamics of particular data can be found in Figs. 3–9. The red dotted lines mark the beginning of periods of anthropogenic transformation of the landscape. On the CHAR graph: 1) The black line — interpolated CHAR; 2) The gray line — background CHAR; 3) The red line — threshold CHAR; 4) The red pluses — local fire episodes. The lithology column and legend is inherited from Fig. 4. Legend: 1 — loose organic gyttja, 2 — porous organic gyttja, 3 — silty gyttja, 4 — laminated silty gyttja, 5 — silty gyttja with wooden remains, 6 — silty peat, 7 — ferruginized silty peat, 8 — sandy clay silt with gravel, 9 — wooden remains. (For interpretation of the references to colour in this figure legend, the reader is referred to the Web version of this article.)

830 years.

The second period (9800–3500 cal yr BP) is characterized by low background and interpolated CHAR values (<2 pieces $cm^{-2}yr^{-1}$), except for a relatively small peak of interpolated CHAR (4.5 pieces $cm^{-2}yr^{-1}$) around 4500 cal yr BP. Seven local fire episodes correspond to this interval. Fire return intervals ranging from 30 to 1800 years.

The interval from 3500 cal yr BP to 350 cal yr BP is characterized by a sharp increase in both interpolated and background CHAR. Interpolated CHAR reaches values of 8–11 pieces $cm^{-2}yr^{-1}$, with maximum values occurring during the intervals of 2500–3400 cal yr BP, 1000–2100 cal yr BP and 650–350 cal yr BP. Background CHAR during this time varies in the range of 0.5–4.5 pieces $cm^{-2}yr^{-1}$ and fire return intervals are significantly reduced to 30–230 years.

5. Discussion

The centennial-resolution multiproxy data obtained in this study offer a reconstruction of the history of basin development, vegetation changes, climate dynamics and human impact for nearly the entire Holocene (since 11200 cal yr BP) in the marginal zone of the last glaciation. The main stages for each environmental proxy are shown in Fig. 10.

5.1. Lake system development and sedimentation

The beginning of sedimentation in the lake Petrovskoe (11100–11200 cal yr BP) started from the deposition of peat on a sandy silt base containing macrocharcoals and plant remains. The peak of CHAR is on the upper boundary of mineral deposits, above which a *Sphagnum* mire formed, that coincides with the idea of the peatland initiation in relation to the fire regime (Novenko et al., 2021). This bog existed during the period of 11100–10300 years ago, was subject to periodic flooding and, possibly, the formation of floating mats and mineralized layers. The sedimentary conditions was unstable.

The response of terrestrial ecosystems to rapid warming 11700 years ago was delayed, and the refugee of dead ice served as habitats for boreal species. The combination of mineralized *Sphagnum* peat composed of boreal *Sphagnum teres* and the presence of pollen of thermophilic taxa at the same level suggests the existence of buried ice, which created more severe conditions on it than on the surrounding moraine hills. Chironomid analysis also indicates cold conditions during this time. As the buried ice melted during the warming period 10500-8300, the boreal phytocoenosis formed on the surface was “projected” onto the bottom of the basin, then flooded with water and buried (and partially mixed) with gyttja. As the buried ice melted, the bog was repeatedly flooded, bringing mineral debris and possibly forming floating mats. Analyses show the coexistence of *Sphagnum* mire, riparian or floating-mat habitats (presence of Nymphaeaceae, *Menyanthes*, *Pediastrum, Typha, Carex* and Polypodiaceae) and open water (pelagic cladocerans, *Potamogeton* pollen). Such phenomenon is well known on the plains within the Baltic basin (Strivins et al., 2017a) and on the Lake Seliger in the upstream of the Volga River (Sapelko et al., 2022).

The onset of the Lake Petrovskoe formation is associated with the final melting of dead ice and fluvial processes, during which peat was partially washed away and mixed with eroded material and organic lake deposits (10,600–9400 cal yr BP). The progressive increase in Loss on Ignition (LOI) values after 9400 cal yr BP indicates a stabilization of conditions in the reservoir, as well as a gradual increase in trophicity and organic content in the sediments. Several negative anomalies in LOI reflect significant erosional events (Fig. 4) corresponding to the period from 10,200 to 9400 cal yr BP in the Early Holocene. In the Late Holocene, brief episodes of erosion are observed at 4200, 3500, 2900–2800, 1800–1700, and 1200–1100 cal yr BP, as well as after 800 cal yr BP. Additionally, following 2800 cal yr BP, stepwise eutrophication occurred. In the interval of 2.2–3.8 m (1100–1530 years ago), there was a prolonged phase characterized by an increased supply of clastic material, possibly due to erosion. Furthermore, at the end of this period, between 2.2 and 2.4 m (1100–1160 cal yr BP), a distinct event occurred that was associated with a very high intensity of soil flushing. After this event, sedimentation stabilized; however, LOI exhibited significant variability.

According to the chironomid record, 9000–8000 cal yr BP the conditions within the lake basin were cold, open and oligotrophic and, as a result, the sedimentation rate was lowest. At the same time, the expansion of broadleaved taxa confirms that warming has occurred at the regional level.

After 8000 cal yr BP, the lake conditions and geomorphological setting became more stable and sedimentation rate increased gradually, while the proportion of organic material in the gyttja composition rose up to the top of the core. The inner dynamics of the reservoir was relatively stable. We can associate increase in MAR and decrease of LOI in the period 2800–2900 BP (the beginning of the Early Iron Age) with human activity caused fires (Fig. 10), soil erosion and increasing eutrophication of the lake. Similar disruptions in trends occurred in the middle of the 1st millennium CE, synchronously with the phenomenon of “*Alnus* decline” in the pollen diagram. The last period of erosion 1200–1100 cal yr BP was short-term and thus is visible in the LOI and in the χ, but is not reflected in the MAR.

The changes in water level identified in the cladoceran record can mostly be attributed to the flooding of the low lake floodplain during wet periods, rather than to a significant decrease in the level of the lake system. The results of the cladocerans and chironomids analyses show acidification of the water last ca. 1000 years. Aquatic vegetation had grown in the lake throughout its entire development.

5.2. Vegetation development, biomes and fire regime

Due to the dimensions of the basin and its geomorphological position, a significant amount of pollen accumulated in the lake’s catchment area within the lake depression (Tauber, 1967). Therefore, we can draw conclusions about the vegetation typical of a microregion that does not extend beyond the marginal glaciation zone. The main stages and specific features of the environmental proxies are combined in Fig. 10, using scales of depth (measured from the water surface and from the bottom), time, Holocene periods (Cohen et al., 2013) and archaeological periods.

The earliest palynological data from this section date back to the end of the early Holocene warming and the beginning of the Preboreal cooling (11200 cal yr BP). We observe the tail end of the "lower maximum" of *Picea* (Khotinskiy, 1977; Giesecke and Bennett, 2004; Latałowa and van der Knaap, 2006), followed by a peak in early Holocene fires, and the final stages of tundra-steppe vegetation continued until 10500 cal yr BP.

The period from 11000 to 10000 cal yr BP marks the final stage of Preboreal cooling, during which boreal mires developed, covering the buried dead ice. At the same time, a regional warming trend led to the appearance and rapid proliferation of thermophilic taxa, primarily *Ulmus*. *Pinus* and *Betula* predominantly constituted the regional vegetation. Local wetland vegetation included *Sphagnum* and fern-sedge-grass communities, with *Betula* and *Salix* in the tree layer. Relatively high values for treeless biomes were observed up to 10000 cal yr BP.

Starting from 10500 cal yr BP, thermophilic species formed closed communities by 9500 cal yr BP, although pine and birch still played significant roles in vegetation formation. Birch and alder (most likely *Alnus glutinosa*), as well as nitrophilic herbs and *Humulus* constituted the local vegetation in the swampy lake floodplain following the lowering of the lake level. Biomisation indicates a rapid onset of *warm mixed forests* and a decrease in *cold deciduous forests*. This aligns with the findings of O.K. Borisova (2019) and T.V. Sapelko et al. (2022), who dated the appearance of thermophilic elements in the forest stands to 10670–10300 cal yr BP, with widespread expansion by 9500 cal yr BP. The prolonged warming gave way to a brief and intense ’8.2 ka event,’

which is reflected in the palynological spectra (*Picea* and *Pinus* rise) and Biomisation affinity scores (changes in favor of *taiga* and *cold conifer corest* biomes, Suppl. 3), albeit with some age uncertainty. This event was characterized by a short, sharp change in forest composition and a rapid return to the main trend (Figs. 5 and 6, Suppl. 3).

Starting around 8000–7500 cal yr BP, broadleaved forests reached their maximum development and diversity, while the presence of boreal forests decreased, likely due in part to the replacement of birch and alder by broadleaved species in drying lake floodplains. After 6000 cal yr BP, the proportion of *Picea* in the vegetation composition gradually increased, indicating a greater role for *taiga* biome. The late re-expansion of *Picea* is supported by data from deposits from the Kosilovo mire (Nosova et al., 2024) located 2 km to the west and other nearby sequences investigated (Tarasov et al., 2019; Sapelko et al., 2022). In the period leading up to the 4.2 ka environmental shift, the *warm mixed forest* biome remained significant. Low fire activity during this period, typical for nemoral forests (Feurdean et al., 2020), resulted in a reduction of pine forests as pyrogenic vegetation. Overall, the results of fire activity reconstruction for the studied region are similar to the results obtained for the large data set analyzed in boreo-nemoral ecoregion (Feurdean et al., 2020).

It is worth noting that the first appearance of Cerealia in several pollen series in the broadleaved-coniferous forest zone of European Russia often coincides in different studies (this paper, Nosova et al., 2019; Sapelko et al., 2022). From that moment, 4200 cal yr BP, human influence increasingly affected the vegetation in the area. Biomisation results indicate a decrease in the prominence of *warm mixed forests,* correlating with stages of anthropogenic vegetation transformation previously identified in the modern broadleaved-coniferous forest zone (Nosova et al., 2019; Ershova et al., 2022). These stages were dated to 4200, 2900–2800, 1500, 1200 and 500 cal yr BP, corresponding respectively to: 1) the absolute limit (Co) of Cerealia, 2) the start of the Early Iron Age (2800 BP), 3) the Migration Period and cultural changes in the region, 4) the Old Russian period (1100–900 BP c) and 5) the onset of the New Age. Each stage involved the degradation of broadleaved elements in forests, significant fluctuations in spruce forests and an increased role of secondary forests dominated by pine and birch. Other NAP-indicators of fire activity (*Pteridium* and *Lycopodium*) support the pyrogenic nature of pine forest expansion. Biomisation also shows a change in the ratio of biomes in favor of boreal ones, attributed to a cooling trend and an increased role of secondary forests with *Betula, Pinus* and *Alnus*.

During the period from 1700 to 1200 cal yr BP a phenomenon characteristic of Eastern and Northern Europe and the Baltic countries, "*Alnus* decline" was observed. In the last ones, this decline occurred from 1400 to 1000 cal yr BP (Strivins et al., 2017), while in Poland and adjacent territories, it took place from 1200 to 1000 cal yr BP (Latałowa et al., 2019) and was attributed to pathogens or anthropogenic factors. The extent of this phenomenon in European Russia requires further study.

Biomisation data indicate a trend toward a decrease in the importance of forest biomes and an increase in open *steppe* biomes from 800 to 300 cal yr BP, which is typical for the coniferous-broadleaf forest zone in European Russia (Novenko et al., 2009; Nosova et al., 2017, 2019; Mazei et al., 2020; Tarasov et al., 2019, 2022).

6. Conclusions

According to our results, Petrovskoe Lake formed in a glacial runoff trough on the top of buried dead ice. Initially, during the early Holocene warming, cold *Sphagnum* mires formed on the surface of gradually melting buried ice and accompanied by periodic flooding. The cold phase of the early Holocene continued until 10500, when the remnants of tundra-steppe vegetation disappeared and thermophilic forest vegetation began to develop. Birch and pine forests predominated until 9500, when thermophilic biomes "took over".

Lake sediments began to form on the peat layer and were accompanied by several large-scale erosion episodes. The unstable period with low MAR and oligotrophic conditions lasted until 9400 cal yr BP, after which the lake regime stabilized. During the existence of the lake, eutrophication arose in several stages, apparently associated with the influx of remains of the thermophilous vegetation surrounding the lake basin during the Holocene Optimum, and during that time the productivity of the lake increased. According to the data obtained, erosion stages (indicated by a lowering of LOI at 4200, 3500, 2800, 1700–1800 and 1200 cal yr BP) during the Late Holocene correlate with sharp increases in MAR, fire activity and stages of anthropogenic transformation.

The Holocene Climatic Optimum was expressed in the stable existence of broadleaved forests from 7000 to 5000 cal yr BP, when Late Holocene cooling began. Starting from 4200 (the first appearance of cultivated cereals) it is difficult to separate the consequences of climate cooling from the results of anthropogenic impact. We have established the stages of anthropogenic transformation of this territory, started 4200, 3600, 2900–2800, 2200, 1500, 1200 and 800 cal yr BP. Both, previously noted for the broadleaved-coniferous forest zone (Nosova et al., 2019; Ershova et al., 2022) and new ones, coincides with fire activity. The maximum anthropogenic transformation began ca. 800 cal yr BP (different from the most common 500 cal yr BP). The combination of anthropogenic and climatic factors caused boreal biomes predomination in the territory since 3000 years ago, consisting of spruce and secondary tree species (pine, birch, alder, willow and aspen).

Funding

This research was funded by the Russian Science Foundation (grant number 23–77–10063 – field work, lithological, radiocarbon, pollen analyses), and realized within the State Task #FMWS-2024-0003 (laboratory processing for lithological analysis, Chironomidae analysis) and State Task #122042700002-6 (laboratory processing for palynological, Cladocera and macrofossil analysis).

CRediT authorship contribution statement

M.B. Nosova: Writing – original draft, Supervision, Software, Resources, Methodology, Investigation, Formal analysis, Data curation, Conceptualization. **A.L. Zakharov:** Writing – original draft, Visualization, Software, Project administration, Methodology, Investigation, Funding acquisition, Conceptualization. **N.G. Lavrenov:** Software, Methodology, Investigation, Formal analysis, Conceptualization. **N.E. Zaretskaya:** Writing – original draft, Supervision, Methodology, Formal analysis, Conceptualization. **N.G. Mazei:** Writing – original draft, Validation, Investigation. **D.A. Kupriyanov:** Writing – original draft, Visualization, Software, Investigation, Formal analysis. **Yu.A. Pastukhova:** Writing – original draft, Visualization, Validation, Methodology, Investigation. **V.O. Bakumenko:** Writing – original draft, Visualization, Validation, Software, Methodology, Investigation. **E.E. Severova:** Writing – original draft, Validation, Investigation. **E.A. Konstantinov:** Writing – original draft, Validation, Supervision, Methodology, Investigation, Data curation, Conceptualization.

Declaration of competing interest

The authors declare the following financial interests/personal relationships which may be considered as potential competing interests: Andrey Zakharov reports financial support was provided by Russian Science Foundation. If there are other authors, they declare that they have no known competing financial interests or personal relationships that could have appeared to influence the work reported in this paper.

Acknowledgments

We are grateful to Nikita Sychev, Lidiya Shasherina, Anna Rudinskaya, Dmitriy Baranov, Elena Garova, Nikolay Luguvoy for their help at fieldwork, Valeriy Pimenov, Lyudmila Lazukova and Anna Mareeva for their help in the laboratory.

Appendix A. Supplementary data

Supplementary data to this article can be found online at https://doi.org/10.1016/j.quaint.2025.109778.

References

Andersen, T., Sæther, O.A., Cranston, P.S., Epler, J.H., 2013. The larvae of orthocladiinae (Diptera: Chironomidae) of the holarctic region—keys and diagnoses. Insect Systemat. Evol. 66, 189–385.

Bakumenko, V., Poska, A., Płóciennik, M., Gasteviciene, N., Kotrys, B., Luoto, T.P., Belle, S., Veski, S., 2024. Chironomidae-based inference model for mean July air temperature reconstructions in the eastern Baltic area. Boreas 53, 401–404. https://doi.org/10.1111/bor.12655.

Birks, H.H., Birks, H.J.B., 2006. Multi-proxy studies in palaeolimnology. Veg. Hist. Archaeobotany 15, 235–251. https://doi.org/10.1007/s00334-006-0066-6.

Birks, H.J.B., Frey, D.G., Deevey, E.S., 1998. Numerical tools in palaeolimnology-progress, potentialities and problems. J. Paleolimnol. 20, 307–332.

Bjerring, R., Becares, E., Declerck, S., et al., 2009. Subfossil Cladocera in relation to contemporary environmental variables in 54 Pan-European lakes. Freshw. Biol. 54 (11), 2401–2417. https://doi.org/10.1111/j.1365-2427.2009.02252.x.

Blaauw, M., Christen, J.A., 2011. Flexible paleoclimate age depth models using an autoregressive gamma process. Bayesian Anal. 6 (3), 457–474. https://doi.org/10.1214/11-BA618.

Blake, G.R., 1965. Bulk density. In: black CA (ed) Part 1. Physical and mineralogical properties, including statistics of measurement and sampling. Agron. Monograp. 9, 374–390. https://doi.org/10.2134/agronmonogr9.1.c30.

Błaszkiewicz, M., 2011. Timing of the final disappearance of permafrost in the central European Lowland, as reconstructed from the evolution of lakes in N Poland. Geol. Q. 55, 361–374.

Bledzki, L.A., Rybak, J.I., 2016. Freshwater Crustacean Zooplankton of Europe: Cladocera & Copepoda (Calanoida, Cyclopoida) Key to Species Identification, with Notes on Ecology, Distribution, Methods and Introduction to Data Analysis. Springer. https://doi.org/10.1007/978-3-319-29871-9.

Blott, S.J., Croft, D.J., Pye, K., Saye, S.E., Wilson, H.E., 2004. Particle size analysis by laser diffraction. Geol. Soc. London, Special Publ. 232 (1), 63–73. https://doi.org/10.1144/gsl.sp.2004.232.01.08.

Borisova, O., 2019. Environmental and climatic conditions of human occupation in the central East European Plain during the Middle Holocene: reconstruction from palaeofloristic data. Quat. Int. 516, 42–57. https://doi.org/10.1016/j.quaint.2018.05.025.

Borisova, O.K., 2021. Landscape and climatic conditions in the central East European Plain in the last 22 thousand years: reconstruction based on paleobotanical data. Water Resour. 48, 886–896. https://doi.org/10.1134/s0097807821060038.

Botany Collection, MSU Russia. Pollen Specimen Database. Available at: http://botany-collection.bio.msu.ru/pollen-speciment (Accessed January 2023 – June 2024).

Brooks, S.J., Langdon, P.G., Heiri, O., 2007. The identification and use of Palaearctic Chironomidae larvae in palaeoecology. Quater. Res. Associat. Technic. Guide 10, 1–275. https://doi.org/10.1007/s10933-007-9191-1.

Chebotareva, N.S., Makarycheva, I.A., 1974. The Last Glaciation of Europe and its Geochronology. Nauka, Moscow (In Russian).

Cohen, K.M., Finney, S.C., Gibbard, P.L., Fan, J.X., 2013. The ICS international chronostratigraphic chart. Episodes J. Int. Geosci. 36 (3), 199–204. https://doi.org/10.18814/epiiugs/2013/v36i3/002.

Davydova, N.N., Subetto, D.A., Khomutova, V.I., Sapelko, T.V., 2001. Late Pleistocene-Holocene paleolimnology of three north-western Russian lakes. J. Paleolimnol. 26, 37–51. https://doi.org/10.1023/a:1011131015322.

Dolukhanov, P.M., Gay, N.A., Miklayayev, A.M., Mazurkiewicz, A.N., 1989. Rudnya-Serteya, a stratified dwelling-site in the Upper Duna basin (a multidisciplinary research). Fennosc. Archaeol. VI, 23–27.

Elovicheva, Y.K., 2001. Evolution of the Natural Environment of the Anthropogene of Belarus. Minsk: Belsans (In Russian).

Elovicheva, Y.K., Bogdel, I., 1987. Reconstruction of palaeoclimate and vegetation of the Byelorussian Holocene using bog and lake deposit data. Palaeohydrol. Temper. Zone III, 152–156.

Eremeev, I.I., Dzjuba, O.F., 2010. Notes on Historical Geography of the Forest Part of the Road from the Varangians to Greeks: Archaeological and Palaeogeographical Researches between the Western Dvina and Ilmen Lake. Nestor-History, St. Petersburg (In Russian).

Eremeev, I.I., Dzyuba, O.F., Lisitsyna, O.V., Buben'ko, O.V., Podgursky, P.N., 2009. New evidence of initial agriculture in the Western Dvina basin. Quat. Int. 203, 67–73. https://doi.org/10.1016/j.quaint.2008.04.026.

Ershova, E.G., Krenke, A.N., Nosova, M.B., 2022. History of the producing economy development in Moscow region and neighboring territories: review of palaeobotanical and archaeological evidence (to the 50th anniversary of the book by Yu.A. Krasnov "Early farming and cattle breeding in the forest zone of Eastern Europe"). Rossijskaja Arheologija 2, 7–19. https://doi.org/10.1016/j.quascirev.2017.05.024 (In Russian).

Feurdean, A., Vannière, B., Finsinger, W., et al., 2020. Fire hazard modulation by long-term dynamics in land cover and dominant forest type in eastern and central Europe. Biogeosciences 17, 1213–1230. https://doi.org/10.5194/bg-17-1213-2020, 2020.

Finsinger, W., Bonnici, I., 2022. Tapas: an R Package to Perform Trend and Peaks Analysis. Zenodo. Available online: https://hal.inria.fr/hal-03607000/. (Accessed 27 August 2024).

Giesecke, T., Bennett, K.D., 2004. The Holocene spread of *Picea abies* (L.) Karst. in Fennoscandia and adjacent areas. J. Biogeogr. 31 (9), 1523–1548. https://doi.org/10.1111/j.1365-2699.2004.01095.x.

Gribova, S.A., Isachenko, T.I., Lavrenko, E.M., 1980. The Vegetation of the European Part of USSR. Nauka, Leningrad (In Russian).

Grimm, E.C., 1987. CONISS: a FORTRAN 77 program for stratigraphically constrained cluster analysis by the method of incremental sum of squares. Comput. Geosci. 13 (1), 13–35.

Grimm, E., 2011. Tilia Version 1.7.16. Illinois State Museum, Research and Collection Center, Springfield, IL.

Gunova, V.S., Sirin, A.A., 1996. Paleogeographic conditions of raised bogs' development in the western Dvina lowland in the Holocene. In: Palynology in Russia: Articles of Russian Palynologists for the IX International Palynological Congress. Huston, Texas, pp. 27–36 (In Russian).

Heiri, O., Lotter, A.F., Lemcke, G., 2001. Loss on ignition as a method for estimating organic and carbonate content in sediments: reproducibility and comparability of results. J. Paleolimnol. 25, 101–110. https://doi.org/10.1023/a:1008119611481.

Higuera, P., 2009. CharAnalysis 0.9: Diagnostic and Analytical Tools for Sediment-Charcoal Analysis User's Guide. Montana State University, Bozeman MT.

Hunter, J.D., 2007. Matplotlib: a 2D graphics environment. Comput. Sci. Eng. 9 (3), 90–95. https://doi.org/10.1109/mcse.2007.55.

Ignatov, M.S., Ignatova, E.A., 2003. Flora of mosses in the middle part of European Russia. T. 1 Sphagnaceae-Hedwiigiaceae., vol. 1 KMK, Moscow (In Russian).

Katz, N.Y., Katz, S.V., Skobeeva, E.I., 1977. Atlas of Plant Residues in Peats. Nedra, Moscow (In Russian).

Khomutova, V.I., 1982. Spore-pollen spectra of bottom sediments of lakes of the North-West of the Russian Plain and their significance for paleolimnology. In: Late Cenozoic History of Lakes in the USSR, pp. 128–131.

Khotinskiy, N.A., 1977. The Holocene of North Eurasia. Nauka, Moscow (In Russian).

Klink, A.G., Pillot, H.K.M., 2003. Chironomidae larvae: key to the higher taxa and species of the lowlands of Northwestern Europe. ETI, Expert Center for Taxonomic Identification. University of Amsterdam.

Konert, M., Vandenberghe, J.E.F., 1997. Comparison of laser grain size analysis with pipette and sieve analysis: a solution for the underestimation of the clay fraction. Sedimentology 44 (3), 523–535. https://doi.org/10.1046/j.1365-3091.1997.d01-38.x.

Konstantinov, E.A., Panin, A.V., Karpukhina, N.V., Bricheva, S.S., Borisova, O.K., Naryshkina, N.N., Gurinov, A.L., Zakharov, A.L., 2021. The riverine past of Lake Seliger. Water Resour. 48, 635–645. https://doi.org/10.1134/s0097807821050110.

Korhola, A., Rautio, M., 2001. Cladocera and other branchiopod crustaceans. In: Tracking Environmental Change Using Lake Sediments: Volume 4: Zoological Indicators, pp. 5–41.

Kozharinov, A.V., Sirin, A.A., Klimenko, V.V., Klimanov, V.A., Maliasova, E.S., Sleptsov, A.M., 2003. 5000 years vegetation and climate dynamics in the Zapadnodvinskaya Lowlands, Tver region. Russ. Bot. J. 88, 90–102 (In Russian).

Kremenetski, K.V., Borisova, O.K., Zelikson, E.M., 2000. The Late Glacial and Holocene history of vegetation in the Moscow region. Paleontol. J. 34 (Suppl. p/1), 67–74.

Krenke, N.A., Ershova, E.G., Ershov, I.N., Raeva, V.A., Ganichev, K.A., Aleksandrovsky, A.L., Lopatin, N.V., Chaukin, S.N., 2022. Radiocarbon dating of archaeological and natural objects of the Smolensk region in 2014-2021. Brief commun. Inst. of Archaeol. (267), 320–344. https://doi.org/10.25681/IARAS.0130-2620.267.320-344 (In Russian).

Kvasov, D.D., Treshnikov, A.F. (Eds.), 1986. General Patterns of the Emergence and Development of Lakes. Methods of Studying the History of Lakes. Nauka, Leningrad, p. 254 (In Russian).

Larocque-Tobler, I., 2014. The Polish sub-fossil chironomids. Palaeontol. Electron. 17 (1), 1–28.

Latałowa, M., van der Knaap, W.O., 2006. Late Quaternary expansion of Norway spruce *Picea abies* (L.) Karst. in Europe according to pollen data. Quat. Sci. Rev. 25 (21–22), 2780–2805. https://doi.org/10.1016/j.quascirev.2006.06.007.

Latałowa, M., Święta-Musznicka, J., Słowiński, M., et al., 2019. Abrupt *Alnus* population decline at the end of the first millennium CE in Europe: the event ecology, possible causes and implications. Holocene 29 (8), 1335–1349. https://doi.org/10.1177/0959683619846978.

Lavrenov, N.G., Ershova, E.G., Krenke, N.A., Zhuravkova, M.M., 2021. Landscapes of Smolensk oblast as a consequence of ancient anthropogenic activity: palaeoecological study of Radomsky Mokh swamp. Povolzhskaya arkheologiya (The Volga River Region Archaeology) 4 (38), 235–246. https://doi.org/10.24852/pa2021.4.38.235.246 (In Russian).

Lavrenov, N., Ershova, E., Pimenov, V., 2024. Mshary mire (source of the Dnieper River, western Russia). Grana 63 (2), 185–187. https://doi.org/10.1080/00173134.2024.2347651.

Maher, B.A., 1998. Magnetic properties of modern soils and Quaternary loessic paleosols: paleoclimatic implications. Palaeogeogr. Palaeoclimatol. Palaeoecol. 137 (1–2), 25–54. https://doi.org/10.1016/s0031-0182(97)00103-x.

Malakhovsky, D.B., Sammet, E.Yu, 1982. Glacial outliers and glaciodislocations of the northwest Russian plain. Mater. Glaciol. Res. 44, 121–128.

Marks, L., 2015. Last deglaciation of northern continental Europe. Cuadernos de Investigación Geográfica 41 (2), 279–293. https://doi.org/10.18172/cig.2698.
Mazei, Y.A., Tsyganov, A.N., Bobrovsky, M.V., et al., 2020. Peatland development, vegetation history, climate change and human activity in the Valdai uplands (Central European Russia) during the Holocene: a multi-proxy palaeoecological study. Diversity 12 (12), 462. https://doi.org/10.3390/d12120462.
Mooney, S., Tinner, W., 2011. The analysis of charcoal in peat and organic sediments. Mires Peat 7, 1–18.
Moore, P.D., Webb, J.A., Collinson, M.E., 1991. Pollen Analysis. Blackwell Scientific Publications, Oxford.
Nosova, M., Severova, E., Volkova, O., 2017. A 6500-year pollen record from the Polistovo-Lovatskaya Mire System (northwest European Russia): vegetation dynamics and signs of human impact. Grana 56 (6), 410–423. https://doi.org/10.1080/00173134.2016.1276210.
Nosova, M.B., Novenko, E.Y., Severova, E.E., Volkova, O.A., 2019. Vegetation and climate changes within and around the Polistovo-Lovatskaya mire system (Pskov Oblast, north-western Russia) during the past 10,500 years. Veg. Hist. Archaeobotany 28, 123–140. https://doi.org/10.1007/s00334-018-0693-8.
Nosova, M.B., Mazei, N.G., Zakharov, A.L., Zazovskaya, E.P., 2024. Kosilovo mire (Toropets district, Tver region, north-western Russia). Grana 1–4. https://doi.org/10.1080/00173134.2024.2412108 (in press).
Novenko, E.Y., 2016. Vegetation and Climate Changes in Central and Eastern Europe in the Late Pleistocene and Holocene at Interglacial and Transitional Stages of Climatic Macrocycles. GEOS, Moscow (In Russian).
Novenko, E.Y., Olchev, A.V., 2015. Early Holocene vegetation and climate dynamics in the central part of the East European Plain (Russia). Quat. Int. 388, 12–22. https://doi.org/10.1016/j.quaint.2015.01.027.
Novenko, E.Y., Volkova, E.M., Nosova, M.B., Zuganova, I.S., 2009. Late Glacial and Holocene landscape dynamics in the southern taiga zone of the East European plain according to pollen and macrofossil records from the Central Forest State Reserve (Valdai Hills, Russia). Quat. Int. 207, 93–103. https://doi.org/10.1016/j.quaint.2008.12.006.
Novenko, E.Y., Tsyganov, A.N., Volkova, E.M., Babeshko, K.V., Lavrentiev, N.V., Payne, R.J., Mazei, Y.A., 2015. The Holocene paleoenvironmental history of central European Russia reconstructed from pollen, plant macrofossil, and testate amoeba analyses of the Klukva Peatland, Tula Region. Quat. Res. 83, 459–468. https://doi.org/10.1016/j.yqres.2015.03.006.
Novenko, E.Y., Tsyganov, A.N., Volkova, E.M., Kupriyanov, D.A., Mironenko, I.V., Babeshko, K.V., Utkina, A.S., Popov, V., Mazei, Y.A., 2016. Mid-and Late Holocene vegetation dynamics and fire history in the boreal forest of European Russia: a case study from Meshchera Lowlands. Palaeogeogr. Palaeoclimatol. Palaeoecol. 459, 570–584.
Novenko, E.Y., Mazei, N.G., Kupriyanov, D.A., Kusilman, M.V., Olchev, A.V., 2021. Peatland initiation in Central European Russia during the Holocene: effect of climate conditions and fires. Holocene 31 (4), 545–555. https://doi.org/10.1177/0959683620981709.
Özer, M., Orhan, M., Isik, N.S., 2010. Effect of particle optical properties on size distribution of soils obtained by laser diffraction. Bull. Eng. Geol. Environ. 16 (2), 163–173. https://doi.org/10.2113/gseegeosci.16.2.163.
PALDAT – database of palynological data. https://www.paldat.org. (Accessed 31 May 2024).
Patton, H., Hubbard, A., Andreassen, K., Auriac, A., Whitehouse, P.L., Stroeven, A.P., Shackleton, C., Winsborrow, M., Heyman, J., Hall, A.M., 2017. Deglaciation of the Eurasian ice sheet complex. Quat. Sci. Rev. 169, 148–172. https://doi.org/10.1016/j.quascirev.2017.05.019.
Pogoda i klimat. www.pogodaiklimat.ru. (Accessed 21 September 2024).
Potito, A.P., Woodward, C.A., McKeown, M., Beilman, D.W., 2014. Modern influences on chironomid distribution in western Ireland: potential for palaeoenvironmental reconstruction. J. Paleolimnol. 52, 385–404. https://doi.org/10.1007/s10933-014-9800-8.
Rdzany, Z., Frydrych, M., 2018. Record of glacial outburst floods in marginal zones and forelands of Scandinavian glaciations in Poland. Acta Univ. Lodz. Folia Geogr. Physica 17, 33–40. https://doi.org/10.18778/1427-9711.17.04.
Reimer, P., Austin, W., Bard, E., et al., 2020. The IntCal20 Northern Hemisphere radiocarbon age calibration curve (0–55 cal kB). Radiocarbon 62 (4), 725–757. https://doi.org/10.1017/rdc.2020.41.
Safronova, I.N., Yurkovskaya, T.K., Mikliaeva, I.M., Ogureeva, G.N., 1999. Zones and Types of Vegetation Zonation in Russia and Adjacent Territories. M. 1: 8 000 000. Moscow: TOO «EKOR».
Sapelko, T., Pozdnyakov, S., Kuznetsov, D., Ludikova, A., Ivanova, E., Guseva, M., Zazovskaya, E., 2019. Holocene sedimentation in the central part of Lake Ladoga. Quat. Int. 524, 67–75. https://doi.org/10.1016/j.quaint.2019.05.028.
Sapelko, T., Kalińska, E., Kuznetsov, D., Naumenko, M., Gałka, M., 2022. Holocene history of the lake and forest island ecosystem at and around Lake Seliger, Valdai hills (east European plain, Russia). Int. J. Earth Sci. 111 (6), 1947–1960. https://doi.org/10.1007/s00531-022-02210-4.
Savitzky, A., Golay, M.J., 1964. Smoothing and differentiation of data by simplified least squares procedures. Anal. Chem. 36 (8), 1627–1639. https://doi.org/10.1021/ac60214a047.
Schmid, P.E., 1993. A key to the larval Chironomidae and their instars from Austrian Danube region streams and rivers. Part 1: Diamesinae, Prodiamesinae and Orthocladiinae. Federal Institute for Water Quality, Vienna.
Spurk, M., Leuschner, H.H., Baillie, M.G., Briffa, K.R., Friedrich, M., 2002. Depositional frequency of German fossil oaks: climatically and non-climatically induced fluctuations in the Holocene. Holocene 12, 707–715.
Stankevich, YaV., 1953. Research of monuments of the first millennium of our era in the upper reaches of the Western Dvina for 1949-1951. Brief Communications of the Institute of the History of Material Culture, vol. 52. USSR Academy of Sciences, Moscow (In Russian).
Stivrins, N., Buchan, M.S., Disbrey, H.R., et al., 2017. Widespread, episodic decline of alder (*Alnus*) during the medieval period in the boreal forest of Europe. J. Quat. Sci. 32 (7), 903–907. https://doi.org/10.1002/jqs.2984.
Stivrins, N., Liiv, M., Heinsalu, A., Gałka, M., Veski, S., 2017a. The final meltdown of dead-ice at the Holocene Thermal Maximum (8500–7400 cal. yr BP) in western Latvia, eastern Baltic. Holocene 27 (8), 1146–1157. https://doi.org/10.1177/0959683616683255.
Sudakova, N.G., Antonov, S.I., 2021. Regional features of the geomorphological structure of the ancient glacial region in the center of the Russian Plain. Geomorfologiya 52 (1), 100–108. https://doi.org/10.31857/S0435428121010120 (In Russian).
Svendsen, J.I., Alexanderson, H., Astakhov, V.I., et al., 2004. Late Quaternary ice sheet history of northern Eurasia. Quat. Sci. Rev. 23, 1229–1271. https://doi.org/10.1016/j.quascirev.2003.12.008.
Tarasov, P.E., Webb III, T., Andreev, A.A., et al., 1998. Present-day and mid-Holocene biomes reconstructed from pollen and plant macrofossil data from the former Soviet Union and Mongolia. J. Biogeogr. 25, 1029–1053. https://doi.org/10.1046/j.1365-2699.1998.00236.x.
Tarasov, P.E., Savelieva, L.A., Long, T., Leipe, C., 2019. Postglacial vegetation and climate history and traces of early human impact and agriculture in the present-day cool mixed forest zone of European Russia. Quat. Int. 516, 21–41. https://doi.org/10.1016/j.quaint.2018.02.029.
Tarasov, P.E., Savelieva, L.A., Kobe, F., Korotkevich, B.S., Long, T., Kostromina, N.A., Leipe, C., 2022. Lateglacial and Holocene changes in vegetation and human subsistence around Lake Zhizhitskoye, East European midlatitudes, derived from radiocarbon-dated pollen and archaeological records. Quat. Int. 623, 184–197. https://doi.org/10.1016/j.quaint.2021.06.027.
Tauber, H., 1967. Investigations of the mode of pollen transfer in forested areas. Rev. Palaeobot. Palynol. 3 (1–4), 277–286.
ter Braak, C.J., Juggins, S., 1993. Weighted averaging partial least squares regression (WA-PLS): an improved method for reconstructing environmental variables from species assemblages. In: Proceedings of the Twelfth International Diatom Symposium, Renesse, the Netherlands. Springer, Dordrecht, pp. 485–502.
The Global Pollen Project. The Open Platform for Pollen Identification https://globalpollenproject.org (Accessed January 2023 – June 2024).
Tishkov, A.A., Gracheva, R.G., Konstantinov, E.A., Samus, A.V., 2023. The key section of the Valdaian peat bog as a source of paleoecological and paleoclimatic information. Doklady Rossijskoj akademii nauk. Nauki o Zemle 509 (1), 105–113. https://doi.org/10.1134/S1028334X22601870.
Velichko, A.A. (Ed.), 2009. Paleoclimates and Paleoenvironments of Extra-tropical Regions of the Northern Hemisphere. Late Pleistocene—Holocene. Atlas-Monograph. GEOS, Moscow (In Russian).
Velitchko, A.A., lsayeva, L.L., Oreshkin, D.B., Faustova, M.A., 1989. The last glaciation of Eurasia. In: The Arctic Seas: Climatology, Oceanography, Geology, and Biology. Springer US, Boston, MA, pp. 729–758. https://doi.org/10.1007/978-1-4613-0677-1_26.
Wohlfarth, B., Tarasov, P., Bennike, O., Lacourse, T., Subetto, D., Torssander, P., Romanenko, F., 2006. Late glacial and Holocene palaeoenvironmental changes in the rostov-yaroslavl' area, west Central Russia. J. Paleolimnol. 35, 543–569. https://doi.org/10.1007/s10933-005-3240-4.
Zaretskaya, N.E., Hartz, S., Terberger, T., Savchenko, S.N., Zhilin, M.G., 2012. Radiocarbon chronology of the Shigir and Gorbunovo archaeological bog sites, middle Urals, Russia. Radiocarbon 54, 783–794. https://doi.org/10.1017/s0033822200047433.
Zazovskaya, E., Mergelov, N., Shishkov, V., Dolgikh, A., Miamin, V., Cherkinsky, A., Goryachkin, S., 2017a. Radiocarbon age of soils in oases of East Antarctica. Radiocarbon 59 (2/1), 489–503. https://doi.org/10.1017/RDC.2016.75.
Zazovskaya, E., Shishkov, V., Dolgikh, A., Alexndrovskiy, A., Skripkin, V., Chichagova, O., 2017b. Organic matter of cultural layers as a material for radiocarbon dating. Radiocarbon 59 (6/2), 1931–1944. https://doi.org/10.1017/RDC.2017.134.

Appendix 4 (Manuscript)

Bakumenko, V., Lanka, A., Poska, A., Vassiljev, J., Alliksaar, T., Heiri, O., Belle, S., Veski, S. (Manuscript). A 14 500 - year multi-proxy reconstruction of climate and environment change in eastern Baltics: case study from Southern Estonia. Maniscript is under review in: Quaternary Science Reviewes.

A 14 500-year multi-proxy reconstruction of climate and environmental change in Eastern Baltics

Varvara Bakumenko[a*], Anna Lanka[a], Anneli Poska[a,b], Jüri Vassiljev[a], Oliver Heiri[v], Simon Belle[d], Tiiu Alliksaar[a], Siim Veski[a]

[a] Department of Geology, Tallinn University of Technology, Ehitajate tee 5, 19086, Tallinn, Estonia

[b] Department of Physical Geography and Ecosystem Science, Lund University, Lund, Sweden

[c] Department of Environmental Sciences, University of Basel, Basel, Switzerland

[d] Department of Aquatic Sciences and Assessment, Swedish University of Agricultural Sciences, Uppsala, Sweden

[*]varvara.bakumenko@taltech.ee

Keywords: Paleolimnology, Cladocera, Chironomidae, pollen, continentality

Abstract

This study presents a 14,500-year high-resolution multi-proxy reconstruction of past climate and environmental changes from Lake Nakri in Southern Estonia. Estonia's geographical position at the intersection of maritime and continental climate zones and boreal and nemoral biomes makes it a highly suitable location for studying past small climate fluctuations. We used Cladocera, Chironomidae, pollen, and loss-on-ignition analyses to reconstruct mean July air temperatures, explore changes in continentality expressed in annual temperature range (ATR), to track environmental changes (trophy, pH, etc.) and lake ecosystem dynamics throughout the late glacial and Holocene. Using Cladocera remains to infer past changes in nutrient status, we found no evidence of significant shifts. Therefore, we conclude that the chironomid-based reconstruction was not biased by such changes. Chironomidae and pollen analysis results were used to reconstruct July air temperatures. The reconstruction curves are coherent and consistently reveal climate events, happened around the 8.2 ka, 7.5 ka, 5.5 ka cold events, Medieval Warm Period, and Little Ice Age. The exception to the otherwise consistent proxy pattern is that Chironomidae data reveal an earlier onset of Early Holocene

warming compared with the pollen record. This discrepancy may be attributed to low local pollen productivity and delayed postglacial vegetation development. The chironomid-based reconstructions show that the Younger Dryas climate was marked by a 3°C drop in summer temperature and increased ATR. The chironomid-based continentality (difference in summer and winter temperatures) reconstruction approach is still under development. We have produced the first tentative chironomid-inferred ATR reconstruction showing trends similar to ones already published. The resulting reconstructions provide critical insights into past regional climate variability and ecosystem responses in eastern temperate-boreal ecotones. New climate curves can serve as a reference for future regional climate studies.

1. Introduction

Transitional regions, characterized by changing climates and biomes, are particularly sensitive to climate variability (Fu, 1992). The Eastern Baltic region exemplifies such a transitional zone, lying along the north-south gradient between boreal and temperate vegetation zones and exhibiting a pronounced west-east shift from oceanic to continental climates (Team, 2008; Heikkilä and Seppä, 2010; Edvardsson et al., 2016). Furthermore, Stonevicius et al. (2018) reported significant change in continentality expressed in annual temperature range (ATR) over the last 50 years. Given that recent climate change in Europe has already led to warmer temperatures and reduced precipitation during the growing season—and these trends are expected to continue—it is important to understand how such changes may impact sensitive ecosystems in transitional climate zones.

Pollen are excellent indicators of regional and local land cover and human impact changes and are one of the most commonly used proxies in past climate reconstructions (Ilyashuk et al., 2009; Salonen et al., 2012; Chevalier et al., 2020), as well as the most abundant type of climate reconstruction in the region (e.g. (Niinemets and Saarse, 2009; Poska et al., 2022; Saarse and Veski, 2001; Seppä and Poska, 2004), with just a few examples of usage of other biotic proxies (Heiri et al., 2014; Stansell et al., 2017; Druzhinina et al., 2020; Šeirienė et al., 2021). However, for Quaternary climate reconstruction in northern and eastern Europe the method also has some limitations. For instance, it has been shown that immigration of plants after deglaciation may lag climate change (Väliranta et al., 2015), and some intervals, such as the Younger Dryas, may presently have no analogues in modern vegetation (Magny et al., 2001). Furthermore, boreal forest can be resistant to minor climate

changes (Stralberg et al., 2020) implying that pollen-based climate reconstructions in the boreal region may not be sensitive to minor changes. Therefore, there is an urgent need for long-term multi-proxy climate and environmental reconstructions using independent climate proxies in Northern Europe and particularly in the Eastern Baltic region, where such studies are currently lacking.

Subfossil chironomids, non-biting midges from the family Chironomidae, are widely used as a proxy to reconstruct past July air temperatures (Tóth et al., 2015; Hájková et al., 2016; Jiménez-Moreno et al., 2023; Rigterink et al., 2024), and have revealed some potential for continentality changes assessment (Self et al., 2011). Even though the relationship between continentality and chironomids remains poorly understood, there are some possible mechanisms which could explain it. Continentality can provide indirect effects on aquatic zoobenthos by altering the timing and length of the growing season (Nishimura & Laroque, 2011), shifting the timing of water turnover (Butcher et al., 2015), and influencing ice-cover duration, which in turn affects both pH (Preston et al., 2016) and dissolved oxygen levels (Zdorovennova et al., 2021). Chironomids are known to be sensitive to changes in in-lake factors, such as pH, dissolved oxygen concentrations and trophic state (Brooks et al., 2001; Luoto, 2011; Nazarova et al., 2011; Ursenbacher et al., 2020). Therefore, it is helpful to account for these potential confounding influences using complementary proxies to support chironomid-based climate reconstructions. Cladocera analysis is a well-established palaeolimnological method for detecting past environmental changes within lakes (Van Damme and Kotov, 2016; Pastukhova et al., 2024), as cladocerans are sensitive to changes in lake water pH, trophic state and conductivity (Lanka et al., 2024; Zawiska et al., 2025) as well as lake water depth (Wang et al., 2024). Loss-on-ignition (LOI) is commonly used in the multi-proxy research (Hamerlík et al., 2016; Yao et al., 2017; Sapelko et al., 2019), provides data on the organic and inorganic carbon content of sediments and can be used a waterbody trophic state evaluation. Combining chironomid-, pollen-, cladoceran- and loss on ignition analysis results will allow us to produce critical quantitative and qualitative palaeoecological datasets often used to complement Chironomide-based palaeoclimate reconstructions (Lotter et al., 1997; Mirosław-Grabowska et al., 2015; Veski et al., 2015; Druzhinina et al., 2020; Šeirienė et al., 2021).

We selected the Lake Nakri (Southern Estonia) palaeo-sequence, which covers the last 14.5 ka cal BP—from the time of ice retreat to the present day— to perform the palaeo-environment reconstruction using Chironomidae, Cladocera, pollen and LOI analysis and compared the results other records from eastern and northern Europe. The objectives of the

current study is to (I) present a new high-resolution multiproxy based palaeolimnological record from Eastern Baltic region (II) reconstruct the late glacial and Holocene climate and environmental dynamics (III) compare the responses of different proxies in respect to July air temperature, annual temperature range and environment changes, and (IV) evaluate the reconstructed fluctuations within the framework of known regional and global climatic and environmental changes.

The outcome of this paper contributes to our overall understanding of past global climate change patterns, produces a novel high resolution environmental change record for the Baltic region, and documents the response of local environments and ecosystems to changing climate aiding in assessments of the potential effects of future changes. The resulting climate reconstructions have the potential to serve as a reference for Eastern Europe.

2. Study site description

Lake Nakri (0.9 ha, 48.5 m a.s.l., 57° 53.703′ N, 26° 16.389′ E), is situated in Southern Estonia (Fig. 1). It is a small shallow (up to 3 m depth) lake with ca 0.25 km^2 catchment area. Based on modern limnological measurements and observations, Lake Nakri has been classified as an eutrophic lake (Secchi depth 1.6 m) with slightly alkaline pH (Lanka et al., 2024) and brownish water color. The lake has a low swampy shoreline and is surrounded by natural mixed spruce-pine dominated boreal forest with fairly low modern land use in catchment. With an average annual air temperature of 5.5°C, mean July temperature of 18°C, mean January temperature of −4°C, and annual precipitation of 675 mm, the region exhibits climatic conditions that are transitional between oceanic and continental climates (Estonian Environment Agency).

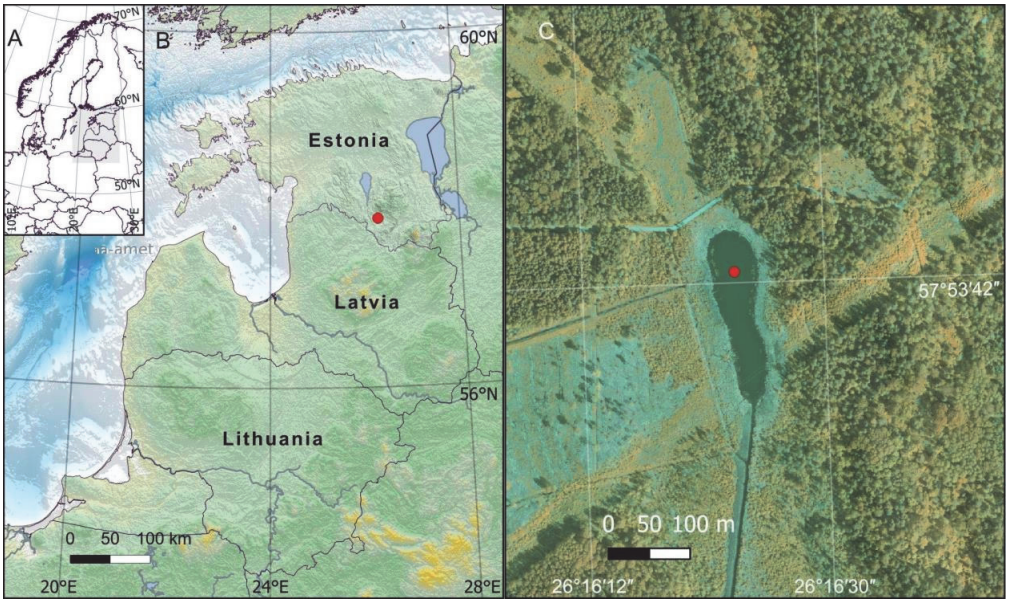

Fig.1 - Overview map (A) and EOTOPO 2022 map (NOAA National Centers for Environmental Information, 2022) of the eastern Baltic (B) and false-color forestry orthophoto (Republic of Estonia Land and Spatial Development Board, 2025) for Lake Nakri (C). Red dot marks the sampling point.

3. Methods

3.1. Sampling strategy

Parallel overlapping sets of 1 m long segments of the lake sediment sequence, covering 1346 cm, were taken using a Russian corer. The coring was conducted from the deepest part of the lake in 2007, 2009 and 2018. The uppermost 58 cm unconsolidated sediments were retrieved with a Wilner sediment sampler. Sediment cores were correlated according to loss-on-ignition curves and radiocarbon dates. Samples for analysis from depths of 0–587 cm were taken from the 2018 core, while deeper samples were obtained from the 2007 and 2009 cores..

The core was described and photographed in the field and subsequently transported to the laboratory for further analysis and documentation. The full sediment sequence (0—1346

cm) was sampled for pollen analysis (163 samples), Chironomidae analysis (149 samples), and LOI analysis (1340 samples). The upper part of the core (0—1028 cm) was also analysed for Cladocera communities (68 samples). Samples for all types of analysis were taken from the same levels if possible.

Lower part of the sequence covering 14.0-9.0 ka cal BP has been published in detail by Amon et al. (2012, 2014).

3.2. Chronology

The chronology of the Lake Nakri sediments was established by the OxCal 4.4 deposition model (Bronk Ramsey, 2009; Ramsey, 2008), where lithological boundaries, coring time (top of the sediment), radiocarbon dating and age determinations derived from spheroidal fly ash particle (SFAP) analysis (Renberg and Wik, 1985; Alliksaar, 2000; Heinsalu et al., 2007) were used. The radiocarbon ages were determined at the Poznan Radiocarbon Laboratory in Poland. The radiocarbon dates were calibrated using the IntCal20 calibration curve (Reimer et al., 2020). For radiocarbon dating, terrestrial plant macrofossils (mainly small branches, *Dryas* leaves, and *Betula* catkin scales). Levels lacking macrofossils were dated using bulk sediment samples.

SFAPs, incomplete combustion products of high-temperature fossil-fuel burning emitted to the environment with flue-gases, are successfully used for dating sediments of post-industrial era (Renberg and Wik, 1985; Rose, 2002). The method has been well-established for Estonia since the beginning of the 20th century (Alliksaar, 2000). Heinsalu et al. (2007) show that the SFAP analysis determined ages are in good correlation with the ^{210}Pb based ages. To count SFAP in sediments the subsamples were subject to sequential pre-treatment with 30% H_2O_2 and 2,7M HCl to remove organic and carbonate matter. The SFAP were counted under the light microscope at 250x magnification together with added Lycopodium spores to calculate SFAP concentration in sediments. The SFAP analysis derived ages were used for the upper 50 cm part of the sediment. The lower part of the sediment was dated by the radiocarbon method.

All ages used in this study are given as median calibrated kiloannum before 1950 CE (ka cal BP). The zonation of all presented proxies follows the formal tripartite subdivision of the Holocene (Walker et al., 2012).

3.3. Lithostratigraphy

To reconstruct changes in sediments organic matter dynamics, organic, carbonate and mineral matter contents of the sediment was determined by loss-on-ignition (LOI) analysis procedure described by Heiri et al. (2001). Measurements were performed on continuous 1 cm thick sediment samples of 1 cm^3 volume. The sediment samples were dried for 24 hours at 105 °C and then burned for 4 hours at 525 °C to determine organic matter (OM) content. The residue was thereafter burned for 2 hours at 950 °C and the weight loss was multiplied by 1.36 to express the amount of carbonaceous matter as carbonate ions (CO_3^{2-}) content (Bengtsson and Enell, 1986). The remaining fraction was deemed as mineral matter.

3.4. Pollen analysis

To reconstruct terrestrial land cover and July air temperatures, pollen analysis was applied. Pollen subsamples of known volume (0.5 cm^3 in the Holocene and 2 cm^3 in the late glacial) and thickness (1 cm) were taken at 5–10 cm intervals. Pollen sample preparation followed a standard acetolysis method (Berglund and Ralska-Jasiewiczowa, 1986) combined with hot HF treatment with 40% and 75% acids to remove inorganic matter (Bennett and Willis, 2001). Lycopodium spores were added to calculate pollen concentration and subsequently the pollen accumulation rate (PAR) (Stockmarr, 1971). At least 500 terrestrial pollen grains were counted at each subsample level, except for the four lowest level samples, where only about 200 grains were observed due to low pollen concentrations. Pollen data were expressed as percentages of the total terrestrial pollen sum. Counts of spores, green algae, charcoal, and other microfossils were calculated as percentages of the total sum of terrestrial pollen.

3.5. Cladocera analysis

To reconstruct lake environmental parameters (trophic state, pH, water depth fluctuations), Cladocera analysis was applied. Sediment subsamples of known volume (1 cm^3) and thickness (1 cm) were taken from the sediment core with an interval of 10-20 cm. Samples for subfossil Cladocera analysis were prepared according to standard procedure (Frey, 1986), heating them for 30 minutes in 10% KOH solution at 85 °C water bath. Afterwards samples were filtered through a sieve with a mesh size of 40 µm and thereafter remains were diluted with 10 ml of water and coloured with Safranin O.

198 Microscope slides were prepared from 100 µl of the diluted, homogenized subsample
199 and examined under a light microscope at 100x-400x magnification. We examined as many
200 slides as was necessary to find at least 70 subfossil Cladocera individuals and examined one
201 extra slide for each sample to identify any previously undetected species (Kurek et al., 2010).
202 Subfossil Cladocera species were identified based on the key by Szeroczynska and Sarmaja-
203 Korjonen (2007). *Daphnia* spp. and *Ceriodaphnia* spp. remains were dominated by
204 postabdominal claws, from which it can be difficult to distinguish between these two groups.
205 Therefore, they were merged under the *Daphnia* spp. group. *Alona gutatta* and *Coronatella*
206 *rectangula* were counted as separate species based on the postabdomen findings but merged
207 in group *C. rectangula*/*A. gutatta* if the head shields or shells were found.

208 ## *3.6. Chironomidae analysis*

209 To reconstruct July air temperatures, ATR and environmental changes (trophy, water
210 level fluctuations), Chironomidae analysis was applied. Chironomidae subsamples of
211 standardized volume (1 cm^3) and thickness (1 cm) were taken at 10 cm intervals. Subsamples
212 were treated according to standard procedures (Brooks et al., 2007). Sediments were water-
213 sieved with a 100-µm mesh size sieve to remove fine particles. In case coarse sediment
214 particles remained, additional deflocculation in the hot KOH (70 °C) for 10 minutes was
215 applied. After deflocculation the sample was water-washed on the 100-µm mesh size.
216 Further, each sample was transferred into a Petri dish from which Chironomidae head
217 capsules were collected with fine forceps under a stereomicroscope at 25X magnification.
218 The obtained head capsules were air-dried and mounted in Aquatex® mounting medium.
219 Taxonomic identification was conducted under the light microscope at 100x–400x
220 magnification. The Nakri lake fossil Chironomidae assemblages' collection is stored in
221 Tallinn University of Technology.
222 Identification of the Chironomidae subfossil head capsules was done by OH (late
223 glacial-early Holocene) and VB (Holocene) with 0.5 ka cal BP (3 samples) of overlap using
224 the same taxonomic approximation according to Brooks et al. (2007) and using identification
225 keys by Klink and Pillot (2003), Andersen et al. (2013) and Larocque-Tobler (2014). All
226 identifications at genus or subfamily taxonomic level (Tanytarsini, *Tanytarsus* spp.,
227 *Paratanytarsus* spp., Tanypodinae, Chironomini, Orthocladiinae) were excluded from the
228 Nakri lake dataset to avoid including broad groups of Chironomidae species with different
229 ecological preferences. *Cricotopus intersectus*-type was merged with *Cricotopus laricomalis*-

type into one type due to the high chance of misidentification of these morphotypes. Morphotype-level identifications for the genera *Ablabesmyia*, *Einfeldia*, *Zalutschia*, *Eukiefferiella*, and *Dicrotendipes* were combined into their respective genus-level groups to align with the varying identification resolutions used elsewhere.

3.7. Training sets for the climate reconstruction

Pollen-based July mean air temperature reconstruction was done based on the modern pollen-climate analogue dataset described by Seppä and Birks (2001).

Chironomid-based mean July air temperature reconstruction proceeded using two training sets: a region specific Finno-Baltic-Polish (FBP) dataset described in detail in Bakumenko et al. (2024) and a Swiss-Norwegian dataset (Heiri et al., 2011), that has been widely used across Europe for reconstructing late Quaternary July air temperature change (e.g. Oliver Heiri et al., 2014; Lapellegerie et al., 2024). Comparing the performance of the two training sets will help determine whether a local training set improves the accuracy of chironomid-based climate reconstructions.

A novel tentative reconstruction of chironomid-based continentality, expressed as ATR (difference in the mean temperature of the coldest and the warmest months) was performed using FBP training seta. The geographic area of the training set includes clear ATR gradient (18.6–27.1 ºC; Fig. 2) as well as a mean July air temperature one (12.1–19.2 ºC; Fig. 2). Moreover, gradients of these climate variables are distributed in different patterns across the region (Fig. 2). While July air temperature continuously increases from North to South, ATR has the highest values in the central Fennoscandia and decreases towards the seas. This difference in distribution makes it potentially possible to calibrate the TS for mean July temperature and ATR independently and separate signals from these two variables.

Modern climate data for the samples in the FBP chironomid calibration dataset sites was extracted from the ERA5 dataset with hourly temporal and 0.25° x 0.25° spatial resolution (Hersbach et al., 2020), downloaded as July and January months mean temperature in °C from the Copernicus Climate Data Store

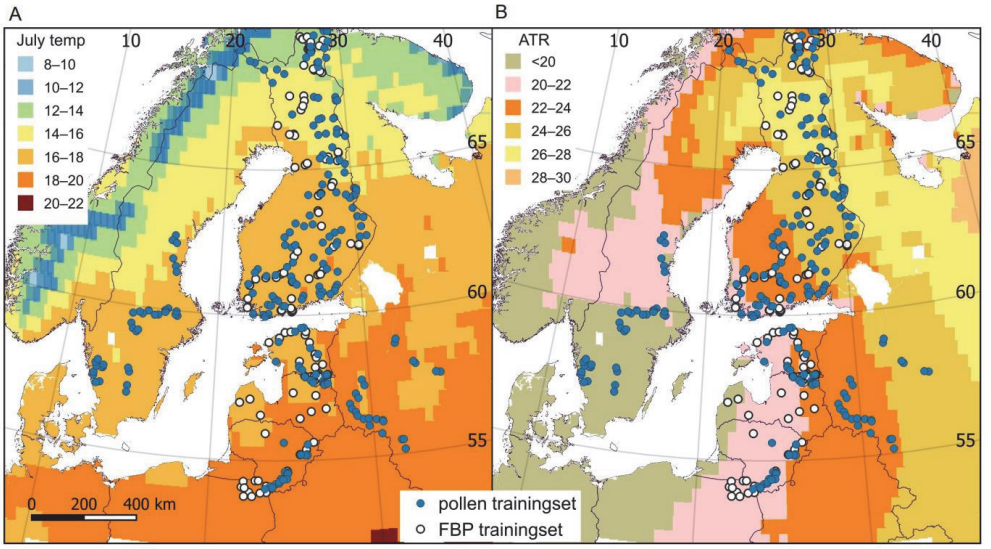

Fig. 2. Location of pollen and Finno-Baltic-Polish (FBP) chironomid training sets. Maps display July mean air temperature (Hersbach et al., 2020) and annual temperature range (ATR).

3.8. Data analysis

Cladocera were grouped based on their habitat preference according to Bledzki and Rybak (2016). Redundancy analysis (RDA; Birks et al., 1997) was used to test the influence of ATR on the Chironomidae assemblages of the FBP training set.

Principal Component Analysis (PCA) was applied to the fossil assemblages of Chironomidae, pollen, and Cladocera to identify potential drivers of assemblages patterns. Pearson correlations were used to examine the relationships between the first two PC axes of each proxy and with other environmental indicators, including LOI, herbs percentages in the pollen spectra, oxygen isotopes inferred from the Greenland ice sheet (GRIP; Rasmussen et al., 2023) and Cladocera *Bosmina longirostris* as an additional marker of trophic change.

The weighted averaging–partial least squares (WA-PLS) regression and calibration (ter Braak and Juggins, 1993) with bootstrapping (9999 permutations; Birks and Birks, 1998) was used for both pollen and chironomid-based climate reconstructions. The best transfer functions were selected as those producing the lowest cross-validated root mean squared error of prediction (RMSEP). The values of R^2, root mean squared error (RMSE), and both

maximum and average bias were used to assess the reliability of the interpolation model. The WA-PLS coefficients for the best performing component of FBP-based reconstruction were used to divide climate dependent Chironomidae taxa, according to Brooks et al. (2007) and Bakumenko et al. (2024), into three groups (typical for cold, moderate, and warm conditions) in respect to the mean July air temperature. The rare taxa deletion (abundance more than 2% at least in one sample) was done for Lake Nakri chironomid assemblages to reduce the influence of random appearances and to increase performance of the WA-PLS (Walker, 2001).

Software program R version 4.1.1. was used to perform numerical analysis and plots. The following packages were used: 'tidyverse' for data visualisation (Wickham et al., 2019), 'dplyr' for data restructuring and basic calculations (Wickham et al., 2022), 'vegan' for ordination (Oksanen et al., 2022). The program C2 (Juggins, 2003) was used to perform pollen- and chironomid-based reconstructions. Stratigraphic diagrams were prepared in Tilia 3.0.1 software.

4. Results

4.1. Litho- and chronostratigraphy

Lake Nakri age-depth model (Fig. 3) is based on 17 radiocarbon dates (Table 1). Radiocarbon date Poz-124700 is considered too old according to SFAP analysis derived ages and not used in the age-depth model. Radiocarbon dates Poz-124704 and Poz-124705 from the bulk sediment are not used in the age-depth model as there are nearby dated macro remains which are preferred; however the omitted dates show similar ages with dated macro remains. The ages for the uppermost sediments were corrected according to the SFAP analysis derived ages, so that 30 cm depth corresponds to 1950±5 CE.

The lowermost part of the sequence (1346–952 cm; 14–11.5 ka cal BP), roughly coinciding with the late glacial, is composed of silt and silty clay with mineral content about 77–91%. There is an increase of organic matter content (up to 7%) in the depth interval 1190–1154 cm (about 13.4–12.8 ka cal BP) (Fig. 3). The Holocene part of the sequence starts with detritius gyttja (952–930 cm; 11.5–10.8 ka cal BP) where organic matter content increases from 8 to 30%, overlain with distinctly laminated gyttja (930–897 cm; 10.8–10.5 ka cal BP). The uppermost part (897–0 cm) of the sediments is homogeneous gyttja with

increasing content of organic matter (up to 60%). Carbonate content is fluctuating but does not in general exceed 20% throughout the sediment sequence (Fig. 3).

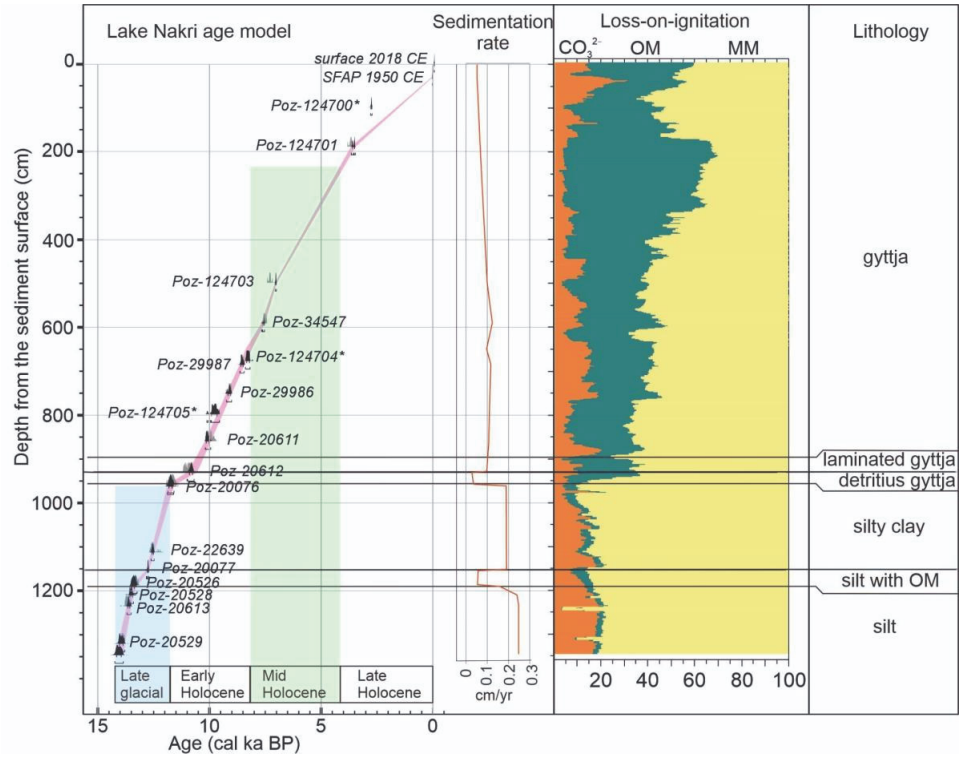

Fig. 3. Lake Nakri age-depth model at 95% probability range (pink curve), sedimentation rate, loss-on-ignition and lithology. The graphs on the age-depth curve show the likelihood (gray) and posterior (black) probability distribution of the calibrated radiocarbon dates. Radiocarbon dates with * are not used in the model.

Table 1 - Lake Nakri ^{14}C dates. * marks the outliers not used in the age-depth model.

Depth from the sediment surface cm	Lab code	^{14}C age yr BP	Calibrated ages cal yr BP at 95.4%	Calibrated ages cal yr BP median	Dated material
98-99	Poz-124700*	2625±30	2590–2490	2540	gyttja

188-189	Poz-124701	3420±35	3730–3560	3630	gyttja
498-499	Poz-124703	6370±40	7060–6990	7030	gyttja
591	Poz-34547	6620±35	7670–7530	7570	wood
682-683	Poz-124704*	7440±50	8380–8170	8260	gyttja
685	Poz-29987	7760±50	8640–8440	8550	wood (branch)
751	Poz-29986	8150±50	9240–9010	9110	bark, seeds, catkins
797-798	Poz-124705*	8770±50	10120–9550	9770	gyttja
859	Poz-20611	8870±50	10190–9940	10100	wood, seeds, catkins
931	Poz-20612	9610±60	11020–10680	10810	seeds, catkins
962	Poz-20076	10150±50	11890–11600	11750	wood
1112.5	Poz-22639	10510±60	12610–12470	12540	wood
1152	Poz-20077	10800±40	12830–12710	12750	wood
1187	Poz-20526	11430±70	13470–13240	13360	plant macro
1210	Poz-20528	11660±70	13600–13400	13510	plant macro
1235	Poz-20613	11810±80	13700–13510	13610	Dryas leaves

1320	Poz-20529	12060±70	14080–13790	13950	plant macro

4.2. Pollen analysis

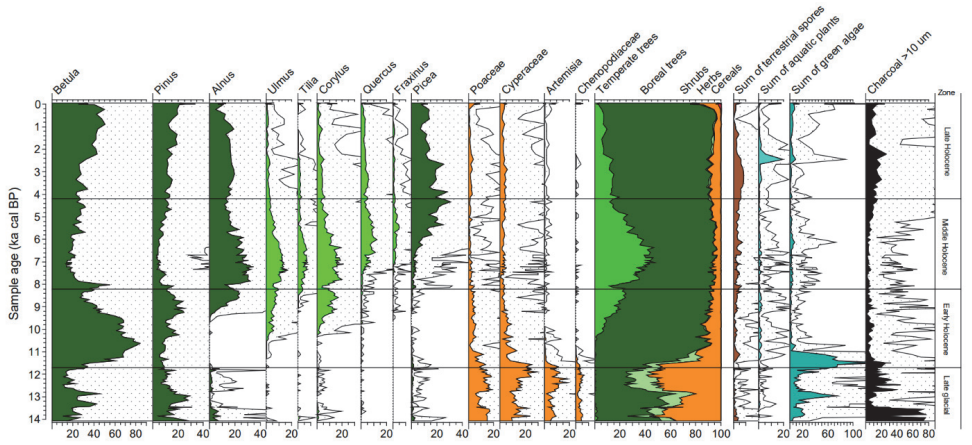

Fig. 4. Subfossil pollen diagram of selected taxa. The relative abundance of taxa is expressed in %. The abundance of charcoal particles is expressed in % of charcoal particles against pollen total sum.

108 microfossil types were identified in Lake Nakri pollen record (Fig. 4). Late glacial is characterised by high herb pollen values and has considerable input of redeposited temperate broadleaved tree pollen. Between 13.5–12.85 ka cal BP the amount of redeposited pollen is lower, and cold tolerant trees like *Betula* (birch) and *Pinus* (pine) expand. The local presence of both is confirmed by finds of *Pinus* stomata and *Betula* macrofossils from the same sediment interval (Amon et al., 2012).

The tree succession at the beginning of the Early Holocene is typical for the area – first *Betula* and then *Pinus* culminate. The first thermophilous trees *Ulmus* (elm) and *Corylus* (hazel) appear ca. 1000 years later. *Alnus* (alder) expands rapidly all over Estonia around 9.5 ka cal BP. Just before the end of Early Holocene ca 8.5 ka cal BP *Tilia* (lime) expands, and the amount of temperate broadleaved trees rises rapidly just to collapse at the Early Holocene – Middle Holocene boundary around 8.2 ka cal BP. The 8.2 ka cooling event is very clear in Lake Nakri pollen data: most of the broadleaved trees alongside with *Alnus* and *Corylus* show a clear drop in relative abundances, *Betula* in contrast flourishes.

During the Middle Holocene the temperate broadleaved trees maximum (up to ca 45%) is visible around 8–6 ka cal BP, showing the typical succession for Estonia with subsequent culminations of *Ulmus*, *Tilia*, *Quercus* (oak) and *Fraxinus* (ash). *Picea* (spruce) expands during the second half of the Middle Holocene and culminates around 4.2 ka cal BP. Low amount and taxonomic richness of herb pollen indicates dense forest cover. Still, first scattered finds of cultivated plants (*Triticum* (wheat) and *Hordeum* (barley)) accompanied by well-known anthropohores like *Plantago lanceolata* (narrowleaf plantain) and an increase in charcoal appear since 5 ka cal BP.

During the Late Holocene, the vegetation was characterized by mixed boreal forests dominated by *Betula*, *Pinus*, *Alnus*, and *Picea*, with a noticeable decline in temperate broadleaved trees. The weak signs of anthropogenic deforestation in the surroundings of Lake Nakri are observable as a slight increase in herb pollen and its taxonomic diversity since 1 ka cal years BP. Sporadic presence of cultivated plants (*Secale* (rye), *Hordeum*, *Triticum* and *Cannabis* (hemp)) suggests small-scale arable farming in the largely natural vicinity of Lake Nakri.

4.3. Cladocera analysis

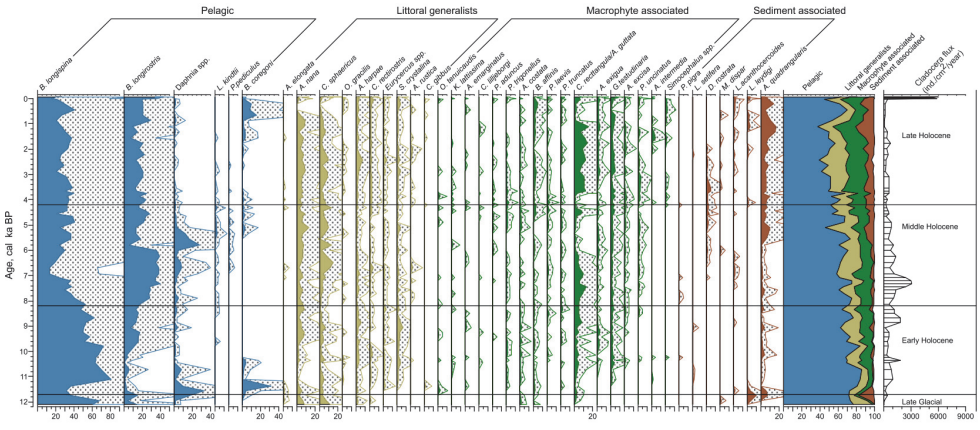

Fig. 5. Subfossil Cladocera diagram of selected taxa. The relative abundance of taxa is expressed in %.

In total 49 cladocera species were identified within the core, with *Bosmina longispina* and *Bosmina longirostris* as the main dominant species (Fig. 5).

The late glacial period is characterised by low total cladocera flux, and changing species composition as in almost each sample a new dominant species emerges.

In the Early Holocene *B. longispina* is the dominant species and several new macrophyte associated species appear. In the Middle Holocene between 8 and 6 ka cal BP *Bosmina longirostris* became the dominant species and an increase of Cladocera flux can be observed. About 5.5 ka cal BP *B. longirostris* is replaced by *Daphnia* spp. as the dominant species.

At the end of the Middle Holocene and throughout the Late Holocene *B. longispina* and *B. longirostris* dominate. The relative abundance of sediment associated species increases, but that seems to be mainly connected to the increase of *Alona quadrangularis* relative abundances. We also observed a slight increase in the relative abundances of macrophyte associated species. Within the last millennium there seems to be a time period, where Cladocera flux reduces almost to the late glacial level, and several species for a time disappear, just to re-appear in the uppermost sediment layers. The highest Cladocera flux was observed in the few uppermost sediment samples that correspond with the time period from 1950 CE forward.

While most of the species appear throughout the core, there are some that seem to be present in some periods and missing in others. Most of the littoral species appear for the first time at the beginning of the Holocene. Species that appear during late glacial and beginning of the Early Holocene but then disappear until the end of Middle Holocene are *Bosmina coregoni, Leydigia leydigi* and *Alona intermedia*. *Alonopsis elongata* appears in almost every sample of late glacial and beginning of the Early Holocene but afterwards appears rather sporadically. *Leptodora kindtii, Polyphemus pediculus,* and *Disparalona rostrata* are predominantly found in the Middle Holocene, with their presence also marking the transition periods at the end of the Early Holocene and the beginning of the Late Holocene.

Species that mostly appear in the Middle Holocene and the Late Holocene are *Alona rustica* and *Leydigia acanthocercoides* and the most characteristic taxon for the Late Holocene is *Simocephalus* spp..

4.4. Chironomidae analysis

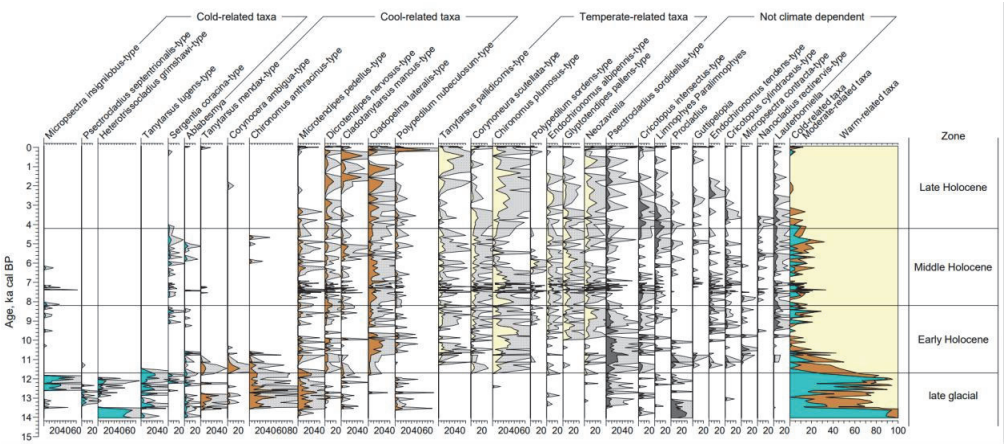

Fig. 6. Subfossil Chironomidae diagram of selected taxa. The relative abundance of taxa is expressed in %. Taxa are sorted by the corresponding WA-PLS coefficients for component 1 of the Finno-Baltic-Polish training set.

44 chironomid head capsules were counted per sample on average with the counting range 30–127 (38 samples counts were under 50). 155 chironomid taxa were identified in the Lake Nakri sequence (Fig. 6), from which 94 taxa were left after rare species removal.

The late glacial period is characterised by the dominance of the widely distributed *Microtendipes pedellus*-type, *Tanytarsus mendax*-type and *Chironomus anthracinus* which were assessed as cool-climate related taxa. Cold-related taxa abundant in the late glacial period include *Tanytarsus lugens*-type, *Psectrocladius septentrionalis*-type, *Micropsectra insignilobus*-type and *Heterotrissocladius grimshawi*-type (overall dominant at 13.5–14.5 ka cal BP). Also, not climate dependent *Procladius* and *Psectrocladius sordidellus*-type and *Cricotopus intersectus*-type were presented.

Throughout the Early Holocene period, cool-related *Dicrotendipes nervosus*-type and *Cladopelma lateralis*-type and temperate-related *Chironomus plumosus*-type and *Corynoneura scutellata*-type are present, as well as generalistic *Psectrocladius sordidellus*-type and *Cricotopus intersectus*-type. Cold-related *Tanytarsus lugens*-type appeared only at the start of the zone. temperate-related *Glyptotendipes pallens*-type, *Neozavrelia* and *Endochironomus albipennis*-type dominate since 10 ka cal BP.

In the Middle Holocene period taxa composition is similar to the Early Holocene one, but with increased counts of cool-related *Cladotanytasus mancus*-type and temperate-related *Polypedilum sordens*-type, as well not climate dependent *Lauterborniella* and *Nanocladius*

rectinervis-type. Also, here cold-related *Sergentia coracina*-type and *Micropsectra insignilobus*-type reappear at low abundances.

The Late Holocene period is marked by peaks of temperate-related *Chironomus plumosus*-type, *Neozavrelia, Tanytarsus pallidicornis*-type and cool-related *Cladopelma lateralis*-type, *Cladotanytarsus mancus*-type. Cool-climate related *Polypedilum nubeculosum*-type becomes overwhelmingly dominant around 0.5 ka cal BP. Cold-related taxa are almost not present in the Late Holocene. Not climate dependent *Psectrocladius sordidellus*-type and *Cricotopus intersectus*-type increased.

4.5. Climate models performance and reconstructions

The chironomid-based July air temperature reconstruction of the Lake Nakri sequence showed similar trends and performance values based on two different training sets (FBP, Swiss-Norwegian; Table 2), although the FBP-based one revealed the smallest error of reconstruction ($RMSEP_{boot}$ = 0.7 °C). Dicrotendipes, Endochironomus, Cladopelma morphotypes were grouped together for Swiss-Norwegian TS-based reconstruction, accounting to following average abundances in the Nakri record: 3.3%, 5.4%, 7.55%. In the FBP training set these taxa are identified to a higher taxonomic resolution (Dicrotendipes notatus-type (0.3% in average), Dicrotendipes nervosus-type (3%), Endochironomus albipennis-type (3.4%), Endochironomus tendens-type (1.4%), Endochironomus impar-type (0.6%), Cladopelma lateralis-type (7.5%), Cladopelma laccophila-type (0.05%)).

The pollen-based July air temperature reconstruction of the Lake Nakri sequence shows in general values similar to the chironomid-based reconstruction using the FBP training set.

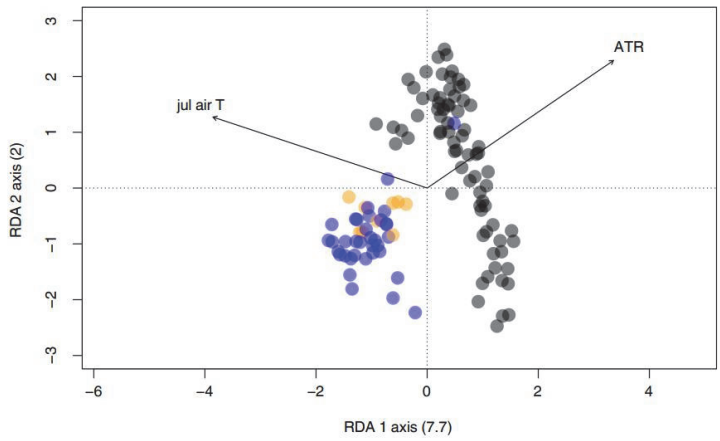

Fig. 7. Redundancy analysis (RDA) of Finno-Baltic-Polish training set using July air temperatures (Jul T; °C) and annual temperature range (ATR; °C). Blue dots indicate lakes from Eastern Baltic (Estonia, Latvia, Lithuania), yellow dots indicate Polish lakes, black dots indicate Finnish lakes.

ATR explained 11 % of variation in the FBP training set based on RDA ($p = 0.001$; $\lambda1: \lambda2 = 1$; Fig. 7). The chironomid-based ATR reconstruction performed with the Finno-Baltic-Polish training set revealed RMSEP of 1.4 °C and R^2 of 0.8 (Table 2).

The chironomid-based reconstructions— derived from both FBP and Swiss-Norwegian training sets— can be characterised by one major climate event - warming transition at the onset of the Holocene (~12–10 ka cal BP; Fig. 9A). Following this, temperatures remained fairly stable around 17–18 °C, punctuated by modest cooling episodes of approximately 0.5–1 °C at intervals of 9.0–8.0, 7.5–7.0, 5.5–5.0 ka and 1–0.5 ka cal BP. Because the upper section of the sediment core lacks dates more recent than 3.5 ka cal BP, interpretations regarding the Medieval Warm Period and the Little Ice Age—though apparent in the curves—should be regarded with caution. The chironomid-inferred ATR reconstruction revealed a major decreasing trend from Younger Dryas (Fig. 9A) towards nowadays. The onset of Holocene is marked by a drastic ATR decrease. This was followed by slight fluctuations interrupted by two pronounced climatic events: 9.0–8.0 ka cal BP increase and 2–0.5 ka cal BP decrease in ATR.

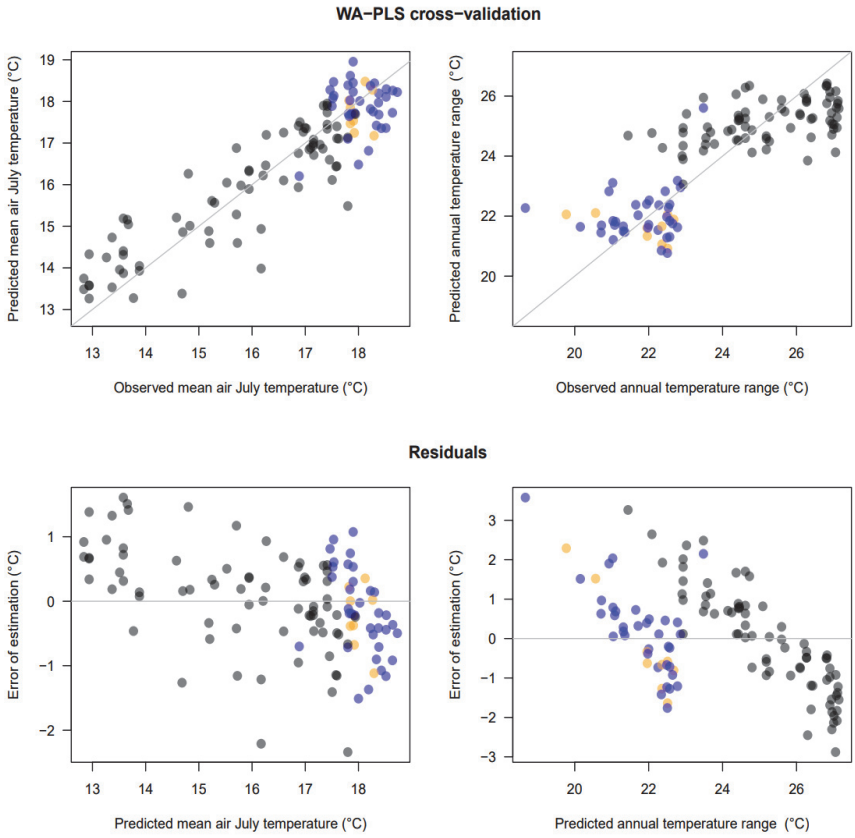

Fig. 8. Diagnostic plots of cross-validated estimates and prediction residuals compared with observed values of the Finno–Baltic–Polish training set calculated with a WA-PLS-based model based on two components using July air temperatures (°C) and annual temperature range (°C). Blue dots indicate lakes from Eastern Baltic (Estonia, Latvia, Lithuania), yellow dots indicate Polish lakes, black dots indicate Finnish lakes.

Table 2. Redundancy analysis (% of explanatory power) and weighted averaging-partial least squares (WA-PLS) inference model results ($RMSEP_{boot}$, R^2_{boot}, RMSE, Average $Bias_{boot}$, Maximum $Bias_{boot}$) for Finno-Baltic-Polish, Swiss-Norwegian chironomid-based and pollen-based training sets.

	Finno-Baltic-Polish training set - July air temperature (Bakumenko et al., 2024)	**Swiss-Norwegian training set - July air temperature (Heiri et al., 2011)**	**Pollen-based reconstruction - July air temperature (Seppä and Birks, 2001)**	**Finno-Baltic-Polish training set - annual temperature range**
Gradient range (°C)	12.1–19.2	3.5–18.4	7.5–17.5	18.6–27.1
% of explanatory power	14.4 (RDA-based)	5.6 (CCA-based)	11.4 (RDA-based)	11.0 (RDA.based)
$RMSEP_{boot}$ (°C)	0.7	1.5	0.7	1.4
RMSE (°C)	0.6	1.3	0.6	0.8
R^2_{boot}	0.9	0.9	0.8	0.8
Average $Bias_{boot}$ (°C)	0.02	–0.03	–0.03	0.04
Maximum $Bias_{boot}$ (°C)	0.7	1	2.9	3.1

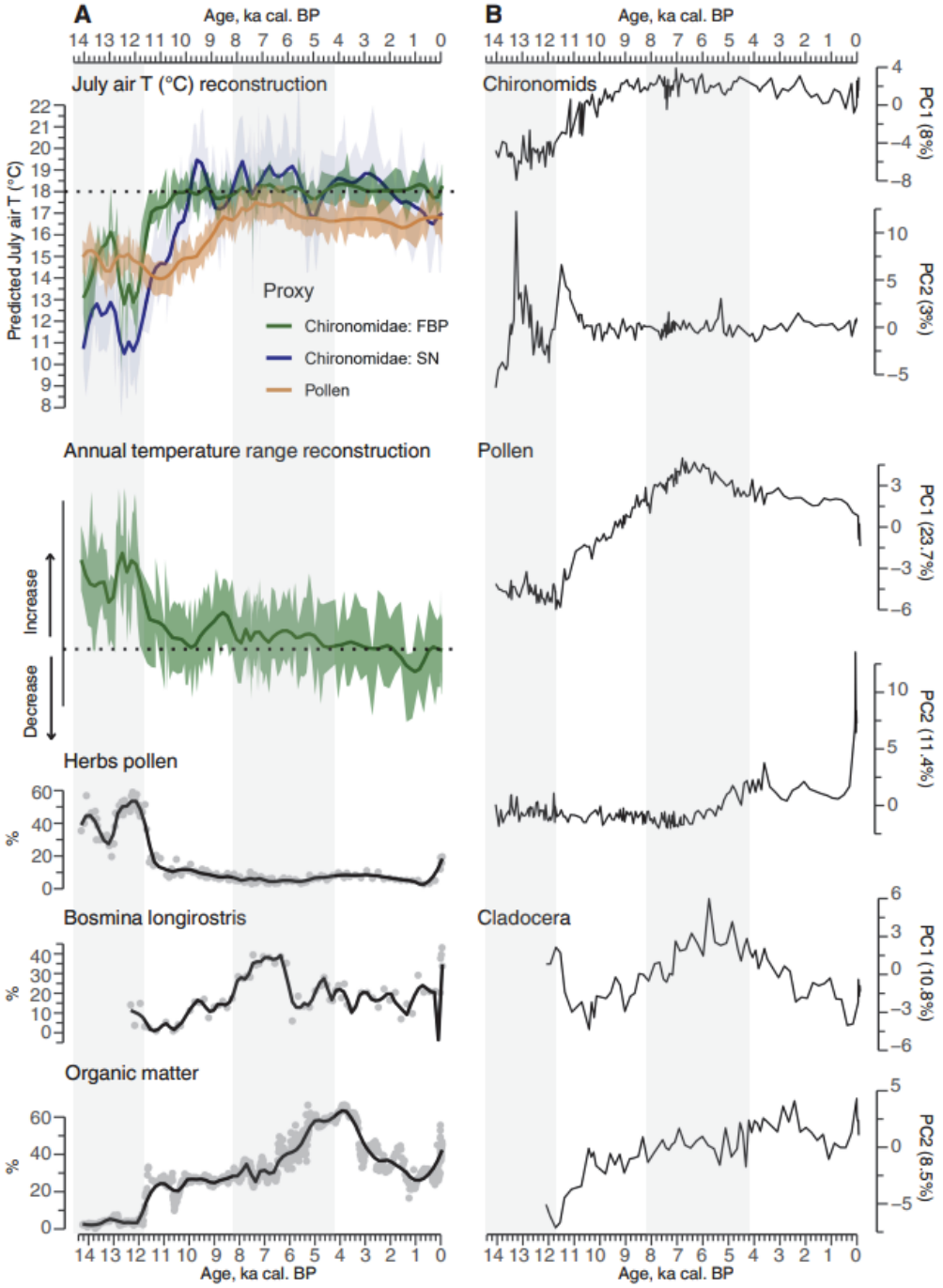

Fig. 9. (A) Chironomid-inferred Finno-Baltic-Polish (FBP) and Swiss-Norwegian (SN) training sets based and pollen-inferred July air temperature (°C) and annual temperature range (°C) reconstructions from Lake Nakri together with indicators of vegetation openness (herb

pollen, %), indicators of trophic changes (*Bosmina longirostris* and organic matter) and (B) PC curves of the Chironomids, Cladoceran and pollen Lake Nakri subfossil assemblages. The horisontal black dotted line indicates modern values of July air temperature and annual temperature range. The gray shading indicates time periods: late glacial (14.5–11.7 ka cal. BP), Early Holocene (11.7 – 8.2 ka cal. BP), Middle Holocene (8.2 – 4.2 ka cal. BP), Early Holocene (4.2 – 0 ka cal. BP).

The PC1 of both chironomid and pollen assemblages from the Lake Nakri record exhibits significant correlations with each other and with GRIP oxygen isotope data (r >0.8; S1). This suggests that both chironomid and pollen assemblages are primarily influenced by climatic factors.

The PC2 of chironomid assemblage suggests that chironomid and pollen assemblage are both driven by the same driver. The strongest correlation of chironomid PC2 (r =0.42; S1) is the herb's proportion in the pollen spectrum, which revealed drastic change in Younger Dryas/Holocene boundary (Fig. 9). The Cladocera PC1 scores had the strongest correlation with herb cover and organic matter curve (correlation index around 0.6; S1), suggesting that Cladocera communities were influenced by changes in vegetation and nutrient availability.

5. Discussion

5.1. Lake environment and climate reconstruction validation

5.1.1. Trophic state

Lake trophic state can influence chironomid-based temperature reconstructions, with more eutrophic lakes being reconstructed as warmer in comparison to oligotrophic lakes (Heiri et al., 2003; Heiri et al., 2014; Tóth et al., 2015). Chironomid taxa that indicate oligotrophic conditions are typically cold-water species, while those associated with eutrophic environments tend to prefer warmer waters, reflecting a positive co-tolerance to both eutrophication and climate change. The research from contemporary lake ecosystems and mesocosm experiments have shown that the zooplankton and phytoplankton communities have a similar reaction to warming as it is to nutrient enrichment (Visconti et al., 2008;

Jeppesen et al., 2009; Moss, 2011). This can lead to difficulties distinguishing between the influence of climate and nutrient availability for aquatic organisms in palaeolimnology. At the same time lake trophic state is expected to change with temperature, as changing climate can affect weathering, nutrient mobilization and primary productivity in lakes (Brodersen and Quinlan, 2006; Velle et al., 2010; Eggermont and Heiri, 2012). Therefore, to some extent, shifts in trophic status can be expected during climate changes. In this case trophic state changes would not bias the Chironomidae based climate reconstructions. However, variations in trophic state and productivity unrelated to temperature (e.g., from human activity) may introduce errors and distort chironomid-derived temperature records.

5.1.2. Proxy choice for climate reconstructions

The performance statistics of the pollen-based transfer function applied to the Nakri record are comparable to those of the chironomid-based reconstructions (Table 2). Climate is usually one of primary drivers of terrestrial vegetation composition is importance of climate for Nakri dataset, was confirmed by the significant correlation of PC1 of pollen, and chironomids with GRIP ice core oxygen isotopes data (Rasmussen et al., 2023; S1). However, the pollen-based reconstruction suggests on average 1 ^{o}C warmer temperatures during the late glacial, an absence of major cooling during the Younger Dryas and a significant delay in Early Holocene warming compared to the chironomid-based reconstructions (Fig. 9). The latter can be explained by the migration delays of the terrestrial vegetation during the late glacial and Early Holocene which can influence the quality of the pollen-based reconstructions, especially in formerly glaciated areas of northern and eastern Europe (Rao et al., 2022; Väliranta et al., 2015; Zani et al., 2023). The Younger Dryas terrestrial vegetation on the other hand may lack suitable modern analogues in contemporary ecosystems (Magny et al., 2001), due to the dry and high continental climate, potentially explaining the warmer temperatures reconstructed from pollen records in the region (Fig. 9). The Younger Dryas pollen spectra are known to contain redeposited thermophilus pollen, which can bias climate reconstructions (Veski et al., 2012).

5.1.3. Chironomid training set choice

WA-PLS based Chironomid-based July air temperature transfer functions using the FBP and Swiss-Norwegian training sets had similar cross-validated performance statistics, such as RMSEP, maximum bias and average bias (Table 2). Additionally, both temperature

reconstructions generally reflected similar climate patterns (Fig. 9) and resemble the temperature development of the GRIP ice core (Rasmussen et al., 2023; Fig. 10). However, the Swiss-Norwegian-based reconstruction indicated colder values during the late glacial and Early Holocene along with more pronounced temperature fluctuations during 9.0-8.0, 7.0-7.5, 6.5-5.5 ka cal BP compared to the FBP-based reconstruction. The causes of differences in reconstructions using different training sets have been previously discussed in the literature (Luoto, 2011; Engels et al., 2014; Kotrys et al., 2020; Bakumenko et al., 2024). These can be attributed to two primary reasons: (1) systematic differences in the estimated values between geographically distinct training sets (Engels et al., 2014; Bakumenko et al., 2024) and (2) mismatches in Chironomidae taxonomic resolution (Heiri and Lotter, 2010). In the Swiss-Norwegian training set, morphotypes optima tend to be lower than those in the FBP-based training set due to the presence of cooler modern analogues (Bakumenko et al., 2024). In the Swiss-Norwegian training set, certain genera are grouped at a broader taxonomic level, whereas in the FBP training set, these taxa are identified with higher taxonomic resolution. . Improving taxonomic resolution can enhance the performance and sensitivity of transfer functions by capturing more ecological details, but also carry a risk of reduced training set reliability if misidentifications occur (Heiri and Lotter, 2010). In this study, we minimized such risks by consistently using established identification keys for modern Chironomidae and rigorously comparing them with fossil specimens from Lake Nakri (see Methods). We suggest that for Nakri the FBP-based training set and transfer function may provide more realistic results, as it encompasses the distribution patterns of the modern Chironomidae taxa from the Baltic lowlands area. However, the general agreement between the two chironomid-based reconstructions based on different calibration data supports that the July air temperature records presented here have successfully captured the major patterns of late glacial and Holocene summer temperature change in the region.

Our tentative reconstruction of ATR based on the FBP calibration dataset features a cross-validated RMSEP of 1.4, which, compared to the ATR range in the dataset (18.6–27.7 ^{o}C) is relatively small. Although the distributions of Chironomidae taxa and assemblages have been observed to correspond to continentality changes (Self et al., 2011) a fully functional training set for the Baltic area has not been developed yet, and the approach has not been tested in downcore reconstructions or on surface sediments from other regions. It has to be kept in mind that chironomid-based continentality reconstructions can be biased by numerous collinear climatic and environmental factors, including July air temperatures (Self et al., 2011) and should be treated with caution. Therefore, we have presented the results of

the ATR reconstruction as a change in trend rather than absolute values. The overall decreasing ATR trend aligns with several independent lines of evidence: isotope-derived reconstructions indicate increasing winter precipitation throughout the Holocene in Estonia (Stansell et al., 2017), and 20th-century instrumental data show a reduction in seasonality in the Eastern Baltic region (Bethere et al., 2017).

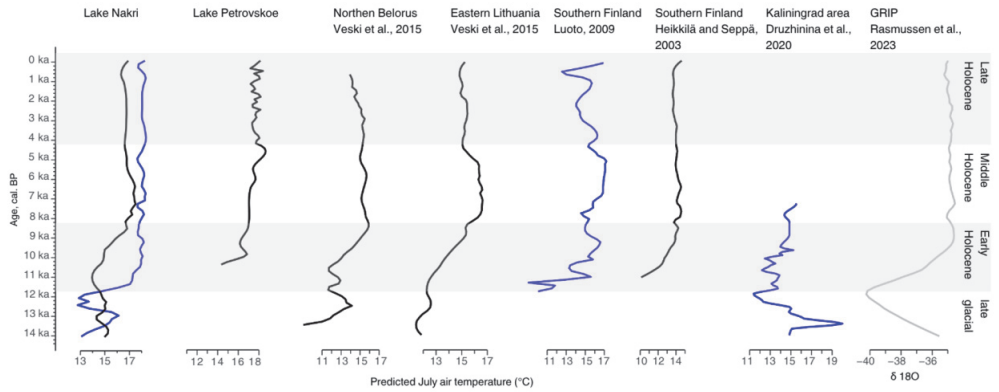

Fig. 10. Lake Nakri Chironomid-based temperature reconstruction based on the Baltic-Finish-Polish calibration data and pollen-based temperature reconstruction in comparison with already published climate reconstructions from Northern and Northeastern Europe and Greenland. Black lines indicate pollen-based reconstructions, black lines indicate chironomid-based reconstructions, gray line indicates δ18O-based reconstruction.

5.2. Lake Nakri palaeoclimate and palaeoenvironment history

5.2.1. Late glacial (14.5–11.7 ka cal BP)

Deglaciation of Estonia took place around 14.7–12.7 ka cal BP (Kalm et al., 2011; Lasberg and Kalm, 2013; Amon et al., 2016; Hughes et al., 2016). The oldest ^{14}C radiocarbon date in the Nakri record is dated to 14.0–13.8 ka cal BP, and the oldest sediments estimated to an age of 14.5 ka cal BP. This represents an extraordinary sedimentary archive, directly capturing conditions during the ice retreat from the region and providing a valuable window into deglaciation dynamics. Based on previous pollen-based studies, late glacial climate and environment in Eastern Baltic revealed two distinct events: the Bölling/Alleröd warming followed by the Younger Dryas cooling (Seppä and Poska, 2004; Laumets et al., 2014). Immigration of plant and animal taxa followed shortly after the ice retreat and the late glacial open tundra biome was dominated by

589 herbs and cold-tolerant shrub species (Amon et al., 2016; Poska et al., 2022). Modern
590 chironomids are known to be sensitive to the presence or absence of vegetation (Ólafsson et
591 al., 2002). This, combined with the significant correlation between PC2 of the Lake Nakri
592 fossil chironomid assemblages and the percentage of herb pollen (S1), highlights the drastic
593 ecological shifts which occured in the region during the late glacial period.
594 During the late glacial period the ecosystem of Lake Nakri was characterised by the
595 presence of green algae with a peak 13 ka cal. BP. Green algae are an important group of
596 primary producers in lakes, and although other algae groups are not represented in pollen
597 slides, the high abundance of green algae suggests increased productivity in the lake. This
598 event coincides with temporal extirpation of oligotrophic and cold-related chironomids
599 *Heterotrissocladius grimshawi*-type, *Tanytarsus lugens*-type and *Micropsectra insignilobus*-
600 type and appearance of eutrophic aquatic vegetation-related chironomids *Cricotopus*
601 *cylindraceus*-type (single appearance in the late glacial) and *Polypedilum nubeculosum*-type
602 (sporadic in late glacial). The trophic increase appears linked to the Bølling-Allerød event,
603 consistent with chironomid records indicating warmer July air temperatures and lower ATR.
604 Previously, the Younger Dryas was mainly characterised by the cold winters and the
605 summer temperature were supposed to be relatively similar to the modern one (Borisova,
606 1997; Davis et al., 2003). Theuerkauf and Joosten (2012) pointed out the uncertainty whether
607 Younger Dryas winters were cold and climate was continental or not. Our data supports the
608 hypothesis that the Younger Dryas cooling also affected summer temperatures (Lotter et al.,
609 2000), and is similar to many chironomid-based summer temperature reconstructions across
610 Europe (Heiri et al., 2014). Besides cold summers, our results suggest that the Younger Dryas
611 period was also characterized by an increase in ATR (Fig. 9) which aligns with reconstructed
612 increase in seasonality based on cryogenic cave carbonates from Great Britain (Töchterle et
613 al., 2024), as well as with model-based reconstructions of Younger Dryas climate (e.g.
614 Renssen et al., 2001). It was also hypothesized that the establishment of tundra biomes,
615 indicated in the Younger Dryas from Lake Nakri sediments, was encouraged by an increase
616 in continentality (Sher et al., 2003; Kienast et al., 2008). The cooler summer temperatures
617 might have not just contributed to changes in terrestrial vegetation, but also affected in lake
618 conditions as during this period cold- and oligotrophic- conditions related to chironomids
619 taxa (*Micropsectra insignilobus*-type, *Tanytarsus lugens*-type) as well as oligotrophy-
620 mesotrophy indicator *B. longispina* dominate (Fig. 5, 6).

5.2.2. Early Holocene (11.7–8.2 ka cal BP)

At the start of the Early Holocene, Characeae disappeared from Lake Nakri (Amon et al., 2012), and green algae abundance reached its highest peak around 11.5 ka cal BP (Fig. 4). Such a regime shift does not necessarily mean increase in nutrients (Scheffer and Van Nes, 2007). Considering the chironomid-inferred rapid warming from 13 up to 18 ºC (Fig. 9) and the connection between climate and productivity (Jeppesen et al., 2009) it is possible that the algae dominated state is a result of temperature increase. At the same time, we observed new macrophyte associated chironomids morphotypes (*Cricotopus cylindraceus*-type, *Lauterborniella*; Fig. 6). While Characeae that were present during the late glacial period (Amon et al., 2012) can easily grow on mineral matter rich sediments (Holzhausen, 2024), this is not the case for many other macrophyte species. Around 11 cal ka BP we observed an increase in organic matter from approximately less than 7% to more than 20% (Fig. 9) and an abrupt decrease in green algae (Fig. 4). When considering these results together with presence of macrophyte associated with Cladocera and Chironomidae taxa (Figs. 5 and 6), it suggests that around this time a new macrophyte dominated lake stage was established. However, it is unlikely that during this time the lake was highly eutrophic, as Cladocera *Bosmina longispina* - a species associated with mesotrophic lakes (Jensen et al., 2013; Lanka et al., 2024) dominates (Fig. 5). Chironomids *Chironomus plumosus*-type, *Procladius*, *Psectrocladius sordidellus*-type are common in the sediments from 11.8 ka cal BP onwards are usually considered indicators for low oxygen concentrations in bottom waters (Brooks et al., 2007) and often occur in eutrophic lakes.

Warmer and more stable climate conditions of Early Holocene led to the replacement of tundra biomes with boreal forests, as evidenced by the Lake Nakri pollen record and similar findings from other parts of the Eastern Baltics (Amon et al., 2016; Poska et al., 2022). Later, ca 8.5 ka cal BP the boreal forests were gradually replaced by temperate broad-leaved ones (Saarse and Veski, 2001; Niinemets and Saarse, 2009; Poska et al., 2022) with a distinct effect of 8.2 ka cold event apparent in the vegetation records (Seppä and Poska, 2004; Niinemets and Saarse, 2009; Seppä et al., 2009; Veski et al., 2015). The cold event is also visible in the chironomid-based reconstruction as a cooling of approximately 1 ºC, reappearance of cold-related oligotrophic taxa (*Micropsectra insignilobus*-type, *Sergentia coracina*-type) and decline in warm-related eutrophic ones (*Chironomus plumosus*-type, *Neozavrelia*) around 9.0–8.5 ka cal BP. In the Cladocera assemblages this event is associated with general reduction in Cladocera flux since 9.0 ka cal BP. Decrease in Cladocera

abundance (represented by Cladcoera flux) can be related to cooling or oligotrophication (Manca et al., 2007; Zawiska et al., 2017). However, in the case of the 8.2 event in Lake Nakri, this change is most likely climate driven, as no changes in Cladocera assemblages that would be indicative of oligotrophication, can be observed (Fig. 5). The pollen-based reconstructions (Heikkilä and Seppä, 2003; Veski et al., 2015) mainly indicate short cooling event around 8.2 ka cal BP and indicate quick recovery of the ecosystem thereafter. However, chironomid-based reconstruction from South Finland and Central Poland support the hypothesis that in our region the 8.2 ka event may have been embedded into a longer summer cooling episode starting at 9.0 ka cal BP (Luoto et al., 2010; Płóciennik et al., 2011). Based on globally distributed multi-proxy data, Mayewski et al. (2004) interprets the interval 9.0–8.0 ka cal BP as a partial return toward more glacial conditions following an orbitally driven delay in Northern Hemisphere deglaciation.

Summarized by (Davis et al., 2003), pollen-based reconstructions from Northern and Eastern Europe suggest that cooling 9.0–8.0 ka cal BP was more pronounced during the winter than during summer. Our data indicated an increase of ATR between 9.0 and 8.0 ka cal BP, which aligns with these findings. A reconstruction based on phosphorus concentrations in stalagmite calcite from western Ireland suggests also an increased temperature seasonality during the 8.2 ka cal BP event (Baldini et al., 2002). Additionally, evidence points to heightened seasonality of precipitation and severe arid events between 9 and 8 ka cal BP across the Northern Hemisphere (Shuman, 2012; Andersen et al., 2017). These events may have been triggered by the weakening of the meridional overturning circulation due to reduced Atlantic meridional overturning circulation, decline in summer insolation and cooling influence of volcanic aerosols (Mayewski et al., 2004; Carlson et al., 2008).

5.2.3. Middle Holocene (8.2–4.2 ka cal BP)

The Middle Holocene is characterized by a generally warm and stable climate, corresponding to the Holocene Thermal Maximum, during which, based on pollen data, temperate broadleaved trees became abundant in the Eastern Baltic area.

At the same time we can observe an increase in productivity in Lake Nakri. Whether this is solely due to rising temperatures, or a combination of warming and nutrient enrichment remains uncertain. In the Cladocera record this period is marked by the increase in relative abundance of *Bosmina longirostris* (8.2–5.8 ka cal BP) and increase in Cladocera

686 influx (8.2–7 ka cal BP). While the first is a well-established indicator for eutrophic
687 conditions (Chen et al., 2010; Adamczuk, 2016), the latter is considered to be representative
688 of either warming or eutrophication (Manca et al., 2007; Zawiska et al., 2017). This phase
689 aligns with a period of warmest temperatures in the pollen- and chironomid- based
690 temperature reconstructions. Rising surface water temperatures can enhance water column
691 stratification, potentially leading to hypolimnetic oxygen depletion (Nickus et al., 2010).
692 Such conditions can facilitate phosphorus release from sediments (Hupfer and Lewandowski,
693 2008), which may be the case for Lake Nakri, as indicated by the disappearance of the
694 oxygen-sensitive Chironomidae morphotype *Micropsectra contracta*-type (Fig. 6; Brooks et
695 al., 2007). Therefore, during the Holocene thermal maximum, both temperature and nutrient
696 enrichment could have contributed to the increase in productivity.
697 Short summer cooling events of approximately 0.5–1°C together with the slight ATR
698 oscillations occurred in our chironomid-based temperature reconstruction around 7.0–7.5 ka
699 and 6.5–5.5 ka cal BP (Fig. 9). A cooling around 7–7.5 ka cal BP was also observed in a
700 chironomid record from Southern Finland (Fig. 6; Luoto et al., 2010), however, no pollen
701 based reconstruction indicates this event. Even though pollen-based reconstructions from
702 eastern Baltic did not reveal any climate changes in this period, pollen-based reconstruction
703 from Sweden indicated winter cooling and increase in continentality 7 ka cal BP (Seppä et
704 al., 2005).
705 The 6.5-5.5 chironomid-inferred cooling trend aligns with an increase in Cladocera
706 *Daphnia* spp. abundancy, which is considered indicative of cooler climate (Nevalainen et al.,
707 2014). A peak in this taxon occurs in Lake Nakri 5.8–5.2 ka cal BP together with decline in
708 *Bosmina longirostris*. This point towards decrease of productivity, which was probably
709 caused by climate. The 6.5–5.5 ka cal cold spell BP has also been observed in pollen-based
710 records from Northern Belarus and Eastern Latvia, as well as in the chironomid-based
711 reconstruction from Southern Finland (Fig. 10; Luoto et al., 2010; Veski et al., 2015). Also,
712 cooling periods with similar age have been reported from the North Atlantic and central
713 Europe (O'Brien et al., 1995; Oppo et al., 2003; Moros et al., 2004; Vollweiler et al., 2006).
714 The average 5.5 ka cal BP summer cooling across North America and Europe was estimated
715 to be at least 0.5°C (Marsicek et al., 2018). The identified possible cause of the described
716 cooling event is a decrease in solar activity, primarily summer insolation, driven by changes
717 in orbital forcing (Mayewski et al., 2004; Shuman, 2012). This reduction led to lower mid-
718 latitude temperatures, glacier advances, a rise in the treeline limit in Scandinavia (Liu et al.,
719 2000; Clement et al., 2000; Braconnot et al., 2004; Mayewski et al., 2004; Liu et al., 2007).

Therefore, this event can be described as a complex response to peak rates of insolation change, involving feedback interactions among multiple components (Shuman, 2012).

5.2.4. Late Holocene (4.2–0 ka cal BP)

The 4.2 ka cal BP, commonly accepted Late Holocene boundary, did not reveal any remarkable changes in the Lake Nakri record. After 4.0 ka cal BP the development of southern mixed boreal forests where late successional temperate taxa are replaced by early successional ones happened in Eastern Baltic (Niinemets and Saarse, 2009; Poska et al., 2022). This coincides with stable chironomid-inferred July air temperatures around 18°C. The relatable stable Cladocera species composition throughout the Late Holocene suggests that by the end of the Middle Holocene, Lake Nakri had reached conditions similar to those observed today. This also aligns with our knowledge that the area has experienced modest, compared to average in Estonia, anthropogenic impact.

Despite the generally stable conditions, some minor climate events were observed in the Late Holocene: 0.5°C July air temperature increased approximately 1–0.5 ka cal BP, followed by a subsequent drop. This period corresponds to the Medieval Warm Period and following cooling can be associated with the Little Ice Age (Diaz et al., 2011; Płóciennik et al., 2011). Similar amplitude changes connected with the Medieval Warm Period and Little Ice Age have been observed from the pollen records in Eastern Latvia and Southern Finland (Heikkilä and Seppä, 2003; Luoto et al., 2010; Veski et al., 2015). The Medieval Warm Period revealed almost no ATR fluctuations (Fig. 9). The data from Southern Finland reports it as a dry and warm period in the Baltic area (Seppä et al., 2009).

The Little Ice Age was indicated by a cooling pattern together with ATR decrease. Also, possible decrease of productivity might have occurred during the Little Ice Age, where several littoral species disappeared, and Cladocera influx was reduced to values similar to the late glacial period (Fig. 5). The chironomid-based reconstruction from Southern Finland (Fig. 7; Luoto et al., 2010) shows more pronounced cooling than observed in Lake Nakri record, which can possibly be attributed to its more northern location. The ATR decrease which aligns with study of Jones et al. (2014), revealing that this event is characterized predominantly by snowy winters with periodic episodes of cool and humid summers. Together, these conditions contributed to a positive glacier mass balance and the advance of glaciers across the Northern Hemisphere (Steiner et al., 2008; Solomina et al., 2015). Several factors may have contributed to this cooling, including a decrease in solar insolation in

northern hemisphere (Wanner et al., 2008) and the atmospheric effects of frequent volcanic eruptions, which often led to cool, humid summers due to increased dust and aerosols (Büntgen et al., 2016; Owens et al., 2017; Strandberg et al., 2023). Additional contributing factors include due to anthropogenic deforestation increased surface albedo (Owens et al., 2017), as well as sea-ice export from the Arctic Ocean (Miles et al., 2020).

6. Conclusions

This study presents a high-resolution, multi-proxy reconstruction of postglacial climate and environmental dynamics from Lake Nakri. The site is situated in the transitional from continental to maritime climate Eastern Baltic region and represents the record of the past 14.5 ka cal BP - from the last deglaciation until modern days. The multi-proxy approach, applied to lake Nakri records included Chironomidae, Cladocera, pollen, and LOI analyses, which made it possible to estimate both climate and environmental changes of the site.

Chironomid- and pollen-based climate reconstructions generally infer the same July air temperature trends. However, pollen-based reconstruction revealed evident lag likely related to postglacial migration dynamics and the absence of modern analogues for late glacial climates. The trophic changes, estimated from Cladocera assemblages, are assessed as relatively minor and not expected to influence the chironomid-based reconstructions drastically.

The chironomid-based July temperature reconstructions, developed using two independent training sets, revealed generally similar patterns. However, the usage of the local training set showed its advantages exhibiting lower error of July air temperature estimation. The chironomid-inferred ATR trends aligned well with published literature and vegetation changes, observed in lake Nakri. Thus, the usage of chironomids as a continentality proxy can be justified.

The chironomid-inferred reconstruction captures major and minor climate events, some of which have already been observed in the literature. The Bølling-Allerød was characterised by increased lake productivity, likely driven by warming. During the Younger Dryas, chironomid assemblages suggest colder summers and increased ATR, accompanied by a cold-adapted, oligotrophic cladocera and chironomid taxa and the development of tundra vegetation. On the Holocene boundary the major climate warming event was observed, which resulted in forest expansion, with boreal forests later replaced by temperate ones. The 8.2 ka cold event, expressed in a ~1°C July air temperature decrease and ATR increase, was

suggested to be a part of a broader 9.0–8.0 ka cal BP cooling episode. The Middle Holocene climate, which incorporates Holocene Thermal Maximum, was characterised by warm and stable climate and the spread of temperate broadleaved forests in the Eastern Baltic. Also, some minor cooling events were indicated by chironomid-inferred reconstructions at ~7.0–7.5 and 6.5–5.5 ka cal BP. The Late Holocene was characterised by warm July air temperatures and development of southern mixed boreal forests in the Eastern Baltic. The Medieval Warm Period was reflected as a July air temperature increase of approximately 0.5 °C with almost no ATR changes. It was followed by the Little Ice Age, which was marked by cooling, decreased ATR. After it, the reconstructed values were close to the modern ones.

The new findings contribute to a broader understanding of how ecosystems of the Eastern Baltic region have responded to past climate forcing and provide a valuable context for anticipating future environmental trajectories under ongoing climate change.

CRediT authorship contribution statement

Varvara Bakumenko: conceptualisation; data curation; investigation; formal analysis; software; visualisation; writing – original draft; writing – review & editing. **Anna Lanka**: conceptualisation; data curation; investigation; formal analysis; software; visualisation; writing – review & editing. **Anneli Poska:** supervision; conceptualisation; data curation; validation; writing – review & editing. **Jüri Vassiljev**: investigation; conceptualisation; formal analysis; software; writing – review & editing. **Oliver Heiri**: investigation; supervision; writing – review & editing. **Tiiu Alliksaar**: investigation; formal analysis; software; writing – review & editing. **Simon Belle**: supervision; conceptualisation; writing – review & editing. **Siim Veski**: supervision; investigation; conceptualisation; writing – review & editing; funding acquisition; resources.

Acknowledgments

This study was financially supported by the Estonian Research Council grants PRG1993 and TK215. Varvara Bakumenko and Anna Lanka was supported by the Doctoral School of Earth Sciences and Ecology, supported by the European Union, European Regional Development

Fund (ASTRA “TTÜ arenguprogramm aastateks 2016–2022”). Anneli Poska was supported by Swedish strategic research area BECC (Biodiversity and Ecosystem Services in a Changing Climate); MERGE (ModElling the Regional and Global Earth system at Lund University).

Declaration of competing interest

The authors declare that they have no known competing financial interests or personal relationships that could have appeared to influence the work reported in this paper.

Supplement 1. Pearson correlations of PC1 and PC2 with each other and some selected environmental parameters: herbs % in the Lake Nakri pollen spectra, % of organic matter, *Bosmina longirostris*, chironomid-inferred annual temperature range (ATR) and oxygen isotopes from GRIP ice core (Rasmussen et al., 2023). Only significant correlations ($p<0.05$) are shown.

	Herbs	**Organic matter**	**ATR**	***Bosmina longirostris***	**Oxygen isotopes**	**PC1 of other proxy**	**PC2 of other proxy**
Chironomids PC1	-0.79	0.77	-0.74	0.46	0.84	0.66 clad 0.87 pollen	
Chironomids PC2	0.42		-0.19				-0.3 clad
Cladocera PC1	-0.64	0.62	-0.51	0.58	0.56	0.66 chir 0.76 pollen	0.26 pollen
Cladocera PC2		0.41		0.26			-0.3 chir

Pollen PC1	-0.9	0.63	0.36	0.63	0.84	0.76 clad 0.87 chir	0.26 clad
Pollen PC2		0.38					

References

Adamczuk, M., 2016. Past, present, and future roles of small cladoceran Bosmina longirostris (O. F. Müller, 1785) in aquatic ecosystems. Hydrobiologia 767, 1–11. https://doi.org/10.1007/s10750-015-2495-7

Alliksaar, T., 2000. Application of spherical fly-ash particles to study spatial deposition of atmospheric pollutants in north-eastern Estonia. Oil Shale 4, 335–50.

Amon, D.J., Ziegler, A.F., Dahlgren, T.G., Glover, A.G., Goineau, A., Gooday, A.J., Wiklund, H., Smith, C.R., 2016. Insights into the abundance and diversity of abyssal megafauna in a polymetallic-nodule region in the eastern Clarion-Clipperton Zone. Sci Rep 6, 30492. https://doi.org/10.1038/srep30492

Amon, L., Veski, S., Heinsalu, A., Saarse, L., 2012. Timing of Lateglacial vegetation dynamics and respective palaeoenvironmental conditions in southern Estonia: evidence from the sediment record of Lake Nakri. J Quaternary Science 27, 169–180. https://doi.org/10.1002/jqs.1530

Amon, L., Veski, S., Vassiljev, J., 2014. Tree taxa immigration to the eastern Baltic region, southeastern sector of Scandinavian glaciation during the Late-glacial period (14,500–11,700 cal. b.p.). Veget Hist Archaeobot 23, 207–216. https://doi.org/10.1007/s00334-014-0442-6

Andersen, N., Lauterbach, S., Erlenkeuser, H., Danielopol, D.L., Namiotko, T., Hüls, M., Belmecheri, S., Dulski, P., Nantke, C., Meyer, H., Chapligin, B., Von Grafenstein, U., Brauer, A., 2017. Evidence for higher-than-average air temperatures after the 8.2 ka event provided by a Central European δ18O record. Quaternary Science Reviews 172, 96–108. https://doi.org/10.1016/j.quascirev.2017.08.001

Andersen, T., Sæther, O., Cranston, P., Epler, J., 2013. The larvae of Orthocladiinae (Diptera: Chironomidae) of the Holarctic region–Keys and diagnoses. Insect Systematics & Evolution.

Bakumenko, V., Poska, A., Płóciennik, M., Gasteviciene, N., Kotrys, B., Luoto, T., Belle, S., Veski, S., 2024. Chironomidae-based inference model for mean July air temperature reconstructions in the eastern Baltic area 53, 401–414. https://doi.org/10.1111/bor.12655

Baldini, J.U.L., McDermott, F., Fairchild, I.J., 2002. Structure of the 8200-Year Cold Event Revealed by a Speleothem Trace Element Record. Science 296, 2203–2206. https://doi.org/10.1126/science.1071776

Bengtsson, L., Enell, M., 1986. Chemical analysis, in: Handbook of Holocene Palaeoecology and Palaeohydrology. John Wiley & Sons Ltd, Chichester, Berglund B.E.(ed.), pp. 423–451.

Bennett, K.D., Willis, K.J., 2001. Pollen, in: Smol, J.P., Birks, H.J.B., Last, W.M., Bradley, R.S., Alverson, K. (Eds.), Tracking Environmental Change Using Lake Sediments: Terrestrial, Algal, and Siliceous Indicators. Springer Netherlands, Dordrecht, pp. 5–32. https://doi.org/10.1007/0-306-47668-1_2

Berglund, E., Ralska-Jasiewiczowa, M., 1986. , in: Handbook of Holocene Palaeoecology and Palaeohydrology. Wiley-Interscience, Chichester.

Birks, H. j. b., Braak, C. j. f. T., Line, J.M., Juggins, S., Stevenson, A.C., Battarbee, R.W., Mason, B.J., Renberg, I., Talling, J.F., 1997. Diatoms and pH reconstruction. Philosophical Transactions of the Royal Society of London. B, Biological Sciences 327, 263–278. https://doi.org/10.1098/rstb.1990.0062

Birks, H.J.B., Birks, H.J.B., 1998. D.G. Frey and E.S. Deevey Review 1: Numerical tools in palaeolimnology – Progress, potentialities, and problems. Journal of Paleolimnology 20, 307–332. https://doi.org/10.1023/A:1008038808690

Bledzki, L.A., Rybak, J.I., 2016. Freshwater Crustacean Zooplankton of Europe: Cladocera & Copepoda (Calanoida, Cyclopoida) Key to species identification, with notes on ecology, distribution, methods and introduction to data analysis. Springer International Publishing, Cham. https://doi.org/10.1007/978-3-319-29871-9

Borisova, O.K., 1997. Younger Dryas landscape and climate in Northern Eurasia and North America. Quaternary International 41–42, 103–109. https://doi.org/10.1016/S1040-6182(96)00041-9

Braconnot, P., Harrison, S.P., Joussaume, S., Hewitt, C.D., Kitoch, A., Kutzbach, J.E., Liu, Z., Otto-Bliesner, B., Syktus, J., Weber, S.L., 2004. Evaluation of PMIP coupled ocean-atmosphere simulations of the Mid-Holocene, in: Battarbee, R.W., Gasse, F., Stickley, C.E. (Eds.), Past Climate Variability through Europe and Africa, Developments in Paleoenvironmental Research. Springer Netherlands, Dordrecht, pp. 515–533. https://doi.org/10.1007/978-1-4020-2121-3_24

Brodersen, K.P., Quinlan, R., 2006. Midges as palaeoindicators of lake productivity, eutrophication and hypolimnetic oxygen. Quaternary Science Reviews, Quaternary beetle research: the state of the art 25, 1995–2012. https://doi.org/10.1016/j.quascirev.2005.03.020

Bronk Ramsey, C., 2009. Bayesian Analysis of Radiocarbon Dates. Radiocarbon 51, 337–360. https://doi.org/10.1017/S0033822200033865

Brooks, S.J., Bennion, H., Birks, H.J.B., 2001. Tracing lake trophic history with a chironomid–total phosphorus inference model. Freshwater Biology 46, 513–533. https://doi.org/10.1046/j.1365-2427.2001.00684.x

Brooks, S.J., Langdon, P.G., Heiri, O., 2007. The identification and use of Palaearctic Chironomidae larvae in palaeoecology. Quaternary Research Association Technical Guide i-vi,1.

Büntgen, U., Myglan, V.S., Ljungqvist, F.C., McCormick, M., Di Cosmo, N., Sigl, M., Jungclaus, J., Wagner, S., Krusic, P.J., Esper, J., Kaplan, J.O., De Vaan, M.A.C., Luterbacher, J., Wacker, L., Tegel, W., Kirdyanov, A.V., 2016. Cooling and societal change during the Late Antique Little Ice Age from 536 to around 660 AD. Nature Geosci 9, 231–236. https://doi.org/10.1038/ngeo2652

Carlson, A.E., LeGrande, A.N., Oppo, D.W., Came, R.E., Schmidt, G.A., Anslow, F.S., Licciardi, J.M., Obbink, E.A., 2008. Rapid early Holocene deglaciation of the Laurentide ice sheet. Nature Geosci 1, 620–624. https://doi.org/10.1038/ngeo285

Chen, G., Dalton, C., Taylor, D., 2010. Cladocera as indicators of trophic state in Irish lakes. J Paleolimnol 44, 465–481. https://doi.org/10.1007/s10933-010-9428-2

Chevalier, M., Davis, B.A.S., Heiri, O., Seppä, H., Chase, B.M., Gajewski, K., Lacourse, T., Telford, R.J., Finsinger, W., Guiot, J., Kühl, N., Maezumi, S.Y., Tipton, J.R., Carter, V.A., Brussel, T., Phelps, L.N., Dawson, A., Zanon, M., Vallé, F., Nolan, C., Mauri, A., de Vernal, A., Izumi, K., Holmström, L., Marsicek, J., Goring, S., Sommer, P.S., Chaput, M., Kupriyanov, D., 2020. Pollen-based climate reconstruction techniques for late Quaternary studies. Earth-Science Reviews 210, 103384. https://doi.org/10.1016/j.earscirev.2020.103384

Clement, A.C., Seager, R., Cane, M.A., 2000. Suppression of El Niño during the Mid-Holocene by changes in the Earth's orbit. Paleoceanography 15, 731–737. https://doi.org/10.1029/1999PA000466

Davis, B.A.S., Brewer, S., Stevenson, A.C., Guiot, J., 2003. The temperature of Europe during the Holocene reconstructed from pollen data. Quaternary Science Reviews 22, 1701–1716. https://doi.org/10.1016/S0277-3791(03)00173-2

Diaz, H.F., Trigo, R., Hughes, M.K., Mann, M.E., Xoplaki, E., Barriopedro, D., 2011. Spatial and Temporal Characteristics of Climate in Medieval Times Revisited. Bull. Amer. Meteor. Soc. 92, 1487–1500. https://doi.org/10.1175/BAMS-D-10-05003.1

Druzhinina, O., Kublitskiy, Y., Stančikaitė, M., Nazarova, L., Syrykh, L., Gedminienė, L., Uogintas, D., Skipityte, R., Arslanov, K., Vaikutienė, G., Kulkova, M., Subetto, D., 2020. The Late Pleistocene–Early Holocene palaeoenvironmental evolution in the SE Baltic region: a new approach based on chironomid, geochemical and isotopic data from Kamyshovoye Lake, Russia. Boreas 49, 544–561. https://doi.org/10.1111/bor.12438

Edvardsson, J., Corona, C., Mažeika, J., Pukienė, R., Stoffel, M., 2016. Recent advances in long-term climate and moisture reconstructions from the Baltic region: Exploring the potential for a new multi-millennial tree-ring chronology. Quaternary Science Reviews 131, 118–126. https://doi.org/10.1016/j.quascirev.2015.11.005

Eggermont, H., Heiri, O., 2012. The chironomid-temperature relationship: expression in nature and palaeoenvironmental implications. Biological Reviews 87, 430–56. https://doi.org/10.1111/j.1469-185X.2011.00206.x

Engels, S., Self, A., Luoto, T., Brooks, S., Helmens, K., 2014. A comparison of three Eurasian chironomid–climate calibration datasets on a W–E continentality gradient and the implications for quantitative temperature reconstructions. Journal of Paleolimnology 51, 529–47. https://doi.org/10.1007/s10933-014-9772-8

Frey, D., 1986. Cladocera Analysis., in: Berglund, B. E. (Ed.),Handbook of Holocene Palaeoecology and Palaeohydrology. John Wiley & Sons Ltd., pp. 667–692.

Hájková, P., Pařil, P., Petr, L., Chattová, B., Matys Grygar, T., Heiri, O., 2016. A first chironomid-based summer temperature reconstruction (13–5 ka BP) around 49°N in inland Europe compared with local lake development. Quaternary Science Reviews 141, 94–111. https://doi.org/10.1016/j.quascirev.2016.04.001

Hamerlík, L., Dobríková, D., Szarlowicz, K., Reczynski, W., Kubica, B., Šporka, F., Bitušík, P., 2016. Lake biota response to human impact and local climate during the last 200 years: A multi-proxy study of a subalpine lake (Tatra Mountains, W Carpathians). Science of The Total Environment 545–546, 320–328. https://doi.org/10.1016/j.scitotenv.2015.12.049

Heikkilä, M., Seppä, H., 2010. Holocene climate dynamics in Latvia, eastern Baltic region: a pollen-based summer temperature reconstruction and regional comparison. Boreas 39, 705–719. https://doi.org/10.1111/j.1502-3885.2010.00164.x

Heikkilä, M., Seppä, H., 2003. A 11,000 yr palaeotemperature reconstruction from the southern boreal zone in Finland. Quaternary Science Reviews 22, 541–554. https://doi.org/10.1016/S0277-3791(02)00189-0

Heinsalu, A., Alliksaar, T., Leeben, A., Nõges, T., 2007. Sediment diatom assemblages and composition of pore-water dissolved organic matter reflect recent eutrophication history of lake peipsi (Estonia/Russia), in: Gulati, R.D., Lammens, E., De Pauw, N., Van Donk, E. (Eds.), Shallow Lakes in a Changing World. Springer Netherlands, Dordrecht, pp. 133–143. https://doi.org/10.1007/978-1-4020-6399-2_13

Heiri, O, Brooks, S., Renssen, H., Bedforf, A., Hazekamp, M., Ilyashuk, B., Jeffers, E., Lang, B., Kirilova, E., Kuiper, S., Millet, L., 2014. Validation of climate model-inferred regional temperature change for late-glacial Europe. Nature Communications 5, 4914. https://doi.org/10.1038/ncomms5914

Heiri, O., Brooks, S.J., Birks, H.J.B., Lotter, A.F., 2011. A 274-lake calibration data-set and inference model for chironomid-based summer air temperature reconstruction in Europe. Quaternary Science Reviews 30, 3445–3456. https://doi.org/10.1016/j.quascirev.2011.09.006

Heiri, Oliver, Brooks, S.J., Renssen, H., Bedford, A., Hazekamp, M., Ilyashuk, B., Jeffers, E.S., Lang, B., Kirilova, E., Kuiper, S., Millet, L., Samartin, S., Toth, M., Verbruggen, F., Watson, J.E., van Asch, N., Lammertsma, E., Amon, L., Birks, H.H., Birks, H.J.B., Mortensen, M.F., Hoek, W.Z., Magyari, E., Muñoz Sobrino, C., Seppä, H., Tinner, W., Tonkov, S., Veski, S., Lotter, A.F., 2014. Validation of climate model-inferred regional temperature change for late-glacial Europe. Nat Commun 5, 4914. https://doi.org/10.1038/ncomms5914

Heiri, O., Lotter, A.F., 2010. How does taxonomic resolution affect chironomid-based temperature reconstruction? J Paleolimnol 44, 589–601. https://doi.org/10.1007/s10933-010-9439-z

Heiri, O., Lotter, A.F., Hausmann, S., Kienast, F., 2003. A chironomid-based Holocene summer air temperature reconstruction from the Swiss Alps. The Holocene 13, 477–484. https://doi.org/10.1191/0959683603hl640ft

Heiri, O., Lotter, A.F., Lemcke, G., 2001. Loss on ignition as a method for estimating organic and carbonate content in sediments: reproducibility and comparability of results. Journal of Paleolimnology 25, 101–110. https://doi.org/10.1023/A:1008119611481

Hersbach, H., Bell, B., Berrisford, P., Hirahara, S., Horányi, A., Muñoz-Sabater, J., Nicolas, J., Peubey, C., Radu, R., Schepers, D., Simmons, A., Soci, C., Abdalla, S., Abellan, X., Balsamo, G., Bechtold, P., Biavati, G., Bidlot, J., Bonavita, M., De Chiara, G., Dahlgren, P., Dee, D., Diamantakis, M., Dragani, R., Flemming, J., Forbes, R., Fuentes, M., Geer, A., Haimberger, L., Healy, S., Hogan, R.J., Hólm, E., Janisková, M., Keeley, S., Laloyaux, P., Lopez, P., Lupu, C., Radnoti, G., de Rosnay, P., Rozum, I., Vamborg, F., Villaume, S., Thépaut, J.-N., 2020. The ERA5 global reanalysis. Quarterly Journal of the Royal Meteorological Society 146, 1999–2049. https://doi.org/10.1002/qj.3803

Holzhausen, A., 2024. What we really know about the dormancy, reproduction, germination and cultivation of charophytes (Characeae). OE 9, e117655. https://doi.org/10.3897/oneeco.9.e117655

Hughes, A.L.C., Gyllencreutz, R., Lohne, Ø.S., Mangerud, J., Svendsen, J.I., 2016. The last Eurasian ice sheets – a chronological database and time-slice reconstruction, DATED-1. Boreas 45, 1–45. https://doi.org/10.1111/bor.12142

Hupfer, M., Lewandowski, J., 2008. Oxygen Controls the Phosphorus Release from Lake Sediments – a Long-Lasting Paradigm in Limnology. International Review of Hydrobiology 93, 415–432. https://doi.org/10.1002/iroh.200711054

Ilyashuk, B., Gobet, E., Heiri, O., Lotter, A.F., van Leeuwen, J.F.N., van der Knaap, W.O., Ilyashuk, E., Oberli, F., Ammann, B., 2009. Lateglacial environmental and climatic changes at the Maloja Pass, Central Swiss Alps, as recorded by chironomids and pollen. Quaternary Science Reviews 28, 1340–1353. https://doi.org/10.1016/j.quascirev.2009.01.007

Jensen, T.C., Dimante-Deimantovica, I., Schartau, A.K., Walseng, B., 2013. Cladocerans respond to differences in trophic state in deeper nutrient poor lakes from Southern Norway. Hydrobiologia 715, 101–112. https://doi.org/10.1007/s10750-012-1413-5

Jeppesen, E., Kronvang, B., Meerhoff, M., Søndergaard, M., Hansen, K.M., Andersen, H.E., Lauridsen, T.L., Liboriussen, L., Beklioglu, M., Özen, A., Olesen, J.E., 2009. Climate Change Effects on Runoff, Catchment Phosphorus Loading and Lake Ecological State, and Potential Adaptations. J of Env Quality 38, 1930–1941. https://doi.org/10.2134/jeq2008.0113

Jiménez-Moreno, G., Heiri, O., García-Alix, A., Anderson, R.S., Jiménez-Espejo, F.J., López-Blanco, C., Jiménez, L., Pérez-Martínez, C., Rodrigo-Gámiz, M., López-Avilés, A., Camuera, J., 2023. Holocene summer temperature reconstruction based on a chironomid record from Sierra Nevada, southern Spain. Quaternary Science Reviews 319, 108343. https://doi.org/10.1016/j.quascirev.2023.108343

Jones, P.D., Harpham, C., Vinther, B.M., 2014. Winter-responding proxy temperature reconstructions and the North Atlantic Oscillation. Journal of Geophysical Research: Atmospheres 119, 6497–6505. https://doi.org/10.1002/2014JD021561

Juggins, S., 2003. Software for ecological and palaeoecological data analysis and visualisation. University of Newcastle, Newcastle upon Tyne.

Kalm, V., Raukas, A., Rattas, M., Lasberg, K., 2011. Pleistocene Glaciations in Estonia, in: Developments in Quaternary Sciences. Elsevier, pp. 95–104. https://doi.org/10.1016/B978-0-444-53447-7.00008-8

Kienast, F., Tarasov, P., Schirrmeister, L., Grosse, G., Andreev, A.A., 2008. Continental climate in the East Siberian Arctic during the last interglacial: Implications from palaeobotanical records. Global and Planetary Change 60, 535–562. https://doi.org/10.1016/j.gloplacha.2007.07.004

Klink, A., Pillot, H., 2003. Chironomidae Larvae: Key to the Higher Taxa and Species of the Lowlands of Northwestern Europe. Expert-Center for Taxonomic Identification.

Kotrys, B., Płóciennik, M., Sydor, P., Brooks, S., 2020. Expanding the Swiss-Norwegian chironomid training set with Polish data. Boreas 49, 89–107. https://doi.org/10.1111/bor.12406

Lanka, A., Poska, A., Bakumenko, V., Dimante-Deimantovica, I., Liiv, M., Stivrins, N., Zagars, M., Veski, S., 2024. Subfossil Cladocera as indicators of pH, trophic state and conductivity: Separate and combined effects in hemi boreal freshwater lakes. Ecological Indicators 167, 112592. https://doi.org/10.1016/j.ecolind.2024.112592

Lapellegerie, P., Millet, L., Rius, D., Duprat-Oualid, F., Luoto, T., Heiri, O., 2024. Chironomid-inferred summer temperature during the Last Glacial Maximum in the Southern Black Forest, Central Europe. Quaternary Science Reviews 345, 109016. https://doi.org/10.1016/j.quascirev.2024.109016

Larocque-Tobler, I., 2014. The Polish sub-fossil chironomids. Palaeontologia Electronica 17, 28. https://doi.org/10.26879/391

Lasberg, K., Kalm, V., 2013. Chronology of L ate W eichselian glaciation in the western part of the E ast E uropean P lain. Boreas 42, 995–1007. https://doi.org/10.1111/bor.12016

Laumets, L., Kalm, V., Poska, A., Kele, S., Lasberg, K., Amon, L., 2014. Palaeoclimate inferred from δ18O and palaeobotanical indicators in freshwater tufa of Lake Äntu Sinijärv, Estonia. J Paleolimnol 51, 99–111. https://doi.org/10.1007/s10933-013-9758-y

Liu, Z., Kutzbach, J., Wu, L., 2000. Modeling climate shift of El Nino variability in the Holocene. Geophysical Research Letters 27, 2265–2268. https://doi.org/10.1029/2000GL011452

Liu, Z., Wang, Y., Gallimore, R., Gasse, F., Johnson, T., deMenocal, P., Adkins, J., Notaro, M., Prentice, I.C., Kutzbach, J., Jacob, R., Behling, P., Wang, L., Ong, E., 2007. Simulating the transient evolution and abrupt change of Northern Africa atmosphere–ocean–terrestrial ecosystem in the Holocene. Quaternary Science Reviews 26, 1818–1837. https://doi.org/10.1016/j.quascirev.2007.03.002

Lotter, A.F., Birks, H.J.B., Eicher, U., Hofmann, W., Schwander, J., Wick, L., 2000. Younger Dryas and Allerød summer temperatures at Gerzensee (Switzerland) inferred from fossil pollen and cladoceran assemblages. Palaeogeography, Palaeoclimatology, Palaeoecology 159, 349–361. https://doi.org/10.1016/S0031-0182(00)00093-6

Lotter, A.F., Birks, H.J.B., Hofmann, W., Marchetto, A., 1998. Modern diatom, cladocera, chironomid, and chrysophyte cyst assemblages as quantitative indicators for the reconstruction of past environmental conditions in the Alps. II. Nutrients. Journal of Paleolimnology 19, 443–463. https://doi.org/10.1023/A:1007994206432

Lotter, A.F., Sturm, M., Teranes, J.L., Wehrli, B., 1997. Varve formation since 1885 and high-resolution varve analyses in hypertrophic Baldeggersee (Switzerland). Aquatic Science 59, 304–325. https://doi.org/10.1007/BF02522361

Luoto, T.P., 2011. The relationship between water quality and chironomid distribution in Finland—A new assemblage-based tool for assessments of long-term nutrient dynamics. Ecological Indicators 11, 255–262. https://doi.org/10.1016/j.ecolind.2010.05.002

Luoto, T.P., Kultti, S., Nevalainen, L., Sarmaja-Korjonen, K., 2010. Temperature and effective moisture variability in southern Finland during the Holocene quantified with midge-based calibration models. J Quaternary Science 25, 1317–1326. https://doi.org/10.1002/jqs.1417

Magny, M., Guiot, J., Schoellammer, P., 2001. Quantitative Reconstruction of Younger Dryas to Mid-Holocene Paleoclimates at Le Locle, Swiss Jura, Using Pollen and Lake-Level Data. Quaternary Research 56, 170–180. https://doi.org/10.1006/qres.2001.2257

Manca, M., Torretta, B., Comoli, P., Amsinck, S.L., Jeppesen, E., 2007. Major changes in trophic dynamics in large, deep sub-alpine Lake Maggiore from 1940s to 2002: a high resolution comparative palaeo-neolimnological study. Freshwater Biology 52, 2256–2269. https://doi.org/10.1111/j.1365-2427.2007.01827.x

Marsicek, J., Shuman, B.N., Bartlein, P.J., Shafer, S.L., Brewer, S., 2018. Reconciling divergent trends and millennial variations in Holocene temperatures. Nature 554, 92–96. https://doi.org/10.1038/nature25464

Mayewski, P.A., Rohling, E.E., Curt Stager, J., Karlén, W., Maasch, K.A., Meeker, L.D., Meyerson, E.A., Gasse, F., Van Kreveld, S., Holmgren, K., Lee-Thorp, J., Rosqvist, G., Rack, F., Staubwasser, M., Schneider, R.R., Steig, E.J., 2004. Holocene climate variability. Quat. res. 62, 243–255. https://doi.org/10.1016/j.yqres.2004.07.001

Miles, M.W., Andresen, C.S., Dylmer, C.V., 2020. Evidence for extreme export of Arctic sea ice leading the abrupt onset of the Little Ice Age. Sci. Adv. 6, eaba4320. https://doi.org/10.1126/sciadv.aba4320

Mirosław-Grabowska, J., Zawisza, E., Jaskółka, A., Obremska, M., 2015. Natural transformation of the Romoty paleolake (NE Poland) during the Late Glacial and Holocene based on isotopic, pollen, cladoceran and geochemical data. Quaternary International, Palaeolandscapes from Saalian to Weichselian: INQUA TERPRO Commission, Peribaltic International Field Symposium, Lithuania 386, 171–185. https://doi.org/10.1016/j.quaint.2015.06.040

Moros, M., Emeis, K., Risebrobakken, B., Snowball, I., Kuijpers, A., McManus, J., Jansen, E., 2004. Sea surface temperatures and ice rafting in the Holocene North Atlantic: climate influences on northern Europe and Greenland. Quaternary Science Reviews, Holocene climate variability - a marine perspective 23, 2113–2126. https://doi.org/10.1016/j.quascirev.2004.08.003

Moss, B., 2011. Allied attack: climate change and eutrophication. IW 1, 101–105. https://doi.org/10.5268/IW-1.2.359

Nazarova, L., Herzschuh, U., Wetterich, S., Kumke, T., Pestryakova, L., 2011. Chironomid-based inference models for estimating mean July air temperature and water depth

from lakes in Yakutia, northeastern Russia. J Paleolimnol 45, 57–71. https://doi.org/10.1007/s10933-010-9479-4
Nevalainen, L., Ketola, M., Korosi, J.B., Manca, M., Kurmayer, R., Koinig, K.A., Psenner, R., Luoto, T.P., 2014. Zooplankton (Cladocera) species turnover and long-term decline of Daphnia in two high mountain lakes in the Austrian Alps. Hydrobiologia 722, 75–91. https://doi.org/10.1007/s10750-013-1676-5
Nickus, U., Bishop, K., Erlandsson, M., Evans, C.D., Forsius, M., Laudon, H., Livingstone, D.M., Monteith, D., Thies, H., 2010. Direct Impacts of Climate Change on Freshwater Ecosystems, in: Kernan, M., Battarbee, R.W., Moss, B. (Eds.), Climate Change Impacts on Freshwater Ecosystems. Wiley, pp. 38–64. https://doi.org/10.1002/9781444327397.ch3
Niinemets, E., Saarse, L., 2009. Holocene vegetation and land-use dynamics of south-eastern Estonia. Quaternary International 207, 104–116. https://doi.org/10.1016/j.quaint.2008.11.015
NOAA National Centers for Environmental Information, 2022. ETOPO 2022 15 Arc-Second Global Relief Model. https://doi.org/10.25921/FD45-GT74
O'Brien, S.R., Mayewski, P.A., Meeker, L.D., Meese, D.A., Twickler, M.S., Whitlow, S.I., 1995. Complexity of Holocene Climate as Reconstructed from a Greenland Ice Core. Science 270, 1962–1964. https://doi.org/10.1126/science.270.5244.1962
Oksanen, J., Simpson, G., Blanchet, F., Kindt, R., Legendre, P., Minchin, P., O'Hara, R., Solymos, P., Stevens, M., Szoecs, E., Wagner, H., Barbour, M., Bedward, M., Bolker, B., Borcard, D., Carvalho, G., Chirico, M., De Caceres, M., Durand, S., Evangelista, H., Fitzjohn, R., Friendly, M., Furneaux, B., Hannigan, G., Hill, M., Lahti, L., McGlinn, D., Ouellette, M., Ribeiro Cunha, E., Smith, T., Stier, A., ter Braak, C., Weedon, J., 2022. vegan: community ecology package. R package version 2.6-4.
Ólafsson, J.S., Adalsteinsson, H., Gíslason, G.M., Hansen, I., Hrafnsdóttir, Th., 2002. Spatial heterogeneity in lotic chironomids and simuliids in relation to catchment characteristics in Iceland. SIL Proceedings, 1922-2010 28, 157–163. https://doi.org/10.1080/03680770.2001.11902566
Oppo, D.W., McManus, J.F., Cullen, J.L., 2003. Deepwater variability in the Holocene epoch. Nature 422, 277–277. https://doi.org/10.1038/422277b
Owens, M.J., Lockwood, M., Hawkins, E., Usoskin, I., Jones, G.S., Barnard, L., Schurer, A., Fasullo, J., 2017. The Maunder minimum and the Little Ice Age: an update from recent reconstructions and climate simulations. J. Space Weather Space Clim. 7, A33. https://doi.org/10.1051/swsc/2017034
Pastukhova, Y., Tsyganov, A., Sapelko, T., Mazei, N., Zharov, A., Mazei, Y., 2024. Paleoecological reconstruction of water level changes in a cascade of lakes on Lunkulansaari Island (Lake Ladoga) based on the analysis of Cladocera remains in lake sediments. Limnology and Freshwater Biology 574–579. https://doi.org/10.31951/2658-3518-2024-A-4-574
Płóciennik, M., Self, A., Birks, H.J.B., Brooks, S.J., 2011. Chironomidae (Insecta: Diptera) succession in Żabieniec bog and its palaeo-lake (central Poland) through the Late Weichselian and Holocene. Palaeogeography, Palaeoclimatology, Palaeoecology 307, 150–167. https://doi.org/10.1016/j.palaeo.2011.05.010

Poska, A., Väli, V., Vassiljev, J., Alliksaar, T., Saarse, L., 2022. Timing and drivers of local to regional scale land-cover changes in the hemiboreal forest zone during the Holocene: A pollen-based study from South Estonia. Quaternary Science Reviews 277, 107351. https://doi.org/10.1016/j.quascirev.2021.107351

Ramsey, C.B., 2008. Deposition models for chronological records. Quaternary Science Reviews, INTegration of Ice-core, Marine and Terrestrial records (INTIMATE): Refining the record of the Last Glacial-Interglacial Transition 27, 42–60. https://doi.org/10.1016/j.quascirev.2007.01.019

Rao, Z., Tian, Y., Guang, K., Wei, S., Guo, H., Feng, Z., Zhao, L., Li, Y., 2022. Pollen Data as a Temperature Indicator in the Late Holocene: A Review of Results on Regional, Continental and Global Scales. Front. Earth Sci. 10, 845650. https://doi.org/10.3389/feart.2022.845650

Rasmussen, S.O., Dahl-Jensen, D., Fischer, H., Fuhrer, K., Hansen, S.B., Hansson, M., Hvidberg, C.S., Jonsell, U., Kipfstuhl, S., Ruth, U., Schwander, J., Siggaard-Andersen, M.-L., Sinnl, G., Steffensen, J.P., Svensson, A.M., Vinther, B.M., 2023. Ice-core data used for the construction of the Greenland Ice-Core Chronology 2005 and 2021 (GICC05 and GICC21). Earth Syst. Sci. Data 15, 3351–3364. https://doi.org/10.5194/essd-15-3351-2023

Reimer, P.J., Austin, W.E.N., Bard, E., Bayliss, A., Blackwell, P.G., Bronk Ramsey, C., Butzin, M., Cheng, H., Edwards, R.L., Friedrich, M., Grootes, P.M., Guilderson, T.P., Hajdas, I., Heaton, T.J., Hogg, A.G., Hughen, K.A., Kromer, B., Manning, S.W., Muscheler, R., Palmer, J.G., Pearson, C., Van Der Plicht, J., Reimer, R.W., Richards, D.A., Scott, E.M., Southon, J.R., Turney, C.S.M., Wacker, L., Adolphi, F., Büntgen, U., Capano, M., Fahrni, S.M., Fogtmann-Schulz, A., Friedrich, R., Köhler, P., Kudsk, S., Miyake, F., Olsen, J., Reinig, F., Sakamoto, M., Sookdeo, A., Talamo, S., 2020. The IntCal20 Northern Hemisphere Radiocarbon Age Calibration Curve (0–55 cal kBP). Radiocarbon 62, 725–757. https://doi.org/10.1017/RDC.2020.41

Renberg, I., Wik, M., 1985. Soot Particle Counting in Recent Lake Sediments an Indirect Dating Method. Ecological Bulletins 37, 53–57.

Renssen, H., Isarin, R.F.B., Jacob, D., Podzun, R., Vandenberghe, J., 2001. Simulation of the Younger Dryas climate in Europe using a regional climate model nested in an AGCM: preliminary results. Global and Planetary Change 30, 41–57. https://doi.org/10.1016/S0921-8181(01)00076-5

Republic of Estonia Land and Spatial Development Board, 2025. False-color forestry NGR orthophoto 06.07.2017.

Rigterink, S., Krahn, K.J., Kotrys, B., Urban, B., Heiri, O., Turner, F., Pannes, A., Schwalb, A., 2024. Summer temperatures from the Middle Pleistocene site Schöningen 13, northern Germany, determined from subfossil chironomid assemblages. Boreas 53, 525–542. https://doi.org/10.1111/bor.12658

Rose, N., 2002. Fly-Ash Particles, in: Last, W.M., Smol, J.P. (Eds.), Tracking Environmental Change Using Lake Sediments, Developments in Paleoenvironmental Research. Springer Netherlands, Dordrecht, pp. 319–349. https://doi.org/10.1007/0-306-47670-3_12

Saarse, L., Veski, S., 2001. SPREAD OF BROAD-LEAVED TREES IN ESTONIA. Proceedings of the Estonian Academy of Sciences. Geology 50, 51. https://doi.org/10.3176/geol.2001.1.05

Salonen, J.S., Seppä, H., Luoto, M., Bjune, A.E., Birks, H.J.B., 2012. A North European pollen–climate calibration set: analysing the climatic responses of a biological proxy using novel regression tree methods. Quaternary Science Reviews 45, 95–110. https://doi.org/10.1016/j.quascirev.2012.05.003

Sapelko, T., Pozdnyakov, S., Kuznetsov, D., Ludikova, A., Ivanova, E., Guseva, M., Zazovskaya, E., 2019. Holocene sedimentation in the central part of Lake Ladoga. Quaternary International, Quaternary Freshwater ecosystem: a paleoclimate, paleolandscapes and biostratigraphy approach 524, 67–75. https://doi.org/10.1016/j.quaint.2019.05.028

Scheffer, M., Van Nes, E.H., 2007. Shallow lakes theory revisited: various alternative regimes driven by climate, nutrients, depth and lake size. Hydrobiologia 584, 455–466. https://doi.org/10.1007/s10750-007-0616-7

Šeirienė, V., Gastevičienė, N., Luoto, T.P., Gedminienė, L., Stančikaitė, M., 2021. The Lateglacial and early Holocene climate variability and vegetation dynamics derived from chironomid and pollen records of Lieporiai palaeolake, North Lithuania. Quaternary International, The Quaternary of Europe and Adjacent Areas: Stratigraphical Perspectives and Tools for Correlations – SEQS-2019 605–606, 55–64. https://doi.org/10.1016/j.quaint.2020.12.017

Self, A., Brooks, S., Birks, H., Nazarova, L., Porinchu, D., Odland, A., Yang, H., Jones, V., 2011. The distribution and abundance of chironomids in high-latitude Eurasian lakes with respect to temperature and continentality: development and application of new chironomid-based climate-inference models in northern Russia. https://doi.org/10.1016/j.quascirev.2011.01.022

Seppä, H., Birks, H.J.B., 2001. July mean temperature and annual precipitation trends during the Holocene in the Fennoscandian tree-line area: pollen-based climate reconstructions. The Holocene 11, 527–539. https://doi.org/10.1191/095968301680223486

Seppä, H., Bjune, A.E., Telford, R.J., Birks, H.J.B., Veski, S., 2009. Last nine-thousand years of temperature variability in Northern Europe. Climate of the Past 5, 523–535. https://doi.org/10.5194/cp-5-523-2009

Seppä, H., Hammarlund, D., Antonsson, K., 2005. Low-frequency and high-frequency changes in temperature and effective humidity during the Holocene in south-central Sweden: implications for atmospheric and oceanic forcings of climate. Clim Dyn 25, 285–297. https://doi.org/10.1007/s00382-005-0024-5

Seppä, H., Poska, A., 2004. Holocene annual mean temperature changes in Estonia and their relationship to solar insolation and atmospheric circulation patterns. Quat. res. 61, 22–31. https://doi.org/10.1016/j.yqres.2003.08.005

Sher, A., Kuzmina, S., Kiseyov, S., Lister, A., 2003. Tundra-steppe environment in Arctic Siberia and the evolution of the woolly mammoth. Presented at the 3rd International Mammoth Conference, 2003 : Program and Abstracts, Occasional Papers in Earth

Sciences, 5 . Palaeontology Program, Department of Tourism and Culture, Government of Yukon, Yokon, Canada, pp. 136–142.
Shuman, B., 2012. Patterns, processes, and impacts of abrupt climate change in a warm world: the past 11,700 years. WIREs Climate Change 3, 19–43. https://doi.org/10.1002/wcc.152
Solomina, O.N., Bradley, R.S., Hodgson, D.A., Ivy-Ochs, S., Jomelli, V., Mackintosh, A.N., Nesje, A., Owen, L.A., Wanner, H., Wiles, G.C., Young, N.E., 2015. Holocene glacier fluctuations. Quaternary Science Reviews 111, 9–34. https://doi.org/10.1016/j.quascirev.2014.11.018
Stansell, N.D., Klein, E.S., Finkenbinder, M.S., Fortney, C.S., Dodd, J.P., Terasmaa, J., Nelson, D.B., 2017. A stable isotope record of Holocene precipitation dynamics in the Baltic region from Lake Nuudsaku, Estonia. Quaternary Science Reviews 175, 73–84. https://doi.org/10.1016/j.quascirev.2017.09.013
Steiner, D., Pauling, A., Nussbaumer, S.U., Nesje, A., Luterbacher, J., Wanner, H., Zumbühl, H.J., 2008. Sensitivity of European glaciers to precipitation and temperature – two case studies. Climatic Change 90, 413–441. https://doi.org/10.1007/s10584-008-9393-1
Stocker, T.F., Qin, D., Xia, Y., Bex, V., Midgley, P.M., 2013. IPCC, 2013: Climate Change 2013: The Physical Science Basis. Contribution of Working Group I to the Fifth Assessment Report of the Intergovernmental Panel on Climate Change. Cambridge University Press, Cambridge, United Kingdom and New York, NY, USA.
Stockmarr, J., 1971. Tables with spores used in absolute pollen analysis. Pollen et spores 615–21.
Stonevicius, E., Stankunavicius, G., Rimkus, E., 2018. Continentality and Oceanity in the Mid and High Latitudes of the Northern Hemisphere and Their Links to Atmospheric Circulation. Advances in Meteorology 1, 5746191. https://doi.org/10.1155/2018/5746191
Stralberg, D., Arseneault, D., Baltzer, J.L., Barber, Q.E., Bayne, E.M., Boulanger, Y., Brown, C.D., Cooke, H.A., Devito, K., Edwards, J., Estevo, C.A., Flynn, N., Frelich, L.E., Hogg, E.H., Johnston, M., Logan, T., Matsuoka, S.M., Moore, P., Morelli, T.L., Morissette, J.L., Nelson, E.A., Nenzén, H., Nielsen, S.E., Parisien, M., Pedlar, J.H., Price, D.T., Schmiegelow, F.K., Slattery, S.M., Sonnentag, O., Thompson, D.K., Whitman, E., 2020. Climate-change refugia in boreal North America: what, where, and for how long? Frontiers in Ecol & Environ 18, 261–270. https://doi.org/10.1002/fee.2188
Strandberg, G., Chen, J., Fyfe, R., Kjellström, E., Lindström, J., Poska, A., Zhang, Q., Gaillard, M.-J., 2023. Did the Bronze Age deforestation of Europe affect its climate? A regional climate model study using pollen-based land cover reconstructions. Climate of the Past 19, 1507–1530. https://doi.org/10.5194/cp-19-1507-2023
Szeroczynska, K., Sarmaja-Korjonen, K., 2007. Atlas of Subfossil Cladocera from Central and Northern Europe Atlas of Subfossil Cladocera from Central and Northern Europe Krystyna Szeroczynska. Library.
Team, B.A., 2008. Assessment of Climate Change for the Baltic Sea Basin. Springer Science & Business Media.

ter Braak, C.J.F., Juggins, S., 1993. Weighted averaging partial least squares regression (WA-PLS): an improved method for reconstructing environmental variables from species assemblages. Hydrobiologia 269, 485–502. https://doi.org/10.1007/BF00028046

Theuerkauf, M., Joosten, H., 2012. Younger Dryas cold stage vegetation patterns of central Europe–climate, soil and relief controls. Boreas 41, 391–407. https://doi.org/10.1111/j.1502-3885.2011.00240.x

Töchterle, P., Baldo, A., Murton, J.B., Schenk, F., Edwards, R.L., Koltai, G., Moseley, G.E., 2024. Reconstructing Younger Dryas ground temperature and snow thickness from cave deposits. Clim. Past 20, 1521–1535. https://doi.org/10.5194/cp-20-1521-2024

Tóth, M., Magyari, E.K., Buczkó, K., Braun, M., Panagiotopoulos, K., Heiri, O., 2015. Chironomid-inferred Holocene temperature changes in the South Carpathians (Romania). The Holocene. https://doi.org/10.1177/0959683614565953

Ursenbacher, S., Stötter, T., Heiri, O., 2020. Chitinous aquatic invertebrate assemblages in Quaternary lake sediments as indicators of past deepwater oxygen concentration. Quaternary Science Reviews 231, 106203. https://doi.org/10.1016/j.quascirev.2020.106203

Väliranta, M., Salonen, J.S., Heikkilä, M., Amon, L., Helmens, K., Klimaschewski, A., Kuhry, P., Kultti, S., Poska, A., Shala, S., Veski, S., Birks, H.H., 2015. Plant macrofossil evidence for an early onset of the Holocene summer thermal maximum in northernmost Europe. Nat Commun 6, 6809. https://doi.org/10.1038/ncomms7809

Van Damme, K., Kotov, A.A., 2016. The fossil record of the Cladocera (Crustacea: Branchiopoda): Evidence and hypotheses. Earth-Science Reviews 163, 162–189. https://doi.org/10.1016/j.earscirev.2016.10.009

Velle, G., Brodersen, K.P., Birks, H.J.B., Willassen, E., 2010. Midges as quantitative temperature indicator species: Lessons for palaeoecology. The Holocene 20, 989–1002. https://doi.org/10.1177/0959683610365933

Veski, S., Seppä, H., Stančikaitė, M., Zernitskaya, V., Reitalu, T., Gryguc, G., Heinsalu, A., Stivrins, N., Amon, L., Vassiljev, J., Heiri, O., 2015. Quantitative summer and winter temperature reconstructions from pollen and chironomid data between 15 and 8 ka BP in the Baltic–Belarus area. Quaternary International 19, 4–11.

Visconti, A., Manca, M., De Bernardi, R., 2008. Eutrophication-like response to climate warming: an analysis of Lago Maggiore (N. Italy) zooplankton in contrasting years. J Limnol 67, 87. https://doi.org/10.4081/jlimnol.2008.87

Vollweiler, N., Scholz, D., Mühlinghaus, C., Mangini, A., Spötl, C., 2006. A precisely dated climate record for the last 9 kyr from three high alpine stalagmites, Spannagel Cave, Austria. Geophysical Research Letters 33, 2006GL027662. https://doi.org/10.1029/2006GL027662

Walker, I.R., 2001. Midges: Chironomidae and Related Diptera, in: Smol, J.P., Birks, H.J.B., Last, W.M. (Eds.), Tracking Environmental Change Using Lake Sediments, Developments in Paleoenvironmental Research. Springer Netherlands, Dordrecht, pp. 43–66. https://doi.org/10.1007/0-306-47671-1_3

Walker, M.J.C., Berkelhammer, M., Björck, S., Cwynar, L.C., Fisher, D.A., Long, A.J., Lowe, J.J., Newnham, R.M., Rasmussen, S.O., Weiss, H., 2012. Formal subdivision of the Holocene Series/Epoch: a Discussion Paper by a Working Group of

INTIMATE (Integration of ice-core, marine and terrestrial records) and the Subcommission on Quaternary Stratigraphy (International Commission on Stratigraphy). Journal of Quaternary Science 27, 649–659. https://doi.org/10.1002/jqs.2565

Wang, W., Xiang, L., Li, Y., Suo, Q., Song, X., Zhang, Y., Huang, C., Muhammad, F., Wang, T., Ren, X., Chen, S., Chen, G., Huang, X., 2024. Modern distribution of Cladocera in lakes of northern China and western Mongolia and its environmental implications. Fundamental Research. https://doi.org/10.1016/j.fmre.2024.09.004

Wanner, H., Beer, J., Bütikofer, J., Crowley, T.J., Cubasch, U., Flückiger, J., Goosse, H., Grosjean, M., Joos, F., Kaplan, J.O., Küttel, M., Müller, S.A., Prentice, I.C., Solomina, O., Stocker, T.F., Tarasov, P., Wagner, M., Widmann, M., 2008. Mid- to Late Holocene climate change: an overview. Quaternary Science Reviews 27, 1791–1828. https://doi.org/10.1016/j.quascirev.2008.06.013

Wickham, H., Averick, M., Bryan, J., Chang, W., McGowan, L.D., François, R., Grolemund, G., Hayes, A., Henry, L., Hester, J., Kuhn, M., Pedersen, T.L., Miller, E., Bache, S.M., Müller, K., Ooms, J., Robinson, D., Seidel, D.P., Spinu, V., Takahashi, K., Vaughan, D., Wilke, C., Woo, K., Yutani, H., 2019. Welcome to the Tidyverse. Journal of Open Source Software 4, 1686. https://doi.org/10.21105/joss.01686

Wickham, H., Francois, R., Henry, L., Muller, K., 2022. Dplyr: a grammar of data manipulation. R package version 1.0.10.

Yao, F., Ma, C., Zhu, C., Li, J., Chen, G., Tang, L., Huang, M., Jia, T., Xu, J., 2017. Holocene climate change in the western part of Taihu Lake region, East China. Palaeogeography, Palaeoclimatology, Palaeoecology 485, 963–973. https://doi.org/10.1016/j.palaeo.2017.08.022

Zani, D., Lischke, H., Lehsten, V., 2023. Climate and dispersal limitation drive tree species range shifts in post-glacial Europe: results from dynamic simulations. Front. Ecol. Evol. 11, 1321104. https://doi.org/10.3389/fevo.2023.1321104

Zawiska, I., Correa-Metrio, A., Rzodkiewicz, M., Wolski, J., 2025. Cladocera assemblages indicate environmental gradients of lake productivity and morphometry in central Europe. Boreas 54, 258–272. https://doi.org/10.1111/bor.70001

Zawiska, I., Luoto, T.P., Nevalainen, L., Tylmann, W., Jensen, T.C., Obremska, M., Słowiński, M., Woszczyk, M., Schartau, A.K., Walseng, B., 2017. Climate variability and lake ecosystem responses in western Scandinavia (Norway) during the last Millennium. Palaeogeography, Palaeoclimatology, Palaeoecology 466, 231–239. https://doi.org/10.1016/j.palaeo.2016.11.034

Curriculum vitae

Personal data

Name:	Varvara Bakumenko
Date of birth:	28.02.1998
Place of birth:	Moscow, Russia
Citizenship:	Russian

Contact data

E-mail:	Bakumenko.varvara@gmail.com

Education

2020–2025	Tallinn University of Technology, PhD
2019–2020	Moscow State University, MSC
2015–2019	Moscow State University, BSC
2013–2015	High school

Language competence

English	Fluent
Russian	Native
Estonian	A2
French	A2

Professional employment

2020–2025	Tallinn University of Technology
2017–2020	Moscow State University

Elulookirjeldus

Isikuandmed

Nimi:	Varvara Bakumenko
Sünniaeg:	28.02.1998
Sünnikoht:	Moskva, Venemaa
Kodakondsus:	Venemaa

Kontaktandmed

E-post:	Bakumenko.varvara@gmail.com

Hariduskäik

2020–2025	Tallinna Tehnikaülikool, PhD
2019–2020	Moskva Riiklik Ülikool, MSC
2015–2019	Moskva Riiklik Ülikool, BSC
2013–2015	Keskharidus

Keelteoskus

Inglise keel	kõrgtase
Vene keel	emakeel
Prantsuse keel	A2
Eesti keel	A2

Teenistuskäik

2020–2025	Tallinna Tehnikaülikool
2017–2020	Moskva Riiklik Ülikool

ISSN 2585-6901 (PDF)
ISBN 978-9916-80-351-6 (PDF)